ZooKeys 1160: 1–59 (2023)
doi: 10.3897/zookeys.1159.98022
https://zookeys.pensoft.net

RESEARCH ARTICLE

A peer-reviewed open-access journal
ZooKeys
Launched to accelerate biodiversity research

Further notes on the taxonomy of the land snail family Clausiliidae Gray, 1855 (Stylommatophora, Helicina) from Myanmar with description of two new species

Nem Sian Man[1], Ngwe Lwin[2], Chirasak Sutcharit[1], Somsak Panha[1]

1 *Animal Systematics Research Unit, Department of Biology, Faculty of Science, Chulalongkorn University, Bangkok, 10330, Thailand* **2** *Fauna and Flora International, No. 35, 3rd Floor, Shan Gone Condo, Myay Ni Gone Market Street, Sanchaung Township, Yangon, Myanmar*

Corresponding author: Somsak Panha (somsak.pan@chula.ac.th)

Academic editor: Thierry Backeljau | Received 25 November 2022 | Accepted 2 April 2023 | Published 3 May 2023

https://zoobank.org/B7E44924-0D3D-4529-987F-19A51FAA115E

Citation: Man NS, Lwin N, Sutcharit C, Panha S (2023) Further notes on the taxonomy of the land snail family Clausiliidae Gray, 1855 (Stylommatophora, Helicina) from Myanmar with description of two new species. ZooKeys 1160: 1–59. https://doi.org/10.3897/zookeys.1159.98022

Abstract

This study presents a complete species list of the door snails inhabiting Myanmar, updated to now include 33 taxa, and provides taxonomic notes together with a re-description of the shell, radula, and genitalia for 13 species and subspecies, including *Oospira philippiana*, the type species of the genus *Oospira*. The snails previously treated as subspecies or synonyms of *Oospira gracilior* and *Oospira magna* are reclassified and recognized as distinct species. The lectotype of *Oospira insignis* has been clarified and an illustration of the original type specimen provided. A long-overlooked species, *Oospira andersoniana*, has been collected and redescribed herein. Two new species from the limestone karsts in the Salween River Basin are introduced: *Oospira luneainopsis* Man & Panha, **sp. nov.** and *Oospira zediopsis* Man & Panha, **sp. nov.** A synoptic view of all clausiliid taxa known from Myanmar is presented along with taxonomic information and distributional records. Photographs of the type materials for all taxa are provided for further comparison or, if unavailable, photographs of the examined specimens or the original figure from the literature.

Keywords

Biodiversity, door snail, endemic, gastropod, limestone, systematics

Table of contents

Introduction

Door snails are well-known land snails belonging to the family Clausiliidae Gray, 1855, and are easily recognized by their usually sinistral fusiform shell and their unique clausilial apparatus: clausilium, plicae and lamellae (Nordsieck 2007; Uit de Weerd and Gittenberger 2013). They are considered to have originated in western Eurasia during the Late Cretaceous before being dispersed worldwide, and now occur in the Ethiopian, Palearctic and Neotropical regions (Nordsieck 2007; Uit de Weerd and Gittenberger 2013). These snails have long fascinated researchers who studied their systematic and evolutionary history, particularly for European taxa (e.g., Giokas et al. 2005; Gittenberger et al. 2012; Koch et al. 2017; Fehér et al. 2018; Hausdorf 2022; Hausdorf and Neiber 2022; Sulikowska-Drozd et al. 2022).

Only two of the seven subfamilies of Clausiliidae have diversified in Southeast Asia: Phaedusinae Wagner, 1922 and Garnieriinae Boettger, 1926 (Uit de Weerd and

Gittenberger 2013). Their ancestors are believed to have colonized and diversified in SE Asia independently over nearly the same period (Nordsieck 2007; Uit de Weerd and Gittenberger 2013). These door snails are ground to arboreal dwellers (tree trunks) that tend to prefer karstic-associated habitats (Stoliczka 1871; Loosjes 1953). Within Indochina, Vietnam has the highest number of reported clausiliid taxa, with ca. 90 nominal species and subspecies in 33 genera and subgenera (Nordsieck 2011; Schileyko 2011; Páll-Gergely and Szekeres 2017; Bui and Szekeres 2019); in contrast, the clausiliids of other countries in Indochina are far less well documented. This is surprising especially in the case of Myanmar, which hosts 14 terrestrial ecoregions (Olson et al. 2001) and has twice the land area of Vietnam, but which has only 31 nominal species and subspecies from four genera (Grego et al. 2021; Szekeres et al. 2021a, b).

Knowledge of Myanmarese door snails was primarily reported during the colonial period in the 19th century by the pioneering western naturalists (see Pholyotha et al. 2020; Man et al. 2022 for further history review). The 'Fauna of British India including Ceylon and Burma' by Gude (1914) was the first, and is still the most important, publication on Myanmarese clausiliids. This early-20th century reference includes 19 nominal species and subspecies belonging to '*Clausilia* Draparnaud, 1805' with various subgenera and 'sections' (Gude 1914). Later, three additional species from northern and south-eastern Myanmar were introduced in the mid-20th and early-21st centuries (Likharev 1962; Nordsieck 1973, 2002a). In 2007, Nordsieck published an updated global list and proposed a reclassification of nearly all known clausiliid species. Then, in 2021, he further published the diagnostic characters, drawings and photographs from the type species and representative materials for Asian Phaedusinae (Nordsieck 2007, 2021). Regarding Myanmarese clausiliids, *Phaedusa* Adams & Adams, 1855 and *Oospira* Blanford, 1872 stand out as the most species-rich genera in this family. Recently, Grego et al. (2021) and Szekeres et al. (2021a, b) reported that the door snail diversity of Myanmar included 27 nominal species and subspecies of three genera; however, these species are mainly recognized on shell features only.

Traditionally, shell morphology employs apomorphic characters for species recognition, including lamellae development, and the number and position of palatal plicae (i.e., Nordsieck 2007, 2021; Uit de Weerd and Gittenberger 2013). Meanwhile, genital anatomy has been used to distinguish taxa when shell features alone are ambiguous (Pholyotha et al. 2020; Sutcharit et al. 2020a; Páll-Gergely and Szekeres 2020). Yet, the reproductive organs of clausiliids have received less attention, with only some scattered investigations in a few Indochinese species (Stoliczka 1871, 1873; Likharev 1962; Nordsieck 1973; Maassen and Gittenberger 2007; Páll-Gergely and Szekeres 2017). Nevertheless, recent studies on European taxa have shown that the genital organs and their internal sculpture, though highly variable, are helpful for more precise species identification (De Mattia et al. 2020, 2021; Páll-Gergely and Szekeres 2020). Lately, Hwang et al. (2022) also discussed some characters involving the genitalia and shell sculpture that should be considered for further taxonomic work on clausiliids at the species level based on a molecular analysis of the genus *Formosana* Boettger, 1877. Prior to our recent study, all former studies on Myanmarese phaedusinids were based on shell characters, except for *Oospira philippiana* (Pfeiffer, 1847), *O. decollata*

(Likharev, 1962), and *O. malaisei* Nordsieck, 1973; the genital anatomy of these three species was described, but only the external features were reported. Therefore, there is a need for more in-depth studies of the reproductive organs of these snails and Southeast Asian clausiliids in general.

Myanmar is actively promoting knowledge of its malacofauna, especially the material obtained under the framework of a joint project between the Forest Department of Myanmar, the Fauna and Flora International (**FFI**), and the Animal Systematics Research Unit (**ASRU**) of Chulalongkorn University, Thailand. This effort has already provided information regarding the distribution, habitat, and essential morphological characters (e.g., genitalia and radula) of the Myanmarese malacofauna, including the description of several new ariophantids and helicarionids taxa (Pholyotha et al. 2020, 2022; Sutcharit et al. 2020a; Sutcharit and Panha 2021) and Streptaxidae (Sutcharit et al. 2020b; Man et al. 2022). In this context, the present study provides an up-to-date species list of the door snails from Myanmar, with taxonomic notes, and with a re-description of the shell, genitalia, and radula morphology of several species. In addition, two species from the limestone karsts in the Salween River Basin are described as new. Hopefully, this article will inspire young Myanmarese zoologists to take an interest in the land snails of their country.

Materials and methods

Sampling and morphological studies

This study was conducted within the MoU (Letter No. 0092) framework between the Forest Department, Ministry of Natural Resources and Environmental Conservation and Forestry, Myanmar and FFI from 2015 to 2016. Specimens were collected throughout northern and southern Myanmar (Fig. 1; Table 1) by the ASRU members and are deposited in the Chulalongkorn University Museum of Zoology (**CUMZ**), Thailand. Living snails were photographed and euthanized following standard two-step method protocols. The snails were immersed in 5% ethanol and then preserved in 70% (v/v) ethanol for anatomical studies (American Veterinary Medical Association 2020). Species identifications were based on the original descriptions, supplemented with Gude (1914), Nordsieck (2002b, 2007), Grego et al. (2021) and Szekeres et al. (2021a, b). Specimens were also compared with available reference collections and type material.

Shell dimensions (height and width), whorl count, coloration and sculpture were assessed from intact adult shells. The parietal wall of the last whorl of one to three shells was removed to observe the shape, size, thickness and numbers of plicae and lamellae, and clausilium morphology. The terminology used for the clausilial apparatus and genitalia in this description is modified from Gude (1914), Loosjes (1953), and Nordsieck (2007, 2021), as shown in Fig. 2. In addition, when ethanol-preserved specimens were available, the genitalia of one to five snails of each species were dissected and observed under an Olympus SZX2-TR30 stereoscopic light microscope.

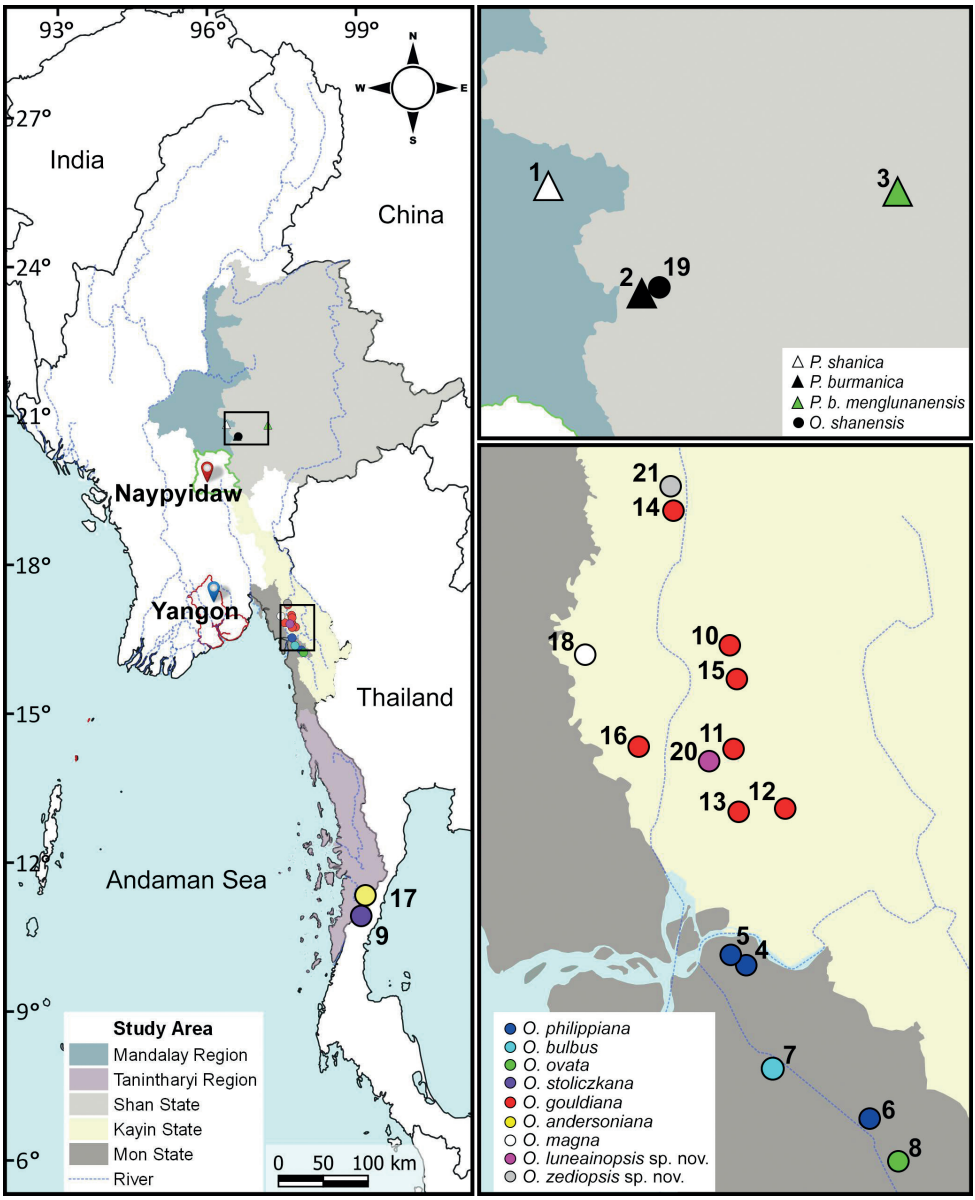

Figure 1. Approximate collecting localities of the *Phaedusa* species (triangles) and *Oospira* species (circles) from Myanmar examined in this study. The numbers correspond to localities listed in Table 1.

The shells, clausilial apparatus and genitalia were then imaged using a digital camera (DSLR D850-Nikon) and a stereo microscope with Cell's Imaging Software. The buccal masses were removed, and the radulae were soaked in 10% (w/v) NaOH, and then cleaned in distilled water. Radulae were photographed under scanning electron microscopy (SEM; JEOL, JSM-6610 LV).

Table 1. Shell measurements of clausiliid species examined in this study. The numbers listed with collection localities correspond to the map in Fig. 1. Asterisks indicate incomplete (apex broken; not decollated) shells. SH: shell height; SW: shell width.

Species no., locality no., and CUMZ no.	Number of specimens	Ranges, mean ± S.D. in mm		SH/SW ratio	Number of whorls
		Shell height	Shell width		
1. *Phaedusa shanica*					
1. Pyinyaung Village, Meiktila, Mandalay (13032, 13033)	46	16.0–18.0 16.88 ± 0.87	3.0–3.4 3.25 ± 0.13	5.0–5.5 5.22 ± 0.26	11–13½
2. *Phaedusa burmanica*					
2. Myin Ma Hti, Kalaw, Shan (13034, 13035)	2	24.0–25.3 24.76 ± 0.68	5.0–5.4 5.16 ± 0.20	4.68–4.9 4.79 ± 0.10	12, 13
3. *Phaedusa bocki menglunanensis*					
3. Aik Kham Cave, Taunggyi, Shan (13036)	3*	22.8, 23.9, 24.0	4.3, 4.5, 5.0	4.8–5.3 5.13±0.29	12–13
4. *Oospira philippiana*					
4. Saddan Cave, Mawlamyine, Mon (13037)	10	21.6–23.0 22.22 ± 0.64	7.0–8.2 7.76 ± 0.45	2.8–3.1 2.86 ± 0.12	5–6
5. Kayon Cave, Mawlamyine, Mon (13038, 13039)	21	21.0–22.6 21.96 ± 0.61	7.2–8.0 7.52 ± 0.30	2.8–3.0 2.92 ± 0.07	5–6
6. Pha Boang Cave, Mawlamyine Mon (13040¸ 13041)	24	25.5–26.6 25.95 ± 0.47	7.9–8.2 8.02 ± 0.12	3.2–3.3 3.23 ± 0.03	6–6½
5. *Oospira bulbus*					
7. Sanbel Cave, Mawlamyine, Mon (13042, 13043)	18	19.39–19.78 19.56 ± 0.17	8.00–8.55 8.30±0.19	2.28–2.42 23.57±0.05	5–5½
6. *Oospira ovata*					
8. Pathein Mountain, Mawlamyine, Mon (13044, 13045)	26	16.8–18.4 17.60±0.59	6.7–7.1 6.92 ± 0.20	2.5–2.7 2.54 ± 0.08	5–5½
7. *Oospira stoliczkana*					
9. Phra Cave, Tanintharyi (13046, 13047)	5	21.6–25 23.47 ± 1.64	6.7–7.1 6.92 ± 0.17	3.1–3.6 3.39 ± 0.22	6–6½
8. *Oospira gouldiana*					
10. Bardai Mountain, Hpa-an, Kayin (13048)	25	24.8–29.0 26.10 ± 1.69	5.7–6.2 5.90 ± 0.21	4.1–4.8 4.42 ± 0.25	10–11
11. Kaw Ka Thaung, Hpa-an, Kayin (13049)	23	25.8–27.8 26.81 ± 0.88	6–7 5.97 ± 0.32	4.3–4.9 4.50 ± 0.28	10–11
12. Lun Nga Mountain, Hpa-an, Kayin (13050)	18	24.0–27.0 26.32 ± 1.41	5.7–6.5 6.11 ± 0.34	4.0–4.9 4.31 ± 0.27	11–12
13. Sadhdan Cave, Hpa-an, Kayin (13051)	2*	25.0, 29.0	5.4, 6.2	4.63–46.7 4.65±0.34	11, 11½
14. Taung Lay Cave, Hpa-an, Kayin (13052)	30	28.1–29.2 28.50 ± 0.47	5.6–5.9 5.80 ± 0.14	4.77–5.21 4.91 ± 0.17	11½–12
15. Waiponla Mountain, Hpa-an, Kayin (13053, 13054)	4*	26.0–27.5 26.42 ±0.72	6.0–7.0 6.52±0.41	3.92–4.33 4.05±0.18	8–8½
16. Rathye Pyan Cave, Hpa-an, Kayin (13055)	1*	21.83	6.1	3.57	6
9. *Oospira andersoniana*					
17. Phra Cave, Tanintharyi (13056, 13057)	34	18.6–22.0 19.75 ± 1.26	4.1–4.4 4.28 ± 0.13	4.3–5.0 4.60 ± 0.22	9–10
10. *Oospira magna*					
18. Bayin Nyi Cave, Hpa-an, Kayin (13058, 13059)	4	21.8–26.3 24.68 ± 1.76	5.3–5.5 5.38 ± 0.08	4.1–4.7 4.58 ± 0.27	10–11
11. *Oospira shanensis*					
19. Nanthe Cave, Kalaw, Shan (13060, 13061)	9	24.5–26.0 25.63 ± 1.00	5.9–0.6 5.93 ± 0.60	4.0–4.6 4.34 ± 0.31	12½–13
12. *Oospira luneainopsis* sp. nov.					
20. Zwekabin Mountain, Hpa-an, Kayin (13062, 13063)	8	18.7–21.6 20.34 ± 1.34	5.6–6.0 5.72 ± 0.16	3.3–3.9 3.50 ± 0.23	7–8
13. *Oospira zediopsis* sp. nov.					
21. Weibyan Cave, Hpa-an, Kayin (13064, 13065)	50	22.4–26.8 24.98 ± 1.43	5.7–6.8 6.25 ± 0.38	3.8–4.2 4.00 ± 0.14	10–11

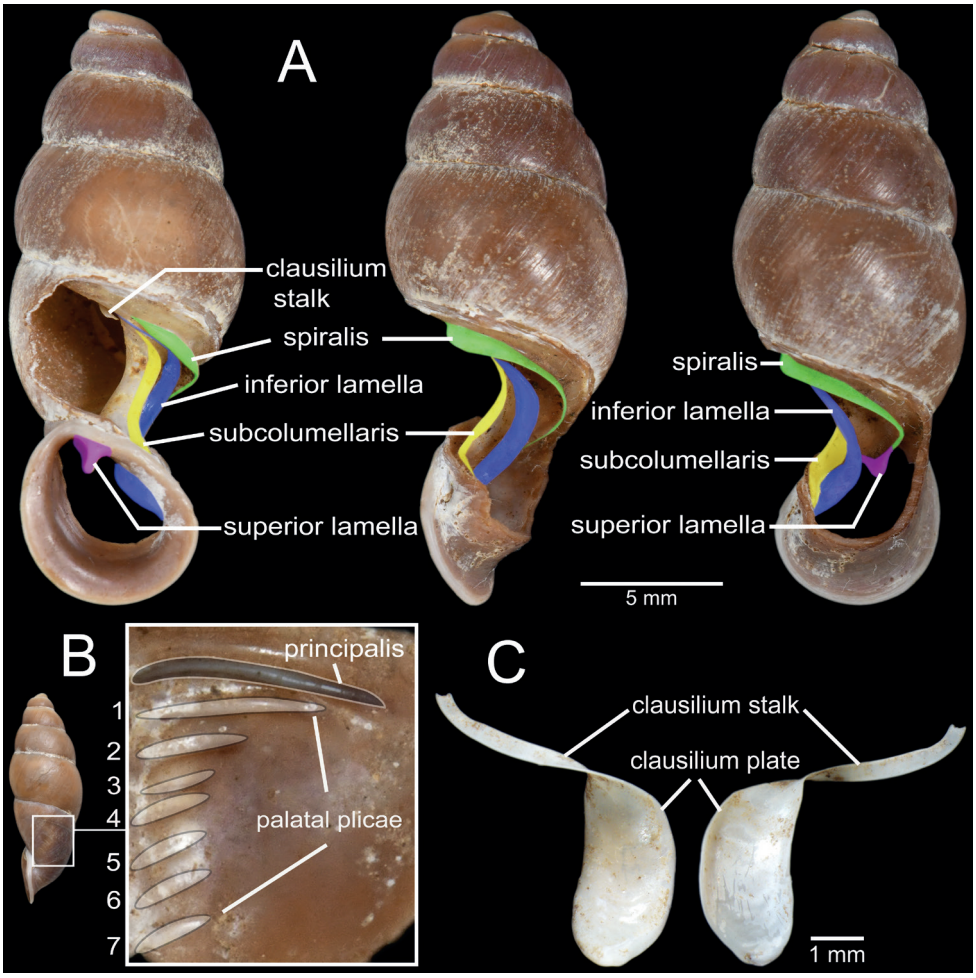

Figure 2. Clausilial apparatus terminology, with *Oospira philippiana* as a representative species **A** apertural, lateral and dorsal views from left to right, respectively, showing the lamellae **B** inside view of last whorl showing principalis and palatal plicae **C** front (left) and back (right) views of clausilium plate. Color indicates each lamella character.

Two nominal species names described as new to science in this work are attributed to the first and last authors (Man and Panha). Thus, a complete citation of the authorship is "Man and Panha in Man et al.".

Anatomical abbreviations

at atrium;
bb bursa (of bursa copulatrix);

db diverticulum (of bursa copulatrix);
dpb distal part of pedunculus (of bursa copulatrix);
ep epiphallus;
fo free oviduct;
p penis;
ppb proximal part of pedunculus (of bursa copulatrix);
pr penial retractor muscle;
v vagina;
vd vas deferens.

Institutional abbreviations

CUMZ Chulalongkorn University Museum of Zoology, Bangkok;
JG-C Jozef Grego collection, Banska Bystrica, Slovakia;
MCZ Museum of Comparative Zoology, Harvard University, Massachusetts;
MNHN Muséum National d'Histoire Naturelle, Paris;
NHMUK The Natural History Museum, London;
SMF Forschungsinstitut und Naturmuseum Senckenberg, Frankfurt am Main;
SMNH Swedish Museum of Natural History, Stockholm;
UF Florida Museum of Natural History, University of Florida, Florida;
ZISP Zoological Institute, Russian Academy of Sciences, St. Petersburg.

Systematics

Family Clausiliidae Gray, 1855
Subfamily Phaedusinae Wagner, 1922

Genus *Phaedusa* Adams & Adams, 1855

Clausilia (*Phaedusa*) Adams & Adams, 1855: 184. Boettger 1877: 54. Pfeiffer and Clessin 1881: 390. Gude 1914: 305.
Phaedusa–Thiele, 1931: 530. Zilch 1959: 389. Schileyko 2000: 599. Nordsieck 2002b: 88. Nordsieck 2007: 30.

Type species. *Clausilia corticina* Pfeiffer, 1842, by subsequent designation of Martens in Albers (1860: 275).

Diagnosis. Shell fusiform, more or less turreted, spire attenuated and shell surface with fine wavy to oblique striations. Palatal plicae short mostly, middle plicae weak to developed and 3 to 7 in number. Superior lamella low, connected to or separated from spiralis, and distinct at transition to spiralis. Inferior lamella spirally ascending and ending close to superior lamella from aperture view. Subcolumellaris visible or invisible in frontal view. Clausilium plate lateral side, rounded and broad.

External features. Animal covered with reticulated, dark gray skin; tentacles short; body and tail with paler color on lateral margin of foot; foot moderately elongated, posteriorly obtusely pointed.

Remarks. Nordsieck (2002b) compiled all the Southeast Asian Phaedusinae and summarized their diagnostic characteristics. Although *Phaedusa* and *Loosjesia* Nordsieck, 2002 are recognized as having spirally ascending inferior lamella, *Phaedusa* possesses shorter or weaker palatal plicae with the inferior lamella more narrowly spiral; in contrast, *Loosjesia* possesses longer and more developed palatal plicae, and much more spiral inferior lamella. *Phaedusa* closely resembles the Indian *Cylindrophaedusa* Boettger, 1877 (Gittenberger et al. 2019).

In the most recent generic classifications and species accounts by Grego et al. (2021) and Szekeres et al. (2021a, b), the genus *Phaedusa* from Myanmar is comprised of eight species, of which only three species were collected and re-described herein.

1 *Phaedusa shanica* (Boettger & Ponsonby, 1888)
Figs 3A, 4A, B, 5A–D, 6A, 19K; Tables 2, 3

Clausilia (*Pseudonenia*) *shanica* Boettger & Ponsonby in Godwin-Austen 1888: 244. Type locality: "Shan Hills, near Pingoung, Burma, at a height of about 2500 feet" [Pinlaung Township, Shan State, Myanmar].
Clausilia [*Phaedusa* (*Pseudonenia*)] *shanica*–Gude 1914: 326, figs 111, 112.
Phaedusa (*Phaedusa*) *shanica*–Nordsieck 2002b: 88. Nordsieck 2007: 32.
Phaedusa shanica–Zilch 1954: 34, pl. 3, fig. 46. Nordsieck 1974: 46, fig. 6, pl. 2, fig. 6. Grego et al. 2021: 27. Szekeres et al. 2021a: 183–185, fig. 11a, b.

Material examined. Limestone hills (Apache Cement Factory), Pyinyaung Village, Meiktila District, Mandalay Region, Myanmar (20°49'39.1"N, 96°23'35.1"E): CUMZ 13032 (6 shells Fig. 4A, B), CUMZ 13033 (40 specimens in ethanol), JG-C2881 (2 shells).

Description. Shell fusiform, turreted, translucent, and pale yellowish brown; spire acute. Shell surface with thin and dense oblique striations; suture distinct. Whorls 11–13½, little convex, regularly growing and attenuated to apex, last whorl somewhat compressed. Aperture obliquely rounded to pear-shaped, basis rounded and narrowing towards parietal sinus; peristome slightly protruded, thickened, and expanded. Superior lamella low, continuous with spiralis, and very low at transition to spiralis to almost separated. Inferior lamella spirally ascending, close to superior lamella and ending at peristome. Subcolumellaris emerged and only visible in oblique view. Principalis running along lateral-dorsal side and anterior end visible through oblique apertural view. Palatal plicae lateral, three: first plica strong and longest; second plica very weak and close to first plica; third plica oblique from subcolumellaris and sometimes almost connected to second plica. Palatal plicae not visible without cracking shell. Clausilium plate lateral side, broad, rounded and slightly thickened at tip.

Genitalia (*n* = 5). Atrium (at) short; penis (p) muscular, cylindrical, and gradually narrower towards epiphallus. Epiphallus (ep) muscular, cylindrical, ca. same as penis length and size, and gradually widening to proximal end. Penial retractor muscle (pr) attached proximally to epiphallus. Vas deferens (vd) slender, and shortly bounded at atrium and penis junction (Fig. 5A). Internal sculpture of penis smooth-surfaced and with 3 to 5 longitudinal folds (Fig. 5B); at transition from penis to epiphallus with irregularly corrugated and wrinkled folds that randomly split and merge (Fig. 5C). Internal sculpture of epiphallus with large papillae arranged in oblique rows (Fig. 5D).

Vagina (v) slender at junction of atrium, then bulging at connection of free oviduct (fo) and distal part of pedunculus (dpb), and almost as long as free oviduct. Distal part of pedunculus large, long, and basally stouter; diverticulum (db) slender, nearly equal to dpb length; proximal part of pedunculus (ppb) large, long, measuring ~ 3/4 of diverticulum length, and bursa copulatrix (bb) ovoid (Fig. 5A).

***Radula*.** Each row contains ~ 47 teeth with half-row formula: central–(lateral)–marginal teeth (1–(11–12)–23). Central tooth symmetrically tricuspid; mesocone large with pointed tip; ectocones triangular and located near the base. Lateral teeth asymmetrically bicuspid with small and pointed ectocone located at base; endocone large with pointed tip. Marginal teeth with asymmetrical tricuspids starting at approximately tooth number 11 or 12; mesocone large with dull tip; endocone and ectocone with small and pointed tips. Marginal teeth gradually reduced in size and becoming multicuspid marginally (Fig. 6A).

Distribution. *Phaedusa shanica* is collected from probably nearby the type locality and likely restricted in Myanmar. It appears to be quite abundant in the limestone hills based on the high numbers collected in our samplings.

Remarks. *Phaedusa shanica* is very similar to *P. theobaldi* (Blanford, 1872) in having two or three palatal plicae which tend to connect at the second and third plicae. *Phaedusa theobaldi* (Fig. 19M) can be distinguished by its less turreted shell, coarser striations, darker horny color, superior lamella and spiralis separated, and not emerged subcolumellaris. These two species are difficult to distinguish at first sight; additional materials from the type locality and the genitalia of *P. theobaldi*, are required to elucidate the relationship between these two species.

Our specimens slightly differ from the type specimen in having three separated palatal plicae, or sometimes second and third plicae well developed and connected (Fig. 4B). According to Nordsieck's (1974: fig. 6) drawing, the lectotype SMF 62260 has only two almost connected first and second palatal plicae, while the probable paralectotype as stated in Gude (1914: fig. 112) has palatal plicae pattern similar to the specimens examined herein. Therefore, we assume that the distinct or indistinct second plica might be attributed to morphological variation. Shell variations among the examined materials for *P. shanica* were observed, including slender to regular fusiform shell, oblique to subquadrate aperture, and the third plica may be well developed and reach to the second plica (Fig. 4B).

In addition, *Phaedusa lypra* (Mabille, 1887) from Shan State also resembles this species in shell form; however, *P. lypra* has a blunter spire, less turreted shell, and wider

aperture sinus (Szekeres et al. 2021a: fig. 10f). *Phaedusa burmanica* (Gude, 1914) and *P. bocki menglunanensis* (Luo, Cheng & Zhang, 1998) from Shan State differ from *P. shanica* in having a larger shell, five distinct palatal plicae that can be seen from outside of shell, wavier and coarser shell surface, and clausilium with a hook (Fig. 4). Regarding the genitalia, *P. shanica* possesses more simple and smooth longitudinal folds and reticulated papillae in the epiphallus, while *P. burmanica* has strongly wavy, irregularly dense, and crowded longitudinal folds along the epiphallus with a distinct fold near the vas deferens (Fig. 5).

2 *Phaedusa burmanica* (Gude, 1914)
Figs 4C, D, 5E–G, 6B, 18F; Tables 2, 3

Clausilia [*Phaedusa* (*Euphaedusa*)] *burmanica* Gude, 1914: 311, fig. 106. Type locality: "Burma, Tonghu" [Taungoo District, Bago Region, Myanmar].
Phaedusa (*Phaedusa*) *burmanica*–Nordsieck 2002b: 88. Nordsieck 2007: 32.
Phaedusa burmanica–Nordsieck 1974: 46, fig. 5, pl. 2, figs 3, 4. Grego et al. 2021: 27. Szekeres et al. 2021a: 181, fig. 10a.

Material examined. Myin Ma Hti Cave, Kalaw City, Shan State, Myanmar (20°35'26.1"N, 96°36'42.6"E): CUMZ 13034 (2 shells + 1 incomplete shell; Fig. 4C, D), CUMZ 13035 (1 specimen in ethanol).

Description. Shell fusiform, turreted, translucent, and pale chestnut-brown; spire acute. Shell surface glossy with thin and dense striations; suture distinct. Whorls 12–13, little convex, regularly growing and attenuated to apex; last whorl compressed. Aperture vertically subquadrate, basis rounded and narrowing towards parietal sinus; peristome slightly protruded, thickened, and expanded. Superior lamella low, continuous with spiralis, and very low at transition to spiralis. Inferior lamella spirally ascending, close to superior lamella and ending at peristome. Subcolumellaris emerged, and visible in oblique view. Principalis running along lateral-dorsal side and anterior end visible through oblique apertural view. Palatal plicae lateral, distinctly five: first plica strong, longest, and nearly connected to principalis anteriorly; second and fifth plicae almost equal and slightly strong; third and fourth plicae weakest and almost not visible. Palatal plicae visible through translucent shell. Clausilium plate lateral side, broad, rounded and with hook.

Genitalia (*n* = 1). Atrium (at) short and slender; penis (p) muscular, cylindrical, broadest at middle part and gradually narrower towards epiphallus. Epiphallus (ep) muscular, cylindrical, ca. same length and size as penis, gradually enlarging to proximal end. Penial retractor muscle (pr) attached proximally to epiphallus. Vas deferens (vd) slender, and shortly bounded at atrium and penis junction (Fig. 5E). Internal sculpture of penis smooth-surfaced and slightly wavy with ca. four longitudinal folds (Fig. 5F). Internal sculpture of epiphallus generally defined as two parts: region near penis with wavy longitudinal folds, then gradually becoming more densely crowded

towards proximal epiphallus; region near vas deferens with strong folds and papillae arranged in oblique rows (Fig. 5G).

Vagina (v) slender at junction of atrium, then bulging at connection of free oviduct (fo) and distal part of pedunculus (dpb), and almost as long as free oviduct. Distal part of pedunculus large, long, basally stouter, and broadest near entrance of diverticulum; diverticulum (db) large, as long as dpb; proximal part of pedunculus (ppb) large, measuring ~ 1/2 diverticulum length, and bursa copulatrix (bb) ovoid (Fig. 5E).

***Radula*.** Each row contains ~ 51 teeth with half-row formula: central–(lateral)–marginal teeth (1–(13–14)–25). Central tooth small, symmetrically tricuspid; mesocone large with dull tip; ectocones very small. Lateral teeth asymmetrically bicuspid: endocone large and with dull tip; ectocone very small, pointed tip and located near the base. Marginal teeth tricuspid starting at approximately tooth number 13 or 14; mesocone long and dull tip; endocone very small and located near tip of mesocone; ectocone small with pointed tip. Marginal teeth gradually becoming polycuspid towards radula margin (Fig. 6B).

Distribution. Apart from the type locality, this species is widely known from Bhamo, Kachin State (Gude 1914) to Shan State and the Mandalay Region in Myanmar (Grego et al. 2021).

Remarks. *Phaedusa bocki menglunanensis* from Shan State can be distinguished from this species by its inferior lamella less spirally ascending, palatal plicae longer, obliquely arranged and more spaced between them, shell surface finer and more curved striations, aperture vertically quadrate, and subcolumellaris distinctly visible in frontal view. *Phaedusa bocki thompsoni* Grego & Szekeres, 2021 also differs from this species in having a more vertical aperture, acute spire, and palatal plicae more on dorsal side (see Szekeres et al. 2021a: fig. 9f).

Variation was observed among the examined specimens in having the superior lamella and spiralis either separated or connected.

3 *Phaedusa bocki menglunanensis* (Luo, Chen & Zhang, 1998)

Figs 4E, F, 19E; Table 2

Hemiphaedusa menglunanensis Luo et al., 1998: 34, fig. 2. Type locality: Menglun, Mengla County, Xishuangbanna Prefecture, Yunnan Province, China. Chen and Zhang 1999: 162, pl. 5, fig. 1a, b. Chen et al. 2016: 111, fig. 2–52a.

Phaedusa (*Phaedusa*) *bocki menglunanensis*–Nordsieck 2007: 32.

Phaedusa bocki menglunanensis–Szekeres et al. 2021a: 180, 181, fig. 9e. Szekeres et al. 2021b: 46.

Material examined. Aik Kham Cave, Taunggyi City, Shan State, Myanmar (20°49'7.0"N, 97°13'42.0"E): CUMZ 13036 (3 incomplete shells, Fig. 4E, F).

Description. Shell fusiform, translucent, and pale yellowish brown; spire regularly acute. Shell surface with fine and coarse striations; suture wide and distinct. Whorls

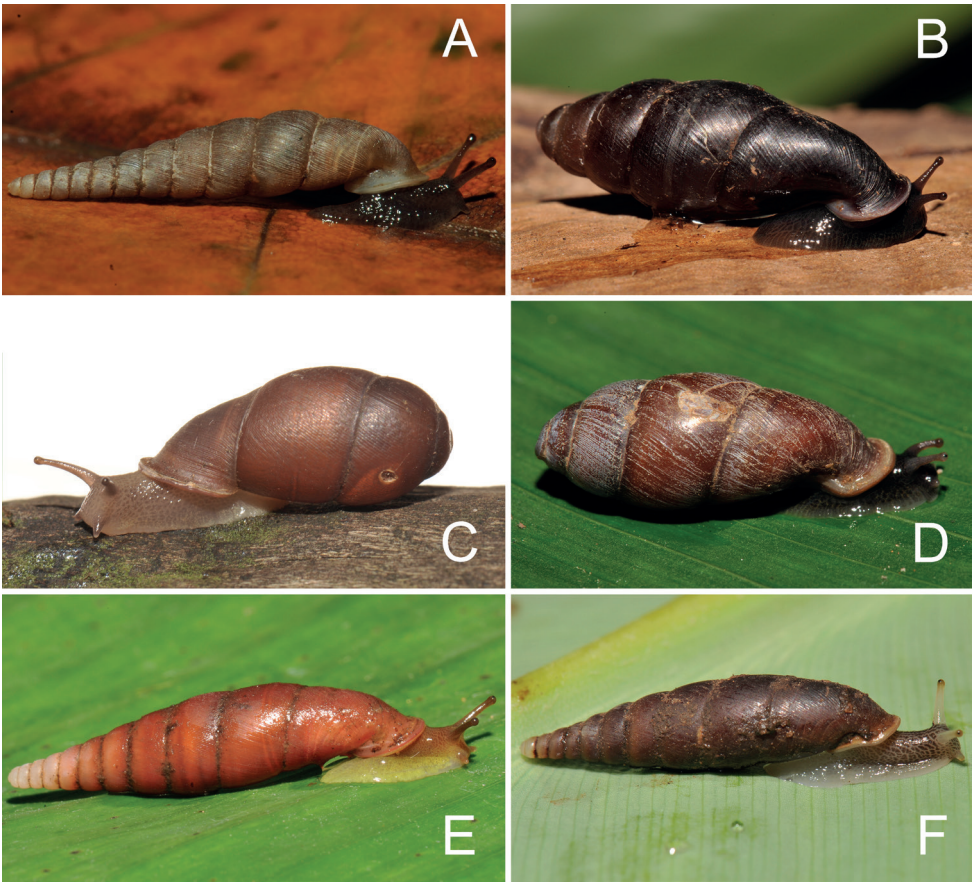

Figure 3. Living snails **A** *Phaedusa shanica* from Pyinyaung Village, Mandalay Region (SH ~ 14 mm) **B** *Oospira philippiana* from Kayon Cave, Mon State (SH ~ 22 mm) **C** *Oospira bulbus* from Sanbel Cave, Mon State (SH ~ 19 mm) **D** *Oospira ovata* from Pathein Mountain, Mon State (SH ~ 16 mm) **E** *Oospira gouldiana* from Kaw Ka Thuang Cave, Kayin State (SH ~ 26 mm) **F** *Oospira shanensis* from Nanthe Cave, Shan State (SH ~ 25 mm).

12 and 13 nearly flattened, regularly increasing, and attenuated to apex. Aperture vertically subquadrate, basis rounded and narrowing towards parietal sinus; peristome protruded, expanded and little reflexed. Superior lamella low, continuous with spiralis, and low at transition to spiralis. Inferior lamella spirally ascending, slightly horizontal before reaching peristome and close to superior lamella. Subcolumellaris emerged, ending at peristome margin, and clearly visible in frontal view. Principalis running along lateral-dorsal side and anterior end visible through oblique apertural view. Palatal plicae lateral, four or five: first plica distinct, longest, and nearly connected to principalis anteriorly; second plica ~ 1/2 of first plica length and remaining plicae oblique, equally spaced, and shorter. Palatal plicae visible through translucent shell. Clausilium plate lateral side, broad, rounded, and with hook.

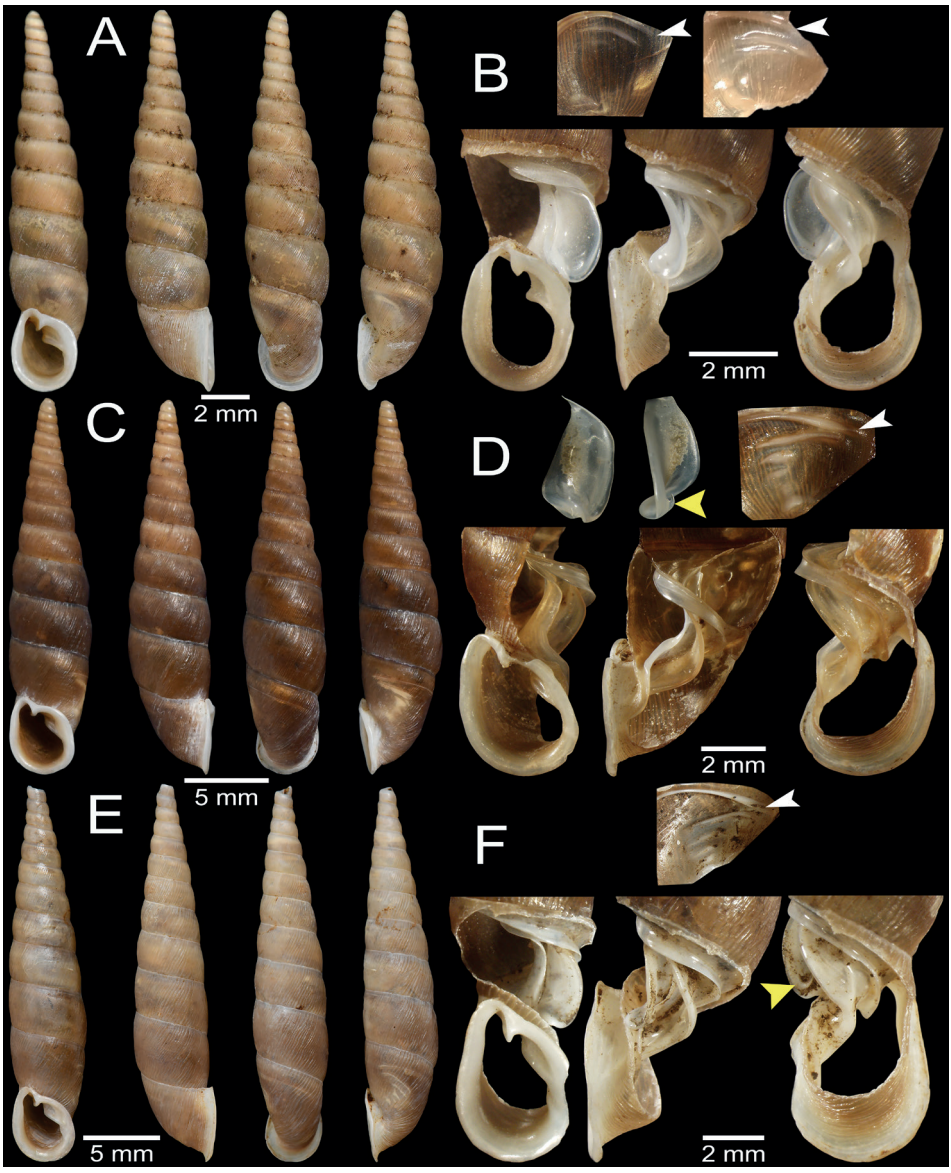

Figure 4. Shell and clausilial apparatus of **A, B** *Phaedusa shanica*, specimen CUMZ 13032 from Pyinyaung Village, Mandalay Region **A** shell **B** clausilial apparatus **C, D** *Phaedusa burmanica*, specimen CUMZ 13034 from Myin Ma Hti Cave, Shan State **C** shell **D** clausilial apparatus and **E, F** *Phaedusa bocki menglunanensis*, specimen CUMZ 13036 from Aik Kham Cave, Shan State **E** shell **F** clausilial apparatus. White arrows indicate principalis and yellow arrows indicate clausilium hook.

Distribution. *Phaedusa bocki menglunanensis* was originally described from Yunnan Province, China, which is near the borders with Vietnam and Laos. It was recently found in Shan State, along the Mekong River near the border with Laos (Szekeres et al. 2021a).

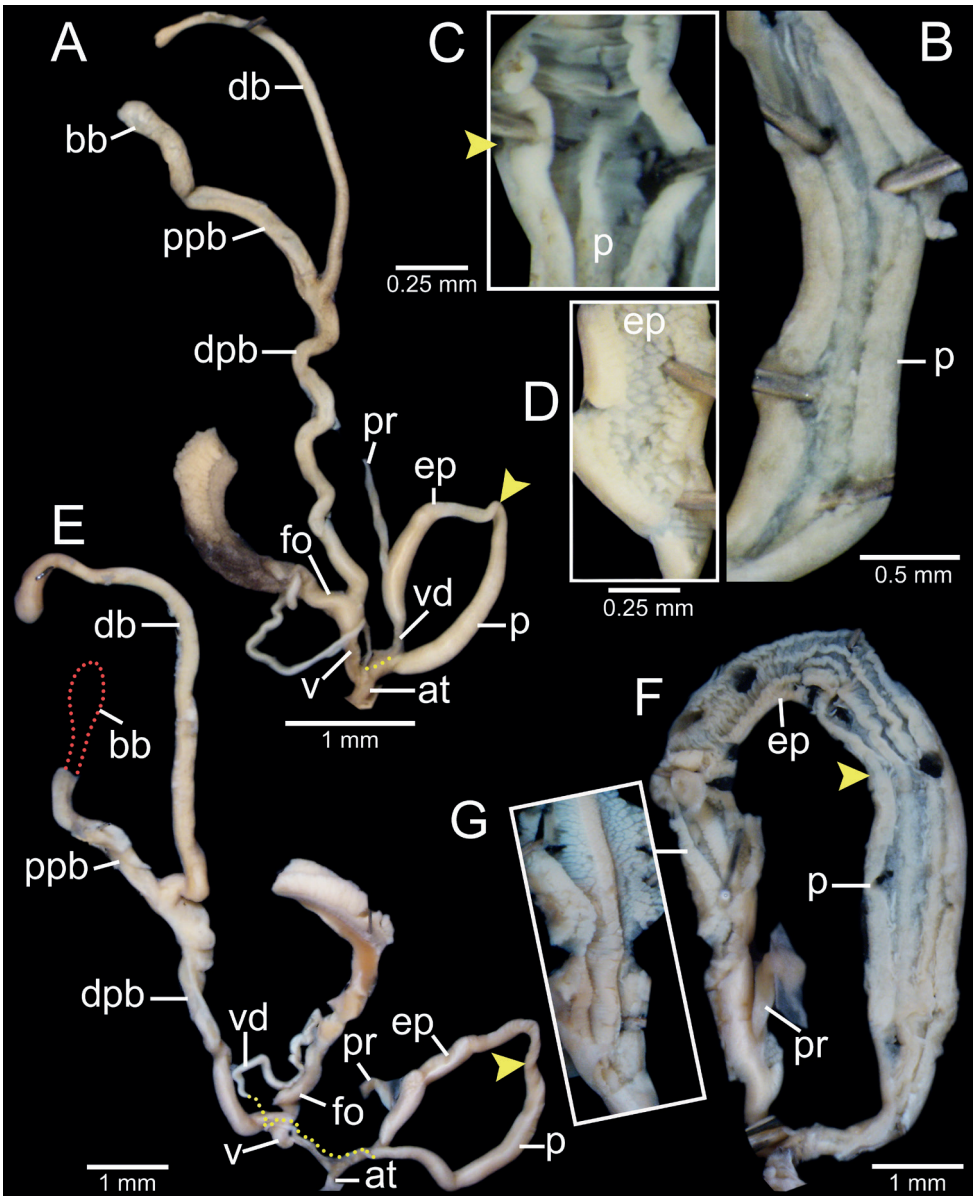

Figure 5. Genital anatomy of **A–D** *Phaedusa shanica*, specimen CUMZ 13033 **A** whole reproductive system **B** internal sculpture of penis **C** transition from penis to epiphallus **D** internal sculpture of epiphallus and **E–G** *Phaedusa burmanica*, specimen CUMZ 13035 **E** whole reproductive system **F** overview internal sculpture of penis and epiphallus **G** internal sculpture of proximal epiphallus. Yellow arrows indicate approximate transitional position from penis to epiphallus.

Remarks. No preserved specimens were found for examination of the genitalia. This subspecies and samples of *P. bocki thompsoni* collected from the same geographical range have a similar shell morphology, but *P. bocki thompsoni* has invisible subcolu-

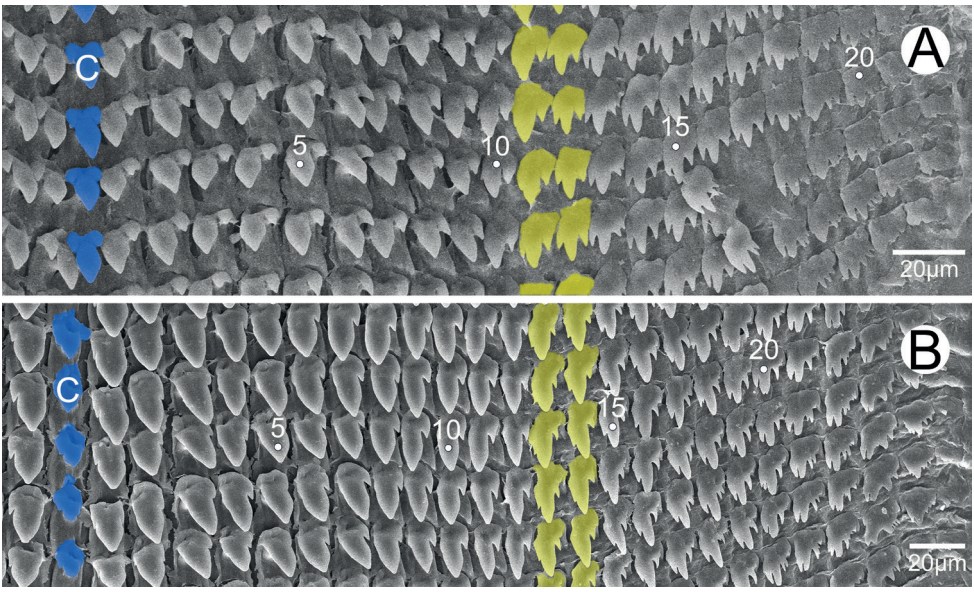

Figure 6. Radula morphology **A** *Phaedusa shanica*, specimen CUMZ 13033 and **B** *Phaedusa burmanica*, specimen CUMZ 13035. Blue color indicates the central teeth row; yellow color indicates the transition from lateral to marginal teeth. 'C' indicates central tooth.

mellaris in frontal view, blunter and turreted spire, and whorls after antepenultimate whorl rapidly attenuated (see Szekeres et al. 2021a: fig. 9f). However, the holotype of *P. bocki thompsoni* from Thailand possesses a subcolumellaris that is visible in frontal view, and four to seven plicae that become shorter and somewhat diffuse towards the base (Szekeres et al. 2021b: fig. 2d). More materials are required for comparison to determine whether the differentiating characters are consistently distinct between these two subspecies.

Genus *Oospira* Blanford, 1872

Clausilia (*Oospira*) Blanford, 1872: 205. Boettger 1877: 64. Gude 1914: 332.
Phaedusa (*Oospira*)–Zilch 1959: 389, 390.
Oospira–Schileyko 2000: 581. Nordsieck 2002b: 86. Nordsieck 2007: 23.

Type species. *Clausilia philippiana* Pfeiffer, 1847, by original designation.

Diagnosis. Shell short to long fusiform, shell surface smooth to with striated ridges, spire blunt to attenuated, whorls few to numerous (6–13). Palatal plicae short to long, mostly developed and 3–10 in number. Superior lamella developed, usually connected to spiralis, distinct or indistinct at transition to spiralis. Inferior lamella

steeply ascending and somewhat ending distant from superior lamella in aperture view. Subcolumellaris usually invisible in frontal view; clausilium plate lateral to ventral side and usually narrow.

External features. Living animals possess reticulated skin; dark gray head; short tentacles; body and tail pale to dark brownish; foot moderately elongated, posterior nearly rounded to bluntly pointed.

Remarks. *Oospira* is the most species-rich genus of the Phaedusinae, and more than a hundred species have been reported from a broad range in Southeast Asia (MolluscaBase 2022). Nordsieck (2002b) united two previously recognized genera, *Acrophaedusa* Boettger, 1877 and *Pseudonenia* Boettger, 1877 to form *Oospira* based on their shared steeply ascending inferior lamella, normal clausilium plate, and mostly palatal plicae form. Perhaps this grouping causes *Oospira* to become widely diverged in shell shape from ovate to fusiform, dark brown to pink, and different aperture shapes which is thought to be a homoplasy. A phylogenetic analysis of phaedusinids genera from Japanese and some southeast Asian taxa, especially from Vietnam, was not in line with traditional taxonomy probably due to parallel or convergent evolution (Motochin et al. 2017; Mamos et al. 2021). However, none of the Indochinese taxa, including *Oospira*, were explored in this phylogenetic work.

The genera *Loosjesia* from Thailand, *Messageriella* Páll-Gergely & Szekeres, 2017 and *Castanophaedusa* Páll-Gergely & Szekeres, 2017 from Vietnam, *Musaphaedusa* Nordsieck, 2018 from Laos, and *Oospira* have a similar shell morphology, especially in the form of the palatal plicae. However, *Loosjesia* can readily be differentiated by its predominantly curved basal inferior lamella with a long transverse palatal plica and clearly visible subcolumellaris (Loosjes 1953; Nordsieck 2002b). *Messageriella* is distinguished by its marginally ending inferior lamella and subcolumellaris, palatal plicae non-parallel and ventral (Páll-Gergely and Szekeres 2017); similarly, *Castanophaedusa* has a rhomboidal aperture which extends to the columellar side and sharply bent basis, marginal and strongly emerged subcolumellaris, palatal plicae ventral and parallel to the principalis (Páll-Gergely and Szekeres 2017). Meanwhile, *Musaphaedusa* has strong sutural papillae, principalis very long, palatal plicae ventral (only two) and strong rib-like striations on the shell surface (Nordsieck 2018).

Regarding the reproductive anatomy of this group, *Oospira penangensis* (Stoliczka, 1873) and *O. philippiana* were the first species examined for their genitalia (Stoliczka 1871, 1873). At present, seven species (including *O. decollata* and *O. malaisei* from Myanmar) have been investigated (Loosjes 1953; Likharev 1962; Nordsieck 1973; Maassen and Gittenberger 2007; Páll-Gergely and Szekeres 2017).

Based on shell morphology, we have divided *Oospira* from Myanmar into two species groups comprised of those with (i) short and ovate fusiform shells and (ii) long and slender fusiform shells. The short and ovate fusiform group includes the species believed to be *Oospira* s.s. (type species *Clausilia philippiana* Pfeiffer, 1847), while the long and slender fusiform group assumed to be the species previously known as '*Pseudonenia* Boettger, 1877' (type species *Clausilia javana* Pfeiffer, 1841).

Oospira species group with short and ovate fusiform shell

In Myanmar, this group is comprised of five species, four of which were collected and examined, while *O. vespa* (Gould, 1856) was not.

4 *Oospira philippiana* (Pfeiffer, 1847)

Figs 2, 3B, 7A–C, 8A–C, 15A, 19H; Tables 2, 3

Clausilia philippiana Pfeiffer, 1847: 69. Type locality: "Mergui in imperio Birmanorum" [near Myeik, Tanintharyi Region, Myanmar]. Küster 1850: 100, pl. 11, figs 7–9. Pfeiffer 1868: 409. Hanley and Theobald 1874: 48, pl. 118, fig. 10. Sowerby 1875: *Clausilia* pl. 4, species 35.

Clausilia (*Phaedusa*) *philippiana*–Adams and Adams 1855: 184. Pfeiffer 1856: 180. Martens 1860: 275. Stoliczka 1871: 174, pl. 6, figs 7−10.

Clausilia (*Oospira*) *philippiana*–Blanford 1872: 205, pl. 9, fig. 14. Nevill 1878: 182. Kobelt 1880: 289, pl. 86, fig. 29. Pfeiffer and Clessin 1881: 392. Tapparone-Canefri 1889: 329. Gude 1914: 333.

Clausilia [*Phaedusa* (*Oospira*)] *philippiana*–Boettger 1878: 56.

Oospira (*Oospira*) *philippiana*–Nordsieck 2002b: 86. Nordsieck 2007: 24.

Oospira philippiana–Nordsieck 2021: 52, pl. 1, fig. 8. Szekeres et al. 2021a: 175, fig. 8c. Szekeres et al. 2021b: 45.

Material examined. Possible syntype SMF 62294/1 ex. H. Dohrn collection from Burma: [Mergui] (Fig. 7A). Saddan Cave, ~ 600 m south of Kayon Cave, Mawlamyine Township, Mawlamyine District, Mon State, Myanmar (16°31'42.8"N, 97°43'2.1"E): CUMZ 13037 (10 adults + 5 juveniles, Fig. 7C). Kayon Cave [formerly called Farm Caves] ~ 10 km from Mawlamyine Township, Mawlamyine District, Mon State, Myanmar (16°32'0.5"N, 97°42'53.5"E): CUMZ 13038 (6 shells; Fig. 2), CUMZ 13039 (15 specimens in ethanol). Pha Boang Cave from Mawlamyine Township, Mawlamyine District, Mon State, Myanmar (16°17'14.04"N, 97°54'4.28"E): CUMZ 13040 (9 adults + 9 juveniles, Fig. 7B), CUMZ 13041 (15 specimens in ethanol).

Description. Shell ovate-fusiform, opaque, and chestnut-brown color; spire blunt. Shell surface nearly smooth or with very thin striations; suture distinct. Whorls 5–6½, convex, regularly growing and bluntly attenuated to apex. Aperture obliquely pear-shaped, basis broader and narrowing towards parietal sinus; peristome detached, thickened, expanded and little reflexed. Superior lamella developed, continuous with spiralis, and low at transition to spiralis. Inferior lamella steeply ascending, distant from superior lamella and ending at peristome. Subcolumellaris emerged, and only visible in oblique view. Principalis running along lateral-dorsal side and anterior end visible through oblique apertural view. Palatal plicae lateral, 7–9: first plica strong and longest; following plicae shorter, parallel, nearly equal in length, gradually reduced towards anterior. Clausilium plate lateral side, slightly broad and rounded at tip.

Table 2. Comparison of shell characters of all species from Myanmar examined in this study.

Species	Inferior lamella	Transition from superior to spiralis lamella	Subcolumellaris in oblique view	Palatal plicae number/ positions	Clausilium position / shape	Spire
P. shanica	spirally ascending	connect to almost separate	visible	3/ 2nd weakest and lateral	lateral/ broad and round	regularly attenuated
P. burmanica	spirally ascending	connect or separate	visible	5/ 3rd and 4th weakest and lateral	lateral/ broad, round and with hook	regularly attenuated
P. bocki menglunanensis	spirally ascending	connect / low at transition to spiralis	visible	4–5/ reduced towards anterior and lateral	lateral/ broad, round and with hook	regularly attenuated
O. philippiana	steeply ascending	connected / distinctly low at transition to spiralis	visible	7–9/ reduced towards anterior and lateral	lateral/ slightly broad	blunt and regularly attenuated
O. bulbus	steeply ascending	connected / distinctly low at transition to spiralis	invisible	5/ nearly equal, reduced towards anterior and lateral	lateral/ narrow	round and rapidly grow
O. ovata	steeply ascending	connected / distinctly low at transition to spiralis	visible	6–7/ gradually reduced towards anterior and lateral	lateral/ narrow	blunt and rapidly grow
O. stoliczkana	steeply ascending	connected / distinctly low at transition to spiralis	visible	8–10/ gradually reduced towards anterior and lateral	lateral/ slightly broad	blunt and regularly attenuated
O. gouldiana	steeply ascending	connected / slightly low at transition to spiralis	invisible	5/ 1st and 4th or 5th longest, parallelly, or irregularly oblique, and lateral	lateral/ narrow	regularly attenuated, 3 to 4 apical whorls white
O. andersoniana	steeply ascending	connected / indistinct at transition to spiralis	invisible	3–5 / 3rd longest, parallelly oblique, and lateral	lateral/ narrow	regularly attenuated
O. magna	steeply ascending	connected / indistinct at transition to spiralis	invisible	4–6 / 4th longest, parallelly oblique, and ventral-lateral (almost horizontal)	ventral/ narrow	regularly attenuated, 3 to 4 apical whorls white
O. shanensis	steeply ascending	connected / indistinct at transition to spiralis	visible	5 / 4th longest and curved, parallel, and ventral-lateral (almost horizontal)	lateral/ broad, round and with hook	regularly attenuated
O. luneainopsis sp. nov.	steeply ascending	connected / slightly low at transition to spiralis	invisible	4 / 4th longest, parallelly oblique, and lateral	lateral/ narrow, slightly pointed at tip	blunt and regularly attenuated
O. zediopsis sp. nov.	steeply ascending	connected / slightly low at transition to spiralis	invisible	4–5 / 4th longest, parallelly oblique, and lateral	lateral/ narrow	regularly attenuated, 4 to 5 apical whorls white

***Genitalia* (*n* = 5).** Atrium (at) short and slender; penis (p) muscular and cylindrical. Epiphallus (ep) muscular, cylindrical, ca. same length and half of the diameter of penis and broadest at middle part. Penial retractor muscle (pr) attaches proximally to epiphallus. Vas deferens (vd) slender, and shortly bounded at atrium and penis junction (Fig. 8A). Internal sculpture of penis consists of two parts: region near atrium ~ 1/3 of penis length with series of irregular transverse folds, chevron-shaped; region near epiphallus becoming smooth surface and relatively thick with 5–7 longitudinal folds (Fig. 8B). Internal sculpture of epiphallus with elevated papillae arranged in oblique rows (Fig. 8C).

Vagina (v) thick and very short, ~ 1/3 of free oviduct (fo) length. Distal part of pedunculus (dpb) large and long; diverticulum (db) long, ~ 2× length and slightly larger diameter than dpb; proximal part of pedunculus (ppb) slender, ca. equal in length to diverticulum, and bursa copulatrix (bb) with distinct ovate shape (Fig. 8A).

Table 3. Comparison of genital characters of all species from Myanmar examined in this study.

Species	Penis / epiphallus	Internal sculpture of penis	Internal sculpture of epiphallus	Distal and proximal lengths of pedunculus
P. shanica	muscular, large / ca. same diameter with penis	smooth surface of longitudinal folds	papillae arranged in oblique rows	distal longer than proximal
P. burmanica	muscular, large / ca. same diameter with penis	wavy surface of longitudinal folds	wavy longitudinal folds and papillae arranged in oblique rows	distal longer than proximal
O. philippiana	muscular, large / narrower than penis	chevron-shaped and smooth surface of longitudinal folds	elevated papillae arranged in oblique rows	distal shorter than proximal
O. bulbus	muscular, large / narrower than penis	chevron-shaped and little wavy surface of longitudinal folds	elevated papillae arranged in oblique rows	distal ca. same as proximal
O. ovata	muscular, large / narrower than penis	V-shaped rows and smooth surface of longitudinal folds	rounded papillae arranged in oblique rows	distal longer than proximal
O. stoliczkana	muscular, large / narrower than penis	nearly V-shaped and oblique smooth surface of longitudinal folds	elevated papillae arranged in nearly oblique rows	distal longer than proximal
O. gouldiana	moderately muscular, slender / nearly same or narrower diameter than penis	smooth surface of longitudinal folds	irregular corrugated folds and papillae arranged in oblique rows	distal ca. same as proximal
O. andersoniana	moderately muscular, slender / nearly same or narrower diameter than penis	smooth surface of longitudinal folds	scattered papillae arranged obliquely to irregularly spaced rows	distal longer than proximal
O. magna	moderately muscular, slender / nearly equal diameter with penis	smooth surface of longitudinal folds	papillae arranged in oblique rows	distal shorter than proximal
O. shanensis	muscular, large / ca. same diameter with penis	corrugated surface of longitudinal folds	reticulated pattern	distal longer than proximal

***Radula*.** Each row contains ≥ 39 teeth with half-row formula: central–(lateral)–marginal teeth (1–(11–12)–19+). Central tooth unicuspid with rounded to blunt tip. Lateral teeth bicuspid: endocone large and rounded tip; ectocone very small, pointed tip and located near the base. Marginal teeth asymmetrically tricuspid starting at approximately tooth number 11 or 12: mesocone large and curved to blunt tip; endocone small and located near tip of mesocone; ectocone triangular, pointed tip and located near the base. Outermost teeth have been lost during the preparation process (Fig. 15A).

Distribution. In Myanmar, this species is reported from Kayin, Mon and Tanintharyi (Gude 1914; Szekeres et al. 2021a, b). In addition, the records outside Myanmar are from Kanchanaburi Province, Thailand (Szekeres et al. 2021b), and further in Andaman Islands, but mentioned as dubious record (see Szekeres et al. 2021a: 177). In this survey, three populations were collected from isolated limestone karsts in Salween River Basin with relatively high abundance.

Remarks. *Oospira stoliczkana* can be distinguished from *O. philippiana* by its elongate ovoid shell, pale color, and higher numbers of plicae. In terms of the genital organs, the male internal sculpture of *O. philippiana* has thicker and denser corrugated folds near the atrium than in *O. stoliczkana* (Fig. 10F). Moreover, *O. vespa* can be differentiated from this species by having an acute spire, aperture more oblique and broader, whorls more expanded.

Among the examined specimens, those from the Pha Boang Cave population (24 shells) have larger and darker shells with more widely spaced and up to nine developed palatal plicae. In contrast, specimens from the Kayon Cave (21 shells) and Saddan

Cave (15 shells) populations are uniform in terms of a smaller shell and seven closer and weaker plicae (Table 1).

No specimens were found at the type locality 'Mergui' [Myeik]; but Szekeres et al. (2021b) reported material from Tanintharyi Region. Instead, multiple populations with high abundance were collected in the vicinity of Salween River Basin in this present study (Fig. 1; Table 1). This agreed with Stoliczka's (1871: 175) statement that the species was 'common at the Farm-caves near Moulmein on limestone hills'.

5 *Oospira bulbus* (Benson, 1863)
Figs 3C, 7D–F, 8D–F, 18E; Tables 2, 3

Clausilia bulbus Benson, 1863: 321. Type locality: "ad ripas fluvii Attaran, non procul ab urbe Moulmein" [banks of Attaran River, Mawlamyine, Mon State, Myanmar]. Pfeiffer 1868: 409. Hanley and Theobald 1870: 12, pl. 24, fig. 5. Sowerby 1875: *Clausilia* pl. 6, species 51.
Clausilia (*Oospira*) *bulbus*–Blanford 1872: 206, pl. 9, fig. 16. Gude 1914: 332.
Clausilia [*Phaedusa* (*Oospira*)] *bulbus*–Boettger 1878: 56.
Oospira (*Oospira*) *bulbus*–Nordsieck 2002b: 86. Nordsieck 2007: 23. Preece et al. 2022: 162, fig. 72e.
Oospira bulbus–Szekeres et al. 2021a: 168, fig. 5c, d.

Material examined. Sanbel Cave, Mawlamyine Township, Mon State, Myanmar (16°22'26.0"N, 97°46'22.6"E): CUMZ 13042 (15 shells; 7D–F), CUMZ 13043 (3 specimens in ethanol), JG-C2882 (1 shell).

Description. Shell oblong-ovate, translucent, and brownish; spire rounded and almost flatted to apex. Shell surface with fine and distinct striations; suture wide and distinct. Whorls 5–5½; penultimate whorl rapidly growing and largest; last whorl compressed and narrower. Aperture obliquely pear-shaped, basis rounded and narrowing towards parietal sinus; peristome detached, thickened, slightly expanded, and not reflexed. Superior lamella sharp, oblique, continuous with spiralis, and low at transition to spiralis. Inferior lamella steeply ascending, distant from superior lamella and ending at peristome. Subcolumellaris emerged and invisible in oblique view. Principalis running along lateral-dorsal side and anterior end visible through oblique apertural view. Palatal plicae lateral, five: first plica longest; following four plicae parallel, equal in length and spacing, and slightly reduced towards anterior. Clausilium plate lateral side and narrow.

Genitalia (*n* = 2). Atrium (at) short and slender; penis (p) muscular and cylindrical. Epiphallus (ep) muscular, cylindrical, ca. same length and half diameter of penis, and broadest at middle part. Penial retractor muscle (pr) attaches proximally to epiphallus. Vas deferens (vd) slender, and shortly bounded at atrium and penis junction (Fig. 8D). Internal sculpture of penis consists of two parts: region near atrium and ~ 1/2 of penis length with series of irregular transverse folds, chevron-shaped;

region near epiphallus becoming smooth, with 5–7 slightly wavy longitudinal folds (Fig. 8E). Internal sculpture of epiphallus with elevated papillae arranged in oblique rows (Fig. 8F).

Vagina (v) thick and short, ~ 1/2 of free oviduct (fo) length. Distal part of pedunculus (dpb) large and long; diverticulum (db) long, ~ 2× in length and slightly smaller in diameter than dpb; proximal part of pedunculus (ppb) slender, ca. equal in length to diverticulum and bursa copulatrix (bb) with distinct ovate shape (Fig. 8D).

Distribution. *Oospira bulbus* has only been reported from Myanmar and is possibly endemic in the limestone hills along the lower course of Attaran River. The specimens examined herein were collected near the type locality.

Remarks. *Oospira ovata* can be separated from this species by its a smoother striated shell, attenuated spire and usually seven plicae. In terms of the genital organs, the male internal sculpture of *O. ovata* has longer V-shaped folds in the region near the atrium and rounded papillae in epiphallus than this species. Although *O. bulbus* has a similar shell form to *Atractophaedus pyknosoma* (Gittenberger & Vermeulen, 2001) from Vietnam, *A. pyknosoma* has a narrower spire, visible subcolumellaris in frontal view, peristome reflected with nearly double lip and first palatal plicae shorter than the following plicae (see Gittenberger and Vermeulen 2001: figs 1–10).

6 *Oospira ovata* (Blanford, 1872)

Figs 3D, 9A–C, 10A–D, 15B, 19G; Tables 2, 3

Clausilia (*Oospira*) *ovata* Blanford, 1872: 206, pl. 9, fig. 17. Type locality: "Ad Nattoung, juxta ripam Attaran fluminis, haud procul a Moulmain in Barma" [Shwe Nat Taung, Mawlamyine, Mon State, Myanmar]. Nevill 1878: 183. Gude 1914: 334.
Clausilia ovata–Hanley and Theobald 1874: 48, pl. 118, fig. 4. Sowerby 1875: *Clausilia* pl. 7, species 60. Pfeiffer 1877: 469.
Clausilia [*Phaedusa* (*Oospira*)] *ovata*–Boettger 1878: 56.
Oospira (*Oospira*) *ovata*–Nordsieck 2002b: 86. Nordsieck 2007: 24.
Oospira ovata–Szekeres et al. 2021a: 175, 176, fig. 8a, b.

Material examined. Pathein Mountain, Mawlamyine Township, Mon State, Myanmar (16°14'7.5"N, 97°56'48.1"E): CUMZ 13044 (25 shells, Fig. 9A–C), CUMZ 13045 (1 specimen in ethanol), JG-C2883 (2 shells).

Description. Shell ovate or pupiform, opaque and chestnut-brown; spire blunt. Shell surface nearly smooth or with very thin growth lines; suture distinct. Whorls 5–5½ convex, rapidly growing; penultimate and antepenultimate whorls equally broad and rounded to apex. Aperture obliquely pear-shaped, basis rounded and narrowing towards parietal sinus; peristome detached, thickened, expanded and little reflexed. Superior lamella well developed, continuous with spiralis and low at transition to spiralis. Inferior lamella steeply ascending, distant from superior lamella and ending at

peristome. Subcolumellaris emerged and only visible in oblique view. Principalis running along lateral-dorsal side and anterior end visible through oblique apertural view. Palatal plicae lateral, six or seven: first plica strong and longest; following plicae short, parallel, equal in length and gradually reduced towards anterior. Clausilium plate lateral side and narrow.

Genitalia (*n* = 1). Atrium (at) short and slender; penis (p) muscular and cylindrical. Epiphallus (ep) muscular, cylindrical, ~ 1.5× diameter of penis, and broadest close to penis. Penial retractor muscle (pr) attaches proximally to epiphallus. Vas deferens (vd) slender and shortly bounded at atrium and penis junction (Fig. 10A). Internal sculpture of penis consists of two parts: region near atrium, ~ 2/3 of penis length with moderately thick transverse folds arranged in V-shaped rows; region near epiphallus with smooth surface and four or five longitudinal folds (Fig. 10B, C). Internal sculpture of epiphallus with rounded papillae arranged in oblique rows (Fig. 10D).

Vagina (v) thick, short, and almost half of free oviduct (fo) length. Distal part of pedunculus (dpb) large and long; diverticulum (db) large, slightly longer, and larger in diameter than dpb; proximal part of pedunculus (ppb) slender, ~ 2/3 diverticulum length and bursa copulatrix (bb) with distinct ovate shape (Fig. 10A).

***Radula*.** Each row contains ~ 61 teeth with half-row formula: central–(lateral)–marginal teeth (1–(12–13)–26). Central tooth unicuspid with dull tip. Lateral teeth bicuspid; endocone large with curved to dull tip; ectocone very tiny to small and pointed tip. Marginal teeth asymmetrically tricuspid starting at approximately tooth number 12 or 13: mesocone large and dull tip; ectocone and endocone small with pointed tips. Outer marginal teeth increasingly asymmetrical and shorter than inner marginal teeth (Fig. 15B).

Distribution. At present, *O. ovata* is only known from Myanmar. Many shells were collected in this study; it is likely endemic to the valley of Attaran River.

Remarks. *Oospira ovata* and *O. philippiana* are generally similar in shell morphology, but *O. ovata* has a more expanded spire. The male internal sculpture of *O. ovata* has longer V-shaped folds in the region near the atrium and rounded papillae pattern in epiphallus, whereas *O. philippiana* has shorter V-shaped folds and more elevated and pointed papillae in epiphallus.

7 *Oospira stoliczkana* (Sykes, 1893)

Figs 9D–F, 10E–H, 19L; Tables 2, 3

Clausilia vespa–Stoliczka 1872: 209, pl. 9, fig. 15a. (non Gould, 1856)
Clausilia vespa–Pfeiffer 1877: 468 (in part).
Clausilia (*Oospira*) *stoliczkana* Sykes, 1893: 166. Type locality: "Tavoy, Burmah" [Dawei, Tanintharyi Region, Myanmar]. Gude 1914: 335.
Oospira (*Oospira*) *stoliczkana*–Nordsieck 2002b: 86. Nordsieck 2007: 24.
Oospira stoliczkana–Szekeres et al. 2021a: 178, 179, fig. 9a.

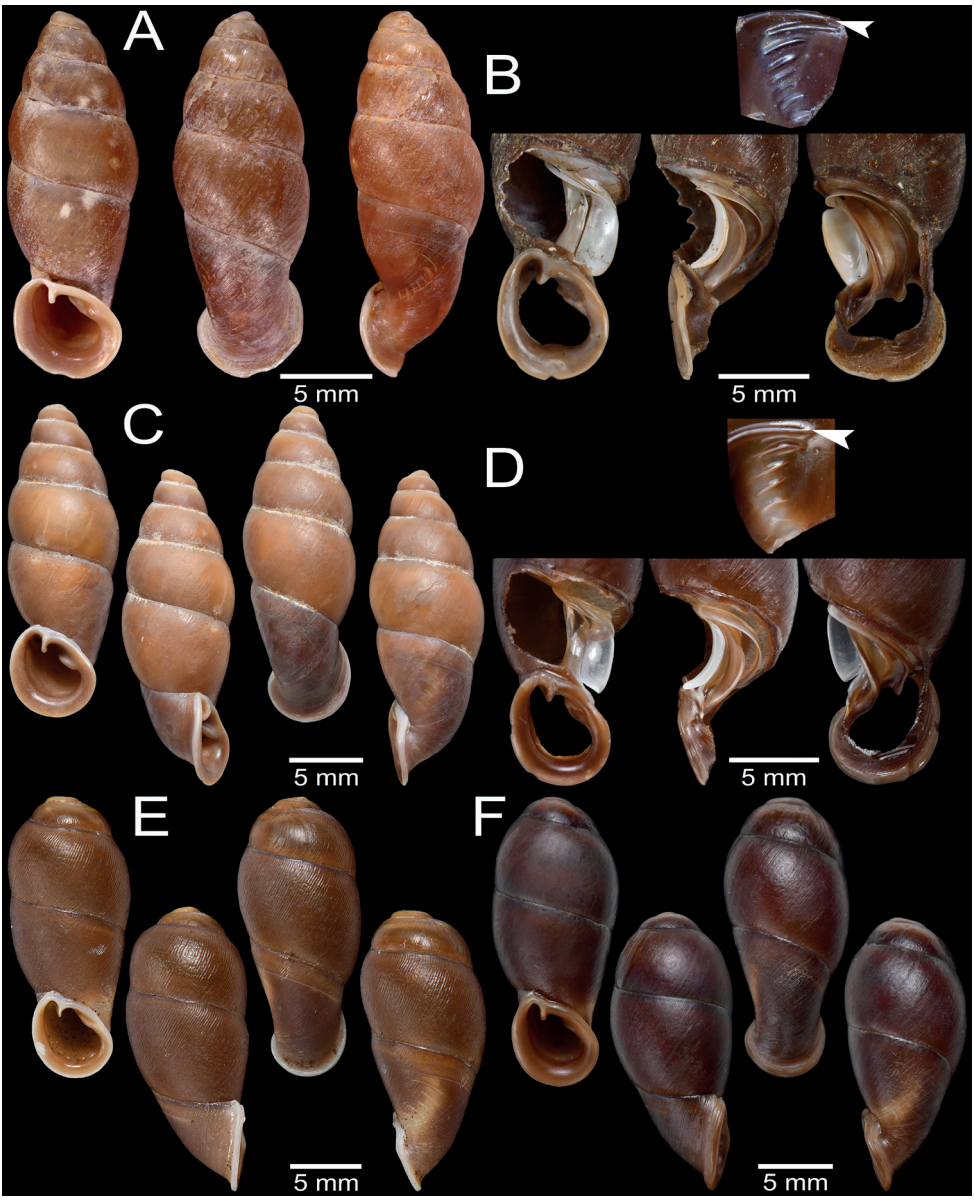

Figure 7. Shell and clausilial apparatus of **A–C** *Oospira philippiana* **A** possible syntype SMF 62294/1 from Burma **B** clausilial apparatus, specimen CUMZ 13040 from Pha Boang Cave, Mon State **C** shell, specimen CUMZ 13037 from Saddan Cave, Mon State and **D–F** *Oospira bulbus*, specimen CUMZ 13042 from Sanbel Cave, Mon State **D** clausilial apparatus **E, F** shells. White arrow indicates principalis.

Material examined. Phra Cave, Tanintharyi Region, Myanmar (11°13'46.2"N, 99°10'34.3"E): CUMZ 13046 (4 shells; Fig. 9D–F), CUMZ 13047 (1 specimen in ethanol).

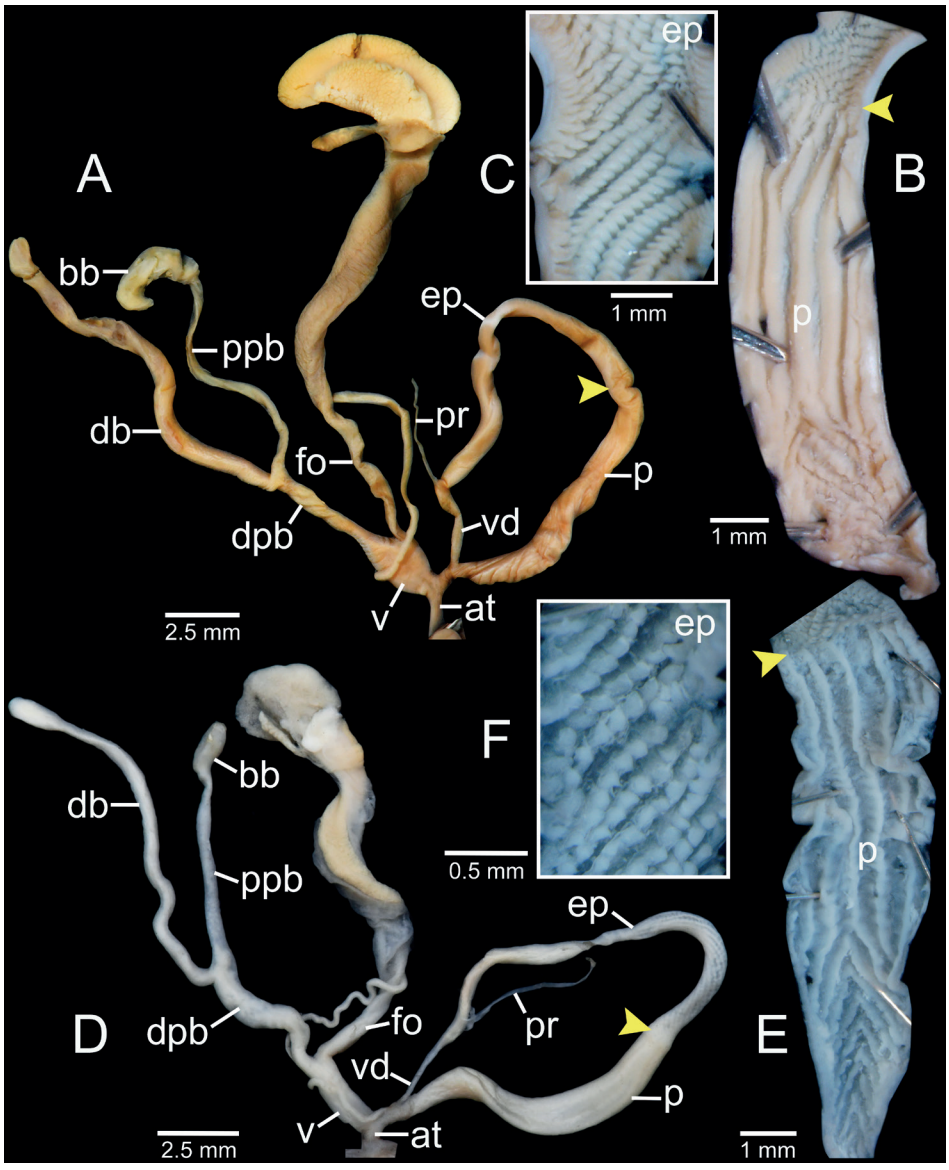

Figure 8. Genital anatomy of **A–C** *Oospira philippiana*, specimen CUMZ 13039 **A** whole reproductive system **B** internal sculpture of penis **C** internal sculpture of epiphallus and **D–F** *Oospira bulbus*, specimen CUMZ 13043 **D** whole reproductive system **E** internal sculpture of penis **F** internal sculpture of epiphallus. Yellow arrows indicate approximate transitional position from penis to epiphallus.

Description. Shell elongate ovoidal, glossy, translucent, and horny brown; spire blunt. Shell surface with very thin striations to smooth surface; suture wide and distinct. Whorls 6–6½, convex, regularly growing and bluntly attenuated to apex. Aperture obliquely pear-shaped, basis rounded and narrowing towards parietal sinus; peristome

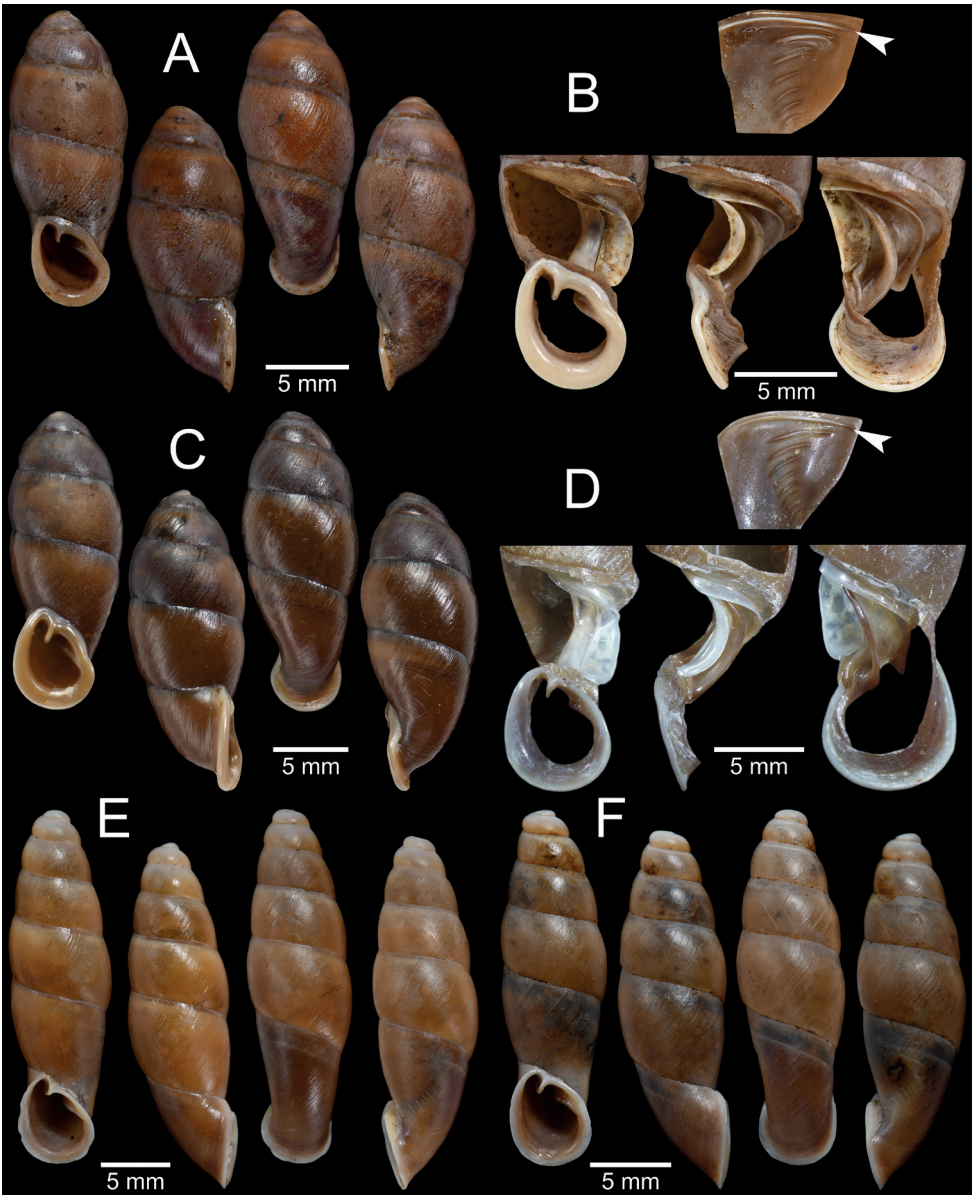

Figure 9. Shell and clausilial apparatus of **A–C** *Oospira ovata*, specimen CUMZ 13044 from Pathein Mountain, Mon State **A, C** shells **B** clausilial apparatus and **D–F** *Oospira stoliczkana*, specimen CUMZ 13046 from Phra Cave, Tanintharyi Region **D** clausilial apparatus **E, F** shells. White arrows indicate principalis.

detached, thin and little expanded. Superior lamella developed, sharp, continuous with spiralis and low at transition to spiralis. Inferior lamella steeply ascending, distant from superior lamella and ending at peristome. Subcolumellaris emerged and only visible in oblique view. Principalis running along lateral-dorsal side and anterior end visible through oblique apertural view. Palatal plicae lateral, 8–10: first plica strong and longest;

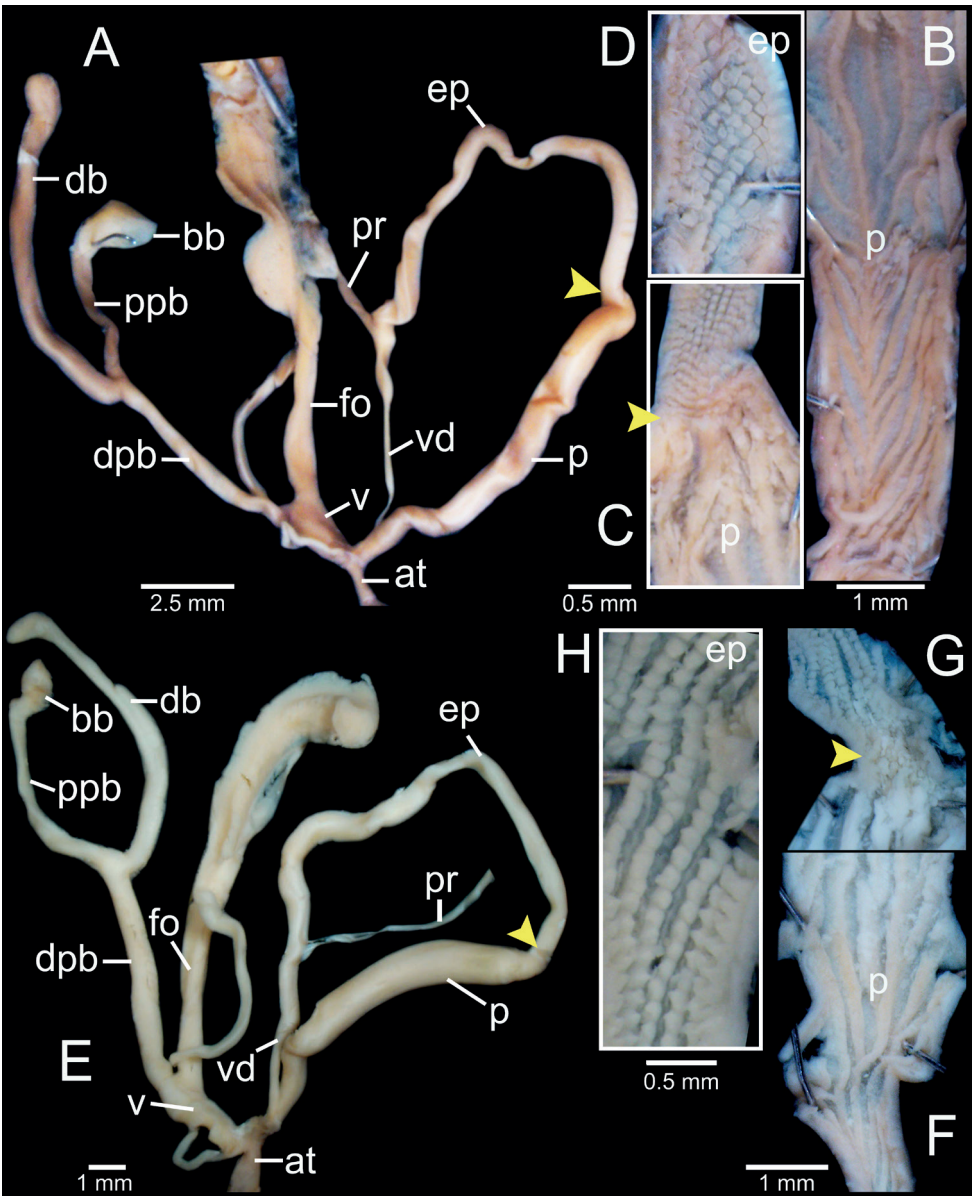

Figure 10. Genital anatomy of **A–D** *Oospira ovata*, specimen CUMZ 13045 **A** whole reproductive system **B** internal sculpture of penis **C** transition from penis to epiphallus **D** internal sculpture of epiphallus and **E–H** *Oospira stoliczkana*, specimen CUMZ 13047 **E** whole reproductive system **F** internal sculpture of penis **G** transition from penis to epiphallus **H** internal sculpture of epiphallus. Yellow arrows indicate approximate transitional position from penis to epiphallus.

following four plicae parallel and equal in length, and remaining plicae shorter, closer, gradually reduced towards anterior. Clausilium plate lateral side and slightly broad at tip.

Genitalia (*n* = 1). Atrium (at) short and slender; penis (p) muscular and cylindrical. Epiphallus (ep) muscular, cylindrical, slightly longer by 1.5× diameter of pe-

nis, and broadest at proximal part. Penial retractor muscle (pr) attaches proximally to epiphallus. Vas deferens (vd) slender, and shortly bounded at atrium and penis junction (Fig. 10E). Internal sculpture of penis consists of two parts: region near atrium, ~ 1/4 length of penis with irregular transverse fleshy folds arranged in nearly V-shaped rows (Fig. 10F); region near epiphallus becoming smooth with oblique longitudinal folds (Fig. 10G). Internal sculpture of epiphallus with elevated papillae arranged in nearly oblique rows (Fig. 10H).

Vagina (v) large, short, and almost half the length of free oviduct (fo). Distal part of pedunculus (dpb) large and long; diverticulum (db) long, ca. same length as dpb; proximal part of pedunculus (ppb) slender, almost equal in length to diverticulum, and bursa copulatrix (bb) small, ovateshape (Fig. 10E).

Distribution. This species is known from Mon State, along with its type locality in Tanintharyi Region; no reports have been made outside Myanmar to date (Szekeres et al. 2021a).

Remarks. *Oospira stoliczkana* can be distinguished from all other species with an ovate-fusiform shell (*O. philippiana*, *O. ovata*, *O. bulbus*, and *O. vespa*) by its elongate ovoidal shell, thinner peristome, and 8 to 10 palatal plicae. Although only one ethanol-preserved specimen could be examined, the internal sculpture of the penis and epiphallus of *O. stoliczkana* differs from *O. philippiana*, *O. bulbus*, and *O. ovata* by its very short V-shaped folds in the region near the atrium and more elevated and pointed papillae in epiphallus.

Some of the examined specimens had a thin and translucent shell, with more distinct palatal plicae.

Oospira species group with long and slender fusiform shell

In Myanmar, this group comprises 15 species including two new ones. Six of these species are examined herein; the remaining nine are *O. arakana* (Stoliczka, 1872), *O. decollata* (Likharev, 1962), *O. fusiformis* (Blanford, 1865), *O. gracilior* (Hanley & Theobald, 1870), *O. insignis* (Gould, 1843), *O. limborgi* Grego & Szekeres, 2021, *O. malaisei* Nordsieck, 1973, *O. mongmitensis* Grego & Szekeres, 2021 and *O. sardicola* Grego & Szekeres, 2021.

8 *Oospira gouldiana* (Pfeiffer, 1857)

Figs 3E, 11, 13A–D, 15C, 18J; Tables 2, 3

Clausilia gouldiana Pfeiffer, 1857: 259. Type locality: “Mergui imperii Birmani” [Myeik Islands, Tanintharyi Region, Myanmar]. Pfeiffer 1860: 123, pl. 34, figs 18–20. Pfeiffer 1868: 409. Stoliczka 1872: 208. Hanley and Theobald 1874: 48, pl. 118, figs 2, 3. Sowerby 1875: *Clausilia* pl. 16, species 148.

Clausilia (*Phaedusa*) *gouldiana*–Blanford 1872: 203, pl. 9, fig. 10.

Clausilia [*Phaedusa* (*Pseudonenia*)] *gouldiana*–Boettger 1878: 54. Pfeiffer and Clessin 1881: 391. Gude 1914: 314–316, fig. 108.

Oospira (*Oospira*) *gouldiana*–Nordsieck 2002b: 86. Nordsieck 2007: 23.
Oospira gouldiana–Szekeres et al. 2021a: 171, fig. 6d–f. Szekeres et al. 2021b: 41.

Materials examined. Bardai Mountain, Hpa-an Township, Hpa-an District, Kayin State, Myanmar (16°59'10.4"N, 97°42'19.8"E): CUMZ 13048 (25 specimens in ethanol, Fig. 11A–C). Kaw Ka Thaung Cave, Hpa-an Township, Hpa-an District, Kayin State, Myanmar (16°49'40.4"N, 97°42'31.0"E): CUMZ 13049 (23 specimens in ethanol, Fig. 11D). Lun Nga Mountain, Hpa-an Township, Hpa-an District, Kayin State, Myanmar (16°44'53.2"N, 97°47'09.5"E): CUMZ 13050 (18 specimen in ethanol). Sadhdan Cave, Hpa-an Township, Hpa-District, Kayin State, Myanmar (16°44'23.4"N, 97°43'04.2"E): CUMZ 13051 (2 incomplete shells). Taung Lay Cave, Hpa-an Township, Hpa-an District, Kayin State, Myanmar (17°11'40.3"N, 97°37'47.0"E): CUMZ 13052 (30 shells; Fig. 11E). Waiponla Mountain, Hpa-an Township, Hpa-an District, Kayin State, Myanmar (16°56'7.4"N, 97°42'56.8"E): CUMZ 13053 (2 incomplete shells, Fig. 11F), CUMZ 13054 (2 specimens in ethanol, lost apical whorls). Rathye Pyan Cave, Hpa-an Twonship, Hpa-an District, Kayin State, Myanmar (16°50'6.2"N, 97°34'14.5"E): CUMZ 13055 (1 incomplete shell).

Description. Shell fusiform, translucent, brownish to reddish pink, and 3–4 white apical whorls; spire regularly attenuated. Shell surface finely striated to nearly smooth surface; suture impressed and distinct. Whorls 10–12 convex, regularly growing or sometimes rapidly growing after antepenultimate whorl and attenuated to apex. Aperture pear-shaped, basis broader and narrowing towards parietal sinus; peristome slightly protruded, thickened, expanded, and indistinctly doubled. Superior lamella developed, continuous with spiralis and slightly low at transition to spiralis. Inferior lamella steeply ascending, distant from superior lamella and ending at peristome. Subcolumellaris emerged and invisible in oblique view. Principalis running along lateral-dorsal side and anterior end visible through oblique apertural view. Palatal plicae lateral, five or six: first plica strong and longest; following plicae short, more or less parallel; fourth or fifth plica longer than middle plicae. Clausilium plate lateral side and narrow.

Genitalia (n = 5). Atrium (at) short and slender; penis (p) long, slender, and shortly narrower at transition to epiphallus. Epiphallus (ep) slender, ca. same length as penis, slightly smaller diameter, and broadest at middle. Penial retractor muscle (pr) attaches proximally to epiphallus. Vas deferens (vd) thin and shortly bounded at penis (Fig. 13A). Internal sculpture of penis with smooth surfaces and five or six thin longitudinal folds (Fig. 13B). Internal sculpture of epiphallus with irregular corrugated pattern (Fig. 13D) and sometimes with distinct irregular transverse fold and papillae arranged in oblique rows.

Vagina (v) thick, cylindrical, and almost half of free oviduct (fo) length. Distal part of pedunculus (dpb) large and middle part broadest; diverticulum (db) slender, very long, ca. same length as distal part and proximal part of pedunculus; proximal part of pedunculus (ppb) slender, nearly same length as (dpb), and bursa copulatrix (bb) ovoid (Fig. 13A).

***Radula*.** Each row contains ≥ 39 teeth with half-row formula: central–(lateral)–marginal teeth (1–(11–12)–19). Central tooth tricuspid with large and triangular mesocone, and ectocones very small and pointed tips. Lateral teeth bicuspid: endocone large and triangular; ectocone very small and pointed tip. Marginal teeth asymmetrically tricuspid starting at approximately tooth number 11 or 12: endocone small located near the tip; mesocone large and dull to blunt tip; ectocone with triangular shape, pointed tip and located near the base (Fig. 15C).

Distribution. *Oospira gouldiana* is the most abundant species of the genus in Myanmar, occurring mainly in the south-eastern part of the country. This species was abundant at seven limestone outcrops in Kayin State (Fig. 1, Table 1). It was recorded from Bago, Kayin, Mon, and Tanintharyi in Myanmar, and the distribution was later expanded to include parts of Thailand (Gude 1914; Szekeres et al. 2021a, b).

Remarks. *Oospira gouldiana* specimens from Taung Lay Cave are quite similar to *O. malaisei* from Kachin State in terms of shell form. But *O. malaisei* (Fig. 17C) shows a more vertical and broader aperture, reflected peristome, closely and rapidly attenuated apical whorls, and inferior lamella more straight ascending at peristome. In contrast, Taung Lay Cave specimens have an oblique and rounded aperture, less reflected peristome, regularly attenuated whitish apical whorls and inferior lamella more spirally ending at peristome. Anatomically, *O. malaisei* possesses an epiphallus of ~ 1/2 the penis length, while in *O. gouldiana* epiphallus and penis have almost equal lengths (see Nordsieck 1973: fig. 26).

Oospira gouldiana also shares a similar shell morphology with *O. insignis* exhibiting a regularly attenuated spire with whitish apical whorls, palatal plicae five, and a broad pear-shaped aperture. Nevertheless, *O. gouldiana* has a more attenuated spire, more parallel palatal plicae, aperture more vertical, and less glossy than *O. insignis*. In addition, this species can easily be separated from *O. shanensis* by its pale color, shorter and oblique palatal plicae, inferior lamella more spirally and closely ascending from spiralis and superior lamella. *Oospira penangensis* differs from this species by its less ventricose, narrower, and more vertical subquadrate aperture, inferior lamella ending straight at peristome and weaker superior lamella from apertural view.

Oospira gouldiana is highly variable in terms of shell color and shape. The typical form was found in the Bardai and Kaw Ka Thaung populations, showing a yellowish to pinkish color with a regular fusiform shape (Fig. 11A, D), while the Taung Lay population have a slenderer shell and the Waiponla population have a more bulging shell (Fig. 11E, F). In addition, the arrangement of palatal plicae shows much variation among the populations. For instance, the Bardai population has irregularly or obliquely arranged plicae (nearly vertical), Kaw Ka Thaung population has parallelly arranged plicae, while the Waiponla and Lun Nga populations have very weak and short parallelly arranged palatal plicae. Furthermore, a very short plica (dot-like) located near the anteriormost palatal plicae next to subcolumellaris is also observed in the Bardai population.

Except for the Sadhdan, Taung Lay, and Rathye Pyan populations, for which genitalia could not be examined, the remaining populations are similar in external

genital morphology, with only slightly differing thickness of the longitudinal folds of the internal sculpture of the penis being observed. However, these four populations inhabit a very small geographical area, hence we attribute this minor difference to morphological variation.

9 *Oospira andersoniana* (Möllendorff, 1882)
Figs 12A, B, 13E–H, 15D, 18B; Tables 2, 3

Clausilia (*Pseudonenia*) *andersoniana* Möllendorff, 1882: 12, pl. 1, fig. 13. Type locality: "In insula Mergui provincise Tenasserim" [Myeik Islands, Tanintharyi Region, Myanmar].
Clausilia [*Phaedusa* (*Pseudonenia*)] *andersoniana*–Gude 1914: 317.

Material examined. The type specimens could not be located in the Senckenberg Museum, Frankfurt (K.-O. Nagel and S. Hof, pers. comm., April 2022). Phra Cave, Tanintharyi Region, Myanmar (11°13'46.2"N, 99°10'34.3"E): CUMZ 13056 (9 shells; Fig. 12A, B), CUMZ 13057 (25 specimens in ethanol), JG-C2880 (2 shells).

Description. Shell fusiform, translucent, and pale yellowish brown color; spire regularly attenuated. Shell surface glossy and almost smooth surface; suture impressed and distinct. Whorls 9–10, little convex, regularly growing and attenuated to apex. Aperture pear-shaped, and basis broader and narrowing towards parietal sinus; peristome protruded, little thickened and expanded. Superior lamella developed, continuous with spiralis, and indistinct at transition to spiralis. Inferior lamella steeply ascending, distant from superior lamella and ending at peristome. Subcolumellaris emerged and invisible in oblique view. Principalis running along lateral-dorsal side and anterior end visible through oblique apertural view. Palatal plicae lateral, 3–5 (usually 3): all plicae very strong, parallel, equal length, spacing, and one or two small plicae sometimes present in middle and at lowest. Clausilium plate lateral side and narrow.

Genitalia (*n* = 5). Atrium (at) short and slender; penis (p) almost cylindrical and shortly narrower at transition to epiphallus. Epiphallus (ep) cylindrical, ca. same length and diameter as penis. Penial retractor muscle (pr) attaches proximally to epiphallus. Vas deferens (vd) thin and shortly bounded at penis (Fig. 13E). Internal sculpture of penis with smooth surfaces and with relatively thickened four or five longitudinal folds (Fig. 13F, G). Internal sculpture of epiphallus with large and scattered papillae arranged obliquely to irregularly spaced rows (Fig. 13H).

Vagina (v) thick, cylindrical, and almost equal to free oviduct (fo) length. Distal part of pedunculus (dpb) large and long; diverticulum (db) thin and ca. same length as dpb; proximal part of pedunculus (ppb) slender, nearly equal in length to diverticulum, and bursa copulatrix (bb) small, ovoid (Fig. 13E).

***Radula*.** Each row contains ~ 45 teeth with half-row formula: central–(lateral)–marginal teeth (1–(10–11)–22). Central tooth tricuspid: mesocone triangular with dull cusp; ectocones small and pointed tip. Lateral teeth bicuspid: endocone large and

with dull cusp; ectocone small with tip pointed laterally. Marginal teeth asymmetrically tricuspid starting at approximately tooth number 10 or 11: endocone very tiny; mesocone large, elongate, blunt tip; ectocone small, triangular, pointed tip. Outermost becoming smaller and more asymmetrical than inner teeth (Fig. 15D).

Distribution. Currently *O. andersoniana* is only known from Tanintharyi Region, Myanmar.

Remarks. This species was described based on two shells collected by the Scottish zoologist, John Anderson (1833–1900), approximately from southern Myanmar, and an illustration was included in the original publication (Möllendorff 1882; Alcock 1902). Then, it was re-described and suggested to be very similar to *O. gouldiana* by Gude (1914). Despite the type specimen being mentioned in the type catalogue of the Clausiliidae in the Naturmuseum Senckenberg by Zilch (1954), this nominal species seems mysterious and is, therefore, listed as uncertain (taxon inquirendum) in MolluscaBase (2022). The type specimens of this species are presumably lost. However, Möllendorff (1882) provided a very detailed description and illustration of the species. Our newly collected specimens from the Tanintharyi Region have a thinly striated shell, smooth surface, thin peristome, mostly nine whorls and three palatal plicae, which matches well with the diagnostic characteristics of this species.

In this survey, *Oospira andersoniana* and *O. stoliczkana* were collected from the same locality in the Tanintharyi Region. These two species are similar in possessing a nearly smooth shell glossy surface, thin peristome, pale yellowish color, and less developed inferior lamella. However, *O. stoliczkana* exhibits a shorter, blunt spire, broader clausilium and several palatal plicae (from 8 to 10).

Compared with the other congeners, *Oospira andersoniana* can be distinguished from *O. insignis*, *O. gouldiana*, and *O. magna* by its less ventricose shell, smoother surface and pale color, peristome and inferior lamella weaker, and palatal plicae longer and more uniformly arranged. In contrast, *O. insignis* possesses oblique palatal plicae, more ventricose and darker colored shell, while *O. gouldiana* has a ventricose shell, spire more attenuated and with whitish apical whorls, inferior lamella more bent, aperture thicker and broader, and palatal plicae closer and more oblique. In addition, *O. magna* can be distinguished from *O. andersoniana* by having a finely and densely striated shell surface, inferior lamella well developed, clausilium in ventral position, and palatal plicae longer and more ventral (nearly horizontal). In terms of the genitalia, *O. andersoniana* has a short male organ, internal penis with large longitudinal folds and epiphallus with a distinct reticulated papillae pattern. In contrast, *O. gouldiana* and *O. magna* possess slender and longer male organs, internal penis with thinner and denser longitudinal folds, and epiphallus with irregularly arranged reticulated papillae patterns. Furthermore, *O. limborgi* Grego & Szekeres, 2021, also described from the Tanintharyi Region, shares some characteristics with this species in having the same number of palatal plicae, nearly triangular aperture, glossy and pale yellowish color (see Szekeres et al. 2021a: fig. 7c).

Shell variation was observed with respect to a small and short plica between the first and second palatal plicae.

10 *Oospira magna* (Gude, 1914)
Figs 12C, D, 14A–D, 19B; Tables 2, 3

Clausilia [*Phaedusa* (*Pseudonenia*)] *gouldiana* var. *magna* Gude, 1914: 316, fig. 109. Type locality: "Moulmain and Phaboo" [Mawlamyine, Mon State and Pabu, Hpa-an, Kayin State, Myanmar].

Materials examined. Bayin Nyi Cave, Hpa-an Township, Kayin State, Myanmar (16°58'10.1"N, 97°29'30.6"E): CUMZ 13058 (3 shells + 6 incomplete shells, Fig. 12C, D), CUMZ 13059 (1 specimen in ethanol).

Description. Shell fusiform, translucent, yellowish brown and 3–4 white apical whorls; spire regularly attenuated. Shell surface nearly smooth to with thin growth lines; suture deep and distinct. Whorls 10–11, convex, regularly growing and attenuated to apex. Aperture oval-pear-shaped, less oblique, basis broader and narrowing towards parietal sinus; peristome protruded, thickened, and slightly expanded. Superior lamella developed, continuous with spiralis, and indistinct at transition to spiralis. Inferior lamella well developed, steeply ascending, distant from superior lamella and ending at peristome. Subcolumellaris emerged and invisible in oblique view. Principalis running along ventral-lateral side and anterior end visible through oblique apertural view. Palatal plicae ventral-lateral, 4–6 (usually 4): first plica strong and longest; second and third plicae short, parallel, oblique, and equal in length; fourth plica longer and stronger than middle plicae. Clausilium plate ventral side and narrow.

Genitalia (*n* = 1). Atrium (at) short and relatively large; penis (p) almost cylindrical and shortly narrower at transition to epiphallus. Epiphallus (ep) slender, ca. same length as penis and smaller diameter. Penial retractor muscle (pr) attaches proximally to epiphallus. Vas deferens (vd) almost same diameter as epiphallus and shortly bounded at penis (Fig. 14A). Internal sculpture of penis with smooth surface and ca. four or five thin longitudinal rows (Fig. 14B), and folds slightly enlarged near epiphallus (Fig. 14C). Internal sculpture of epiphallus with large papillae arranged in oblique rows (Fig. 14D).

Vagina (v) thick, cylindrical, and almost equal in length to free oviduct (fo). Distal part of pedunculus (dpb) cylindrical and long; diverticulum (db) very long, slightly enlarged at basis, then gradually slenderer, ~ 3× times length of dpb; proximal part of pedunculus (ppb) slender, slightly short, ~ 3/4 diverticulum length; bursa copulatrix (bb) large, ovoid (Fig. 14A).

Distribution. *Oospira magna* is only recorded from the southern part of the country to the limestone area of the Salween River Basin in Mon and Kayin States, Myanmar.

Remarks. Originally, *Oospira magna* was proposed as a subspecies of *O. gouldiana* based on its distinct less ventricose shell and seven palatal plicae (Gude 1914). Later Szekeres et al. (2021b) recognized this as a morphological variation within the variable species, *O. gouldiana*. From our recent field survey, several specimens were collected, and their shell morphology matched well with the diagnostic characters of *O. magna*. Although *O. magna* is highly similar to *O. gouldiana* in shell form, it can be distinguished mainly by having a less ventricose shell, almost uniform and ventrally longer

palatal plicae, more developed inferior spiral lamella, aperture less oblique, last whorl more compressed, spiralis starting deeply ventral, and clausilium ventrally seated. In genitalia, *O. gouldiana* exhibits a long distal part of pedunculus almost the same length as the proximal part of pedunculus and an internal sculpture of epiphallus with a thin and irregular corrugated pattern. These differences in the shell and genitalia characters are greater than the intraspecific variation and those characters were not observed as a morphological variation among the *O. gouldiana* populations examined; therefore, we have raised *O. magna* to a distinct species. *Oospira zediopsis* sp. nov. differ from *O. magna* by its a more ventricose shell with a smoother surface, apical whorl rapidly attenuated, dark reddish color, clausilium and palatal plicae laterally seated, and inferior lamella straight ascending.

11 *Oospira shanensis* Grego & Szekeres, 2021

Figs 3F, 12E, F, 14E–H, 15E, 19J; Tables 2, 3

Oospira shanensis Grego & Szekeres in Szekeres et al. 2021a: 177, 178, fig. 8e, f. Type locality: "Shan" [Shan State, Myanmar].

Material examined. Limestone outcrop at Nanthe Cave, Kalaw City, Shan State, Myanmar 20°35'16.6"N, 96°37'57.2"E: CUMZ 13060 (5 shells, Fig. 12E, F), CUMZ 13061 (4 specimens in ethanol).

Description. Shell fusiform, opaque, and dark yellowish color; 5–6 apical whorls rapidly attenuated. Shell surface glossy and almost smooth; suture impressed and distinct. Whorls 12½–13, last four whorls regularly growing and then rapidly attenuated to apex. Aperture obliquely or elliptical, basis oblique and broadest and narrowing towards parietal sinus; peristome attached, thickened, and expanded. Superior lamella developed, continuous with spiralis and indistinct at transition to spiralis. Inferior lamella steeply ascending, anterior end weakly visible in apertural view, very distant from superior lamella and ending at peristome. Subcolumellaris emerged and visible in oblique view. Principalis running along ventral-lateral side and anterior end visible through oblique apertural view. Palatal plicae ventral-lateral, five: equally spaced, fourth plica curved most, two middle plicae equally shorter than first and fourth; fifth plica can only be seen when shell is opened. Clausilium plate lateral side, broad, rounded and with hook.

Genitalia (*n* = 2). Atrium (at) small and short; penis (p) almost cylindrical and gradually narrower at transition to epiphallus. Epiphallus (ep) cylindrical and ca. same length and diameter as penis. Penial retractor muscle (pr) attaches proximally to epiphallus. Vas deferens (vd) very thin and shortly bounded at penis (Fig. 14E). Internal sculpture of penis with 3 to 4 large corrugated longitudinal folds (Fig. 14G). Internal sculpture of epiphallus with finely reticulated pattern arranged on two or three large longitudinal folds (Fig. 14H).

Vagina (v) very thin and ~ 1/3 of free oviduct (fo) length. Distal part of pedunculus (dpb) long and enlarged, cylindrical; diverticulum (db) long, enlarged at basal

and gradually reduced and becoming slender at terminal, and nearly same length as dpb; proximal part of pedunculus (ppb) short, ~ 3/4 diverticulum length, and bursa copulatrix (bb) small, ovoid (Fig. 14E).

***Radula*.** Central and lateral teeth contain ≥ 23 teeth with half-row formula: central–(lateral)–marginal teeth (1–(10–11)+). Central tooth tricuspid: mesocone large and triangular; ectocone small and located near the base. Lateral teeth bicuspid: endocone large and bluntly pointed tip; ectocone small and pointed tip. Marginal teeth asymmetrically tricuspid starting at approximately tooth number 10 or 11 (Fig. 15E). Most marginal teeth part lost during the cleaning process.

Distribution. This species is presently only known from Shan State, Myanmar.

Remarks. Among all the Myanmar's *Oospira* species studied herein, this is the only species with a clausilium hook (Fig. 12F), and the clausilium plate is broader than in all other congeners. The presence of the hook in other phaedusinid taxa has been documented and is assumed to provide an advantage in trapping air bubbles to avoid drowning (see Páll-Gergely and Szekeres 2017).

Oospira sardicola can be distinguished from *O. shanensis* by having paler glossy yellowish color, wider and less oblique aperture, and less ventricose shell (Szekeres et al. 2021b). This species can clearly be recognized from *O. gouldiana* and *O. magna* by its more ventricose shell, inferior lamella straight ascending and reduced to the peristome and clausilium more rounded, broader, and in lateral position. Moreover, *O. shanensis* has a relatively short male organ, epiphallus larger than the penis, diverticulum narrower to the proximal end, and the internal sculpture is distinctly different from *O. gouldiana* and *O. magna*.

Oospira mongmitensis, *O. sardicola*, and *O. shanensis* were recorded from Shan State. All of them are similar in possessing distinct palatal plicae which can be seen through the shell, but different in their pale to dark color, more or less bulging shell and aperture oblique to nearly vertical (Szekeres et al. 2021a, b). Furthermore, *O. sardicola* and *O. mongmitenis* have distinct sutural papillae. These three species; *O. mongmitensis*, *O. sardicola*, and *O. shanensis* from Shan State are notably different from their congeners from southern Myanmar showing anterior end of inferior lamella reduced at peristome.

Our specimens show variation in the development of palatal plicae, especially as the fourth or fifth plicae are horizontal to oblique.

12 *Oospira luneainopsis* Man & Panha, sp. nov.

https://zoobank.org/B8866312-31E1-4E9A-993D-6A3E025C8F17
Figs 16A–C, 18P; Table 2

Type material. ***Holotype*** CUMZ 13062 (Fig. 16A). Measurements: shell height 20 mm, shell width 5.8 mm, and 7 whorls. ***Paratypes*** CUMZ 13063 (8 shells; Fig. 16B, C), NHMUK 20220504 (2 shells).

Type locality. Limestone outcrop at Zwegabin Mountain, Hpa-an Township, Hpa-an District, Kayin State, Myanmar (16°48'44.5"N, 97°40'25.5"E).

Etymology. The specific name *luneainopsis* is a compound of 'lun-eain', which in the Myanmar language refers to a bobbin used for traditional Myanmar weaving, and the Greek suffix *-opsis* meaning 'having the appearance of or like'. It refers to the bobbin shape of the shell of this species.

Diagnosis. Shell ovate-fusiform, decollated with smooth surface and dense striations near suture. Last whorl neck subquadrate; aperture nearly roundish; peristome detached. Inferior lamella straight ascending and reaching at peristome; palatal plicae four, distinct, equally, and parallelly arranged, and superior lamella developed.

Description. Shell ovate-fusiform, decollated, opaque, pinkish brown; spire blunt. Shell surface smooth to with fine growth lines on last whorl, denser near suture and last whorl neck subquadrate; suture impressed and distinct. Whorls 7–8, convex, regularly growing, and bluntly attenuated to apex. Aperture nearly round; peristome detached, thickened, expanded and little reflexed. Superior lamella developed, continuous with spiralis, and slightly low at transition to spiralis. Inferior lamella steeply ascending, distant from superior lamella and ending at peristome. Subcolumellaris emerged and invisible in oblique view. Principalis running along lateral-dorsal side and anterior end visible through oblique apertural view. Palatal plicae lateral, four: first and fourth plicae strong and longest; remaining plicae parallel and equal length; sometimes tiny lowest plica present. Clausilium plate lateral side, narrow and slightly pointed at tip.

Distribution. *Oospira luneainopsis* sp. nov. is only known from the type locality.

Remarks. No ethanol preserved specimens were available for anatomical study. This species can be distinguished from *O. gouldiana*, *O. magna*, and *O. zediopsis* sp. nov. by its small size, decollated, fewer whorls, roundish aperture, more spiral inferior lamella, and equal palatal plicae. This new species is clearly distinct from *O. decollata* by its spiral inferior lamella visible from aperture, smoother shell, pink color, and more bulging whorls.

Compared to the Vietnamese dextral species, *O. duci* Maassen & Gittenberger, 2007 exhibits thinner and oblique aperture, sinus higher, obviously emerged subcolumellaris, very fine striations and more ventrally unequal palatal plicae than this species.

13 *Oospira zediopsis* Man & Panha, sp. nov.

https://zoobank.org/FB4630CA-1F88-437F-88C8-8187A9ECAA1E
Figs 16D–F, 19Q; Table 2

Type material. ***Holotype*** CUMZ 13064 (Fig. 16E). Measurement: shell height 25 mm, shell width 6.5 mm and 10 whorls. ***Paratypes*** CUMZ 13065 (50 shells; Fig. 16D, F), NHMUK 20220508 (2 shells) and JG-C 2884 (2 shells).

Type locality. Weibyan Cave, Hpa-an Township, Hpa-an District, Kayin State, Myanmar (17°13'38.2"N, 97°37'24.0"E).

Etymology. The specific name *zediopsis* is a compound word; 'zedi' is one of several terms in the Myanmar language that refer to a stupa or pagoda, and the Greek suffix *-opsis* means 'having the appearance of or like'. It refers to the Myanmar pagoda-like shell shape of this species.

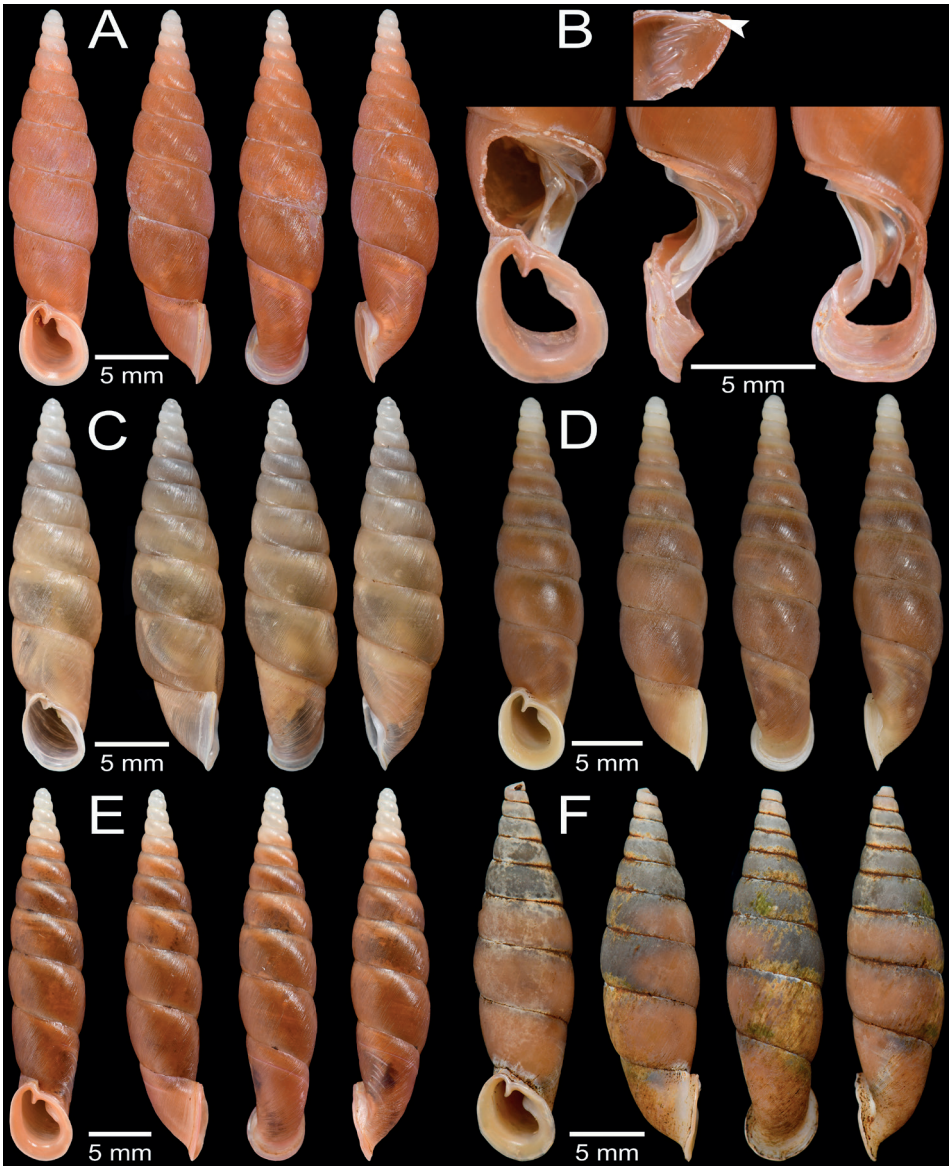

Figure 11. Shell and clausilial apparatus of *Oospira gouldiana* **A–C** specimen CUMZ 13048 from Bardai Mountain, Kayin State **A** typical pinkish shell form **B** clausilial apparatus **C** not fully adult shell **D** yellowish shell form, specimen CUMZ 13049 from Kaw Ka Thaung Cave, Kayin State **E** slender shell form, specimen CUMZ 13052 from Taung Lay Cave, Kayin State **F** ovate shell form, specimen CUMZ 13053 from Waiponla Mountain, Kayin State. White arrow indicates principalis.

Diagnosis. Shell fusiform, with four to five white apical whorls, and nearly smooth shell surface. Inferior lamella straight ascending or almost flattened, palatal plicae lateral, equally oblique, superior lamella distinct at transition to spiralis, and clausilium plate lateral side and less bent inwards.

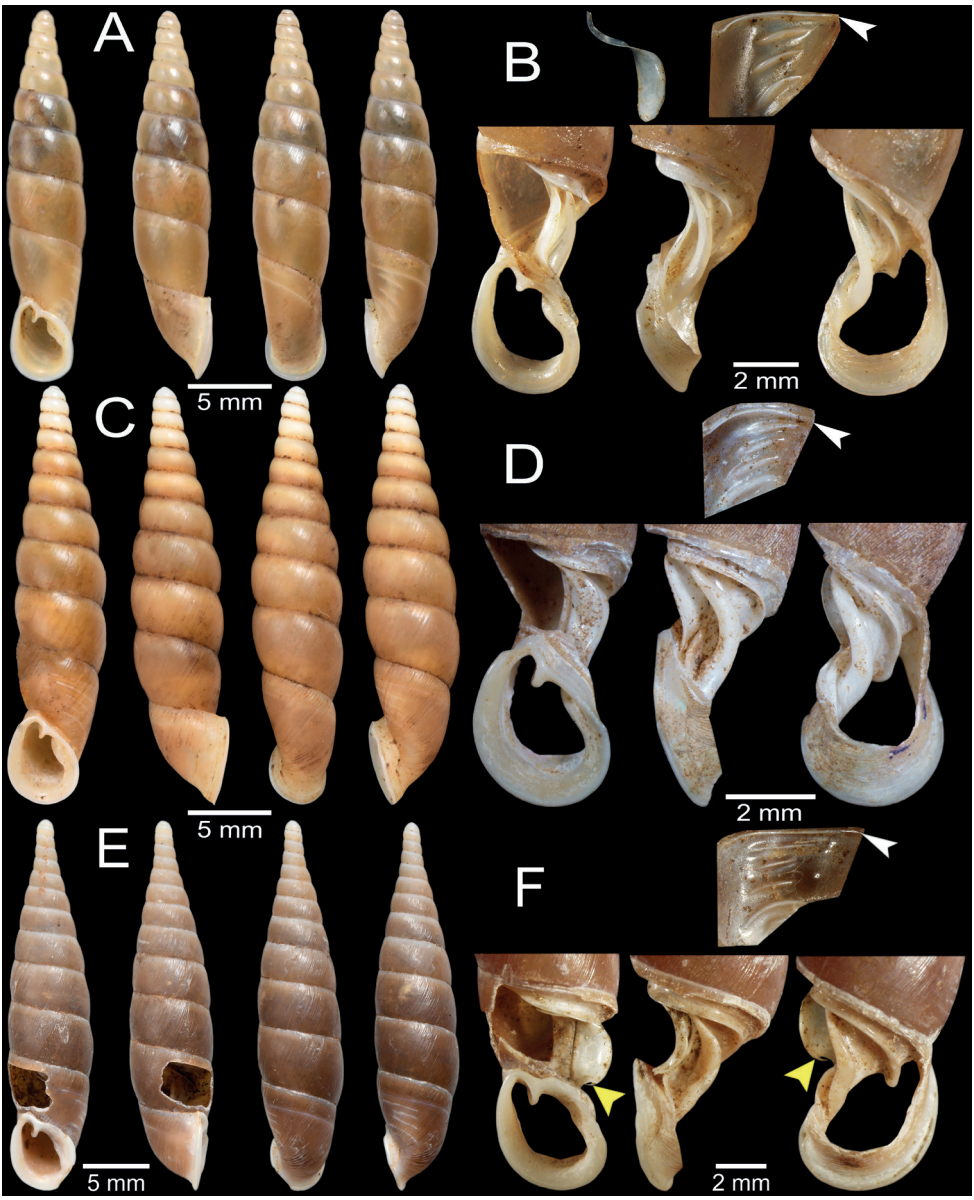

Figure 12. Shell and clausilial apparatus of **A, B** *Oospira andersoniana*, specimen CUMZ 13056 from Phra Cave, Tanintharyi Region **A** shell **B** clausilial apparatus **C, D** *Oospira magna*, specimen CUMZ 13058 from Bayin Nyi Cave, Kayin State **C** shell **D** clausilial apparatus and **E, F** *Oospira shanensis*, specimen CUMZ 13060 from Nanthe Cave, Shan State **E** shell **F** clausilial apparatus. White arrows indicate principalis and yellow arrows indicate clausilium hook.

Description. Shell fusiform, opaque, and chestnut-brown color; 4–5 apical whorls white and rapidly attenuated. Shell surface smooth to with very thin growth lines; suture impressed and distinct. Whorls 10–11, convex, regularly growing, and attenuated

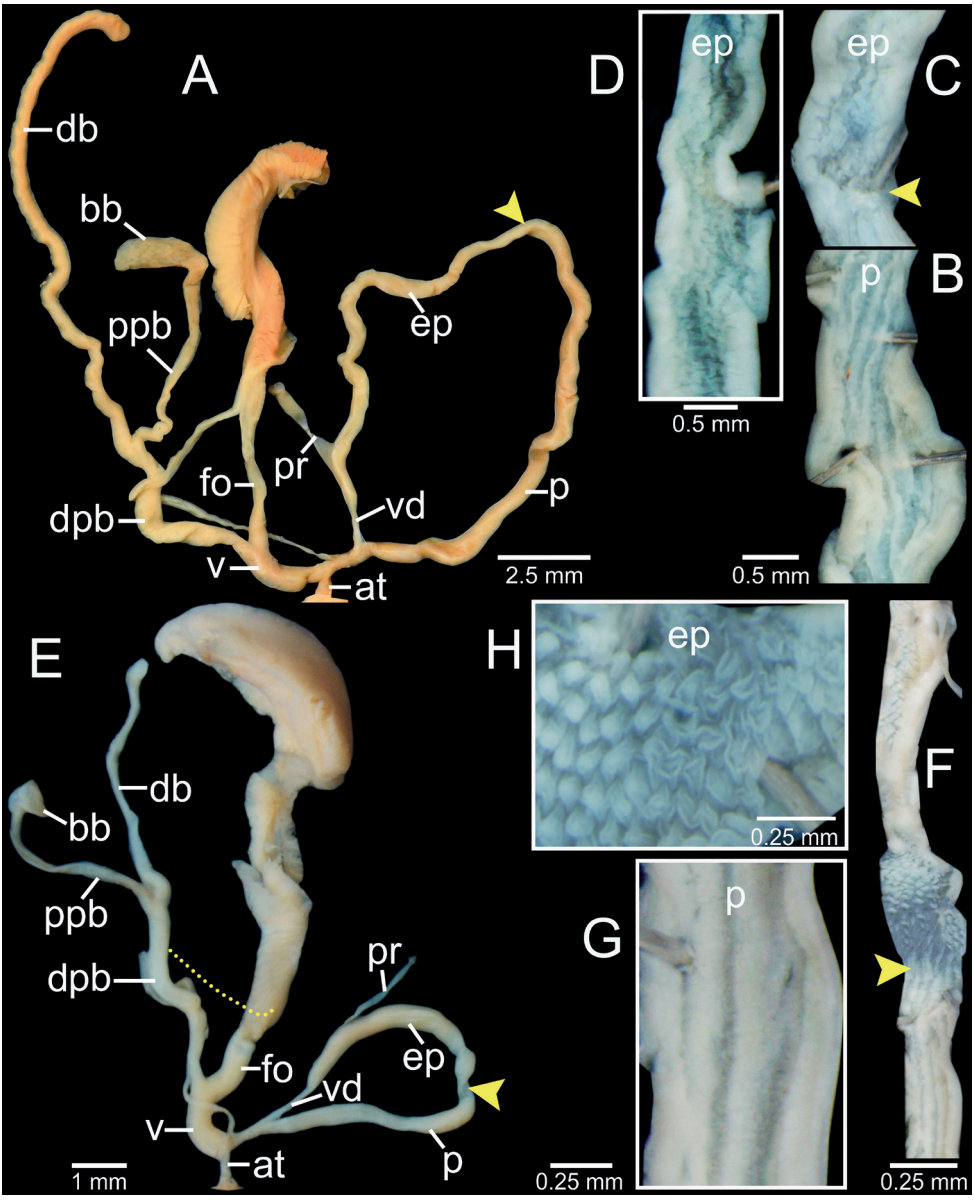

Figure 13. Genital anatomy of **A–D** *Oospira gouldiana*, specimen CUMZ 13049 **A** whole reproductive system **B** internal sculpture of penis **C** transition from penis to epiphallus **D** internal sculpture of epiphallus and **E–H** *Oospira andersoniana*, specimen CUMZ 13057 **E** whole reproductive system **F** overview of internal sculpture of penis and epiphallus **G** internal sculpture of penis **H** internal sculpture of epiphallus. Yellow arrows indicate approximate transitional position from penis to epiphallus.

to apex. Aperture obliquely pear-shaped, and basis rounded; peristome slightly protruded, large, relatively thickened and slightly expanded. Superior lamella developed, connected to spiralis and slightly low at transition to spiralis. Inferior lamella steeply

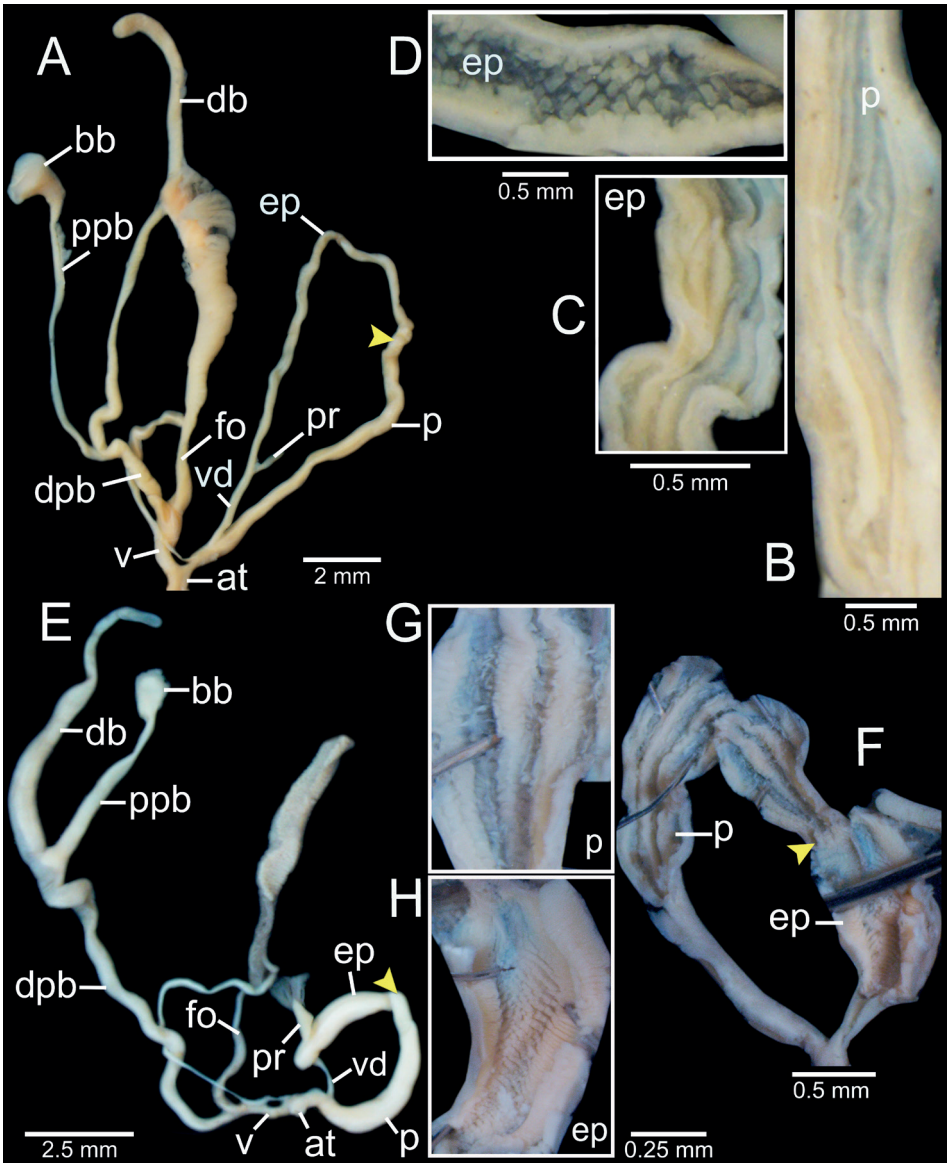

Figure 14. Genital anatomy of **A–D** *Oospira magna*, specimen CUMZ 13059 **A** whole reproductive system **B** internal sculpture of penis near atrium **C** internal sculpture of penis near epiphallus **D** internal sculpture of epiphallus and **E–H** *Oospira shanensis*, specimen CUMZ 13061 **E** whole reproductive system **F** overview internal sculpture of penis and epiphallus **G** internal sculpture of penis **H** internal sculpture of epiphallus. Yellow arrows indicate approximate transitional position from penis to epiphallus.

ascending, distant from superior lamella and ending at peristome. Subcolumellaris emerged and invisible in oblique view. Principalis running along lateral-dorsal side and anterior end visible through oblique apertural view. Palatal plicae lateral, four or five:

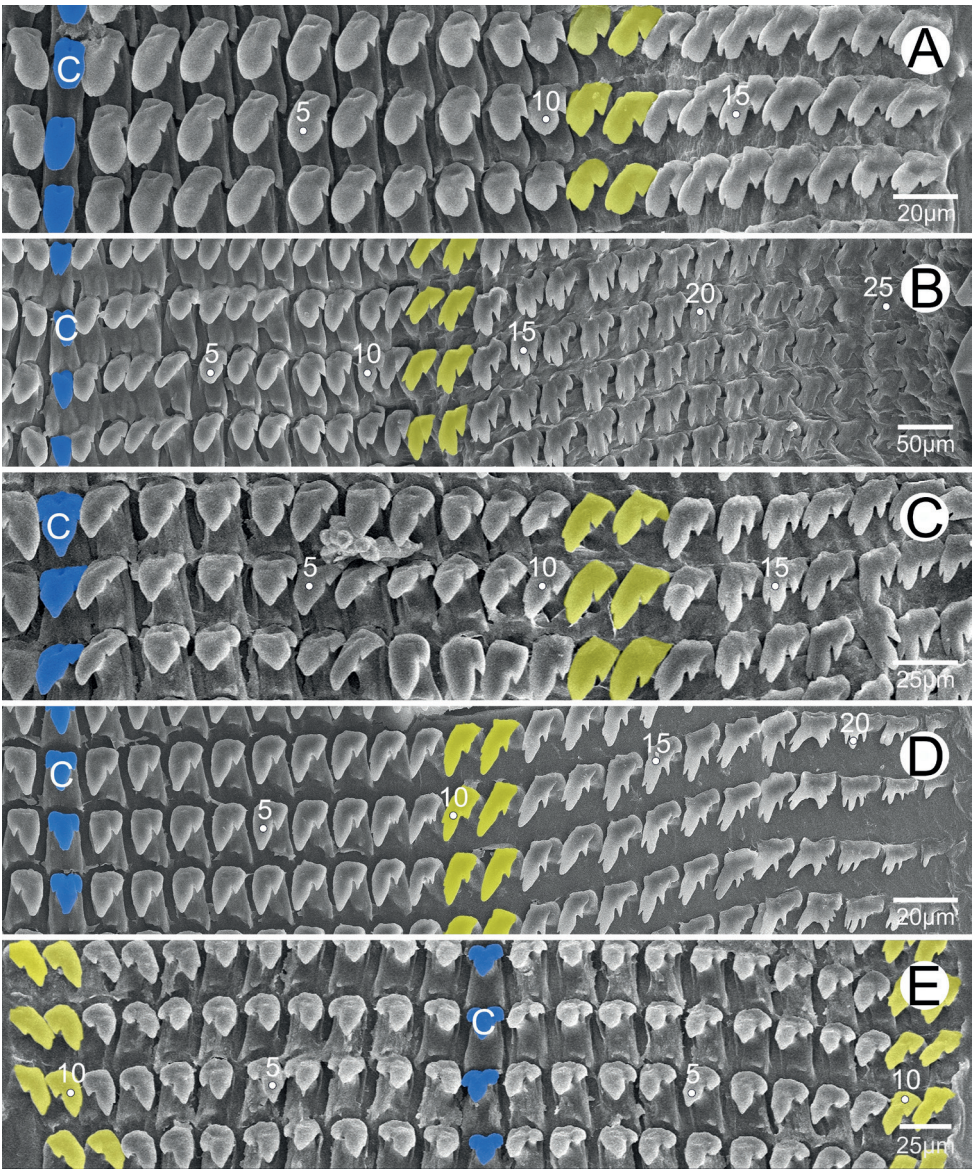

Figure 15. Radula morphology **A** *Oospira philippiana*, specimen CUMZ 13039 **B** *Oospira ovata*, specimen CUMZ 13044 **C** *Oospira gouldiana*, specimen CUMZ 13049 **D** *Oospira andersoniana* CUMZ 13057 **E** *Oospira shanensis*, specimen CUMZ 13061. Blue color indicates central teeth row; yellow color indicates the transition from lateral to marginal teeth. 'C' indicates central tooth.

first and fourth plicae strongest and longest; remaining plicae parallel and equal length; fifth plica smallest. Clausilium plate lateral side and narrow.

Distribution. This species is only known from the type locality with plentiful shells collected.

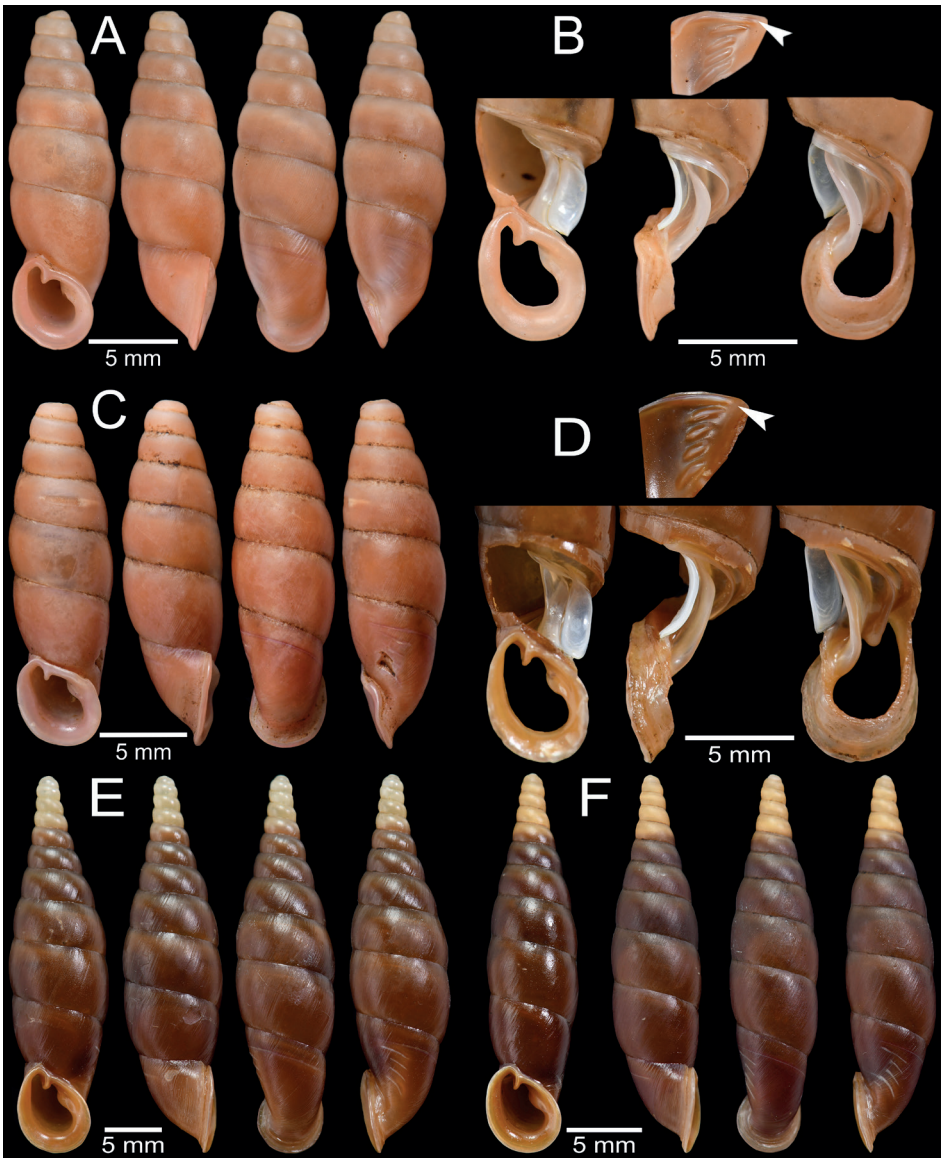

Figure 16. Shell and clausilial apparatus of **A–C** *Oospira luneainopsis* sp. nov. **A** shell of holotype CUMZ 13062 from Zwekabin Mountain, Kayin State **B, C** paratypes CUMZ 13063 from the type locality **B** clausilial apparatus **C** shell and **D–F** *Oospira zediopsis* sp. nov. **D** clausilial apparatus of paratype CUMZ 13065 from the type locality **E** shell of holotype CUMZ 13064 from Weibyan Cave, Kayin State and **F** shell of paratype CUMZ 13065 from the type locality.

Remarks. No ethanol preserved specimens were available for anatomical study. *Oospira gouldiana* can be distinguished from *O. zediopsis* sp. nov. by its less ventricose shell, denser and stronger striations, more spiral inferior lamella, palatal plicae and clausilium

more ventrally positioned, and principalis not visible from the aperture view. Likewise, *O. shanensis* can be differentiated from this new species by wider spacing between spiralis and inferior lamella, anterior end of inferior lamella reduced at peristome, longer palatal plicae, attached peristome, and clausilium wider and with a hook. Furthermore, *O. zediopsis* sp. nov. can be differentiated from *O. insignis* by its more attenuated spire, narrower and more oblique aperture, shorter and more equal palatal plicae.

Discussion

Among the 33 clausiliid taxa recorded from Myanmar, 13 species are redescribed here based on the shell, genitalia, and radular morphologies, including two new species. The remaining 20 species are known from literature, and images of the type specimens, authenticated specimens or original illustrations are provided for further comparison (Figs 18, 19). All examined clausiliid genitalia in Myanmar show simple male organs (penis, epiphallus, penial retractor muscle, and vas deferens) and these differ mainly in the length of penis, diverticulum, and pedunculus. Internally, the epiphallus is more variable with two or three patterns on the surface, and different numbers of simple longitudinal folds in penis. The genitalia of the recently reported *Phaedusa bhutanensis* Nordsieck, 1974 from Bhutan is similar to the Myanmar *Phaedusa* species examined in this study in having a distinctly long diverticulum, pedunculus and developed male organs (see Gittenberger et al. 2019: figs 27b, 28, 29). Overall, the external shell morphology, including shape, size, whorl number, and color is useful in recognizing the Myanmar clausiliids at first glance.

In Myanmar, *Oospira* is one the most diverse stylommatophoran genera. It comprises 20 species of which ten are redescribed herein, including the type species, *O. philippiana*. Based on the shell, clausilial apparatus and genital morphology, the genus is generally divided into two groups: (1) short and ovate fusiform shell group (including type species), and (2) long and slender fusiform shell group. The first group tends to have palatal plicae reduced towards the anterior, inferior lamella straight ascending and superior lamella distinct from spiralis at its transition point, a well-developed penis, diverticulum, and proximal of pedunculus almost similar in length, internal wall of epiphallus with equally and obliquely arranged papillae, and internal wall of penis consists of two shapes: oblique V-shaped near atrium and transitioning to longitudinal folds near epiphallus. The second group possess palatal plicae that are not reduced towards the anterior, inferior lamella more spirally ascending (S-shape) and superior lamella indistinct from spiralis at it transition point, slender to narrowly cylindrical penis, generally diverticulum longer than proximal of pedunculus in length, internal wall of epiphallus with irregularly arranged papillae, and internal wall of penis consists of longitudinal folds throughout the entire chamber. Additionally, the central tooth of group (1) has a more rounded cusp than group (2), which has a triangular shape and pointed cusp. These differences in shell and clausilial apparatus between the two groups rather agree with the diagnostic characters of the *Pseudonenia* Boettger, 1877

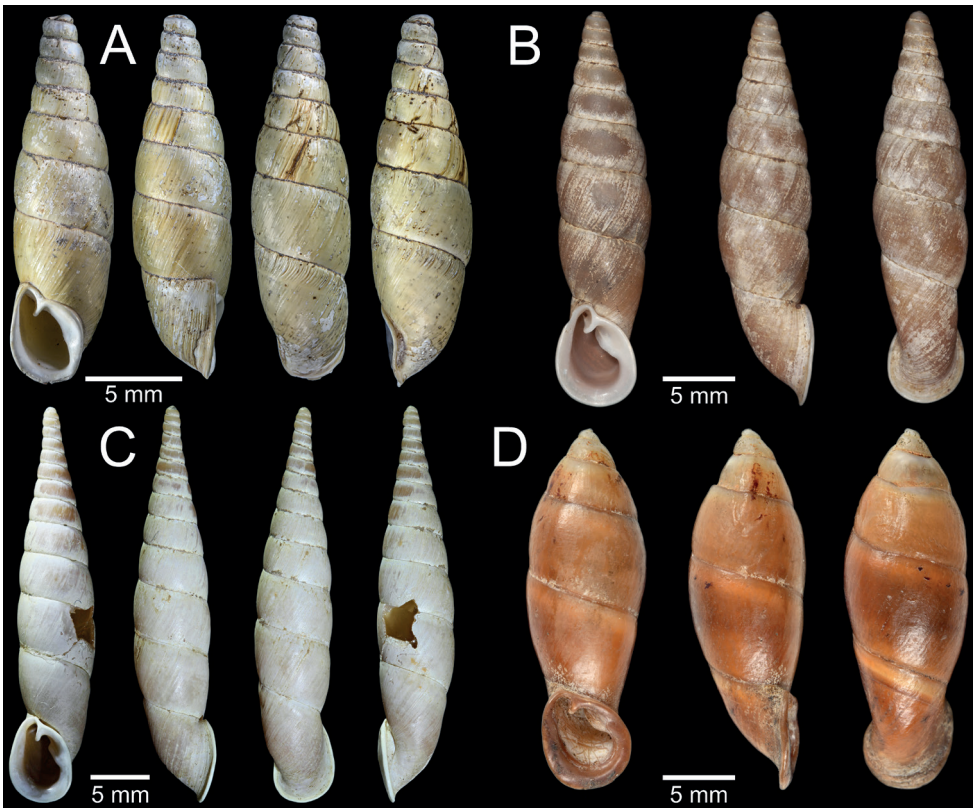

Figure 17. Shell of **A** *Oospira decollata*, paratype ZISP from West Burma, near Pakoku on Mount Victoria. 2200 m a.s.l. **B** *Oospira insignis*, lectotype USNM 117120 from Tavoy, Burmah **C** *Oospira malaisei*, holotype SMNH 3014 from NO-Birma: Pungkataung ca. 3000 ft. and **D** *Oospira vespa*, lectotype MCZ 169455 from Tavoy, British Burma. Photo: A Persson, SMNH (**C**).

(see Gude 1914). However, further supporting evidence and the morphological and anatomical information of its type species are needed to elucidate and resolve the taxonomy of these groups.

Although the clausiliids seem evenly distributed throughout Myanmar, *Phaedusa* is distributed in the northeast to southwest, while *Oospira* occurs widely along the northernmost to the southernmost parts of the country (Fig. 1; Table 1). Based on our surveys, the southern part of Myanmar, including Kayin and Mon States and the Tanintharyi Region, has the largest number of species recorded, and seven species are assumed to be endemic to this area. Allopatric speciation caused by massive and isolated limestone karsts in the topography of the Salween River Basin and the Tenasserim Range possibly plays an important role in the high endemicity of clausiliids. Recent studies on streptaxid and helicarionid snails have shown a similar pattern (Sutcharit et al. 2020a; Man et al. 2022; Pholyotha et al. 2022). However, alternative forces of sympatric speciation and resource partitioning cannot be ignored. For example,

O. andersoniana and *O. stoliczkana* in Tanintharyi are sympatric based on this study. The lower abundance of one species compared to the co-occurring species may reflect the high level of competition (Table 1).

Despite the numbers of the Myanmar clausiliids are increasing, the taxonomic placements of some species are still questionable, for example, *Oospira gouldiana* and *O. insignis* which are morphologically highly variable and have overlapping distributions. Previous studies have attempted to reveal their differentiation, but this remains ambiguous (Stoliczka 1872; Gude 1914; Szekeres et al. 2021a, b). This work, therefore, provides baseline information for future studies, especially with respect to the phylogenetic interpretation of the short and ovate shell group that is endemic in Mon State and the long and slender shell group, with its wider distribution from Shan State to Kayin State and the Tanintharyi Region.

Alphabetical list of additional clausiliid taxa recorded from Myanmar

Below is an alphabetical list of 20 clausiliid species and subspecies belonging to the genera *Cylindrophaedusa*, *Indonenia* Ehrmann, 1927, *Oospira*, and *Phaedusa* that have been reported to occur in Myanmar, but that were not found during this study. The usages of each taxon name are provided in Grego et al. (2021) and Szekeres et al. (2021a, b). The original combination of the taxon name with reference to pages, plates, and/or figures that made the names available is mentioned. The type locality mentioned in the original publication and the distribution record in Myanmar is included. If possible, the modern name and/or regional names of the type locality are provided in square brackets. In addition, the unique name-bearing types (syntype, holotype, and lectotype) are illustrated; only for those that were unavailable or could not be located, the paratypes or paralectotypes or a representative specimen are given. Where necessary, remarks are given on the status of its nominal taxon, type specimens, and other necessary information.

1 *Cylindrophaedusa bacillum* (Hanley & Theobald, 1870)
Fig. 18D

Clausilia bacillum Hanley & Theobald, 1870: 12, pl. 24, fig. 1. Type locality: "Nanclai, Khasi Hills". Sowerby 1875: *Clausilia* pl. 6, species 48.
Clausilia (? *Medora*) *bacillum*–Blanford 1872: 200, pl. 9, fig. 3.
Clausilia (*Phaedusa*) *bacillum*–Tapparone-Canefri 1889: 328, 329. Gude 1914: 305.
Hemiphaedusa bacillum–Nordsieck 1973: 72, pl. 3, fig. 10.
Cylindrophaedusa (*Montiphaedusa*) *bacillum*–Szekeres et al. 2021a: 161, 162, fig. 3e.

Distribution. In Myanmar, this species is known from Schegoo (presumably Shwegu), Bhamo City in Kachin State; no further materials have been reported from Myanmar after its mention in Tapparone-Canefri (1889) and Gude (1914).

2 *Oospira arakana* (Stoliczka, 1872)
Fig. 18C

Clausilia arakana Stoliczka, 1872: 210, pl. 9, fig. 20. Type locality: "Mai-i in provincia Sandoway" [Mwa-ywa, Thandwe Township, Rakhine State]. Hanley and Theobald 1874: 48, pl. 118. figs 8, 9. Sowerby 1875: *Clausilia* pl. 9, species 78.
Clausilia (*Phaedusa*) *arakana*–Gude 1914: 312.
Oospira arakana–Nordsieck 1974: 47, fig. 8, pl. 2, fig. 8. Szekeres et al. 2021a: 165, fig. 4d.

Distribution. This species is probably endemic to Rakhine State, Myanmar.

3 *Oospira decollata* (Likharev, 1962)
Figs 17A, 18G

Pseudonenia decollata Likharev, 1962: 11–13, figs 1, 2. Type locality: "Nat Ma Taung, Chin State, Myanmar".
Oospira (*Oospira*) *decollata*–Nordsieck 2002b: 86. Nordsieck 2007: 23.
Oospira decollata decollata–Szekeres et al. 2021a: 168.

Distribution. This species was recorded from Nat Ma Taung, also called Victoria Mountain, Chin State, and as such it is the westernmost clausiliid species recorded in Myanmar. Another subspecies, *O. decollata muspratti* Grego & Szekeres, 2021 was recently reported from Naga Hills, India (Szekeres et al. 2021a).

4 *Oospira fusiformis* (Blanford, 1865)
Fig. 18I

Clausilia fusiformis Blanford, 1865: 80. Type locality: "Arakan Hill, west of Henzada" [Rakhine State or west of Hinthada Township, Ayeyarwady Region]. Hanley and Theobald 1870: 12, pl. 24, fig. 6. Sowerby 1875: *Clausilia* pl. 7, species 62.
Clausilia (*Phaedusa*) *fusiformis*–Gude 1914: 321.
Oospira fusiformis–Szekeres et al. 2021a: 169–171, fig. 6b, c.

Distribution. In Myanmar, this species is known from Rakhine State and Ayeyarwady Region, and also reported from the Bago Region (Gude 1914). In addition, *O. fusiformis* was recorded from 'Zwekabin Hill near Mawlamyine', which the current administration defines as Zwekabin Mountain in Hpa-an District, Kayin State; however, it was noted as dubious by Szekeres et al. (2021a: 171).

Remarks. Blanford (1865) described this species based on a single specimen and also noted that the examined specimen was an immature shell because the shell was thin, and the peristome not continuous. Later, Blanford (1872) provided a re-description based on a fully adult specimen received from W. Theobald that had a thickened, expanded, and continuous peristome.

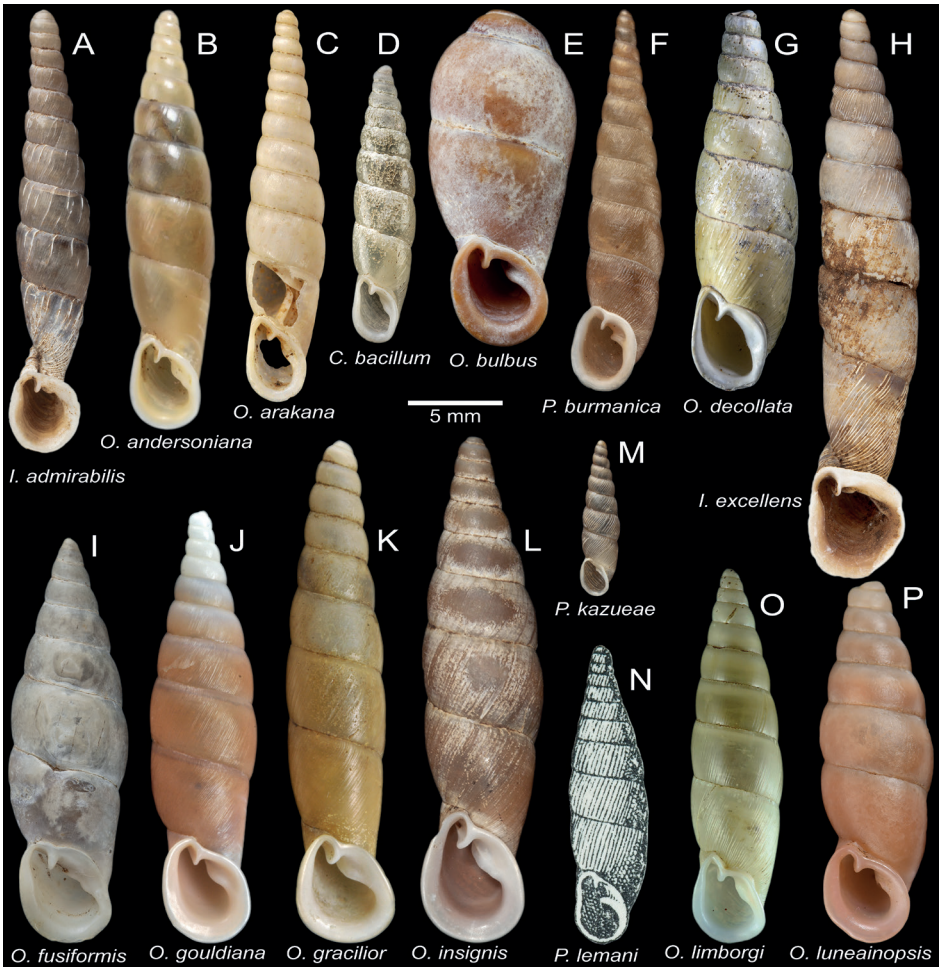

Figure 18. Synoptic view of the clausiliid species recorded from Myanmar **A** *Indonenia admirabilis*, holotype NHMUK 20200185 **B** *Oospira andersoniana*, specimen CUMZ 13054 **C** *Oospira arakana*, lectotype NHMUK 1888.12.4.1037 **D** *Cylindrophaedusa bacillum*, specimen NHMUK 1906.2.2.345 **E** *Oospira bulbus*, possible syntype NHMUK 1903.7.1.1278 **F** *Phaedusa burmanica*, holotype NHMUK 1888.12.4.1058 **G** *Oospira decollata*, paratype ZISP **H** *Indonenia excellens*, specimen NHMUK 20200189 **I** *Oospira fusiformis*, holotype NHMUK 1906.2.2.380 **J** *Oospira gouldiana*, lectotype NHMUK 196548 **K** *Oospira gracilior*, lectotype NHMUK 1907.12.30.243 **L** *Oospira insignis*, lectotype USNM 117120 **M** *Phaedusa kazueae*, holotype NHMUK 20200187 **N** *Phaedusa lemani* (after Gude, 1914: fig. 107) **O** *Oospira limborgi*, holotype NHMUK 1903.7.1.1266, and **P** *Oospira luneainopsis* sp. nov., holotype CUMZ 13062.

The specimen identified as *Oospira insignis* Szekeres et al. (2021a: 172, fig. 7a) is similar to *O. fusiformis* (Fig. 18I) in terms of shell morphology. Blanford (1872) also knew these similarities and suggested uniting the two species; however, further evidence from the shell and genitalia from topotypic specimens will be necessary to verify their species status.

5 *Oospira gracilior* (Hanley & Theobald, 1870)
Fig. 18K

Clausilia insignis var. *gracilior* Hanley & Theobald, 1870: 12, pl. 24, fig. 3. Type locality: "Burma, Moulmain" [Mawlamyine Township, Mon State, Myanmar].
Clausilia (*Phaedusa*) *gracilior*–Gude 1914: 318, 319, fig. 110.

Distribution. In Myanmar, this species is known from Mon State.

Remarks. Hanley and Theobald (1870) introduced this species as a variety of *O. insignis* but did not provide a description. Later Gude (1914) treated it as a separate species and made a complete re-description. We treat this taxon as a distinct species, following Gude (1914), because it clearly differs from *O. insignis* s.s. in being less ventricose, with blunt spire, and the aperture nearly triangular that is broader at its basis; however, no materials for this species have been recollected since the original description.

6 *Oospira insignis* (Gould, 1843)
Figs 17B, 18L

Clausilia insignis Gould, 1843: 140. Type locality: "Tavoy, British Burma" [Dawei, Tanintharyi Region, Myanmar]. Gould 1844: 458, pl. 24, fig. 8. Johnson 1964: 92, pl. 36, fig. 9.
Clausilia (*Phaedusa*) *insignis*–Gude 1914: 319.
Oospira insignis–Nordsieck 2021: 6, pl. 1, fig. 6. Szekeres et al. 2021a: 172, fig. 7a. Szekeres et al. 2021b: 41, fig. 1b.

Distribution. In Myanmar, this species is originally known from Dawei, Tanintharyi Region. Subsequent records were from Mon and Kayin states in Myanmar, and the range was further extended to include Tak and Kanchanaburi provinces in Thailand (Gude 1914; Szekeres et al. 2021a, b).

Remarks. *Oospira insignis* was the first clausiliid discovered from Myanmar, introduced by A.A. Gould based on specimens from the American missionary and naturalist Francis Mason (1799–1874). In the original description, Gould (1843) did not clearly state the number of examined specimens or the type specimen deposition. Later, Gould (1844) re-described this species with an illustration. When Johnson (1964) catalogued Gould's type specimen, he clearly designated the lectotype USNM 117120 as the unique name-bearing type. However, Nordsieck (2007: pl. 1, fig. 1) and Nordsieck (2021: pl. 1, fig. 6) illustrated a specimen BM(NH) 1996183 [=NHMUK] from the Cuming collection and used the term 'lectotype', but this seems invalid; recently, Szekeres et al. (2021a) designated this specimen as the lectotype. This specimen lot NHMUK 1996183a ex. Cuming collection consisted of three shells with no clear evidence that they originated from Gould's collection. Although Johnson (1964) catalogued Gould's type specimens in the Museum of Comparative Zoology, Harvard University, he stated that some unlocated types might presumably be deposited in the NHM, London, because Gould brought some specimens to compare to the Cuming collection. Presum-

ably, Nordsieck (2007) and Szekeres et al. (2021a) may have overlooked the previous lectotype designated by Johnson (1964), which clearly stated that the specimen USNM 117120 ex. Lea collection ex. Gould's collection consists of a single shell as the lectotype. Therefore, the USNM 117120 specimen is the sole name-bearing type of this species. The latter restriction of the lectotype by Nordsieck (2007) and Szekeres et al. (2021a) is invalid (ICZN, 1999: Art. 74.1). Additionally, the specimen NHMUK 1996183 is potentially a part of Gould's type series and is here recognized as the possible paralectotype.

7 *Oospira limborgi* Grego & Szekeres, 2021
Fig. 18O

Oospira limborgi Grego & Szekeres in Szekeres et al. 2021a: 172–174, fig. 7c. Type locality: "Tanintharyi Region, Myanmar".

Distribution. In Myanmar, this species is known only from Tanintharyi Region.

8 *Oospira malaisei* Nordsieck, 1973
Figs 17C, 19C

Oospira malaisei Nordsieck, 1973: 81, 82, pl. 3, fig. 3. Type locality: "Punkataung bei Myitkyina (3000 ft), NO-Birma" [near Punkataung, Myintkyina Township, Kachin State, Myanmar]. Szekeres et al. 2021b: 41–43.

Distribution. This species was introduced from Kachin State, and no subsequent materials have been recorded from Myanmar. Recently, provisionally classified specimens belonging to this species were reported from Mae Hong Son Province in Thailand (Szekeres et al. 2021b). In addition, it was further reported from Yunnan, China, and included in a molecular analysis (Hwang et al. 2022).

9 *Oospira mongmitensis* Grego & Szekeres, 2021
Fig. 19F

Oospira mongmitensis Grego & Szekeres in Szekeres et al. 2021b: 43, fig. 1d. Type locality: "Momeit" [Mongmit, Shan State, Myanmar].

Distribution. In Myanmar, this species is only known from Shan State.

10 *Oospira sardicola* Grego & Szekeres, 2021
Fig. 19I

Oospira sardicola Grego & Szekeres in Szekeres et al. 2021b: 46, 47, fig. 2c. Type locality: "Ruby Mines, Burmah" [around Mongmit, Shan State, Myanmar].

Distribution. In Myanmar, this species is only known from Shan State.

11 *Oospira vespa* (Gould, 1856)
Figs 17D, 19P

Clausilia vespa Gould, 1856: 13. Type locality: "Tavoy" [Dawei, Tanintharyi Region, Myanmar].
Clausilia (*Oospira*) *vespa*–Gude 1914: 336, fig. 116.
Oospira vespa–Szekeres et al. 2021a: 180, fig. 9c.

Distribution. In Myanmar, this species is known from Tanintharyi Region and Salween Valley (Sykes, 1893).

Remarks. *Oospira vespa* is the second clausiliid species introduced by Gould (1856). It was described based on a collection by the American naturalist, F. Mason, from Tavoy, British Burma. In the original publication, Gould (1856) provided only a brief description, without the arrangement and morphology of plicae, illustration, or number of examined specimens. Later, Johnson (1964) catalogued Gould's type specimens and found two specimens, which validly designated a specimen lot MCZ 169455 as the lectotype, which is figured herein (Fig. 17D).

While describing *Oospira stoliczkana* from Myanmar, Sykes (1893) re-described *O. vespa* based on a specimen from 'Salwin Valley'. Then, it was re-described based on Gould's original type series (Gude 1914). Between the two species, *O. vespa* can be distinguished from *O. stoliczkana* by having a more acute spire, and only five or six palatal plicae. In contrast, *O. stoliczkana* possesses a blunt spire, and 8 to 10 palatal plicae.

12 *Phaedusa kazueae* Hunyadi & Szekeres, 2021
Fig. 18M

Phaedusa kazueae Hunyadi & Szekeres in Grego et al. 2021: 25–27, fig. 5b. Type locality: "Montawa Cave, SW of Taunggyi, Shan State, Myanmar".

Distribution. In Myanmar, this species is only known from Shan State.

13 *Phaedusa lemani* (Gude, 1914)
Fig. 18N

Clausilia (*Phaedusa*) *lemani* Gude, 1914: 313, 314, fig. 107. Type locality: "Arakan, Burma" [Rakhine State, Myanmar].

Distribution. In Myanmar, this species is only known from Rakhine State and no further materials have been mentioned to date.

14 *Phaedusa lypra* (Mabille, 1887)
Fig. 19A

Clausilia lypra Mabille, 1887: 117. Type locality: "Tonkin" [Vietnam].

Phaedusa (*Phaedusa*) *lypra*–Nordsieck 2002b: 88.
Phaedusa lypra–Grego et al. 2021: 27, fig. 5c. Szekeres et al. 2021a: 183, fig. 10e, f.

Distribution. In Myanmar, this species is known from Shan State and Mandalay Region (Grego et al. 2021). *Phaedusa lypra* has a wide geographical distribution, ranging from China to Thailand, Vietnam, and India (Szekeres et al. 2021a).

15 *Phaedusa theobaldi* (Blanford, 1872)
Fig. 19M

Clausilia (? *Medora*) *theobaldi* Blanford, 1872: 201, pl. 9, fig. 5. Type locality: "Tonghu in provincia Barmana" [Taungoo Township, Bago Region, Myanmar].
Clausilia (*Phaedusa*) *theobaldi*–Gude 1914: 310.
Phaedusa theobaldi–Nordsieck 1974: 45, fig. 4, pl. 2, figs 1, 2. Grego et al. 2021: 27, fig. 5d. Szekeres et al. 2021a: 185, fig. 11c–e.

Distribution. In Myanmar, this species was first known from Bago Region. Later, the range was expanded records from Rakhine and Kayah States in Myanmar and from Thailand (Gude 1914; Grego et al. 2021; Szekeres et al. 2021b).

16 *Phaedusa bocki thompsoni* Grego & Szekeres, 2021
Fig. 19N

Phaedusa bocki thompsoni Grego & Szekeres in Szekeres et al. 2021b: 46, fig. 2d. Type locality: "Doi Tung, Chiang Rai Province, Thailand".

Distribution. In Myanmar, a single specimen was recorded in Shan State (Szekeres et al. 2021a). This subspecies was originally described from northern Thailand with several specimens.

17 *Indonenia admirabilis* Grego & Szekeres, 2021
Fig. 18A

Indonenia admirabilis Grego & Szekeres in Grego et al. 2021: 22, figs 2b, 3, 4. Type locality: "Phruno River Cave, Maw Ti Do, Hpruso District, Kayah State, Myanmar". Szekeres et al. 2021a: 157, fig. 2a.

Distribution. In Myanmar, this species is only known from Kayah State.

18 *Indonenia excellens* (Nordsieck, 2002)
Fig. 18H

Tropidauchenia (*Indonenia*) *excellens* Nordsieck, 2002a: 16, fig. 6. Type locality: "Karen Mountains, 1200–1300m" [Kayin or Kayah State, Myanmar].

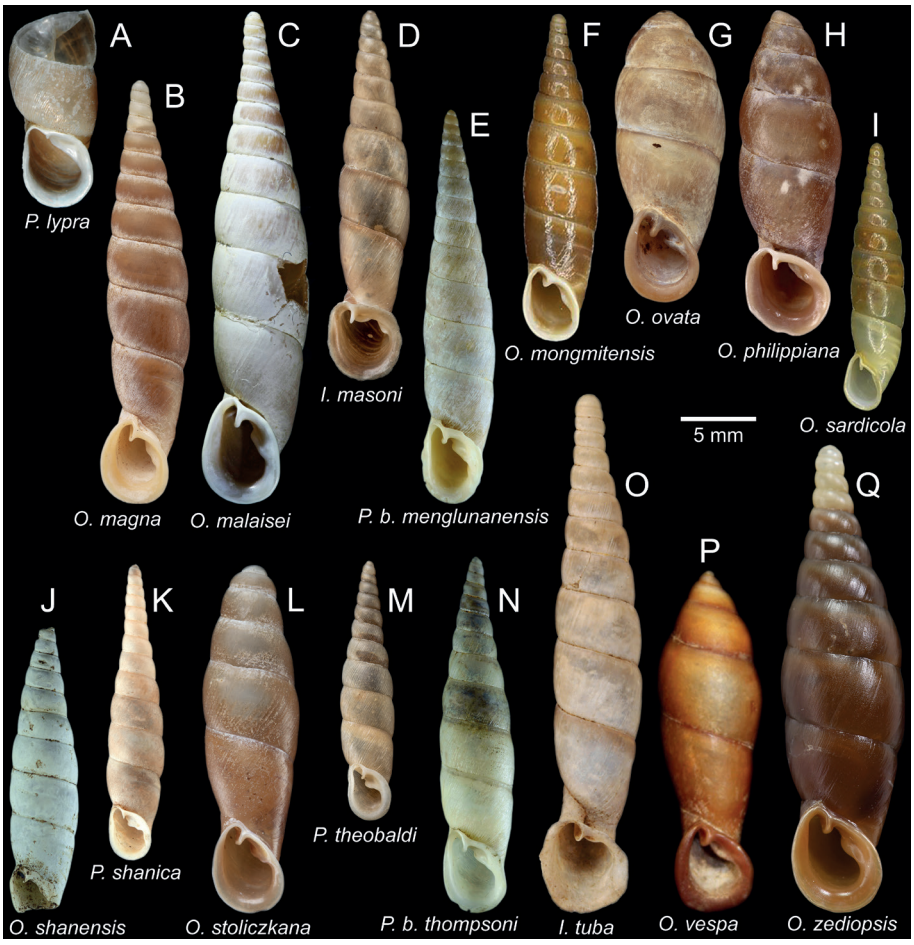

Figure 19. Synoptic view of the clausiliid species recorded from Myanmar **A** *Phaedusa lypra*, syntype MNHN-IM-2000-2502-7 **B** *Oospira magna*, lectotype NHMUK 1901.3.17.156 **C** *Oospira malaisei*, holotype SMNH 3014 **D** *Indonenia masoni*, lectotype NHMUK 1888.12.4.1034 **E** *Phaedusa bocki menglunanensis*, specimen NHMUK 1903.7.1.3652 **F** *Oospira mongmitensis*, holotype UF 117571 (after Szekeres et al. 2021b: fig. 1d) **G** *Oospira ovata*, lectotype NHMUK 1906.2.2.378 **H** *Oospira philippiana*, possible syntype SMF 62294/1 **I** *Oospira sardicola*, holotype UF 117570 (after Szekeres et al. 2021b: fig. 2c) **J** *Oospira shanensis*, holotype NHMUK 1903.7.1.3544 **K** *Phaedusa shanica*, lectotype SMF 62260 **L** *Oospira stoliczkana*, holotype NHMUK 1888.12.4.1031 **M** *Phaedusa theobaldi*, lectotype NHMUK 1888.12.4.1056 **N** *Phaedusa bocki thompsoni*, specimen NHMUK 1903.7.1.1163 **O** *Indonenia tuba*, lectotype NHMUK 1907.12.30.241 **P** *Oospira vespa*, paralectotype MCZ 169456 and **Q** *Oospira zediopsis* sp. nov., holotype CUMZ 13064. Photo: P. Maestrati, MNHN (**A**), A Persson, SMNH (**C**).

Indonenia excellens–Nordsieck 2007: 37, pl. 6, fig. 4. Szekeres et al. 2021a: 157, fig. 2b, c.

Distribution. In Myanmar, this species is known from Kayin or Kayah States, originally given type locality was uncertain. Recently, it was reported from Shan State (Grego et al. 2021).

19 *Indonenia masoni* (Theobald, 1864)
Fig. 19D

Clausilia masoni Theobald, 1864: 246. Type locality: "Tonghu" [Taungoo Township, Bago Region, Myanmar]. Hanley and Theobald 1870: 12, pl. 24, fig. 8. Sowerby 1875: *Clausilia* pl. 8, species 69.
Clausilia (? *Nenia*) *masoni*–Blanford 1872: 206, pl. 9, fig. 18.
Clausilia (*Garnieria*) *masoni*–Gude 1914: 331.
Indonenia masoni–Nordsieck 2007: 37. Szekeres et al. 2021a: 157, fig. 2d.

Distribution. In Myanmar, this species is only known from Bago Region.

20 *Indonenia tuba* (Hanley, 1868)
Fig. 19O

Clausilia tuba Hanley, 1868: 343. Type locality: "Shan, province" [Shan State, Myanmar]. Hanley and Theobald 1870: 12, pl. 24, fig. 9. Sowerby 1875: *Clausilia* pl. 8, species 72.
Clausilia (*Garnieria*) *tuba*–Gude 1914: 331, fig. 115.
Indonenia tuba–Szekeres et al. 2021a: 157–159, fig. 2e, f.

Distribution. In Myanmar, this species is known from Shan State and the Upper Salween Valley (Hanley 1868).

Acknowledgements

The senior author is grateful to all members of the Animal Systematics Research Unit (ASRU), Chulalongkorn University for their kind help during field trips in Myanmar. The authors are indebted to AJ Baldinger (MCZ, Massachusetts), V. Héros and P Maestrati (project ERECOLNAT: ANR-11-INBS-0004, MNHN, Paris); J Ablett, F Naggs, and H Taylor (NHM, London), R Janssen, K-O Nagel, and S Hof (SMF, Frankfurt), A Persson (SMNH, Stockholm), J Slapcinsky (UF, Florida), PV Kijashko (ZISP, St. Petersburg), B. Páll-Gergely (Centre for Agricultural Research, Budapest), and D Mierzwa-Szymkowiak (Museum and Institute of Zoology, Warsaw) for kindly providing the authors with the shell photographs of material housed in the type collections. The work in Thailand was funded by the Thailand Research Fund (TRF-DPG628001), Center of Excellence on Biodiversity (BDC-PG4-163008) and additional support by CU-ASEAN Scholarships and the 90th Anniversary of Chulalongkorn University Fund to NSM. The field trips in Myanmar were partially funded through grants received from FFI and TRF-RTA 5880002. We thank the personnel of the Apache Cement Company for sponsoring our surveys in the Mandalay Region. We also thank the Ministry of Natural Resources and the Environmental Conservation Forest Department for the collection and export permits. We also express our gratitude for the comments from reviewers that improved the manuscript and to DJ Anderson for linguistic polishing.

References

Adams H, Adams A (1855 [1854–1858]) The Genera of Recent Mollusca; Arranged according to their Organization (Vol. 2). van Voorst, London, 661 pp. [Published in parts: Vol. 2: 93–284 (1855)]

Albers JC (1860) Die Heliceen, nach Natürlicher Verwandtschaft Systematisch Geordnet. Zweite Ausgabe, nach dem Hinterlassenen Manuskript Besorgt, von Eduard Von Martens. Wilhelm Engelmann, Leipzig, 359 pp. https://doi.org/10.5962/bhl.title.11218

Alcock A (1902) John Anderson, FRS. Proceedings of the Asiatic Society of Bengal [1901]: 40–44.

American Veterinary Medical Association (2020) AVMA Guidelines for the Euthanasia of Animals: 2020 Edition. https://www.avma.org/sites/default/files/2020-01/2020-EuthanasiaFinal-1-17-20

Benson WH (1863) Characters of new land-shells from the Andaman Islands, Burmah, and Ceylon, and of the animal of *Sophina*. Annals and Magazine of Natural History, Series 3 11(65): 318–323. https://doi.org/10.1080/00222936308681435

Blanford WT (1865) Contributions to Indian malacology, 5. Descriptions of new land shells from Arakan, Pegu, and Ava; with notes on the distribution of described species. Journal of the Asiatic Society of Bengal 34: 66–105.

Blanford WT (1872) Monograph of Himalayan, Assamese, Burmese and Cingalese *Clausilia*. Journal of the Asiatic Society of Bengal 41: 199–206.

Boettger O (1877) Clausilienstudien. Paleontographica (Neue Folge) (Supplement 3), Leipzig 6/7: 1–122. https://doi.org/10.5962/bhl.title.11463

Boettger O (1878) Systematisches Verzeichnis der lebenden Arten der Landschnecken-Gattung *Clausilia* Drap. Mit ausführlicher Angabe der geographischen Verbreitung der einzelnen Species. Bericht über die Thätigkeit des Offenbacher Vereins für Naturkunde 17/18: 18–101.

Bui TC, Szekeres M (2019) A new species of the genus *Oospira* Blanford, 1872 (Gastropoda, Pulmonata, Clausiliidae) from central Vietnam. Ruthenica 29(4): 185–189. https://doi.org/10.35885/ruthenica.2019.29(4).3

Chen DN, Zhang GQ (1999) Fauna Sinica: Mollusca, Gastropoda, Pulmonata, Stylommatophora, Clausiliidae. Science Press, Beijing, 210 pp. [In Chinese]

Chen YX, Tian M, Fan B (2016) Terrestrial Molluscs in Yunnan. China Science Publishing, Beijing, 276 pp. [In Chinese]

De Mattia W, Fehér Z, Mason K, Haring E (2020) An integrative approach to the taxonomy and systematics within the genus *Montenegrina* Boettger, 1877 (Mollusca, Gastropoda, Clausiliidae). Journal of Zoological Systematics and Evolutionary Research 58(3): 691–808. https://doi.org/10.1111/jzs.12407

De Mattia W, Reier S, Haring E (2021) Morphological investigation of genital organs and first insights into the phylogeny of the genus *Siciliaria* Vest, 1867 as a basis for a taxonomic revision (Mollusca, Gastropoda, Clausiliidae). ZooKeys 1077: 1–175. https://doi.org/10.3897/zookeys.1077.67081

Fehér Z, Mason K, Szekeres M, Haring E, Bamberger S, Páll-Gergely B, Sólymos P (2018) Range-constrained co-occurrence simulation reveals little niche partitioning among rock-

dwelling *Montenegrina* land snails (Gastropoda: Clausiliidae). Journal of Biogeography 45(6): 1444–1457. https://doi.org/10.1111/jbi.13220

Giokas S, Pafilis P, Valakos E (2005) Ecological and physiological adaptations of the land snail *Albinaria caerulea* (Pulmonata: Clausiliidae). The Journal of Molluscan Studies 71(1): 15–23. https://doi.org/10.1093/mollus/eyi001

Gittenberger E, Vermeulen JJ (2001) *Oospira* (*O.*) *pyknosoma* spec. nov. (Gastropoda, Pulmonata, Clausiliidae) an impressive clausiliid species from Vietnam. Basteria 65: 123–129.

Gittenberger E, Hamann TD, Asami T (2012) Chiral speciation in terrestrial pulmonate snails. PLoS ONE 7(4): e34005. https://doi.org/10.1371/journal.pone.0034005

Gittenberger E, Leda P, Sherub S, Gyeltshen C (2019) The subfamily Phaedusinae in Bhutan (Gastropoda, Pulmonata, Clausiliidae). Basteria 83(4–6): 133–144.

Godwin-Austen HH (1888) On some land-molluscs from Burmah, with description of some new species. Proceedings of the Zoological Society of London 56(1): 240–245. https://doi.org/10.1111/j.1469-7998.1888.tb06701.x

Gould AA (1843) Shells not long since announced as having been received from the Rev. Francis Mason, missionary at Tavoy, in British Burmah. Proceedings of the Boston Society of Natural History 1: 139–141.

Gould AA (1844) Description of land shells from the province of Tavoy, in British Burmah. Boston Journal of Natural History 4: 452–459.

Gould AA (1856) Descriptions of new species of shells. Proceedings of the Boston Society of Natural History 6: 11–16. www.biodiversitylibrary.org/page/9493210

Gray JE (1855) Catalogue of Pulmonata or Air-Breathing Mollusca in the Collection of the British Museum, Part I. Taylor and Francis, London, 192 pp.

Grego J, Hunyadi A, Szekeres M (2021) New and little-known species of Southeast Asian Clausiliidae (Gastropoda: Pulmonata). Journal of Conchology 44: 21–29.

Gude GK (1914) The Fauna of British India, Including Ceylon and Burma. Mollusca, II. Taylor and Francis, London, 520 pp.

Hanley S (1868) Description of a rare new Indian *Clausilia*. Annals and Magazine of Natural History, Series 4 1(5): e343. hhttps://doi.org/10.1080/00222936808695710

Hanley S, Theobald W (1870–1876) Conchologica Indica: Illustrations of the Land and Freshwater Shells of British India. Reeve, London, 160 pp. https://doi.org/10.5962/bhl.title.14456

Hausdorf B (2022) Phylogeny and biogeography of extant and extinct *Fusulus* (Stylommatophora: Clausiliidae). Journal of Molluscan Studies 88(3): eyac023. https://doi.org/10.1093/mollus/eyac023

Hausdorf B, Neiber MT (2022) Phylogeny and evolution of the land snail tribe Clausiliini (Gastropoda: Clausiliidae). Molecular Phylogenetics and Evolution 175: e107562. https://doi.org/10.1016/j.ympev.2022.107562

Hwang CC, Ger MJ, Wu SP (2022) Within-island diversification in the land snail genus *Formosana* (Gastropoda, Clausiliidae) in Taiwan. Zoologica Scripta 51(5): 562–588. https://doi.org/10.1111/zsc.12557

International Commission on Zoological Nomenclature (ICZN) (1999) International Code of Zoological Nomenclature (4th Edn.). International Trust for Zoological Nomenclature, London, 306 pp.

Johnson RI (1964) The recent Mollusca of Augustus Addison Gould: Illustrations of the types described by Gould with a bibliography and catalog of his species. Bulletin – United States National Museum 239: 1–182. https://doi.org/10.5479/si.03629236.239

Kobelt W (1880 [1879–1881]) Illustrirtes Conchylienbuch, 2. Bauer and Raspe, Nürnberg, 145–391.

Koch EL, Neiber MT, Walther F, Hausdorf B (2017) High gene flow despite opposite chirality in hybrid zones between enantiomorphic door snails. Molecular Ecology 26(15): 3998–4012. https://doi.org/10.1111/mec.14159

Küster HC (1850 [1844–1862]) Die Schliessschnecken und die verwandten Gattungen (*Clausilia*, *Balea*, *Cylindrella*, *Megaspira*): In Abbildungen nach der Naturmit Beschreibungen. Systematisches Conchylien-Cabinet von Martini und Chemnitz 1(14): 1–355. [pls 1–38. [pp. 33–72, pls 5, 9, 11 (1850); pp. 89–150 (1853)]]

Likharev IM (1962) A new species of the Clausiliidae (Gastropoda, Pulmonata) from Burma. Trudy Zoologicheskogo Instituta Akademii Nauk S.S.S.R. 30: 11–13. [in Russian]

Loosjes FE (1953) Monograph of the Indo-Australian Clausiliidae. Beaufortia 31: 1–226.

Luo TC, Chen DN, Zhang GQ (1998) On three new species of Clausiliidae from China (Pulmonata: Stylommatophora: Clausiliidae: Phaedusinae). Guizhou Science 16: 31–35. [in Chinese]

Maassen WJM, Gittenberger E (2007) Three new clausiliid land snails from Tonkin, northern Vietnam (Gastropoda: Pulmonata: Clausiliidae). Zoölogische Mededeelingen 81: 175–186.

Mabille J (1887) Sur quelques mollusques du Tonkin. Bulletins de la Société Malacologique de France 4: 73–164.

Mamos T, Uit de Weerd DU, von Oheimb PV, Sulikowska-Drozd A (2021) Evolution of reproductive strategies in the species-rich land snail subfamily Phaedusinae (Stylommatophora: Clausiliidae). Molecular Phylogenetics and Evolution 158: 1–8. https://doi.org/10.1016/j.ympev.2020.107060

Man NS, Siriboon T, Lin A, Sutcharit C, Panha S (2022) Revision of the carnivorous land snail family Streptaxidae (Stylommatophora, Achatinina) in Myanmar, with description of four new species. ZooKeys 1110: 39–102. https://doi.org/10.3897/zookeys.1110.85399

Möllendorff OF (1882) Descriptions of some new Asiatic *Clausilia*. Journal of the Asiatic Society of Bengal 51(2): 12–13.

MolluscaBase [Eds] (2022) MolluscaBase. *Oospira* W. T. Blanford, 1872. https://www.molluscabase.org/aphia.php [Accessed on 3 September 2022]

Motochin R, Wang M, Ueshima R (2017) Molecular phylogeny, frequent parallel evolution, and new system of Japanese clausiliid land snails (Gastropoda: Stylommatophora). Zoological Journal of the Linnean Society 181(4): 795–845. https://doi.org/10.1093/zoolinnean/zlx023

Nevill G (1878) Hand List of Mollusca in the Indian Museum, Calcutta. Part I. Gastropoda, Pulmonata and Prosobranchia-Neurobranchia. Calcutta, 338 pp. https://doi.org/10.5962/bhl.title.11957

Nordsieck H (1973) Zur Anatomie und Systematik der Clausilien, 12. Phaedusinae, 1: Phaedusen aus Nepal und ihre systematische Stellung innerhalb der Unterfamilie. Archiv für Molluskenkunde 103: 63–85.

Nordsieck H (1974) Zur Anatomie und Systematik der Clausilien, 14. Phaedusinae, 2: *Phaedusa bhutanensis* n. sp. und ihre Beziehungen zu benachbarten Arten. Archiv für Molluskenkunde 104: 41–49.

Nordsieck H (2002a) Revision of the Garnieriinae (Gastropoda: Stylommatophora: Clausiliidae), with descriptions of new taxa. Stuttgarter Beiträge zur Naturkunde (Ser. A) 640: 1–23.

Nordsieck H (2002b) Annotated checklist of the Southeast Asian Phaedusinae, with the description of new taxa (Gastropoda, Pulmonata, Clausiliidae). Basteria 66: 85–100.

Nordsieck H (2007) Worldwide Door Snails. ConchBooks, Hackenheim, 214 pp.

Nordsieck H (2011) Clausiliidae of Vietnam with the description of new taxa (Gastropoda: Stylommatophora). Archiv für Molluskenkunde 140(2): 149–173. https://doi.org/10.1127/arch.moll/1869-0963/140/149-173

Nordsieck H (2018) The door snail from the banana tree in Laos (Gastropoda, Stylommatophora, Clausiliidae, Phaedusinae). Conchylia 48(3–4): 47–50.

Nordsieck H (2021) Taxonomic important shell characters of Asiatic Phaedusinae (Gastropoda, Stylomatophota, Clausiliidae). Acta Conchyliorum 20: 1–56.

Olson DM, Dinerstein E, Wikramanayake ED, Burgess ND, Powell GV, Underwood EC, D'amico JA, Itoua I, Strand HE, Morrison JC, Loucks CJ, Allnutt TF, Ricketts TH, Kura Y, Lamoreux JF, Wettengel WW, Hedao P, Kassem KR (2001) Terrestrial Ecoregions of the World: A New Map of Life on Earth A new global map of terrestrial ecoregions provide an innovative tool for conserving biodiversity. Bioscience 51(11): 933–938. https://doi.org/10.1641/0006-3568(2001)051[0933:TEOTWA]2.0.CO;2

Páll-Gergely B, Szekeres M (2017) New and little-known Clausiliidae (Gastropoda: Pulmonata) from Laos and southern Vietnam. Journal of Conchology 42: 507–521.

Páll-Gergely B, Szekeres M (2020) A revision of the genus *Sumelia* Neubert, 1995 (Gastropoda: Eupulmonata: Clausiliidae) with the introduction of a new genus and a subgenus. Journal of Conchology 43(5): 449–459.

Pfeiffer L (1841) Symbolae ad historiam Heliceorum. Sectio prima. Fischer, Kassel 1: 1–88. https://doi.org/10.5962/bhl.title.11903

Pfeiffer L (1842) Symbolae ad historiam Heliceorum. Sectio prima. Fischer, Kassel 2: 1–147. https://doi.org/10.5962/bhl.title.11903

Pfeiffer L (1847) Diagnosen neuer Heliceen. Zeitschrift für Malakozoologie 4(5): 65–71.

Pfeiffer L (1856) Versuch einer Anordnung der Heliceen nach natürlichen Gruppen. Malakozoologische Blätter 2: 112–185.

Pfeiffer L (1857) Diagnosen interessanter Novitäten. Malakozoologische Blätter 3(17): 256–261.

Pfeiffer L (1860) Novitates Conchologicae. Series prima, Mollusca extramarina. Beschreiber und Abbildung, neuer oder kritischer Land-und Süsswasser-Mollusken. Fischer, Kassel 1: 121–138. [pls. 34–36.]

Pfeiffer L (1868) Monographia Heliceorum Viventium. Brockhaus, Leipzig 6: 1–598.

Pfeiffer L (1877) Monographia Heliceorum Viventium. Brockhaus, Leipzig 8: 1–729.

Pfeiffer L, Clessin S (1881) Nomenclator Heliceorum Viventium: quo Continetur Nomina Omnium Hujus Familiae Generum et Specierum Hodie Cognitarum, Disposita ex Affinitate Naturali. Fischer, Kassel, 617 pp.

Pholyotha A, Sutcharit C, Tongkerd P, Lin A, Panha S (2020) Taxonomic revision of the land snail genera *Macrochlamys* Gray, 1847 and *Sarika* Godwin-Austen, 1907 (Eupulmonata: Ariophantidae) from south-eastern Myanmar, with descriptions of three new species. Molluscan Research 40(2): 183–204. https://doi.org/10.1080/13235818.2020.1723041

Pholyotha A, Sutcharit C, Lin A, Panha S (2022) Uncovering local endemism from southeastern Myanmar: Description of the new karst-associated terrestrial snail genus *Burmochlamys* (Eupulmonata, Helicarionidae). ZooKeys 1110: 1–37. https://doi.org/10.3897/zookeys.1110.82461

Preece RC, White TS, Raheem DC, Ketchum H, Ablett J, Taylor H, Webb K, Naggs F (2022) William Benson and the origins of the golden age of malacology in British India: Biography, illustrated catalogue and evaluation of his molluscan types. Tropical Natural History (Supplement 6): 1–434.

Schileyko AA (2000) Treatise on recent terrestrial pulmonate molluscs, Part 5: Clausiliidae. Ruthenica (Supplement 2): 565–729.

Schileyko AA (2011) Checklist of land pulmonate molluscs of Vietnam (Gastropoda: Stylommatophora). Ruthenica 21: 1–68.

Sowerby GB (1875) Conchologia Iconica: or Illustration of the shells of molluscous animals Volume 20. Monograph of the genus *Clausilia*, plates 1–17.

Stoliczka F (1871) Notes on terrestrial Mollusca from the neighbourhood of Moulmein (Tenasserim Provinces), with descriptions of new species. Journal of the Asiatic Society of Bengal 40: 143–177.

Stoliczka F (1872) Postscript to the monograph of Himalayan and Burmese Clausiliae. Journal of the Asiatic Society of Bengal 41: 207–210.

Stoliczka F (1873) On the land-shells of Penang Island, with descriptions of the animals and anatomical notes; part second, Helicacea. Journal of the Asiatic Society of Bengal 42: 11–38.

Sulikowska-Drozd A, Maltz TK, Janiszewska K (2022) Flexible embryonic shell allies large offspring size and anti-predatory protection in viviparous snails. Scientific Reports 12(1): e17881. https://doi.org/10.1038/s41598-022-22651-w

Sutcharit C, Panha S (2021) Systematic review of the dextral *Hemiplecta* Albers, 1850 (Eupulmonata, Ariophanitdae) from Thailand with description of a new species and list of all the Indochinese species. ZooKeys 1047: 101–154. https://doi.org/10.3897/zookeys.1047.65735

Sutcharit C, Jeratthitikul E, Pholyotha A, Lin A, Panha S (2020a) Molecular phylogeny reveals high diversity and endemism in the limestone karst-restricted land snail genus *Sophina* Benson, 1859 from Myanmar (Eupulmonata: Helicarionidae), with description of four new species. Journal of Zoological Systematics and Evolutionary Research 58(4): 957–981. https://doi.org/10.1111/jzs.12420

Sutcharit C, Lin A, Panha S (2020b) Two new species of the carnivorous snail genus *Discartemon* from Thailand and Myanmar (Eupulmonata: Streptaxidae). The Raffles Bulletin of Zoology (Supplement 35): 149–155.

Sykes ER (1893) On *Clausilia vespa*, Gould, and its allies. The Conchologist 2: 165–167.

Szekeres M, Grego J, Páll-Gergely B, Ablett JD (2021a) Clausiliidae (Gastropoda; Pulmonata) from India, Myanmar, Pakistan, and Sri Lanka in the collection of the Natural History Museum, London. Journal of Conchology 44: 155–187.

Szekeres M, Grego J, Slapcinsky J (2021b) Clausiliidae (Mollusca: Gastropoda: Pulmonata) from Continental Southeast Asia in the collection of the Florida Museum of Natural History. Bulletin of the Florida Museum of Natural History 58: 39–50.

Tapparone-Canefri C (1889) Viaggio di Leonardo Fea in Birmania e regioni vicine. Xviii. Molluschi terrestri e ďacqua dolce. Annali del Museo Civico di Storia Naturale di Genova, Series 2 7: 295–365.

Theobald W (1864) Notes on the variation of some Indian and Burmese Helicidae, with an attempt at their re-arrangement, together with descriptions of new Burmese Gastropoda. Journal of the Asiatic Society of Bengal 33: 238–250.

Thiele J (1931 [1929–1935]) Handbuch der Systematischen Weichtierkunde. Gustav Fischer, Jena, 1134 pp. [pp. 1–376 (1929); pp. 377–778 (1931); pp. 779–1022 (1934); pp. 1023–1134 (1935)]

Uit de Weerd DR, Gittenberger E (2013) Phylogeny of the land snail family Clausiliidae (Gastropoda, Pulmonata). Molecular Phylogenetics and Evolution 67(1): 201–216. https://doi.org/10.1016/j.ympev.2013.01.011

Wagner AJ (1922) Ergänzungen und Erläuterungen zur Systematik der Clausiliiden. Annales Zoologici Musei Polonici Historiae Naturalis 1(2/3): 96–111.

Zilch A (1954) Die Typen und Typoide des Natur-Museums Senckenberg, 12: Mollusca, Clausiliidae (1): Phaedusinae, Neniinae. Archiv für Molluskenkunde 83: 1–63.

Zilch A (1959) Gastropoda, Euthyneura. In: Schinderwolf OH (Ed.) Handbuch der Paläozoologie. Gebrüder Borntraeger, Berlin 6: 1–400.

ZooKeys 1160: 61–74 (2023)
doi: 10.3897/zookeys.1160.103417
https://zookeys.pensoft.net

RESEARCH ARTICLE

A peer-reviewed open-access journal
ZooKeys
Launched to accelerate biodiversity research

Two new Palaearctic species of *Xynobius* Foerster (Hymenoptera, Braconidae, Opiinae)

Yunjong Han[1*], Cornelis van Achterberg[2*], Heung-Sik Lee[3], Hyojoong Kim[1]

1 *Animal Systematics Laboratory, Department of Biological Science, Kunsan National University, Gunsan, 54150, Republic of Korea* **2** *Naturalis Biodiversity Center, P.O. 9517, 2300 RA Leiden, Netherlands* **3** *Animal and Plant Quarantine Agency, Gimcheon, 39660, Republic of Korea*

Corresponding author: Hyojoong Kim (hkim@kunsan.ac.kr)

Academic editor: J. Fernandez-Triana | Received 13 March 2023 | Accepted 14 April 2023 | Published 3 May 2023

https://zoobank.org/B658A31C-AA99-4F8D-B851-A5C4FB955F95

Citation: Han Y, van Achterberg C, Lee H-S, Kim H (2023) Two new Palaearctic species of *Xynobius* Foerster (Hymenoptera, Braconidae, Opiinae). ZooKeys 1160: 61–74. https://doi.org/10.3897/zookeys.1160.103417

Abstract

Two new and very similar species of the genus *Xynobius* Foerster, 1863 are described and illustrated, *X. subparallelus* Han & van Achterberg, **sp. nov.** from Japan (Honshu) and *X. setosiscutum* van Achterberg, **sp. nov.** from Norway. Three species are newly reported from Norway: *Xynobius aciculatus* (Thomson, 1895), *X. comatus* (Wesmael, 1835), and *X. polyzonius* (Wesmael, 1835). *X. polyzonius* (Wesmael, 1835) and *X. sapporanus* (Fischer, 1963) are new combinations. Identification keys to the *Xynobius* species known from Norway and Japan are added.

Keywords

Japan, key, new species, Norway, parasitoid, setose mesoscutum

Introduction

Opiinae is a large subfamily of the family Braconidae with approximately 2,000 valid species and 39 genera according to Yu et al. (2016). It is a common group of parasitoid wasps containing mainly mining or fruit-infesting dipterous larvae and has a world-wide distribution. Wharton (e.g. 1987, 1988, 1997) published important updates and

* Contributed equally as the first authors.

some additions for the existing keys to the genera of Opiinae, but the number of genera remains a matter of discussion because the limits of some genera, especially of *Opius* Wesmael, 1835 and *Eurytenes* Foerster, 1863, are uncertain. We follow Li et al. (2013) and treat the genus *Xynobius* Foerster, 1863 as a valid genus separate from *Opius* Wesmael, 1835, not included within it as was done in the past.

During a visit to Osaka Museum of Natural History the first author discovered a remarkably setose species from Japan (Honshu), and the second author discovered a similar species from south-west Norway among Malaise-trap material. These new taxa are compared, described, and illustrated below.

Material and method

The Japanese specimen was collected by using a sweep net. The Norwegian specimens were collected in a Malaise trap and were chemically treated with a mixture of xylene + alcohol 96% and amylacetate (AXA-method; van Achterberg 2009). For identification of the subfamily Opiinae, see van Achterberg (1990, 1993, and 1997); for references to the Opiinae, see Yu et al. (2016).

Morphological terminology follows van Achterberg (1988, 1993), including the abbreviations for the wing venation. Measurements are taken as indicated by van Achterberg (1988); for the length and the width of a body part the maximum length and width is taken, unless otherwise indicated. The length of the mesosoma is measured from the anterior border of the mesoscutum up to the apex of the propodeum and of the first tergite from the posterior border of the adductor up to the medio-posterior margin of the tergite.

Observations, photographic images, and descriptions were made either under a digital stereo microscope (VHX-1000, Keyence) or with a Canon 5Ds 50.6-megapixel camera combined with a Canon MP-E 65 mm f/2.8 1–5× macro lens, Laowa KX-800 macro twin flash, and an electronic WeMacro Z-stepper rail. The photos were stacked with Helicon Focus v. 7 software (HeliconSoft, Kharkiv, Ukraine).

The type specimens are deposited in the Osaka Museum of Natural History (**OMNH**) at Osaka, Naturalis Biodiversity Center (**RMNH**) at Leiden and Museum Stavanger (MSC) at Stavanger.

Systematics

Genus *Xynobius* Foerster, 1863
Figs 1–11

Xynobius Foerster, 1863: 235. Type species (by original designation): *Xynobius pallipes* Foerster, 1863 (= *Opius caelatus* Haliday, 1837).

Aclisis Foerster, 1863: 267. Type species (by original designation): *Aclisis isomera* Foerster, 1863 (= *Opius caelatus* Haliday, 1837). Synonymized by Fischer (1972).

Holconotus Foerster, 1863: 259 (not Schmidt-Göbel 1846). Type species (by original designation): *Opius comatus* Wesmael, 1835). Synonymized by van Achterberg (2004).

Aulonotus Ashmead, 1900: 368 (new name for *Holconotus* Foerster). Type species (by original designation): *Opius comatus* Wesmael, 1835). Synonymized by Tobias and Jakimavicius (1986).

Eristernaulax Viereck, 1913: 362. Type species (by original designation): *Eristernaulax leucotaenia* Viereck, 1913). Synonymized by van Achterberg (2004).

Stigmatopoea Fischer, 1984: 610, 611 (as subgenus of *Opius* Wesmael), 1998: 25 (key to species); Wharton 1988: 356; 2006: 338 (as subgenus of *Eurytenes* Foerster, 1863; possible paraphyly in *Xynobius*). Type species (by original designation): *Opius macrocerus* Thomson, 1895. Synonymized by van Achterberg (2004).

Xynobiotenes Fischer, 1998: 23 (as subgenus of *Eurytenes* Foerster, 1863). Type species (by original designation): *Opius scutellatus* Fischer, 1962. Synonymized by Li et al. (2013).

***Xynobius subparallelus* Han & van Achterberg, sp. nov.**

https://zoobank.org/ED84A031-AD98-4616-943A-9895E5BF4AF6

Type material. ***Holotype***, ♀ (OMNH), "Japan: Naihara, Totsukawa, Yoshino District, 34°05'49"N, 135°52'20"E, 11.viii.2013, SW [= collected by sweeping], Shunpei Fujie, OMNH"

Diagnosis. This species belongs to the *Xynobius comatus* group on account of the evenly and conspicuously setose middle lobe of the mesoscutum and scutellum (Figs 3, 4), but it differs from all other species by the subparallel-sided first tergite (Fig. 5;

Figure 1. *Xynobius subparallelus* Han & van Achterberg, sp. nov., holotype, ♀, Japan, habitus, lateral.

about 1.8× longer than its apical width), short temple (Fig. 8; eyes in dorsal view about 2.1× longer than temple), irregularly and weakly striate second tergite (Fig. 6), and vein m-cu of the fore wing that gradually merges into vein 2-CU1 (Fig. 2, but this character is rather variable in *X. setosiscutum*). In addition, the notauli are largely absent on the mesoscutal disc (Fig. 4, a derived character state in common with *X. setosiscutum* sp. nov. from Norway), and the second tergite is longitudinally striate (Fig. 6).

Description. Female; length of body 2.7 mm, of fore wing 2.6 mm and of antenna about 3.4 mm.

***Head*.** Antenna with 33 segments (Fig. 10), 1.2× longer than body; margin of antennal sockets strongly protruding, depression between antennal sockets (Fig. 7); length of eye in dorsal view 2.1× longer than temple (Fig. 8); height of head 1.35× longer than height of eye; vertex and frons punctate, setose except for large, smooth interspaces on vertex; no median keel on frons (Fig.7); width of clypeus twice longer than its maximum height; hypoclypeal depression large (Fig. 7); length of the maxillary palp 1.4× longer than height of head; malar sulcus absent; occipital carina absent dorsally; mandible robust (Fig. 1), symmetric, gradually widened basally.

***Mesosoma*.** Length of mesosoma 1.4× longer than its height (Fig. 3); pronope absent but with transverse crenulated groove (Fig. 4); mesopleuron largely smooth, but precoxal sulcus medially impressed and coarsely crenulate (Fig. 3); mesopleural sulcus largely smooth; notauli absent on disc except for a pair of short, deep impressions anteriorly (Fig. 4); mesoscutum and scutellum shiny, punctulate, and densely setose; medio-posterior depression of mesoscutum round and rather small (Fig. 4); scutellar sulcus medium-sized and distinctly crenulate; scutellum flat and only posteriorly narrowly sculptured; propodeum reticulate-rugose, with short medio-longitudinal carina anteriorly but posteriorly largely smooth between carinae (Figs 5, 9).

***Wings*.** Fore wing (Fig. 2): pterostigma narrow elliptical, gradually narrowed apically; vein 1-SR+M sinuate; vein 2-SR distinctly oblique; vein 3-SR 1.7× longer than vein 2-SR; vein SR1 slightly curved; r:3-SR:SR1 = 4:26:46; vein m-cu distinctly antefurcal; second submarginal cell elongated; first subdiscal cell transverse and elongated (Fig. 2). Hind wing: vein m-cu oblique and only pigmented; vein 1r-m 0.5× as long as vein 1-M.

***Legs*.** Length of hind femur 5.3× longer than its width (Fig. 11).

***Metasoma*.** Length of first tergite 1.8× longer than its apical width, its surface rugose with longitudinal striae and rather flat in lateral view (Fig. 5); dorsope distinctly present (Figs 5, 9); second tergite finely and irregularly longitudinally striate medially (Fig. 6) and distinctly longer than third tergite; second metasomal suture absent (Fig. 6); following tergites smooth and with few setae posteriorly; length of setose part of ovipositor sheath 0.5× longer than length of first tergite and nearly 0.1× as long as fore wing, slightly protruding beyond apex of metasoma (Fig. 1).

***Colour*.** Generally dark brown dorsally (Fig. 1); head, scape, mesopleuron and pronotum, yellowish brown; legs and palpi, pale brownish yellow.

Distribution. Japan (Honshu).

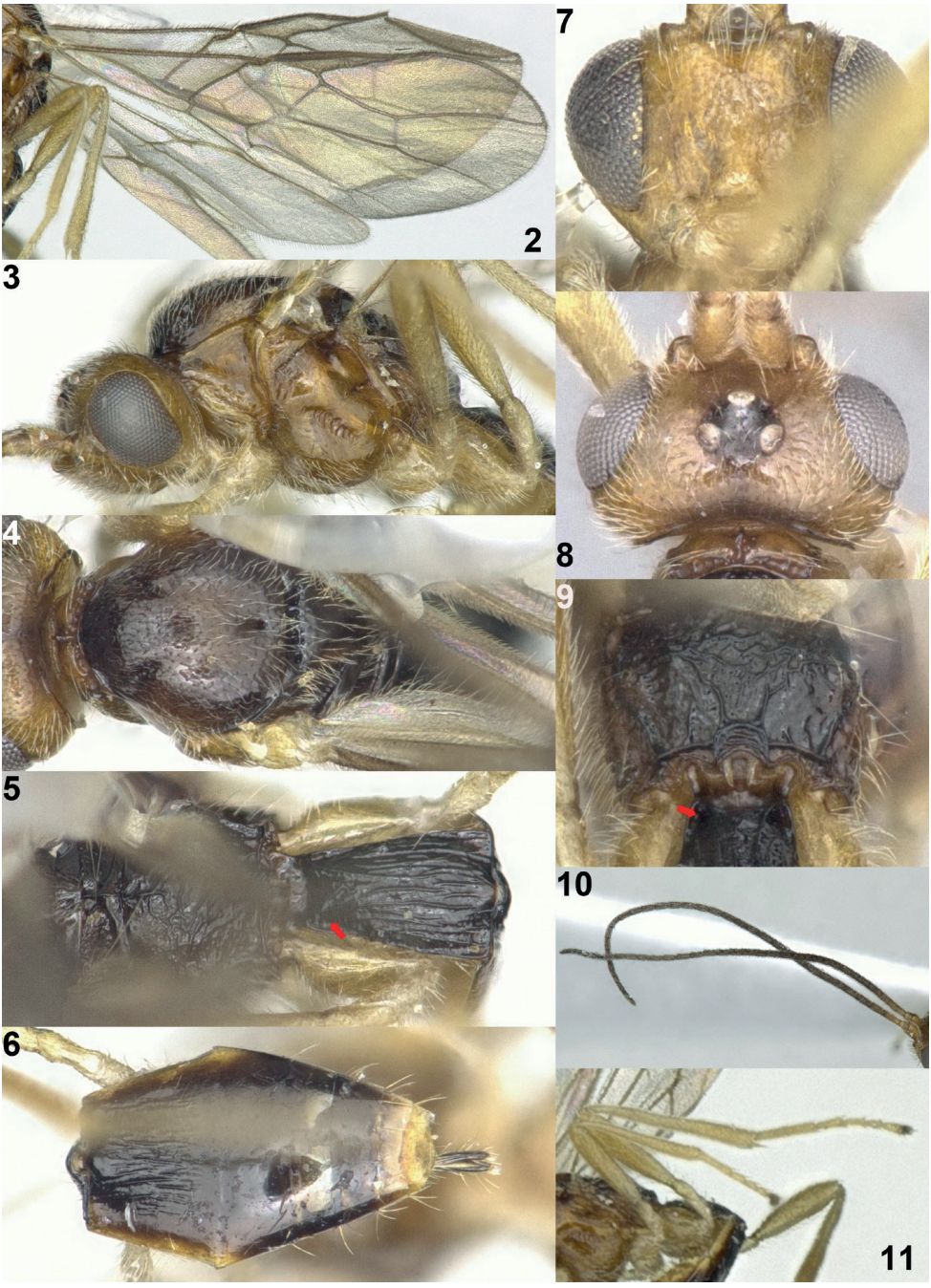

Figures 2–11. *Xynobius subparallelus* Han & van Achterberg, sp. nov., holotype, ♀, Japan **2** wings **3** mesosoma lateral **4** mesosoma dorsal **5** propodeum and 1st metasomal segment dorsal **6** 2nd and following metasoma segments dorsal **7** head anterior **8** head dorsal **9** propodeum posterior and 1st metasomal segment basal **10** antenna **11** hind leg lateral. The arrow indicates the dorsope.

Biology. Unknown.

Etymology. Named after the subparallel-sided first metasomal tergite; "*sub*" is Latin for "less than" and "*parallelus*" is Latin for "equidistantly sides".

Remarks. The new species has a distinct dorsope, symmetric mandible, vein r much shorter than vein 2-SR and a large hypoclypeal depression; therefore, it belongs to the genus *Xynobius*. Most important is the slender (subparallel-sided) first metasomal tergite, the irregularly and weakly longitudinally striate second tergite, the entirely setose mesoscutum and the reduced notauli (absent on most of mesoscutal disc and only distinct and crenulate anteriorly). In the key by Tobias (1998), this species runs to the subgenus *Apodesmia* Foerster sensu Tobias and (surprisingly) to *O.* (*Opius*) *angusticellularis* Tobias, 1998. This species has little to do with the new species because the mesosoma is only slightly longer than high in lateral view, the second and third metasomal tergites are granulate and the antenna has 22–24 segments. The new species runs in Chen and Weng (2005) to *Opius* (*Apodesmia*) *isabella* Chen & Weng, 2005, but it belongs to the genus *Apodesmia* Foerster, 1863 because the occipital carina is connected to the hypostomal carina ventrally, the second and third tergites are more or less coriaceous, and the clypeus is only 1.2× wider than long. Actually, the new species is similar to *Xynobius wengi* van Achterberg & Li, 2013 because of the setose mesoscutum and scutellum and striate second metasomal tergite. However, *X. wengi* has the crenulate notauli present on the mesoscutal disc (only apical quarter absent; notauli nearly entirely absent on disc in *X. subparallelus*), vein m-cu of the fore wing postfurcal or subinterstitial (distinctly antefurcal in *X. subparallelus*), the first metasomal tergite about 1.3× longer than wide apically (about 1.8× in *X. subparallelus*), and the second tergite regularly and coarsely striate (irregularly and finely striate *X. subparallelus*).

***Xynobius setosiscutum* van Achterberg, sp. nov.**

https://zoobank.org/4CEA8E68-639C-4AD0-AEFD-041D92A8708C

Figs 12–23

Type material. ***Holotype***, ♀ (RMNH), "Norway: RY, Sokndal, Skittmyr, 58.3509°N, 6.3054°E, 20.vii.–8.viii.2020, MT [= Malaise trap], J. Birkeland, RMNH'21". ***Paratypes*** (5): 1 ♂ (RMNH), topotypic, but 10–20.vii.2020; 1 ♀ (MSC), "Norway: RY, Ra, Hølland, 58.5245°N, 5.8352°E, 29.vi. –16.vii.2020, MT, A.T. Mjøs, RMNH'21"; 1 ♀ (RMNH), "Norway: RY, Time, Mossige, 58.6900N 5.7239E, 17.ix.–11.x.2020, MT, A.T. Mjøs, RMNH'21"; 1 ♀ (RMNH), "Norway: RI, Hjelmeland, 59.2312°N, 6.1653°E, 16.ix.–31.x.2020, MT, A.T. Mjøs, RMNH'21"; 1 ♀ (RMNH), "Norway: ROY, Sokndal, Rekvei, Long. lat. 58.2035°N, 6.1559°E, Malaise trap, 7.ix.2019, J. Birkeland".

Diagnosis. Antenna with 32–34 segments, flagellum dark brown but apical segments more or less brown; temple medium-sized (Fig. 19; roundly narrowed and eye in dorsal view 2.6× longer than temple); mesoscutum and scutellum evenly and conspicuously setose (Fig. 15); notauli largely absent on mesoscutal disc (a derived character state in common with *X. subparallelus* sp. nov. from Japan); hind femur comparatively

Figure 12. *Xynobius setosiscutum* van Achterberg, sp. nov., holotype, ♀, Norway, habitus, lateral.

robust (Figs 12, 17; about 4× longer than wide); pterostigma narrow elliptical and gradually narrowed apically (Fig. 13); vein m-cu of fore wing distinctly antefurcal and posteriorly angulate with vein 2-CU1 (Fig. 13); first tergite distinctly widened posteriorly (Fig. 16; 1.2–1.4× longer than its apical width in ♀, about 1.6× longer in ♂); second tergite regularly and costate-like striate (Fig. 16) and third tergite smooth; setose part of ovipositor sheath shorter than first metasomal tergite (Fig. 17) and at most slightly protruding beyond apex of metasoma. The new species is very similar

to *X. subparallelus* sp. nov. from Japan because of the reduction of the notauli and the conspicuous setosity of the mesoscutum and scutellum. However, it differs by having the first tergite distinctly widened posteriorly (subparallel-sided in *X. subparallelus*), distinctly wider temple (comparatively narrow), apex of third and fourth metasomal tergites yellow (blackish or dark brown), second tergite regularly and coarsely striate (finely and irregularly striate) and hind femur less slender, about 4× longer than wide (more robust, about 5× longer than wide).

Description. Holotype, ♀, length of body 3.0 mm, of fore wing 3.3 mm.

***Head*.** Antenna with 34 segments and 1.2× as long as fore wing; third segment 1.4× longer than fourth segment, length of third, fourth and penultimate segments 4.7×, 3.3×, and 2.5× their width, respectively (Figs 21, 22); width of head 1.8× its median length in dorsal view; no depression behind stemmaticum; vertex flattened and punctulate; OOL: diameter of ocellus: POL= 37:15:22 (Fig. 19); frons largely flattened and setose (Fig. 18); face finely punctate, shiny and with conspicuously long setae (Fig. 18); clypeus convex dorsally, semi-circular, largely smooth (except punctulation because of very long setae) and its ventral margin thick and concave, width of clypeus 2.1× its maximum height and 0.5× minimum width of face; hypoclypeal depression large and deep (Fig. 18); eye in dorsal view 2.6× longer than temple and temple behind eye roundly narrowed (Fig. 19); occipital carina distinct but dorsally finer and medio-dorsally absent (Fig. 19); temple and malar space smooth; length of malar space 0.8× basal width of mandible and 0.2× height of eye; malar suture nearly complete, shallow; mandible slightly twisted apically, both teeth robust, basally symmetric or nearly so, basal half with lamelliform ventral carina (Figs 18, 20); length of maxillary palp 1.3× height of head; labial palp segments elongate.

***Mesosoma*.** Length of mesosoma 1.5× its height (Fig. 14); laterally pronotum smooth only anteriorly, medially and posteriorly with few crenulae; dorsal pronope absent, medial area rather short, laterally with narrow groove; propleuron weakly evenly convex, with long setae, shiny and smooth (Fig. 14); mesopleuron smooth except for coarsely crenulate precoxal sulcus medially (Fig. 14); mesosternum densely setose; postpectal carina absent; pleural sulcus smooth or nearly so; mesosternal sulcus narrow and finely crenulate; metapleuron largely smooth dorsally and ventrally rugulose, long setose (Fig. 14); mesoscutum steeply raised above pronotum, densely setose, rather shiny and punctulate; notauli short, only impressed anteriorly and absent on most of mesoscutum, rather deep and largely smooth (Fig. 15); medio-posterior depression of mesoscutum rather deep medially, linear and medium-sized; transverse suture of mesoscutum present; scutellar sulcus deep and broad medially, with four carinae and medially 0.2× as long as scutellum; scutellum largely smooth and setose, punctulate, weakly convex, with narrow subposterior depression (Fig. 15); side of scutellum partly punctate (Fig. 15); propodeum largely vermiculate-rugose but posteriorly largely smooth between carinae, anteriorly with short medio-longitudinal carina (Figs 15, 16).

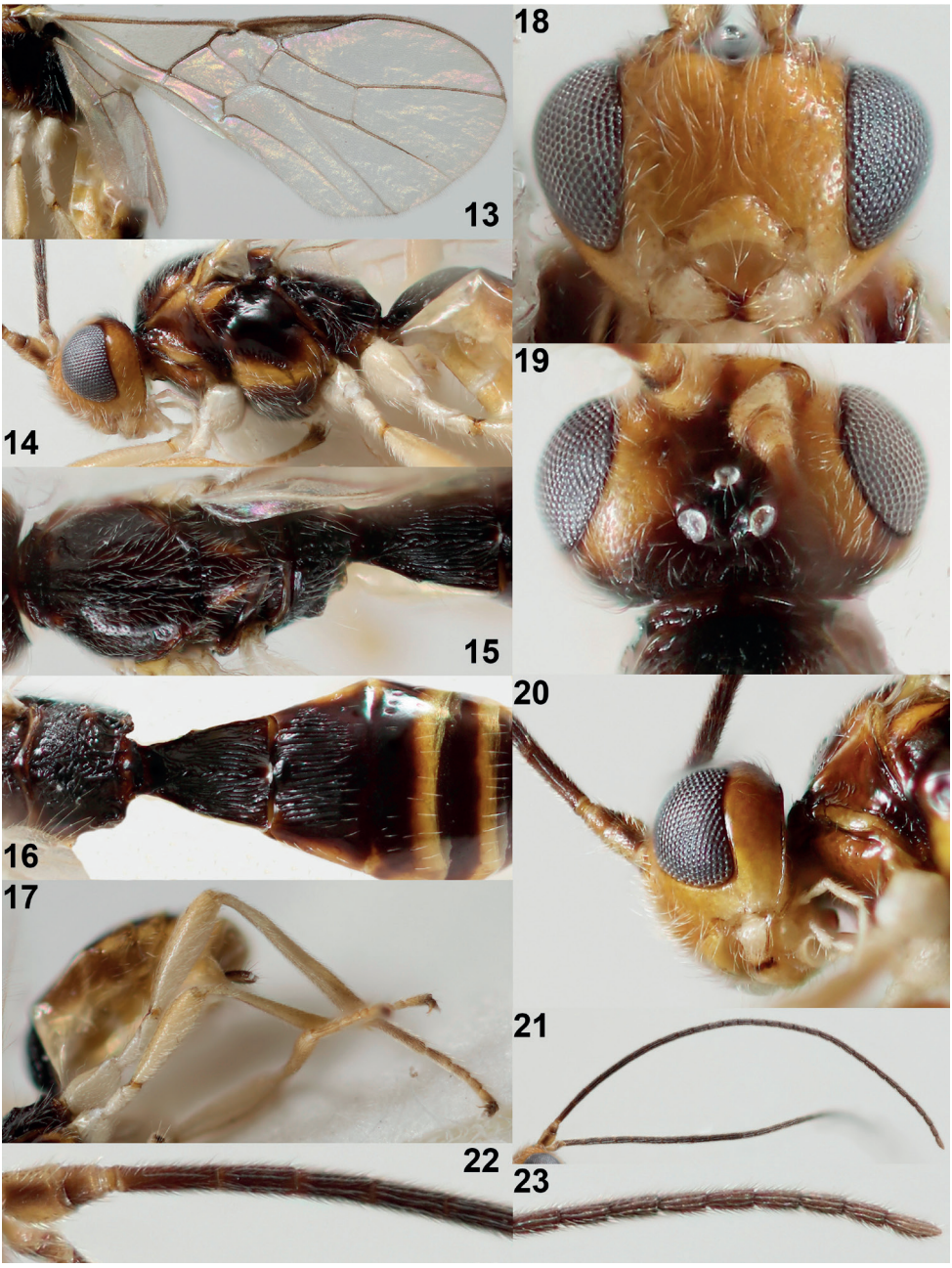

Figures 13–23. *Xynobius setosiscutum* van Achterberg, sp. nov., holotype, ♀, Norway **13** wings **14** head and mesosoma lateral **15** mesosoma dorsal **16** propodeum and 1st to 4th metasomal segments dorsal **17** hind leg and metasoma lateral **18** head anterior **19** head dorsal **20** mandible latero-ventral **21** antenna **22** base of antenna **23** apex of antenna.

***Wings*.** Fore wing (Fig. 13): pterostigma elongate-elliptical, 5× as long as its maximum width and gradually merging into vein 1-R1; vein M+CU1 weakly curved and only distal quarter sclerotized; 1-R1 reaching wing apex; r:3-SR:SR1 = 4:45:72; 2-SR:3-SR:r-m = 20:45:16; vein r slightly widened, its length 0.3× width of pterostigma, arising far before middle of pterostigma; 2-SR straight; m-cu distinctly antefurcal, largely unpigmented and slightly curved, angled with 2-CU1; cu-a slightly postfurcal and vertical; 1-CU1 widened; vein 3-CU1 distinctly longer than vein CU1b (Fig. 13). Hind wing: M+CU:1-M:1r-m = 20:21:12; cu-a straight; m-cu present.

***Legs*.** Second to fourth fore tarsal segments hardly longer than wide; hind femur, tibia and basitarsus 4.0×, 9.6×, and 5.3× as long as wide, respectively (Fig. 17); hind femur densely and long setose.

***Metasoma*.** First tergite 1.2× as long as wide apically and slightly widened apically, dorsope rather small, its surface convex medially and largely coarsely striate, dorsal carinae distinct in basal third of tergite (Fig. 16); second tergite regularly costate-like striate and following tergites smooth; second suture absent dorsally, except laterally; setose part of ovipositor sheath 0.04× as long as fore wing (entire sheath 0.06×), 0.3× first tergite, and 0.1× as long as hind tibia; sheath slightly protruding beyond apex of metasoma; hypopygium truncate ventro-apically, membranous medially and about 0.6× as long as first tergite (Fig. 17).

***Colour*.** Black or blackish brown; scape and pedicel largely (but dorsally partly dark brown), mandible, palpi, coxae, trochanters and trochantelli and femora basally ivory or whitish; hind tarsus infuscate; remainder of legs, head except occiput, vertex and frons medially, mesoscutum antero-laterally, scutellum laterally, pronotum partly, mesopleuron antero-dorsally and ventrally, third to fifth tergites apically, sixth and seventh tergites, and metasoma ventrally yellow; scutellum mainly dark reddish brown; pronotum medially and propleuron, pterostigma, and most veins brown; antenna dark brown, ventrobasally yellowish, apically nearly brown; ovipositor sheath dark brown; wing membrane subhyaline (Fig. 13).

***Variation*.** Length of body 2.9–3.1 mm, of fore wing 3.2–3.5 mm (of ♂ 2.9 mm); antennal segments in ♀ 32 (2) and 34 (2) and in ♂ 33 (1); flagellum dark brown or brown; mesoscutum posteriorly entirely black or partly brown and medio-posterior depression droplet-shaped or linear; vein m-cu of fore wing angled with vein 2-CU1 or gradually merging into vein 2-CU1; hind femur 4.0–4.2× longer than wide; first tergite 1.2–1.4× longer than wide apically in ♀ (about 1.6× longer in ♂); length of setose part of ovipositor sheath 0.03–0.04× fore wing (exposed sheath 0.06–0.08×).

Distribution. Southwestern Norway.

Biology. Unknown.

Etymology. Named after the entirely and conspicuously setose mesoscutum; "*setosus*" is Latin for "bristly", and "*scutum*" is Latin for "shield".

Remarks. This species runs to the subgenus *Allotypus* Foerster sensu Fischer, and with difficulty to *Opius saevulus* Fischer, 1958 (mesosoma less than 1.5× longer than high in lateral view) or *O. irregularis* Wesmael, 1835 (mesosoma 1.5× longer than high in lateral view), in the keys by Fischer (1972). Both of these species have nothing in common with the new species and both belong to the genus *Apodesmia* Foerster, 1863

because the occipital carina is curved and connected to hypostomal carina. Actually, the new species is more related to *X. aciculatus* (Thomson, 1895) because they share the setose middle lobe of the mesoscutum, the striate second tergite, the (at least partly) yellow face and clypeus, and the comparatively robust first tergite in females. The new species has the lateral mesoscutal lobes largely setose medially (glabrous in *X. aciculatus*); vein 3-CU1 of fore wing distinctly longer than vein CU1b (about of equal length); vein r of fore wing widened and shorter (narrow and longer); antenna of ♀ with 32–34 segments (with 28–31 segments); sixth metasomal tergite yellow largely dark brown); second tergite coarsely striate (finely striate); notauli largely absent on mesoscutal disc (notauli complete on disc); and vein m-cu of fore wing antefurcal (postfurcal).

Key to Norwegian species of the genus *Xynobius* Foerster

Notes. The following species are new for Norway and based on material received from Jarl Birkeland and Alf Tore Mjøs (RMNH). *Xynobius aciculatus* (Thomson): RY, Sokndal, Skittmyr; RI, Hjelmeland; *X. comatus* (Wesmael): RI, Suldal, Skumpanes; *X. polyzonius* (Wesmael): RY, Sokndal, Skittmyr. The new combination is based on the examination of the type series.

1 Temples and face densely punctate; scutellum densely rugose; pronotal side (except dorsally) extensively rugose; hind coxa rather dull and densely sculptured; [antenna with about 50 segments; clypeus strongly protruding forwards] ..... ***X. caelatus*** **(Haliday, 1837)**

– Temples smooth or nearly so; face at most remotely punctate; scutellum smooth or largely so; pronotal side (except medial and posterior grooves) smooth or nearly so; hind coxa shiny and smooth or sparsely punctulate **2**

2 Pterostigma behind vein r subparallel-sided or slightly concave; [= "*Stigmatopoea* Fischer, 1986"]; [notauli on mesoscutal disc largely absent posteriorly; antenna with 46–57 segments] ..... ***X. macrocerus*** **(Thomson, 1895)**

– Pterostigma behind vein r slightly to strongly narrowed (Fig. 13)..... **3**

3 Precoxal sulcus smooth or granulate; malar suture (rather) deep; head (except more or less clypeus) blackish or dark brown; propodeum without a distinct median carina anteriorly or weakly developed; [notauli largely absent on disc] **4**

– Precoxal sulcus distinctly crenulate(-rugose) submedially; malar suture absent, very short or shallow; head partly or largely brownish yellow; propodeum with a distinct median carina anteriorly or a pentagonal areola medially **5**

4 Antennal segments of ♀ 38–42; area below pterostigma with brownish patch, rarely obsolescent; vein M+CU1 of fore wing largely sclerotized; [fourth antennal segment robust; propleuron crenulate posteriorly] ..... ***X. geniculatus*** **(Thomson, 1895)**

– Antennal segments of ♀ 26–35; area below pterostigma hyaline; basal half of vein M+CU1 of fore wing unsclerotized; [basal antennal segments comparatively stout and dark brown] ..... ***X. maculipes*** **(Wesmael, 1835)**

5 Second metasomal tergite completely smooth **and** notauli largely absent on disc of mesoscutum; pronope large to medium-sized and deep; mandible without ventro-basal carina; second metasomal tergite yellowish or yellowish brown; basal half of vein M+CU1 of fore wing sclerotized; eyes of ♀ nearly touching mandibular condyle because of short malar space..... .....***X. polyzonius*** **(Wesmael, 1835) comb. nov.**

– Second tergite coarsely striate **or** notauli at least present on anterior half of mesoscutal disc; pronope small, obsolescent or absent; mandible with a short ventro-basal carina; second tergite blackish or dark brown; basal half of vein M+CU1 of fore wing unsclerotized; eyes of ♀ remain distinctly removed from mandibular condyle because of moderately long malar space.....**6**

6 Antenna of ♀ with 22–24 segments, at most 1.2× longer than body; apex of metasoma of ♀ dark brown; hind femur at least partly very finely and densely sculptured and with long setae dorsally; hind tibia densely erect setose; [middle lobe of mesoscutum evenly setose] ....***X. comatus*** **(Wesmael, 1835)**

– Antenna of ♀ with 28–34 segments, 1.3–1.5× longer than body; apex of metasoma of ♀ yellow; hind femur smooth and with medium-sized setae dorsally; hind tibia adpressed setose **7**

7 Lateral mesoscutal lobes glabrous medially, only laterally with long setae; notauli completely developed on mesoscutal disc; vein 3-CU1 of fore wing about as long as vein CU1b; antenna of ♀ with 28–31 segments; sixth metasomal tergite largely dark brown; second tergite finely striate; vein m-cu of fore wing postfurcal .....***X. aciculatus*** **(Thomson, 1895)**

– Lateral mesoscutal lobes largely setose medially; notauli largely absent on mesoscutal disc; vein 3-CU1 of fore wing distinctly longer than vein CU1b; antenna of ♀ with 32–34 segments; sixth metasomal tergite yellow; second tergite coarsely striate; vein m-cu of fore wing antefurcal ....***X. setosiscutum*** **van Achterberg, sp. nov.**

Key to Japanese species of the genus *Xynobius* Foerster

Notes. The number of included species for Japan is based on the list by Yu et al. (2016); only *Xynobius sapporanus* (Fischer, 1963) is added as a new combination. Types of *X. macrocerus*, *X. sapporanus* and *X. subparallelus* have been examined.

1 Scutellum coarsely punctate; [pterostigma subparallel-sided; antenna with 50–54 segments].....***X. japanus*** **(Fischer, 1963)**

– Scutellum smooth.....**2**

2 Middle mesoscutal lobe evenly setose.....**3**

– Mesoscutal lobes glabrous medially, only along notauli with some long setae **4**

3 Fore wing membrane with a large Y-shaped dark brown patch below para- and pterostigma (smaller in ♂); notauli largely impressed on mesoscutal disc; body black ..... ***X. sapporanus*** **(Fischer, 1963) comb. nov.**

– Fore wing membrane hyaline, without dark patch; notauli largely absent on mesoscutal disc; body dark brown or yellowish brown ..... ***X. subparallelus*** **Han & van Achterberg, sp. nov.**

4 Propodeum largely sculptured and without medio-longitudinal carina **5**

– Propodeum largely smooth or anteriorly with a medio-longitudinal carina.... **7**

5 Vein m-cu of fore wing interstitial or antefurcal; second metasomal tergite smooth; [antenna with about 37 segments]..... ***X. laticella*** **(Tobias, 1998)**

– Vein m-cu of fore wing postfurcal and/or second tergite sculptured **6**

6 Second metasomal tergite superficially rugulose; antenna with about 25 segments and slightly longer than body..... ***X. kamikochiensis*** **(Fischer, 1963)**

– Second tergite smooth; antenna with 32 or 33 segments and about 1.3× longer than body ..... ***X. claricoxa*** **(Fischer, 1963)**

7 Pterostigma wide elliptical and distinctly narrowed distally; antenna with 29–31 segments; second metasomal tergite largely longitudinally rugose ..... ***X. kotenkoi*** **(Fischer, 1998)**

– Pterostigma subparallel-sided and slightly widened distally; antenna with 50–53 segments; second tergite smooth.... ***X. macrocerus*** **(Thomson, 1895)**

Acknowledgements

We give special thanks to Shunpei Fujie from OMNH for making the Japanese specimen available and to Jarl Birkeland and Alf Tore Mjøs for collecting the Norwegian specimens and making them available. This research was supported by the Korea Environment Industry and Technology Institute (KEITI) through the Exotic Invasive Species Management Program funded by the Korea Ministry of Environment (MOE) (2018002270005). It was also supported by the Basic Science Research Program through the National Research Foundation of Korea (NRF) funded by the Ministry of Education (NRF-2022R1A2C1091308).

References

Ashmead WH (1900) Some changes in generic names in the Hymenoptera. Canadian Entomologist 32(12): 368–368. https://doi.org/10.4039/Ent32368a-12

Chen J-H, Weng R-Q (2005) Systematic Studies on Opiinae of China (Hymenoptera: Braconidae). Fujian Science and Technology Publishing House, Fuzhou, [iii + 2 + 9 +] 269 pp.

Fischer M (1972) Hymenoptera Braconidae (Opiinae I). (Paläarktische Region). Das Tierreich. 91(1973): 1–620.

Fischer M (1984) Neue Bestimmungsschlüssel für paläarktische Opiinae, neue Subgenera, Redeskriptionen und eine neue Art (Hymenoptera, Braconidae). Annalen des Naturhistorischen Museums in Wien, Serie B 88/89: 607–662.

Fischer M (1998) Neue taxonomische Untersuchungen über Madenwespen der Alten Welt mit besonderer berücksichtigung der Gattungen Eurytenes Förster, Aulonotus Ashmead, Biosteres Förster und der Untergattung Gastrosema Fischer (Hymenoptera, Braconidae: Opiinae). Linzer Biologische Beitrage 30(1): 21–51.

Foerster A (1863) Synopsis der familien und gattungen der Braconiden. Verhandlungen des Naturhistorischen Vereins der Preussischen Rheinlande und Westfalens 19: 225–288.

Li X-Y, van Achterberg C, Tan J-C (2013) Revision of the subfamily Opiinae (Hymenoptera, Braconidae) from Hunan (China), including thirty-six new species and two new genera. ZooKeys 268: 1–186. https://doi.org/10.3897/zookeys.326.5911

Tobias VI (1998) Alysiinae (Dacnusini) and Opiinae. In: Ler PA (Ed.) Keys to the Insects of Russian Far East (Vol. 4). Neuropteroidea, Mecoptera, Hymenoptera 3. Dal'nauka, Vladivostok, 299–411.

Tobias VI, Jakimavičius A (1986) Alysiinae and Opiinae. In: Medvedev GS (Ed.) Opredelitel Nasekomych Evrospeiskoi Tsasti SSSR 3, Peredpontdatokrylye 4. Opr. Faune SSSR 147(3)5: 7–231

van Achterberg C (1988) Revision of the subfamily Blacinae Foerster (Hymenoptera, Braconidae). Zoölogische Verhandelingen 249: 1–324.

van Achterberg C (1990) Illustrated key to the subfamilies of the Holarctic Braconidae (Hymenoptera: Ichneumonoidea). Zoologische Mededelingen Leiden 64(1): 1–20.

van Achterberg C (1993) Illustrated key to the subfamilies of the Braconidae (Hymenoptera: Ichneumonoidea). Zoölogische Verhandelingen 283: 1–189.

van Achterberg C (1997) Revision of the Haliday collection of Braconidae (Hymenoptera). Zoölogische Verhandelingen 314: 1–115.

van Achterberg C (2004) New Indo-Australian subgenera and species of the genera *Xynobius* Foerster and *Ademoneuron* Fischer (Hymenoptera: Braconidae: Opiinae). Zoölogische Mededeelingen 78: 313–329.

van Achterberg C (2009) Can Townes type Malaise traps be improved? Some recent developments. Entomologische Berichten 69(4): 129–135.

Viereck HL (1913) Descriptions of six new genera and twelve new species of Ichneumonflies. Proceedings of the United States National Museum 46(2031): 359–386. https://doi.org/10.5479/si.00963801.2031.359

Wharton RA (1987) Changes in nomenclature and classification of some opiine Braconidae (Hymenoptera). Proceedings of the Entomological Society of Washington 89: 61–73.

Wharton RA (1988) Classification of the braconid subfamily Opiinae (Hymenoptera). Canadian Entomologist 120(4): 333–360. https://doi.org/10.4039/Ent120333-4

Wharton RA (1997) Generic relationships of opiine Braconidae (Hymenoptera) parasitic on fruit-infesting Tephritidae (Diptera). Contributions of the American Entomological Institute 30(3): 1–53.

Wharton RA (2006) The species of *Sternaulopius* Fischer (Hymenoptera: Braconidae, Opiinae) and the braconid sternaulus. Journal of Hymenoptera Research 15: 317–347.

Yu D, van Achterberg C, Horstmann K (2016) Taxapad 2016. Ichneumonoidea 2015. Taxapad Interactive Catalogue Database on flash-drive. Ottawa, Canada.

ZooKeys 1160: 75–87 (2023)
doi: 10.3897/zookeys.1160.103644
https://zookeys.pensoft.net

RESEARCH ARTICLE

A peer-reviewed open-access journal
ZooKeys
Launched to accelerate biodiversity research

Two new species of crab spiders from Xiaolong Mountains in Gansu Province, China (Araneae, Thomisidae)

Rui Zhang[1], Feng Zhang[1]

1 *Key Laboratory of Zoological Systematics and Application of Hebei Province, Institute of Life Science and Green Development, College of Life Sciences, Hebei University, Baoding, Hebei 071002, China*

Corresponding author: Feng Zhang (dudu06042001@163.com)

Academic editor: Shuqiang Li | Received 17 March 2023 | Accepted 5 April 2023 | Published 3 May 2023

https://zoobank.org/9F9C145E-8272-4FB9-8B06-06E66E55B364

Citation: Zhang R, Zhang F (2023) Two new species of crab spiders from Xiaolong Mountains in Gansu Province, China (Araneae, Thomisidae). ZooKeys 1160: 75–87. https://doi.org/10.3897/zookeys.1160.103644

Abstract

Two new species of crab spider are described from the Xiaolong Mountains in Gansu Province, China: *Ebelingia spirala* **sp. nov.** (♂♀) and *Lysiteles longensis* **sp. nov.** (♂♀). Detailed morphological characters, a distribution map, photographs, and illustrations of the habitus and copulatory organs are given for each species.

Keywords

Ebelingia, *Lysiteles*, new species, taxonomy

Introduction

As the seventh largest family of spiders worldwide, Thomisidae Sundevall, 1833 currently contains 171 genera and 2710 species from all over the world (WSC 2023). It has undergone regional revisions in Canada (Dondale and Redner 1978), Japan (Ono 2009), and China (Song et al. 1999; Tang et al. 2007, 2008; Tang and Li 2010a, b). Although crab spiders have been revised, species reassigned, and unknown sexes described in recent decades, there are still many species needing in-depth study (Liu et al. 2022).

The genus *Ebelingia* Lehtinen, 2004 and *Lysiteles* Simon, 1895 are mainly distributed in eastern and southern Asia. Currently, only three species of *Ebelingia* are known (WSC 2023): *E. forcipata* Song & Zhu, 1993, *E. hubeiensis* Song & Zhao, 1994, and *E. kumadai* Ono, 1985. All three species are distributed in China. *E. forcipate* and *E. hubeiensis* are endemic to China, mainly distributed in Fujian, Hubei, and Jiangxi provinces. There are no reports of this genus in Gansu Province. There are 63 *Lysiteles* species worldwide. The Chinese *Lysiteles* fauna is extraordinarily rich with 45 species (WSC 2023). More than half of the species are distributed in southern China, such as Yunnan, Guizhou, and Hubei Provinces, and Hainan Island. Only three species were reported in Gansu Province.

To enrich the diversity of *Ebelingia* and *Lysiteles* in Gansu Province, a survey from Xiaolong Mountains was carried out by colleagues of Hebei University. After a careful examination of thomisid materials, two new species, *Ebelingia spirala* sp. nov. and *Lysiteles longensis* sp. nov., were recognized. Illustrations of diagnostic structures and a distribution map are presented.

Materials and methods

All specimens are preserved in 95% ethanol. Specimens were examined and measured under a Leica M205A stereomicroscope. Photographs were taken using an Olympus BX51 microscope equipped with a Kuy Nice CCD and were imported into Helicon Focus v. 7 for image stacking. Final figures were retouched using Adobe Photoshop 2020. Eye sizes were measured as the maximum diameter in dorsal view. Leg measurements are shown as total length (femur, patella, tibia, metatarsus, and tarsus). All measurements are given in millimetres. The holotypes of the new species are deposited in the Museum of Hebei University (**MHBU**), Baoding, China. The paratypes are in the Museum of Baoding University.

Abbreviations used: **AME**, anterior median eyes; **ALE**, anterior lateral eyes; **AME–ALE**, distance between AME and ALE; **AME–AME**, distance between AMEs; **PME**, posterior median eyes; **PME–PLE**, distance between PME and PLE; **PME–PME**, distance between PMEs; **PLE**, posterior lateral eyes.

Taxonomy

Family Thomisidae Sundevall, 1833

Genus *Ebelingia* Lehtinen, 2004

Type species. *Misumenops kumadai* Ono, 1985 from Japan.

Diagnosis. See Lehtinen (2004).

Comments. This genus includes only three species, all of which are distributed in East Asia. Among them, *E. forcipata* and *E. hubeiensis* are endemic to China and recorded from Fujian, Hubei, and Jiangxi provinces. No species were recorded from Gansu Province.

Distribution. China, Japan, Korea, Russia (Far East).

***Ebelingia spirala* sp. nov.**

https://zoobank.org/95C67764-CC97-4FE4-87BE-29FC005D40C4

Figs 1–8

Type material. ***Holotype*:** ♂, China: Gansu Province, Maiji district, Liqiao town, Baihua Forest Farm, 34°19.93'N, 106°23.18'E, 1844 m, 23 May 2021, Rui Zhang leg. ***Paratypes*:** 1♂3♀, with same data as holotype; 2♀, Niangniangba town, Baiyin village, 34°17.2'N, 105°55.97'E, 1524 m, 31 May 2021, Rui Zhang leg; 1♀, Hui County, Jialing town, Xiaolongshan National Nature Reserve, 33°40.52'N, 106°18.67'E, 1647 m, 7 June 2021, Zhaoyi Li leg.; 1♂, Qingshui County, Shanmen Town, Shanmen Village, 34°41.4'N, 106°21.72'E, 1630 m, 24 June 2022, Zhaoyi Li leg.

Etymology. The specific name is derived from the Latin "*spira*" (meaning "a coil"), referring to the shape of RTA in ventral view, adjective.

Diagnosis. Male of this new species resembles those of *E. forcipata* Song & Zhu, 1993 (see Liu et al. 2022: 51, figs 4A–E, 5A–F) and *E. hubeiensis* Song & Zhao, 1994 (see Song and Zhao 1994: 115, fig. 4E, F) in having short embolus, flat tegulum, and a bifurcated RTA, but can be distinguished by the following combination of characters: (1) RTA about half the length of tibia (vs almost as long as tibia); (2) the presence of spiral thread on dorsal branch of RTA (vs smooth RTA). Female of *E. spirala* sp. nov. is similar to that of *E. hubeiensis* in having central concavity on anterior hood but can be distinguished by the L-shaped, long spermathecae (vs same length and width in *E. hubeiensis*).

Description. Male (*holotype*). Habitus as in Figs 1, 2. Total length 2.88. Carapace 1.27 long, 1.21 wide, opisthosoma 1.60 long, 1.22 wide, the whole dorsum of body with dense setae. Carapace chestnut-coloured, medially with yellowish band. Ocular area white. Eye sizes and interdistances: AME 0.06, ALE 0.09, PME 0.05, PLE 0.08, AME–AME 0.14, AME–ALE 0.15, PME–PME 0.20, PME–PLE 0.22, AME–PME 0.15, ALE–PLE 0.16. MOA 0.18 long, front width 0.27, back width 0.50. Sternum slightly longer than wide. Chelicerae, endites, and labium yellow. Femora and patellae of legs I–II and legs III–IV reddish brown, other segments of legs I–II dark brown. Leg measurements: I 5.73 (1.59, 0.62, 1.52, 1.43, 0.57); II 5.63 (1.68, 0.56, 1.32, 1.38, 0.69); III 2.34 (0.74, 0.30, 0.48, 0.49, 0.32); IV 2.52 (0.66, 0.36, 0.54, 0.62, 0.34). Leg spination: I Fe: p2; II Fe: d2; III Fe: d2; Ti: d1; IV: Pa: d1; Ti: d2. Opisthosoma dorsum yellowish, with cardiac pattern, posterior with irregular stripes; venter yellow, with black stripes.

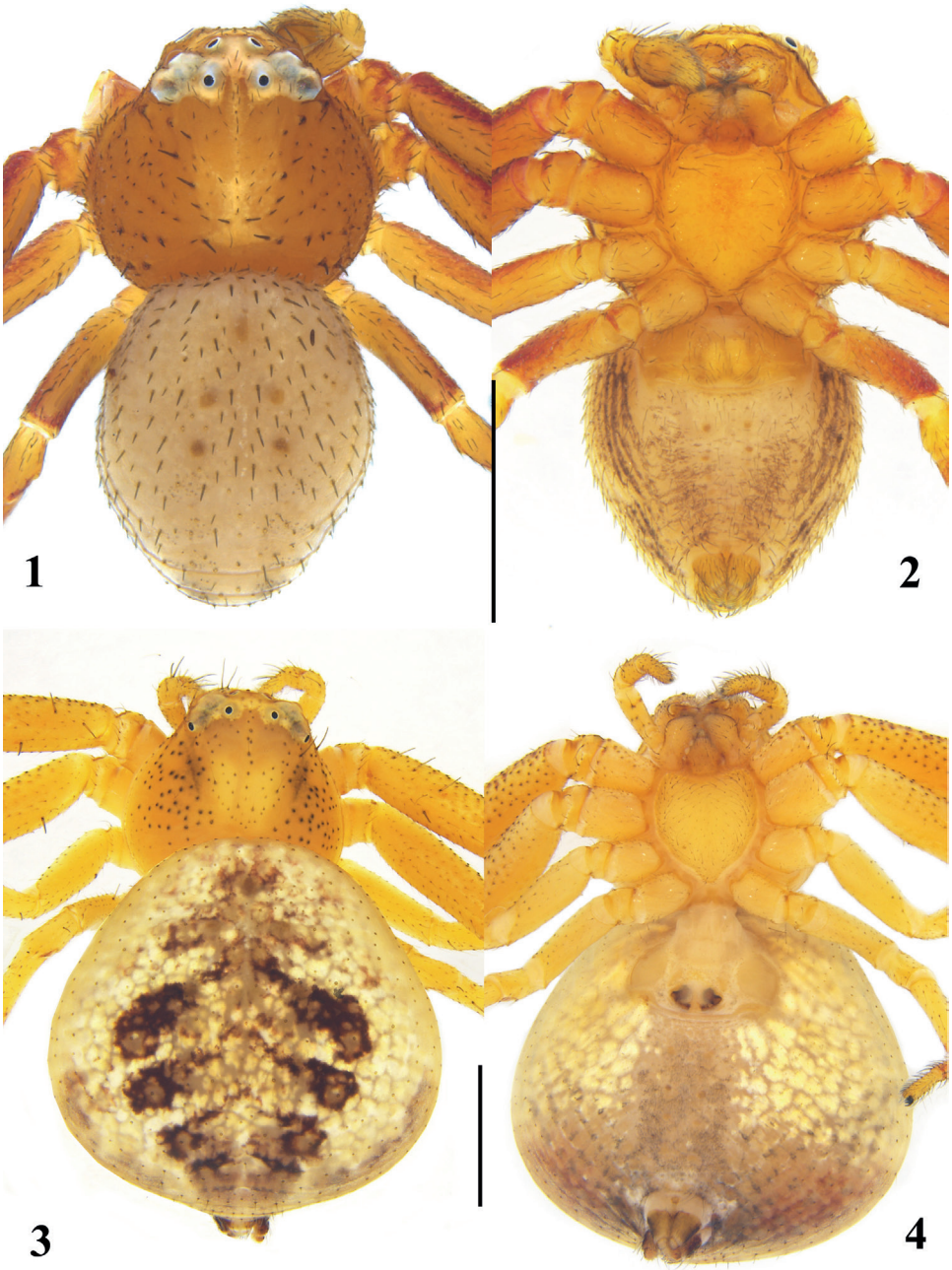

Figures 1–4. *Ebelingia spirala* sp. nov. **1, 2** male habitus (**1** dorsal view **2** ventral view) **3, 4** female habitus (**3** dorsal **4** ventral). Scale bars: 1 mm.

Palp (Figs 5, 6). Tibia with two apophyses, short ventral and bifurcated retrolateral: ventral part blunt and longer than ventral tibial apophysis in retrolateral view, dorsal one with spirals. Ventral tibial apophysis short, with blunt apex. Cymbium

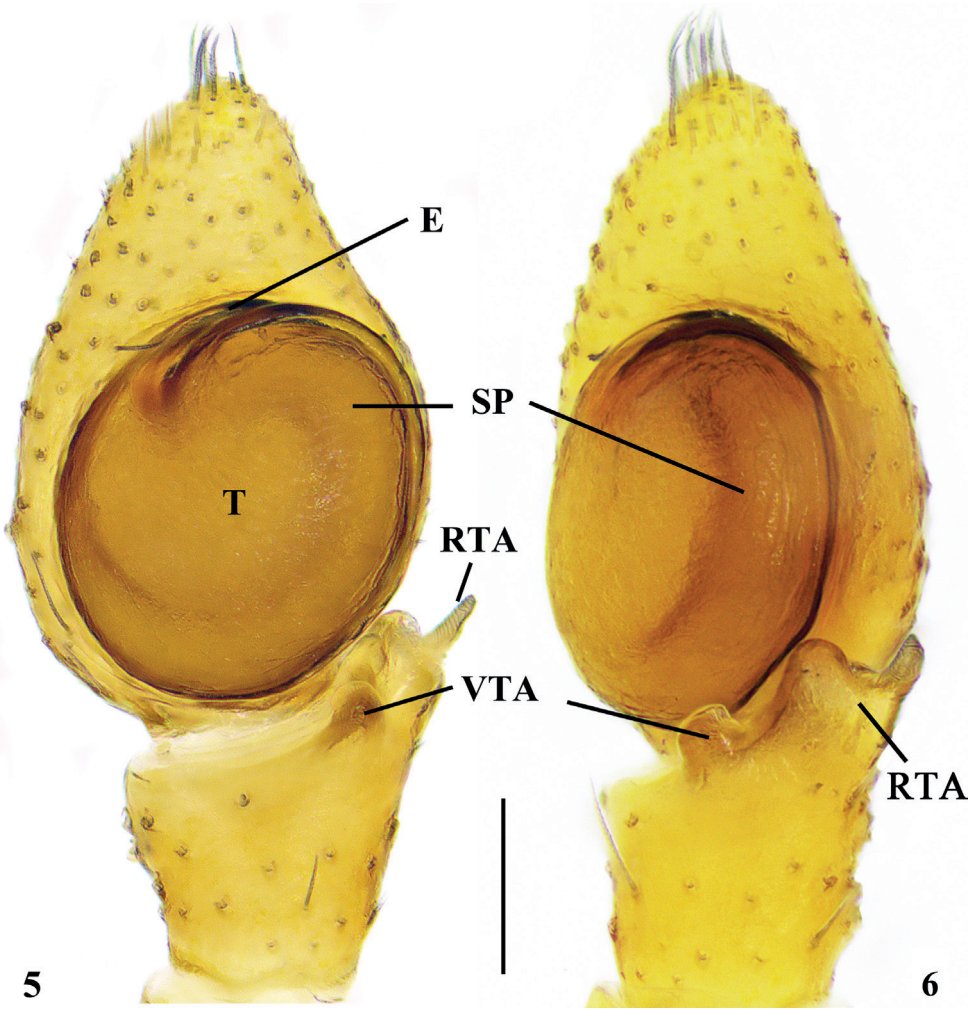

Figures 5, 6. *Ebelingia spirala* sp. nov. **5, 6** left male palp (**5** ventral view **6** retrolateral view). E = embolus; RTA = retrolateral tibial apophysis; SP = spermophore; T = tegulum; VTA = ventral tibial apophysis. Scale bar: 0.1 mm.

1.25× longer than wide. Tegulum oval 1.25× longer than wide, tegular ridge at 11 o'clock position. Spermophore wide, encircling almost whole tegulum. Embolus short, originating from ~11 o'clock position and terminating at 1 o'clock position.

Female. Habitus as in Figs 3, 4. Total length 4.38. Prosoma 1.53 long, 1.57 wide. Opisthosoma 2.85 long, 2.88 wide. Carapace chestnut-coloured, medially with yellowish band, laterally with black spots. Eye sizes and interdistances: AME 0.06, ALE 0.09, PME 0.05, PLE 0.10, AME–AME 0.19, AME–ALE 0.17, PME–PME 0.29, PME–PLE 0.26, AME–PME 0.20, ALE–PLE 0.17. MOA 0.27 long, front width 0.31, back width 0.39. Chelicerae, sternum, and labium yellow. Endites and legs chestnut-coloured. Venter of leg I and II with numerous reddish-brown spots. Leg

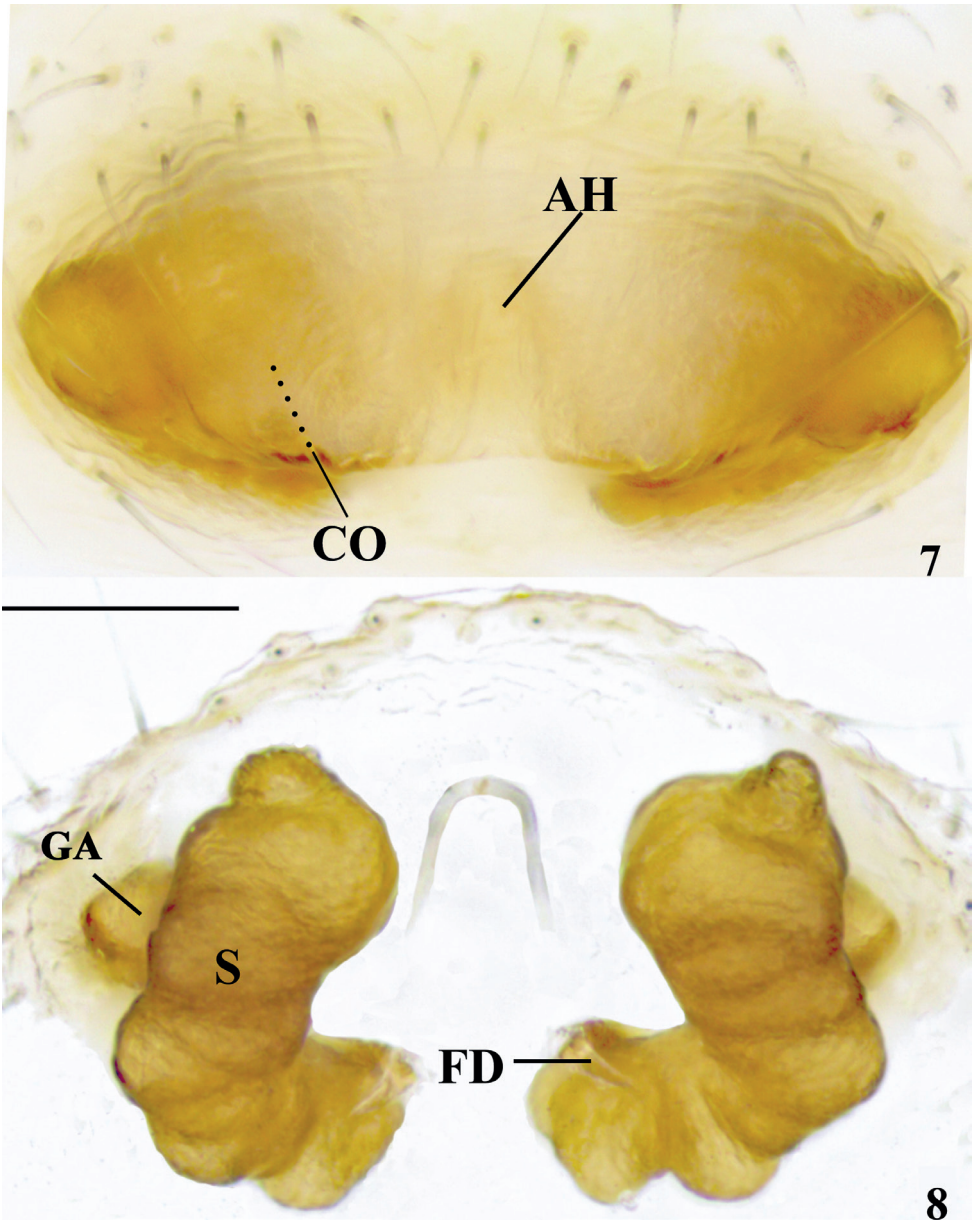

Figures 7, 8. *Ebelingia spirala* sp. nov. **7, 8** epigyne/vulva (**7** ventral view **8** dorsal view). AH = anterior hood; CO = copulatory opening; FD = fertilization duct; GA = glandular appendage; S = spermatheca. Scale bar: 0.1 mm.

measurements: I 5.58 (1.77, 0.74, 1.30, 1.12, 0.65); II 5.14 (1.24, 0.75, 1.37, 1.09, 0.69); III 2.60 (0.78, 0.43, 0.70, 0.39, 0.30); IV 2.86 (0.89, 0.45, 0.58, 0.53, 0.41). Leg spination: I Fe: d1, p4; Pa: d2; Ti: v3; Mt: p4, r4; II Fe: d1; Pa: d1; Ti: p2, r3; Mt:

d3, p5, r5; III Fe: d1; Pa: d1; Ti: d3, v4; IV: Fe: d2; Pa: d2; Ti: d2, v2. Opisthosomal dorsum yellow, with white spots at the sides and brown symmetrical patches in the middle; venter with a few white spots at the sides.

Epigyne (Figs 7, 8). Epigyne almost 2× wider than long, with a deep Ω-shaped anterior hood, about 2× longer than wide. Copulatory openings (Fig. 7) located at posterolateral part of anterior hood. Spermathecae L-shaped, separated by more than width of anterior hood. Fertilization ducts short.

Distribution. Known only from the type locality in Gansu Province, China (Fig. 17).

Genus *Lysiteles* Simon, 1895

Type species. *Lysiteles catulus* Simon, 1895 from Tamil Nadu, India.

Diagnosis. See Tang et al. (2007) and Tang and Li (2010a, b).

Comments. This genus includes 63 species mainly distributed in eastern Asia. It has never been revised in full, although new species have been described now and then in various papers. Most of the 44 *Lysiteles* species have been recorded from China, and three species have been recorded from Gansu Province.

Distribution. Bhutan, China, India, Japan, Korea, Nepal, Pakistan, Philippines, Russia, Vietnam.

Lysiteles longensis sp. nov.

https://zoobank.org/873582B1-1E1F-48AC-91F7-76FE3C658BE6
Figs 9–16

Type material. ***Holotype*****:** ♂, China: Gansu Province, Qingshui County, Shanmen town, Shanmen village, 34°40.72'N, 106°23.98'E, 1735 m, 22 May 2021, Rui Zhang leg. ***Paratypes*****:** 2♂6♀, with same data as holotype; 2♂9♀, Dangchuan town, 34°19.73'N, 105°15.77'E, 1711 m, 24 May 2021, Zhaoyi Li leg.; 1♂3♀, Qingshui County, Shanmen town, Shanmen village, 34°42.32'N, 106°25.1'E, 1635 m, 3 August 2021, Rui Zhang leg.; 3♂6♀, Qingshui County, Shanmen town, Daji village, 34°37.45'N, 106°20.25'E, 1784 m, 23 June 2022, Xinyuan Bai leg.

Etymology. The specific name refers to the type locality. “Long” is a short name for Gansu, adjective.

Diagnosis. Male *L. longensis* sp. nov. is similar to that of *L. silvanus* Ono, 1980 (see Ono 1980: 212, figs 28–30) in having a long RTA and twisted embolus, but it differs by the following combination of characters: (1) tegulum large and reniform, ca 3/4 of cymbium cavity (vs small, semicircular, and ca 1/2 of cymbium cavity); (2) the lowest point of embolus above the tegulum (vs the lowest point at 1/2 of the tegulum); (3) RTA straight, pointing dorsally (vs RTA flexed, pointing ventrally). Female is similar to that of *L. silvanus* (see Ono 1980: 212, figs 25–27) in having a broad atrium with a sclerotized, transversally extending plate and widely separated copulatory openings,

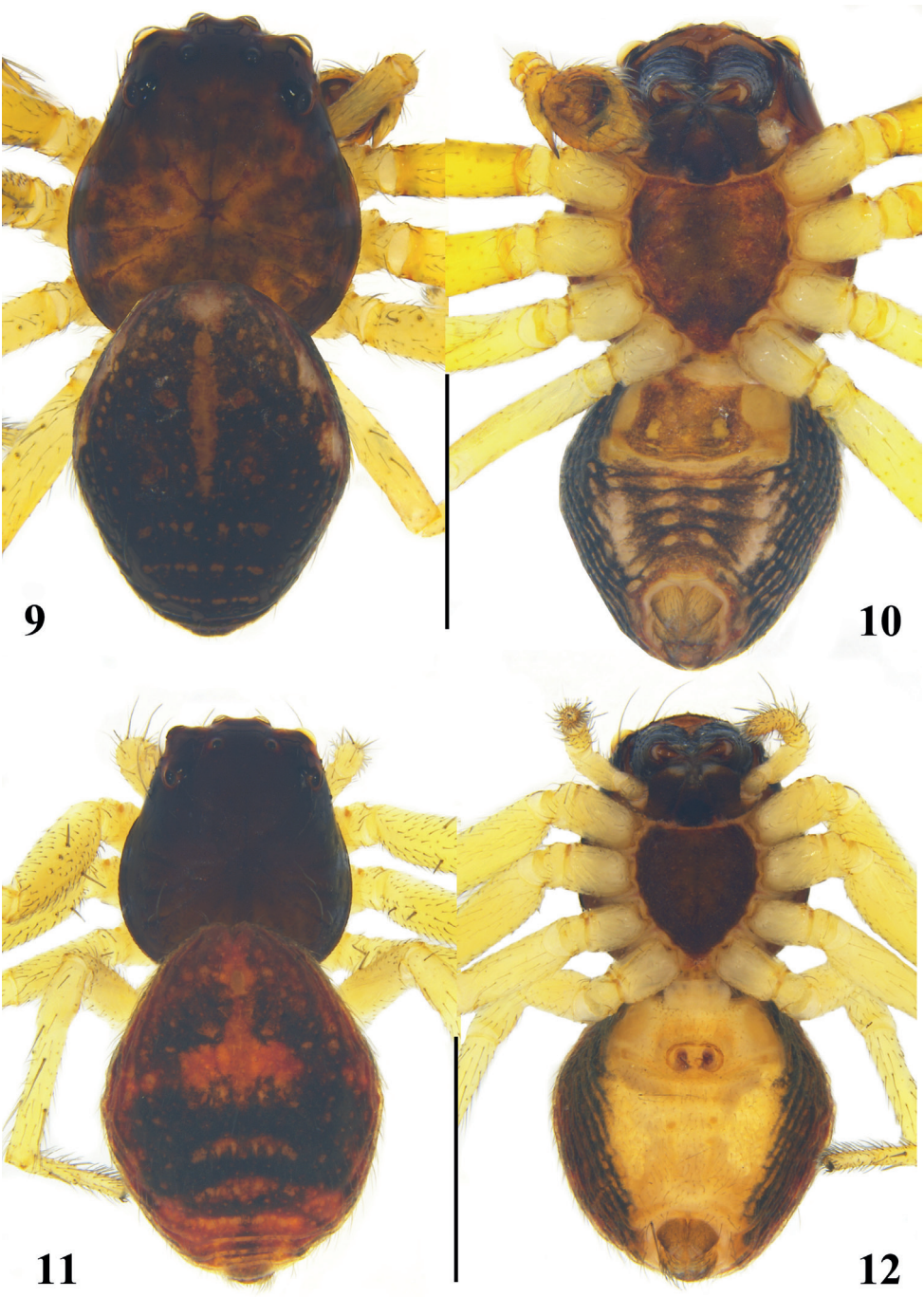

Figures 9–12. *Lysiteles longensis* sp. nov. **9, 10** male habitus (**9** dorsal view **10** ventral view) **11, 12** female habitus (**11** dorsal view **12** ventral view). Scale bars: 1 mm.

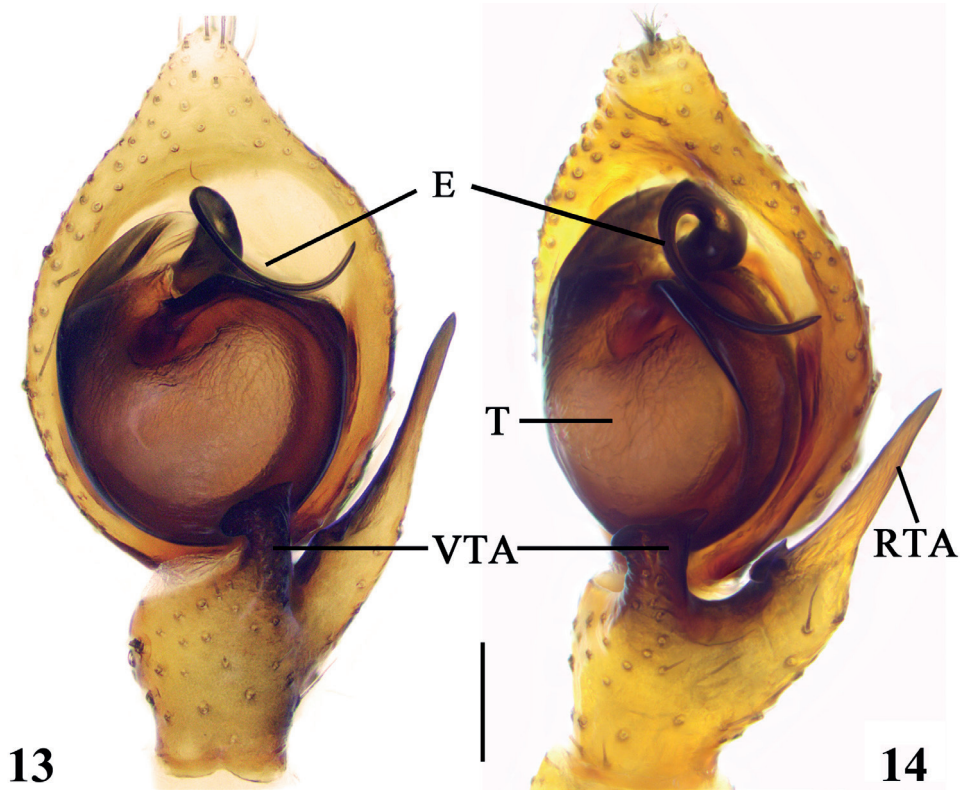

Figures 13, 14. *Lysiteles longensis* sp. nov., left male palp (**13** ventral view **14** retrolateral view). E = embolus; RTA = retrolateral tibial apophysis; T = tegulum; VTA = ventral tibial apophysis. Scale bar: 0.1 mm.

but it can be easily distinguished by the short, thick, and spherical copulatory duct (vs slender and strongly twisted).

Description. Male (*holotype*). Habitus as in Figs 9, 10. Total length 2.89. Carapace 1.31 long, 1.19 wide. Opisthosoma 1.58 long, 1.19 wide. Carapace reddish brown. Eye sizes and interdistances: AME 0.06, ALE 0.11, PME 0.04, PLE 0.08, AME–AME 0.14, AME–ALE 0.13, PME–PME 0.25, PME–PLE 0.24, AME–PME 0.25, ALE–PLE 0.23. MOA 0.24 long, front width 0.26, back width 0.33. Chelicerae, labium and maxillae blackish brown. Legs yellowish and spinous. Leg measurements: I 4.83 (1.37, 0.46, 1.18, 1.06, 0.76); II 5.06 (1.41, 0.55, 1.28, 1.04, 0.78); III 2.88 (0.86, 0.40, 0.79, 0.45, 0.38); IV 2.93 (0.84, 0.39, 0.82, 0.49, 0.39). Leg spination: I Fe: d3, p3; Ti: d3, p1, r1, v4; Mt: p3, r3, v1; II Fe: d3, p2; Pa: d2, p1, r1; Ti: d1, p3, r2, v3; Mt: p3, r3, v4; III Fe: d3; Pa: d1, r1; Ti: d1, p2, r1; Mt: p2, r1; IV: Fe: d4; Pa: d1, r1; Ti: d2, p2, r2; Mt: p1, r1. Opisthosoma dorsum blackish brown, anterior with longitudinal reddish-brown stripe, posterior part with 3 transverse, reddish-brown stripes,

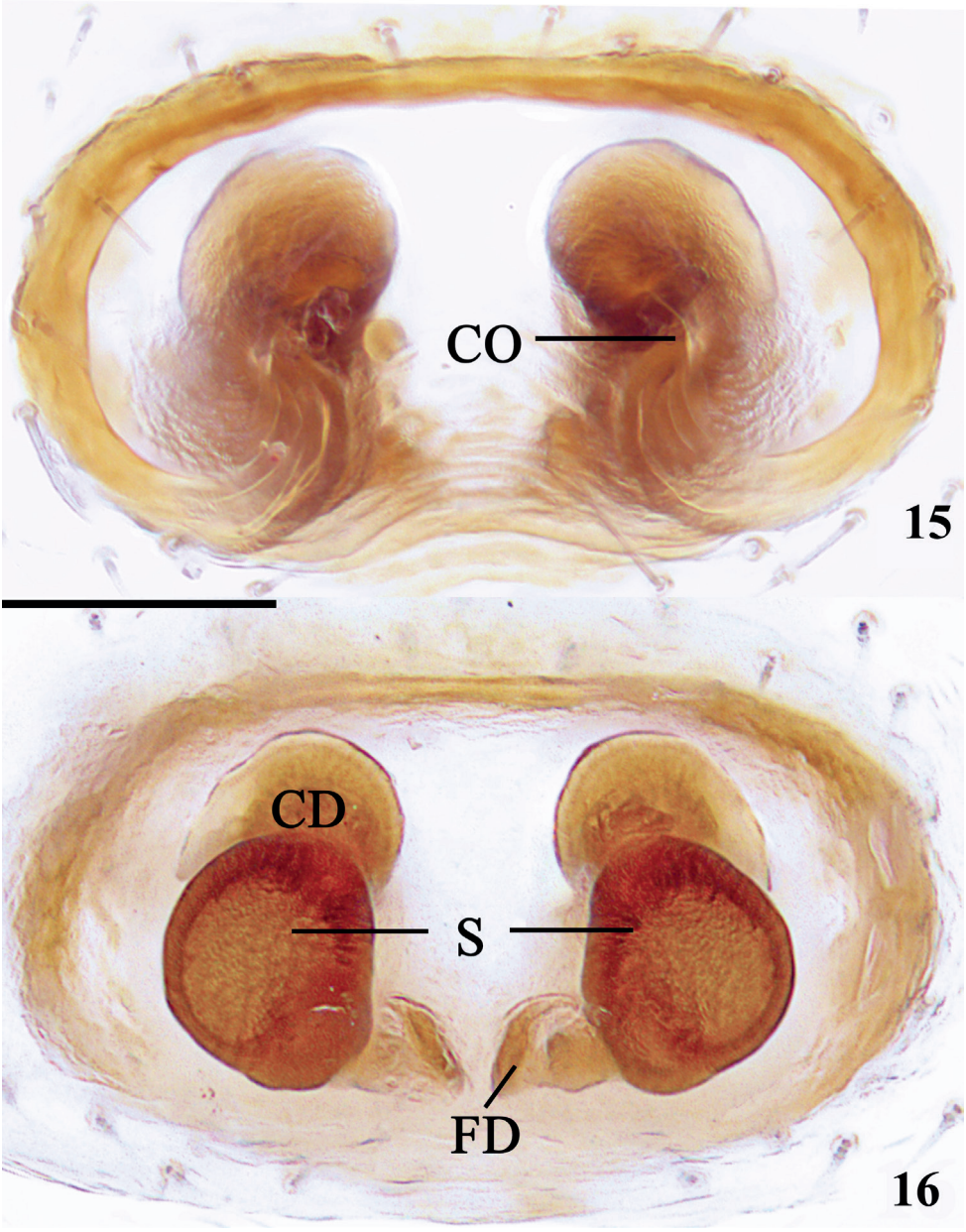

Figures 15, 16. *Lysiteles longensis* sp. nov., epigyne/vulva (**15** ventral view **16** dorsal view). CD = copulatory duct; CO = copulatory opening; FD = fertilization duct; S = spermatheca. Scale bar: 0.1 mm.

and lateral with many small, scattered, brown spots; venter with 4 pairs of longitudinal yellow spots in the middle; spinnerets brown.

Palp (Figs 13, 14). Retrolateral tibial apophysis longer than tibia, with small, basal protuberance (Fig. 14), apically pointed; ventral tibia apophysis digitiform, 1.5× longer

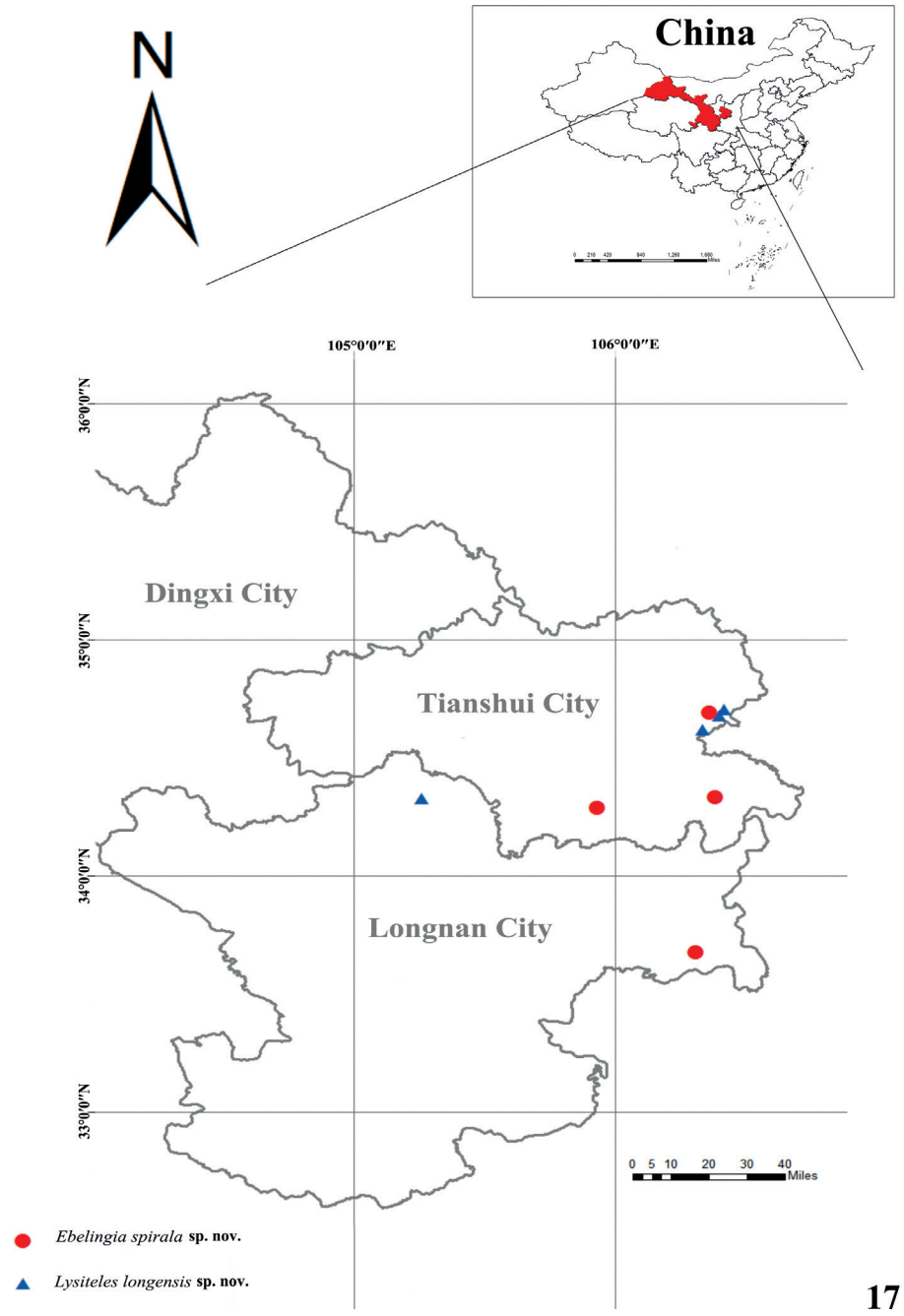

Figure 17. Records of the new species from the Xiaolong Mountains in Gansu Province, China.

than wide, short and broad, apically curved; extending along tegular margin. Embolus with thick base and a strong, dorsally bent apical end. Tip lopped and in counterclockwise direction, base at about 10 o'clock, tip at about 2 o'clock; tegulum as long as wide.

Female. Habitus as in Figs 11, 12. Total length 3.27. Prosoma 1.38 long, 1.17 wide. Opisthosoma 1.89 long, 1.60 wide. Carapace blackish brown. Other characteristics as those of males. Eye sizes and interdistances: AME 0.06, ALE 0.09, PME 0.05, PLE 0.10, AME–AME 0.19, AME–ALE 0.17, PME–PME 0.29, PME–PLE 0.26, AME–PME 0.20, ALE–PLE 0.17. MOA 0.27 long, front width 0.31, back width 0.39. Sternum, chelicerae, labium, and maxillae blackish brown. Legs yellowish and spinous. Leg measurements: I 4.26 (1.32, 0.38, 0.99, 0.96, 0.61); II 4.20 (1.31, 0.41, 1.00, 0.91, 0.57); III 2.49 (0.58, 0.33, 0.68, 0.50, 0.40); IV 2.71 (0.65, 0.40, 0.68, 0.55, 0.43). Leg spination: I Fe: d1, p3; Pa: d1; Ti: d3, p2, r3, v1; Mt: p4, r4; II Fe: d2; Ti: d2, p2, r2, v1; Mt: p3, r3, v2; III Fe: d2; Pa: d1; Ti: d2, p2, r2; Mt: p2, r2, v1; IV: Fe: d1; Pa: d1; Ti: d1, p2, r1; Mt: p1, r1. Opisthosoma dorsum with symmetrical, longitudinal, reddish-brown stripes and lateral with scattered patches. Venter yellow in the middle and black at the sides.

Epigyne (Figs 15, 16). Epigyne ca 1.7× wider than long. Atrium large, sclerotized plate oval, copulatory openings originate medially; sclerotic fold well developed. Copulatory ducts thick, as wide as spermathecae; spermathecae suboval, 1.4× wider than long, spaced by about 0.5 diameters of the vulva.

Distribution. Known only from the type locality in Gansu Province, China (Fig. 17).

Acknowledgements

We are grateful to the subject editor Dr. Shuqiang Li and the reviewer Dr. Yuri Marusik for providing significant comments on the manuscript. We are also grateful to Dr. Xinping Wang (University of Florida) for improving the English of the manuscript, and to Ph.D. Zhaoyi Li and Mr. Xinyuan Bai (Hebei University) for collecting specimens. Thanks are given to Mr. Qi Liu and Ms. Shuqin Huo for their assistance during the fieldwork. This work was supported by the National Natural Science Foundation of China (no. 32170468).

References

Dondale CD, Redner JH (1978) The Crab Spiders of Canada and Alaska, Araneae: Philodromidae and Thomisidae. The Insects and Arachnids of Canada, Part 5. Research Branch, Canada Department of Agriculture, Ottawa, 255 pp.

Lehtinen PT (2004) Taxonomic notes on the Misumenini (Araneae: Thomisidae: Thomisinae), primarily from the Palaearctic and Oriental regions. In: Logunov DV, Penney D (Eds) European Arachnology (Proceedings of the 21st European Colloquium of Arachnology, St.-Petersburg, 4–9 August 2003). Arthropoda Selecta, Special Issue 1: 147–184.

Liu KK, Ying YH, Fomichev AA, Zhao DC, Li WH, Xiao YH, Xu X (2022) Crab spiders (Araneae, Thomisidae) of Jinggang Mountain National Nature Reserve, Jiangxi Province, China. ZooKeys 1095: 43–74. https://doi.org/10.3897/zookeys.1095.72829

Ono H (1980) Thomisidae aus Japan III. Das Genus *Lysiteles* Simon 1895 (Arachnida: Araneae). Senckenbergiana Biologica 60: 203–217.

Ono H (2009) The Spiders of Japan with Keys to the Families and Genera and Illustrations of the Species. Tokai University Press, Kanagawa, 739 pp.

Song DX, Zhao JZ (1994) Four new species of crab spiders from China. Acta Arachnologica Sinica 3: 113–118.

Song DX, Zhu MS, Chen J (1999) The Spiders of China. Hebei Science and Technology Publishing House, Shijiazhuang, 640 pp.

Tang G, Li SQ (2010a) Crab spiders from Hainan Island, China (Araneae, Thomisidae). Zootaxa 2369(1): 1–68. https://doi.org/10.11646/zootaxa.2369.1.1

Tang G, Li SQ (2010b) Crab spiders from Xishuangbanna, Yunnan Province, China (Araneae, Thomisidae). Zootaxa 2703(1): 1–105. https://doi.org/10.11646/zootaxa.2703.1.1

Tang G, Yin CM, Peng XJ, Ubick D, Griswold C (2007) Five crab spiders of the genus *Lysiteles* from Yunnan Province, China (Araneae: Thomisidae). Zootaxa 1480(1): 57–68. https://doi.org/10.11646/zootaxa.1480.1.2

Tang G, Yin CM, Peng XJ, Ubick D, Griswold C (2008) The crab spiders of the genus *Lysiteles* from Yunnan Province, China (Araneae: Thomisidae). Zootaxa 1742(1): 1–41. https://doi.org/10.11646/zootaxa.1742.1.1

World Spider Catalog (2023) World Spider Catalog. Version 24. Natural History Museum Bern. [Accessed 17 Feb. 2023] https://doi.org/10.24436/2

ZooKeys 1160: 89–108 (2023)
doi: 10.3897/zookeys.1160.100844
https://zookeys.pensoft.net

RESEARCH ARTICLE

A peer-reviewed open-access journal
ZooKeys
Launched to accelerate biodiversity research

Description of a new montane freshwater crab (Arthropoda, Malacostraca, Decapoda, Potamonautidae) from the Eastern Cape, South Africa

Nasreen Peer[1], Gavin Gouws[2], Lazola Maliwa[3], Nigel Barker[4], Paul Juby[4], Renzo Perissinotto[5]

1 *Department of Botany and Zoology, Stellenbosch University, Merriman Avenue, Stellenbosch, 7600, South Africa* **2** *National Research Foundation – South African Institute for Aquatic Biodiversity, Private Bag 1015, Grahamstown, 6140, South Africa* **3** *Albany Museum, 40 Somerset Street, Grahamstown, 6139, South Africa* **4** *Department of Plant and Soil Sciences, University of Pretoria, Private Bag X20, Hatfield, 0028, Pretoria, South Africa* **5** *Institute for Coastal & Marine Research, Nelson Mandela University, Gqeberha, 6031, South Africa*

Corresponding author: Nasreen Peer (peer.nasreen@gmail.com)

Academic editor: Célio Magalhães | Received 20 January 2023 | Accepted 6 March 2023 | Published 4 May 2023

https://zoobank.org/970DD66E-66DD-402A-BC38-BEAA5D7E6B1F

Citation: Peer N, Gouws G, Maliwa L, Barker N, Juby P, Perissinotto R (2023) Description of a new montane freshwater crab (Arthropoda, Malacostraca, Decapoda, Potamonautidae) from the Eastern Cape, South Africa. ZooKeys 1160: 89–108. https://doi.org/10.3897/zookeys.1160.100844

Abstract

A new species of freshwater crab, *Potamonautes amathole* **sp. nov.**, is described from the Winterberg-Amathole mountain range in the Eastern Cape Province, South Africa. Morphologically, *P. amathole* Peer & Gouws, **sp. nov.** most closely resembles *P. tuerkayi* but can be distinguished by key morphological characters including the variation in the shape of the subterminal segment of gonopod 2 between both species. Genetically, *P. amathole* Peer & Gouws, **sp. nov.** is placed within the clade of small-bodied, mountain-dwelling crabs including *P. parvispina*, *P. parvicorpus*, *P. brincki*, *P. tuerkayi*, *P. baziya*, and *P. depressus*. The new species is found in slow-moving mountain streams and pools at high altitudes. The continued discovery and description of new freshwater crab species reinforces the need for ongoing research, especially in under-sampled regions.

Keywords

Afrotropical Region, Brachyura, high altitude streams, molecular analyses, morphology, taxonomy

Introduction

In South Africa, the genera *Potamonautes* and *Maritimonautes* represent the freshwater crabs with a total of 26 described species since the last published descriptions (Daniels et al. 2022). Although the freshwater crabs in South Africa are a fairly well-studied group, morphological and molecular analyses continue to reveal new undescribed species, many of which are cryptic and have thus been mistaken for previously described species (Daniels et al. 1998, 2022; Phiri and Daniels 2014, 2016; Peer et al. 2017).

Recently, several new species have been described from natural forest habitats (Peer et al. 2015; Daniels 2017; Daniels et al. 2019, 2021), which only comprise a small percentage of South Africa's total land cover (0.4%) but boast the highest biodiversity per hectare (Geldenhuys and MacDevette 1989). Although mostly fragmented, the Knysna and Amathole Forest complexes are the two largest remaining patches of natural forest in South Africa, with the latter situated in the Amathole Mountain Range along the Great Escarpment (Mucina and Rutherford 2006). The Great Escarpment, as outlined by Clark et al. (2011a), refers to a semi-continuous mountain range that transcends many southern African borders, experiencing a range of climatic conditions.

Aside from high forest biodiversity, the Amathole Mountain Range, forming part of the escarpment between the Sneeuberg range in the west and the Drakensberg range in the east, is considered to display great diversity across habitat types, as well as high levels of endemism in terms of flora (Clark et al. 2011a). Despite this, habitats in the region are still poorly sampled in terms of fauna (Kok et al. 2012; Taylor et al. 2020).

In this paper, we describe *P. amathole* sp. nov. from the Hogsback and Katberg Forests in the Amathole Mountains of the Eastern Cape. NP and GG wrote the taxonomic part of this study, including the description of the new species, while the contribution of the other authors dealt with genetic analyses, natural history, and ecological observations.

Materials and methods

Crab collection

Crabs were collected from three localities (Table 1, Fig. 1) located in the Winterberg-Amathole mountain range.

Crabs were collected by hand or net and preserved in 70% ethanol.

Table 1. Localities of the three sample sites.

Site name	Coordinates
Katberg State Forest	32°28.43'S, 26°40.10'E
Hogsback Arboretum	32°35.42'S, 26°56.05'E
Hogsback Waterfall	32°36.40'S, 26°57.80'E

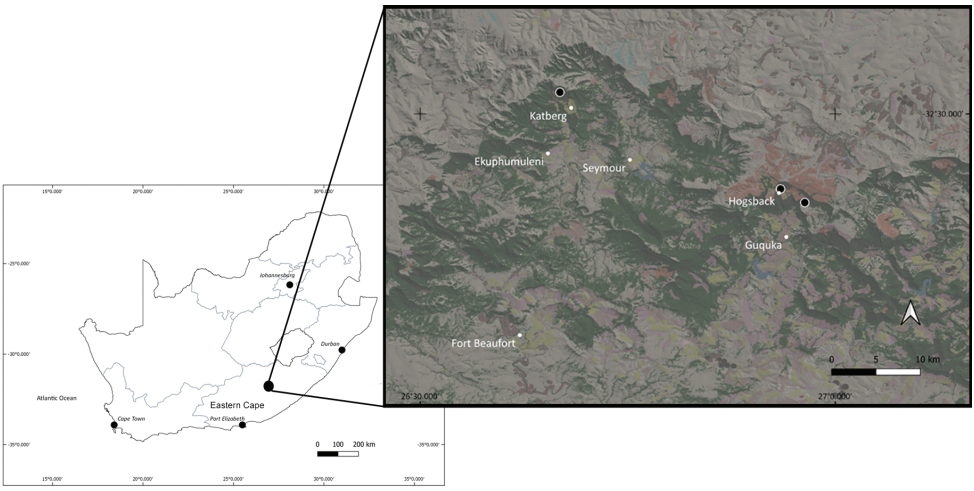

Figure 1. Map showing the location of the Amathole Mountain Range sampling sites (black markers) in relation to nearby towns and villages (white points). South Africa National Land Cover (SANLC) 2018 map layer shows land cover to be predominantly indigenous forest and plantations with residential area nearby.

Genetic analyses

The genetic placement and relationships of the proposed new species were examined using data generated in two sequential studies.

For the first study, total genomic DNA was extracted from 0.5–1 mg of pereiopod muscle tissue from specimens collected from Hogsback and Katberg during 2013. Tissue was rinsed in sterile water and DNA was extracted using an Invisorb Spin Tissue Mini Kit (Invitek Molecular, Berlin), following the manufacturer's protocol.

A fragment of the large ribosomal subunit 16S mitochondrial marker was amplified by Polymerase Chain Reaction, using the primers of Cunningham et al. (1992: 16Sar and 16Sbr). PCRs were completed in 50 µL volumes, comprising 1 X PCR reaction buffer, 5 µL template DNA, 2 mM $MgCl_2$, 0.2 mM deoxynucleotide triphosphate (dNTP), 0.2 µM of each primer, and 0.5 U *Taq* polymerase. The thermocycling profile included an initial denaturing at 95 °C for 5 min, 30 cycles of 95 °C for 45 s, 45 °C for 45 s and 72 °C for 1.5 min, followed by a final extension of 72 °C for 5 min. Amplification was confirmed by gel electrophoresis in a 0.5% agarose gel stained with SYBR Green (ThermoFisher Scientific, Waltham, Massachusetts) and viewed with a UV-transilluminator. PCR products were purified with an Invisorb PCRapace Quick purification kit (Invitek Molecular). Purified products were cycle-sequenced in both forward and reverse directions using the ABI Big Dye Sequencing kit v. 3.1. (Applied Biosystems, Austin, Texas). Cycle-sequencing products were precipitated using a NaAc-ethanol procedure (Sambrook and Russell 2001) and analysed on an ABI 3100 Genetic Analyser at Rhodes University, South Africa. Consensus sequences were created from the forward and reverse sequences of each sample, correcting base ambiguities, using SEQUENCHER v. 4.5 (GeneCodes Corporation).

In the second study, DNA was extracted from specimens collected from Hogsback during 2018, using a PureLink Miniprep kit (Invitrogen, Carlsbad, California). A fragment of the protein-coding mtDNA cytochrome *c* oxidase subunit I (COI) gene was amplified and sequenced using the approach described by Gouws et al. (2015). Sequences were checked and edited as described therein.

Data analyses

Data sets for each of the 16S and COI fragments included data generated in the present study and published data for all described southern African *Potamonautes* species, as compiled previously (Gouws et al. 2015). GenBank accession numbers and sources for the published data are provided in Suppl. material 1: table S1. *Potamonautes danielsi*, described by Peer et al. (2017), was represented by an individual (NPP2) from Network E within a wider lineage of *P. sidneyi* in the study by Gouws et al. (2015); this individual was sampled from the type locality (Mtamvuna River) of *P. danielsi*. Similarly, the *P. brincki* sequences included by Gouws et al. (2015) were ascribed to *P. tuerkayi* in the present study. The latter species was described as distinct from *P. brincki* by Wood and Daniels (2016) with the type locality being Fernkloof, from where the aforementioned *P. brincki* specimens were sampled for the study by Daniels et al. (2002). An alternative COI sequence (Wood and Daniels 2016: GenBank accession number KU561507) was included for *P. brincki*; unfortunately, no other 16S sequence was available. The *P. lividus* specimen from Eswatini (formerly Swaziland) included in the study by Gouws et al. (2015) has subsequently been assigned to *P. valles* (Daniels et al. 2022). The previously-compiled data were also supplemented with data for other South African species described subsequent to the Gouws et al. (2015) study, including *P. baziya* (Daniels et al. 2021: GenBank accession number 16S – OK482902, COI – OK489798), *P. mariepskoppie* (Daniels et al. 2021: 16S – OK482901, COI – OK489797), *P. ngoyensis* (Daniels et al. 2019: 16S – MK607207, COI – MK607221), *P. ntendekaensis* (Daniels et al. 2019: 16S – MK607196, COI – MK607210) and *P. mhlophe* (Daniels 2017: 16S – MF693159, COI – MF693167). In a recent systematic revision, Cumberlidge and Daniels (2022) reassigned several of the *Potamonautes* species included by Gouws et al. (2015) to the genera *Arcopotamonautes* (*A. bellarussus*, *A. lirrangensis*, *A. platynotes* and *A. raybouldi*), *Maritimonautes* (*M. calcaratus*, *M. choloensis*, *M. namuliensis* and *M. obesus*) and *Rotundopotamonautes* (*R. ohdneri* and *R. subukia*). The representatives of *Maritimonautes* were used as outgroups in the present study, due to their basal placement relative to *Potamonautes* (Cumberlidge and Daniels 2022). Representatives of other genera were excluded from these analyses.

ClustalX2 (Larkin et al. 2007) was used to align the COI partition, while the 16S data were aligned using MAFTT 6.956 (Katoh and Toh 2008) with an iterative refinement strategy (L-INS-i) (Katoh et al. 2005). As corresponding 16S and COI sequences were not successfully obtained for every individual included in the present study, the 16S and COI data sets were analysed separately. Phylogenetic relationships were determined using Maximum Likelihood (ML) analyses, as implemented in PAUP*4.0a168

(Swofford 2003). Prior to execution, the optimal models of nucleotide substitution for each of the 16S and COI data sets were identified using jModelTest 2.1.4 (Darriba et al. 2012), with model selection determined using the Akaike (1974) Information Criterion. In the ML analyses, heuristic tree searches were executed, with TBR branch-swapping of a tree obtained through a random addition of taxa, with 100 such replicates employed. Due to computational constraints, nodal support was evaluated through Bayesian Posterior Probabilities (BPPs), with values above 0.95 being regarded as evidence of support. These were generated through Bayesian inferences as described in Gouws et al. (2015) but sampling the posterior distribution every 5 000 generations. Uncorrected sequence divergences among individuals were calculated using PAUP.

Morphological measurement and description

Morphological variables were measured using a pair of Vernier callipers. A Canon Powershot G12 digital camera was used to photograph carapaces and appendages, while a Nikon SMZ25 microscope fitted with a Nikon Digital Sight DS-Fi2 camera was used for macro-examination and to take photos of gonopods and mouthparts.

Abbreviations for depositories and provinces

ISAM Iziko South African Museum, Cape Town, South Africa;
EC Eastern Cape;
WC Western Cape;
KZN KwaZulu–Natal.

Abbreviations for all morphological and morphometric characters (following Gouws et al. 2001):

AW6 Width of sixth abdominal segment;
CH Carapace height;
CL Carapace length;
CLDL Left cheliped, dactyl length;
CRDL Right cheliped, dactyl length;
CRPL Right cheliped, propodus length;
CRPW Right cheliped, propodus width;
CWA Distance between exorbital teeth;
CWW Carapace widest width;
CWP Carapace posterior width;
ED Distance between orbits;
MCPL Major cheliped propodus length;
MCPW Major cheliped propodus width;
ML Merus length;
MW Merus width;

PFCD Distance between postfrontal crest and anterior margin;
P2ML Pereopod 2, merus length;
P2MW Pereopod 2, merus width;
s2/s3 First sternal groove (suture between the second and third sulci);
s3/s4 Second sternal groove (suture between the third and fourth sulci).

Results

Genetic analyses

New sequences generated in the present study were lodged in GenBank (16S: accession numbers OQ559329–OQ559337; COI: OQ558909–OQ558911). The 16S alignment was 549 nucleotides in length. The ML analysis, using the parameters of the optimal model (base frequencies: A = 0.369, C = 0.122, G = 0.163 and T = 0.346; rate matrix: $R_{A\leftrightarrow C}$ = 0.571, $R_{A\leftrightarrow G}$ = 5.756, $R_{A\leftrightarrow T}$ = $R_{G\leftrightarrow T}$ = 1.000, $R_{C\leftrightarrow G}$ = $R_{C\leftrightarrow T}$ = 2.251; α = 0.341 for the gamma distribution of rate variation), produced the topology (-lnL = 3754.743) presented in Fig. 2.

The COI alignment was 660 nucleotides in length. The optimal model had base frequencies of A = 0.292, C = 0.184, G = 0.154 and T = 0.371, a rate matrix of $R_{A\leftrightarrow C}$ = 4.203, $R_{A\leftrightarrow G}$ = 10.249, $R_{A\leftrightarrow T}$ = 2.385, $R_{C\leftrightarrow G}$ = $R_{G\leftrightarrow T}$ = 1.000, $R_{C\leftrightarrow T}$ = 31.047, a proportion of invariant sites (I = 0.549) and a gamma distribution of rate variation (α = 1.280). The tree produced by the ML analysis is shown as Fig. 3.

The topologies produced by the analyses of the 16S and COI data were congruent with respect to, and reflected, the major phylogenetic divisions reported previously for the southern African *Potamonautes* radiation (e.g., Daniels 2017; Daniels et al. 2019, 2021; Cumberlidge and Daniels 2022). These include a clade of small-bodied, mountain-dwelling crabs i.e., *Potamonautes baziya* Daniels, Barnes, Marais & Gouws, 2021, *P. brincki* (Bott, 1960), *P. clarus* Gouws, Stewart & Coke, 2000, *P. depressus* (Krauss, 1843), *P. parvicorpus* Daniels, Stewart & Burmeister, 2001, *P. parvispina* Stewart, 1997 and *P. tuerkayi* Wood & Daniels, 2016; a clade of robust, large-bodied riverine species i.e. *P. barbarai* Phiri & Daniels, 2014, *P. barnardi* Phiri & Daniels, 2014, *P. bayonianus* (de Britto Capello, 1864), *P. dentatus* Stewart, Coke & Cook, 1995, *P. granularis* Daniels, Stewart & Gibbons, 1998, *P. perlatus* (H. Milne Edwards, 1837), *P. sidneyi* Rathbun, 1904, *P. unispinus* Stewart & Cook, 1998 and *P. warreni* Calman, 1918); a clade of species largely inhabiting forests in the Indian Ocean Coastal Belt (IOCB) (*P. danielsi* Peer & Gouws, 2017, *P. isimangaliso* Peer & Gouws, 2015, *P. lividus* Gouws, Stewart & Reavell, 2001 and *P. valles* Daniels, Busschau, Gullacksen, Marais, Gouws & Barnes, 2022); and a clade of mostly burrowing IOCB or tropical highland species with *P. flavusjo* Daniels, Phiri & Bayliss, 2014, *P. mariepskoppie* Daniels, Barnes, Marais & Gouws, 2021, *P. mulanjeensis* Daniels & Bayliss, 2012, *P. mutareensis* Phiri & Daniels, 2013, *P. ngoyensis* Daniels, Busschau & Cumberlidge, 2019 and *P. ntendekaensis* Daniels, Busschau & Cumberlidge, 2019. Discrepancies between the two topologies concerned the placement of *P. dentatus* and *P. mhlophe*

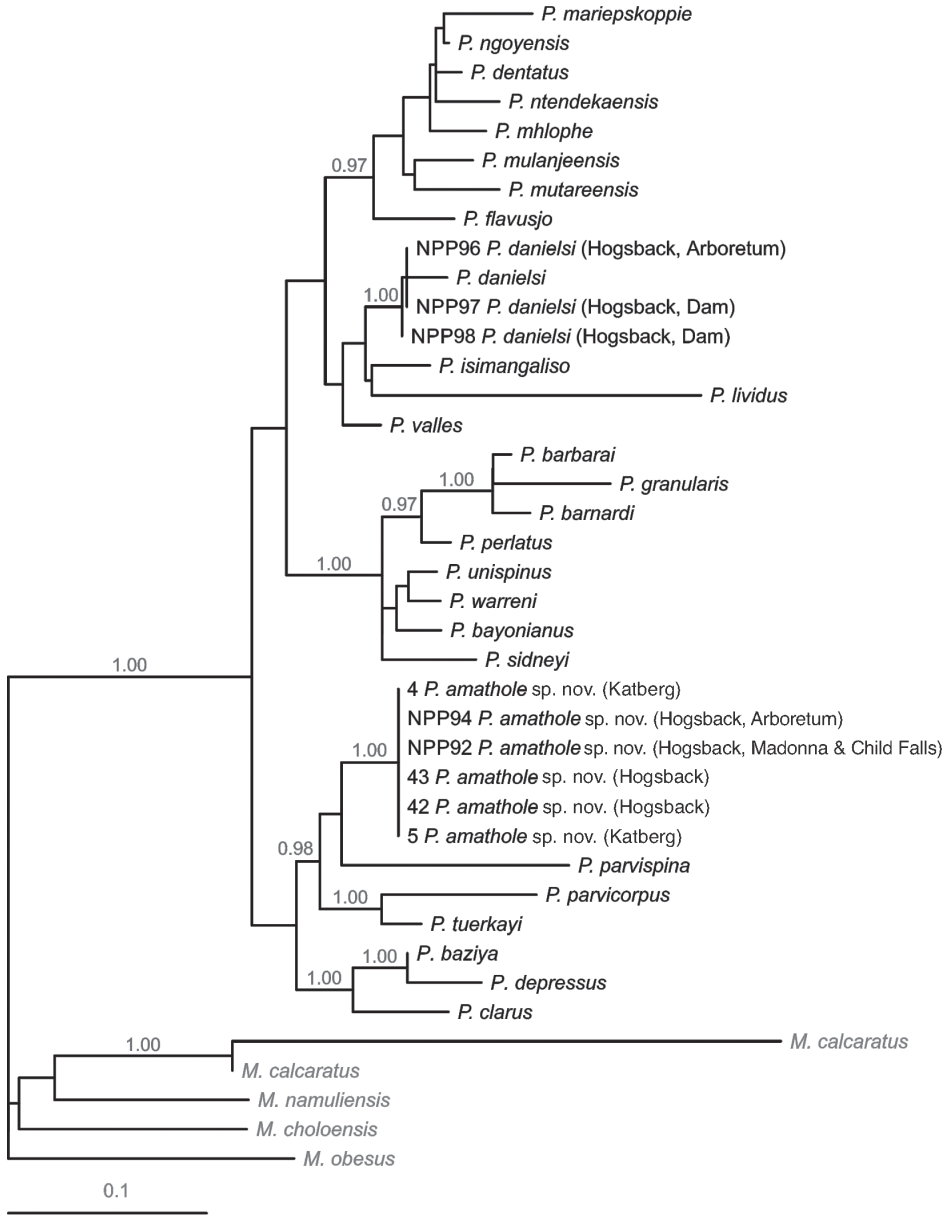

Figure 2. The most likely topology (-lnL = 3754.743) obtained in the Maximum-Likelihood analysis of a 549 nucleotide 16S rRNA alignment, depicting relationships between potamonautid freshwater crabs sampled from Hogsback and Katberg (Eastern Cape, South Africa) and known southern African *Potamonautes* species. Nodal support in the form of Bayesian Posterior Probabilities (BPPs) are indicated above the branches, with only BPPs > 0.95 shown. Species of *Maritimonautes* are included as outgroups.

Daniels, 2017 (see Figs 2 and 3); the generally accepted phylogenetic placement of these species is within the last of the aforementioned clades (see Daniels 2017; Daniels et al. 2019, 2021; Cumberlidge and Daniels 2022), as in the 16S topology.

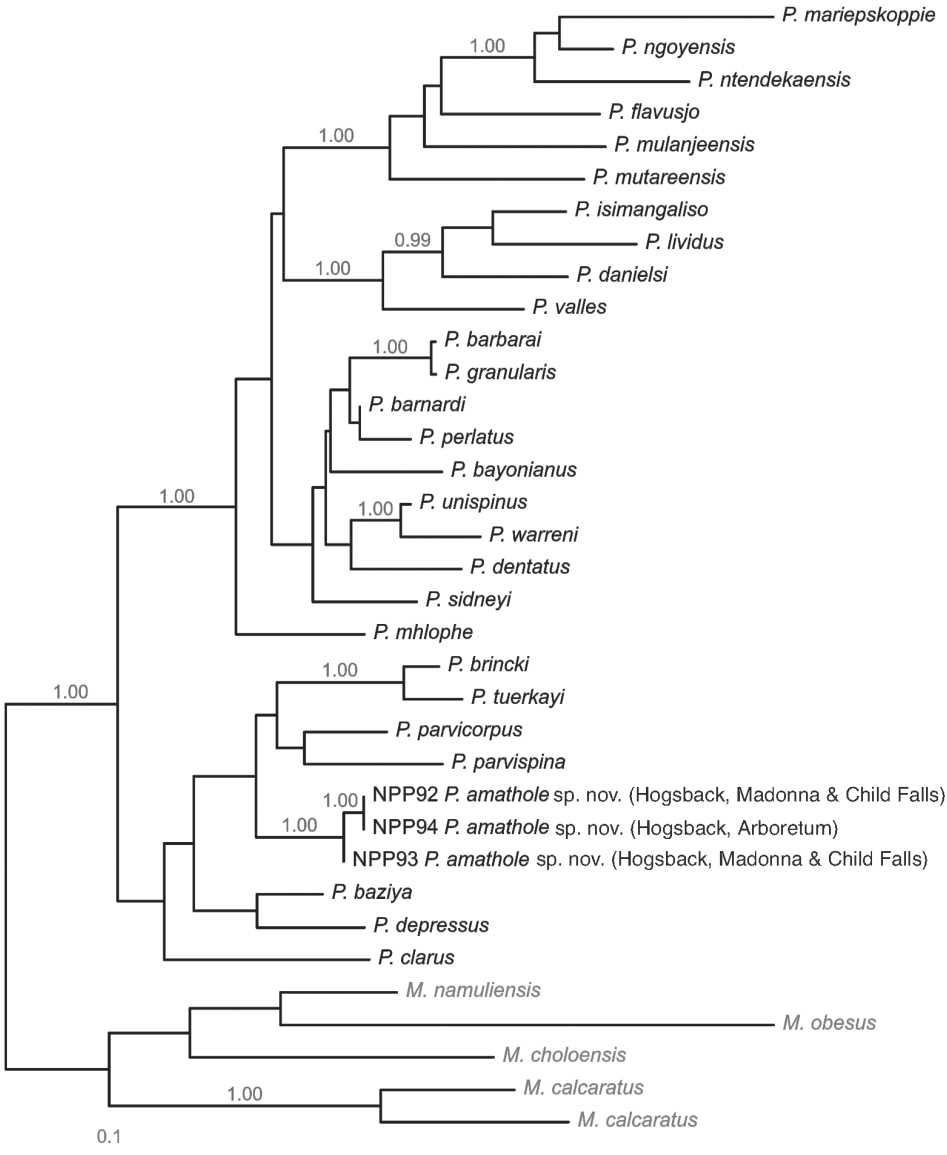

Figure 3. The most likely topology (-lnL = 5093.453) obtained in the Maximum-Likelihood analysis of a 660 nucleotide mtDNA cytochrome *c* oxidase subunit I (COI) alignment, depicting relationships between potamonautid freshwater crabs sampled from Hogsback (Eastern Cape, South Africa) and known southern African *Potamonautes* species. Nodal support in the form of Bayesian Posterior Probabilities (BPPs) are indicated above the branches, with only BPPs > 0.95 shown. Species of *Maritimonautes* are included as outgroups.

Of relevance to the current study, the crabs sampled from Hogsback and Katberg were placed in two separate clades. In the 16S topology, samples from Hogsback and Katberg were placed within the clade of small-bodied, mountain-dwelling species, sister to *P. parvispina*, in a larger well-supported clade (BPP = 0.98) of mountain-dwell-

ing species from the Western Cape (*P. parvicorpus*, *P. parvispina*, and *P. tuerkayi*), which was sister to a clade containing those (*P. baziya*, *P. clarus*, and *P. depressus*) from the Drakensberg in the Eastern Cape and KwaZulu-Natal. Other samples from Hogsback, including one collected sympatrically with the aforementioned at the Hogsback Arboretum, were allied to *P. danielsi* within the clade of IOCB forest-dwelling species with high support (BPP 1.00). In the COI topology, where only samples from Hogsback were included, these were placed similarly within the clade of mountain-dwelling species. These results suggest the presence of two distinct species among the crabs sampled from Hogsback and Katberg.

Uncorrected sequence divergences among individuals are presented in Suppl. material 1: table S2. The Hogsback specimens within the clade of IOCB species were 1.5% divergent from *P. danielsi*. Given their close affinity and the general trends in terms of sequence divergence, and the strong support (BPP = 1.00) for the clade formed by these specimens and *P. danielsi*, it is considered that these are conspecific. The Hogsback and Katberg specimens within the mountain-dwelling clade were 5.4 to 8.9% divergent from the other species in this clade and were 5.8 to 8.3% divergent from their sister-taxon (*P. parvispina*). In the context of the above divergences among known species, the Hogsback and Katberg specimens in this clade are considered to be a distinct species, described below. The Hogsback specimens were also 7.6–8.0% divergent from those collected in sympatry or near-sympatry but belonging to the IOCB clade.

For the COI data, where the only specimens included from Hogsback belonged to the clade of mountain-dwelling species, uncorrected sequence divergences between these specimens and other species in that clade ranged from 7.4 to 10.9%. With the exception of the comparison between *P. barbarai* and *P. granularis* (0.5%), previously described species were 2.4 to 18.4% divergent. Comparatively, these divergences again support the taxonomic distinctiveness of the Hogsback (and, by extension, Katberg) specimens.

Taxonomic description

Genus *Potamonautes*

***Potamonautes amathole* Peer & Gouws, sp. nov.**
https://zoobank.org/E47B3AFA-479B-496E-B7E3-F1F13849CEC2

Type series. *Holotype*: male, CL = 25.3 mm (Table 2), cascading stream in the Katberg State Forest (32°28'26.4"S, 26°40'05.9"E, elevation 1070 m), 25 October 2018, L. Maliwa, N. Miranda and N. Peer legit (MB-A094813). Allotype: female, CL = 24.9 mm (Table 2), collection details as per holotype (MB-A094814). ***Paratypes*:** (Table 2) collection details same as above, MB-A094815 (8 ♂, 4 ♀). Hogsback Arboretum, MB-A094816 (2 ♀), 32°35'25.2"S, 26°56'02.7"E, elevation 1235 m, 24 October 2018, L. Maliwa, N. Miranda and N. Peer legit. Madonna and Child Waterfall, Hogsback, MB-A094817 (1 ♂, 1 ♀); 32°36'24.4"S, 26°57'48.2"E, elevation 1092 m, 24 October 2018, L. Maliwa, N. Miranda and N. Peer legit.

Table 2. Ranges of measurements (mm) for 12 morphometric variables of the *Potamonautes amathole* sp. nov. holotype and paratypes collected from Katberg and Hogsback, as well as *P. brincki*, *P. tuerkayi*, *P. parvispina*, and *P. parvicorpus* from published sources.

Variable	*Potamonautes amathole* sp. nov.			*Potamonautes brincki* Stewart, 1997		*Potamonautes tuerkayi* Wood & Daniels, 2016	*Potamonautes parvispina* Stewart, 1997		*Potamonautes parvicorpus* Daniels, Stewart & Burmeister, 2001	
	Holotype	Males (n = 11)	Females (n = 8)	Males	Females	Holotype	Males	Females	Males	Females
CL	25.3	19.5–25.3	19.3–25.5	15.5–26.9	9.1–25.3	20	20.8–28.7	22.7–28.4	11.85–24.08	9.13–24.71
CWW	37.3	27.8–37.5	26.8–35.5	20.4–38.2	11.4–35.1	30	28.9–42.0	31.5–41.3	15.9–36.24	11.41–34.99
CWP	12.5	10.0–14.3	10.5–15.0	16.8–28.6	9.8–27.7	10	23.3–32.6	25.6–32.8	12.75–26.38	9.84–27.95
CH	12.8	9.0–12.8	8.5–12.0	4.5–7.7	4.5–13.6	10	10.3–16.4	12.4–15.3	5.68–13.48	4.47–13.12
PFCD	3.8	3.0–3.8	2.5–3.8	2.6–3.9	1.4–3.6	4	3.2–4.6	3.7–4.5	2.06–4.27	1.42–3.82
ED	13.5	9.5–13.8	9.0–12.5	7.7–13.4	4.7–12.4	-	10.7–15.3	11.7–14.5	7.03–13.28	4.73–14.07
CWA	25	18.5–24.5	17.8–23.8	15.1–26.5	9.3–24.6	10	21.7–29.2	22.2–27.6	12.57–24.09	9.27–23.84
AW6	8	6.0–7.8	15.0–21.8	13.1–42.7	6.6–22.7	-	5.6–8.1	13.5–24.7	3.62–7.63	3.10–21.57
MCPL	39	22.0–37.0	15.0–21.5	5.1–17.7	2.4–8.4	32	19.8–42.1	19.2–24.2	9.60–25.08	6.59–19.15
MCPW	16.1	9.0–15.3	5.0–7.3	8.2–17	4.5–13.9	12	8.0–19.4	7.3–9.1	3.34–12.81	2.41–10.84
P2ML	15	11.0–15.5	8.8–12.5	7.8–14.9	3.1–23.2	12	11.2–18.5	12.7–14.8	6.21–14.20	1.92–12.62
P2MW	4	3.0–4.0	3.0–4.3	3.6–5.9	1.9–5.6	3	4.4–5.5	5.2–5.4	2.76–4.77	1.92–4.44

Diagnosis. *Potamonautes amathole* sp. nov. exhibits a smooth carapace, flank and epibranchial region, with a rounded anterolateral margin and a narrow posterior end. Postfrontal crest complete. Dactyl of major cheliped highly arched. Pereopod 4 is longest. Bi-lobed maxillary palp with no flange.

Description of holotype. ***Carapace*** (Fig. 4). Cephalothorax ovoid, dorsally flattened, maximum height and width at anterior third (CH/CL = 0.5, CWW/CL = 1.47). Branchial region rounded. Anterior margin straight, lying on same horizontal plane as anterolateral margin; anterolateral margin slightly granulated. Urogastric grooves well-defined; cardiac and cervical grooves well-defined where attached to urogastric groove, becoming poorly defined and shallow towards edge of carapace. Epigastric lobes well-defined by two indentations forked from midpoint of postfrontal crest. Postfrontal crest complete, straight, and distinct, curving down at epibranchial region, sloping backwards to join anterolateral margin. Exorbital teeth present. Epibranchial teeth absent. Carapace brown with orange-brown to purple-brown limbs when alive.

Sternites (Fig. 4b). Sternites 1 and 2 fused, no sulcus. Second sulcus (s2/s3) prominent across sternum and third sulcus (s3/s4) complete, deep, projecting down medially towards abdomen.

Third maxilliped (Figs 4c, 5e). Filling entire buccal frame except oval respiratory openings at top lateral corners. Ischium slightly scabrous, absence of vertical groove. Flagellum on exopod of third maxilliped curving upwards at distal ends.

Mandibular palp (Fig. 5c, d). Consists of two segments. Terminal segment undivided, with dense tuft of setae on posterior proximal surface, margins hirsute. Subterminal segment short, thickened distally, almost round in appearance.

Figure 4. *Potamonautes amathole* sp. nov. male holotype (MB-A094813) **a** dorsal view **b** ventral view, and **c** cephalothorax, frontal aspect. Scale bar: 10 mm.

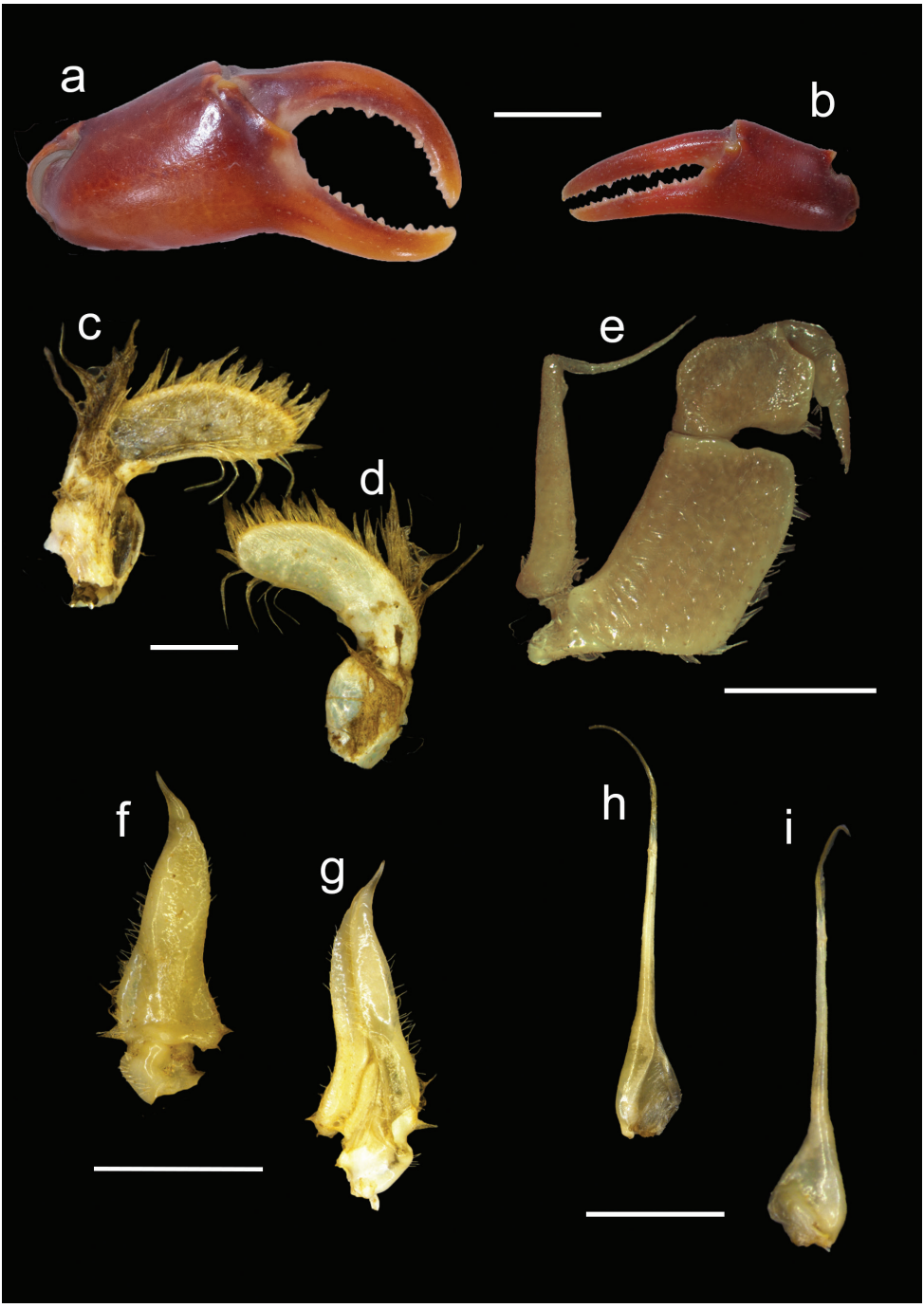

Figure 5. *Potamonautes amathole* sp. nov. male holotype (MB-A094813) **a** major cheliped **b** minor cheliped **c** right mandibular palp posterior view **d** right mandibular palp anterior view **e** 3rd maxilliped **f** left gonopod 1 anterior view **g** left gonopod 1 posterior view **h** left gonopod 2 posterior view, and **i** left gonopod 2 anterior view. Scale bars: 10 mm (**a, b**); 1 mm (**c, d**); 5 mm (**e–i**).

Pereopods (Figs 4a, c, 5a, b). General right-handedness. Inequality of chelae (CRDL/CLDL = 1.41). Dactyl of major chela highly arched, large interspace formed in major cheliped when fingers closed, slim interspace formed when minor cheliped closed. Propodus fairly slim (CRPW/CRPL = 0.41), exhibiting 17 cutting teeth on major dactyl and 15 cutting teeth on pollex, some larger and more prominent. Carpi on either side with one prominent tooth and two rudimentary teeth. Meri granulated with spine on anterior surface. Slender pereopods (P2: ML/MW = 3.75; P5: ML/MW = 3.61), pereopod 4 longest, pereopod 5 shortest. Ventral margins of propodi smooth, dorsal margins bearing fine serration, dactyli serrated, ending in sharp points.

Pleon (Fig. 4b). Somites 1–6 four sided, with triangular distally-rounded terminal segment (telson). First 5 somites broad and short; somite 6 and telson longer.

Pleopods (Fig. 5f–i). Gonopod 1 terminal segment short, 0.24 length of subterminal segment, widest at base, tapering, ends in sharp point at distal end of terminal segment. Medial margin slightly irregular, inner lateral margin curved, margins hirsute. Terminal segment curves away from medial line when viewed posteriorly. Longitudinal groove extending the length of both subterminal and terminal segment, visible on dorsal surface. Gonopod 2 consisting of two segments; terminal segment 0.57 times length of subterminal segment, filamentous; subterminal segment widest at base, tapering gently inward 0.4 of length, forming narrow process supporting terminal segment. Gonopod 2 with straight subterminal segment, terminal segment curves inward toward medial line.

Variation. The major cheliped is not always distinctly arched, especially in females and juveniles.

Live colouration. Colouration varies between orange-brown to a darker purple-brown when alive. Tips of the dactyli may be paler in colour, displaying as orange or paler brown/purple.

Distribution. Currently known only from the Katberg State Forest, the Hogsback State Forest, Madonna and Child Falls and the Hogsback Arboretum, all situated in the Amathole Mountain Range in the Eastern Cape province of South Africa.

Etymology. The species is named after the Amathole Mountains, part of the Winterberg-Amathole mountain range complex, located on the Great Escarpment in the Eastern Cape. It is currently thought to be endemic to this region. The isiXhosa name 'Amathole' translates to 'calves' in English and refers to the mountain range, the forest, and the municipal district.

Remarks. *Potamonautes amathole* sp. nov. is genetically and morphologically most similar to the Western Cape small-bodied montane freshwater crabs, i.e., *P. brincki* (Bott, 1960), *P. parvispina* Stewart, 1997, *P. parvicorpus* Daniels, Stewart & Burmeister, 2001, and *P. tuerkayi* Wood & Daniels, 2016. Morphologically, the species can be most easily distinguished from *P. parvispina* by the latter's small but pronounced epibranchial tooth. *Potamonautes parvicorpus* bears slightly arched chelipeds, an arched carapace, and a poorly developed postfrontal crest, while the new species has highly arched major chelipeds, a flattened carapace and a distinct postfrontal crest. *Potamonautes brincki* also has an arched carapace as well as a partitioned terminal segment of the

mandibular palp with a setae-covered flange. *Potamonautes amathole* sp. nov. has a unilobed terminal segment of the mandibular palp with no flange. Of all the Western Cape montane freshwater crabs, *P. tuerkayi* is the most similar to *P. amathole* sp. nov. However, *P. tuerkayi* has a sharply tapering subterminal segment of gonopod 2, forming a rounded subterminal base, while in *P. amathole* sp. nov. this tapering is gradual, forming a sloping instead of a rounded base. Geographically, the above-mentioned species are all confined to the Cape Fold Mountain region, with *P. amathole* sp. nov. being the first described small-bodied montane freshwater crab from the Eastern Cape part of the Great Escarpment.

Potamonautes depressus and *P. clarus* are two species of highland river crabs in the Drakensberg Mountain range. Although superficially similar to *P. amathole* sp. nov. in terms of a flattened carapace and slender limbs, morphological differences do exist in the structure of the mandibular palp and carapace depression. In *P. clarus*, a bright orange species, the mandibular palp has a flange on the terminal segment, while this is absent in *P. amathole*. *Potamonautes depressus* has an extremely flattened carapace, with CH/CL ranging from 0.38–0.43. In *P. amathole* sp. nov., this depression of the carapace is less extreme with a ratio ranging from 0.43–0.51. Both of these species are confined to fast-flowing rivers in the Drakensberg highlands. In most other *Potamonautes* spp., pereopod 3 is the longest. However, in *P. amathole* sp. nov., pereopod 4 appears to be the longest.

Habitat and ecology. Hogsback and Katberg are both situated in the Keiskamma River catchment. Both sites consist of Southern Mistbelt Forest (FoZ 3), known to be tall, multi-layered, species-rich forests dominated by *Afrocarpus falcatus*, *Celtis africana*, *Calodendrum capense*, *Vepris lanceolata*, and *Zanthoxylum davyi* (Mucina and Rutherford 2006). Within the forest and grassland, patches of Eastern Temperate Freshwater Wetlands (AZf3) can be found (Mucina and Rutherford 2006).

The Hogsback (Madonna and Child) Waterfall site is situated inside the Hogsback State Forest. The habitat is represented by a tall, high-flowing stream with different biotopes and pools rich in macro-invertebrate diversity, i.e., Ephemeroptera, Coleoptera, Hemiptera, Diptera, Trichoptera, Odonata, and Plecoptera (Griffiths et al. 2015). The substrate is largely bedrock with sand and large stones. The site is characterised by a diversity of flora species, including *Canthium ciliatum*, *Protorhus longifolia*, *Afrocarpus falcatus*, and *Scolopia mundii* (Hawley et al. 2004; Mucina and Rutherford 2006).

The second site is situated inside the Hogsback Arboretum Park, downstream from the 39 Steps Waterfall. The habitat is represented by a small stream with pools and the substrate is largely sand with rocks. The edge of the stream is represented by marginal vegetation (i.e., *Pseudoschoenus inanis*) with tree canopy cover and burrows (Griffiths et al. 2015). The site is characterised by a diversity of planted flora species.

The Katberg site is situated in the montane Katberg State Forest. This habitat is comprised of a trickling stream on a very steep slope. The habitat is represented by low and clean water with some other macro-invertebrate diversity, i.e., Ephemeroptera, Coleoptera, Hemiptera, Diptera, Trichoptera, and Odonata (Griffiths et al. 2015). The substrate is largely bedrock with sand and stones. The edge of the stream is represented

by marginal vegetation with dense tree canopy cover and burrows. The site is characterised by a diversity of flora species, including *C. ciliatum*, and *P. longifolia* (Hawley et al. 2004; Mucina and Rutherford 2006).

At the Hogsback Arboretum site, *P. amathole* sp. nov. co-occurs with *P. danielsi*. *Potamonautes danielsi* is also found at the nearby Municipal Dam.

Discussion

Resolving the distribution of southern African potamonautids is often difficult due to the general cryptic nature of this genus (Daniels et al. 2022). However, despite this, *Potamonautes amathole* sp. nov. can be distinguished from its sister species both genetically and morphologically. Providing detailed descriptions and highlighting morphological differences also facilitates accurate species records and highlights potentially new species, not just by the scientific community but also from citizen scientist observations (Daniels et al. 2022). Considering that more extensive sampling is required to fully explore potamonautid diversity, especially in high altitude and under-sampled regions, these citizen science observations play a significant role in the taxonomy of freshwater brachyurans.

16S Sequence divergences among previously known species ranged from 2.1 to 16.9%; the exception being the comparison between *P. dentatus* and *P. mhlophe* (1.5%). The indication of the *P. danielsi* Hogsback population, alongside the morphological identification of the specimen used in a study by Gouws et al. (2018), extends the known range of *P. danielsi* (see Peer et al. 2017) further south-westward and into the broader Amathole Forest and the Albany Thicket vegetation biomes (sensu Mucina and Rutherford 2006).

Although South African freshwater crabs have been extensively researched, we continue to find and describe new species (Daniels et al. 2021, 2022). This is partly due to ongoing efforts to target poorly sampled areas. Although the group has been well-studied in the KwaZulu-Natal and Western Cape provinces, this paper describes only the second montane freshwater crab from the Eastern Cape (the first being *P. baziya*). In KZN, two montane freshwater crabs, i.e., *P. clarus* and *P. depressus*, together with *P. baziya* represent the Drakensberg Escarpment species, with all three being closely related. In the Western Cape, *P. parvispina*, sister species to *P. amathole* sp. nov., is located within the Cederberg region. Myburgh and Daniels (2022) considered the speciation of the three additional Western Cape montane species, i.e., *P. brincki*, *P. tuerkayi*, and *P. parvicorpus*, and found an east/west separation defined by the Cape Fold Mountains. The results from this study and that of Daniels et al. (2021) indicate that *P. amathole* sp. nov. diverged before the separation of the Cape Fold montane species. Several routes of palaeo- and current connectivity along the Great Escarpment have been demonstrated for floristic species (Clark et al. 2011a, b; Janks 2014) with Galley et al. (2007) proposing a radiation from the Cape in a north-east direction towards the Drakensberg mountains, passing through the Winterberg-Amathole mountain range.

A similar pattern of connectivity has been proposed for some invertebrate species including coleopterans (Bilton 2015) and ephemeropterans (Taylor et al. 2020), although this requires more in-depth investigation.

Barnes and Daniels (2019), in a study of onychophoran velvet worms from forests in the Winterberg-Amathole mountain range, highlighted that connectivity is often disrupted by forest fragmentation, especially in poorly conserved areas. This reinforces the need to target the under-sampled regions of South Africa, including the Great Escarpment, in order to properly describe biodiversity along this gradient and understand the phylogeographic patterns that occur along this system. This information, especially regarding endemic species, is crucial to highlight the need for more effective protection of South Africa's freshwater systems.

Acknowledgements

Dr NAF Miranda is thanked for his invaluable efforts in the field. This work is based on the research supported by the South African Research Chairs Initiative of the Department of Science and Technology (DST) and National Research Foundation (NRF) of South Africa. Any opinion, finding, and conclusion or recommendation expressed in this material is that of the author(s) and the NRF does not accept any liability in this regard. The genetic study presented here was partly supported by a Competitive Programme for Rated Researchers (CPRR13082029507) grant from the National Research Foundation.

References

Akaike H (1974) A new look at the statistical model identification. Institute of Electrical and Electronics Engineers Transactions on Automatic Control 19(6): 716–723. https://doi.org/10.1109/TAC.1974.1100705

Barnes A, Daniels SR (2019) On the importance of fine-scale sampling in detecting alpha taxonomic diversity among saproxylic invertebrates: A velvet worm (Onychophora: *Opisthopatus amaxhosa*) template. Zoologica Scripta 48(2): 243–262. https://doi.org/10.1111/zsc.12338

Bilton D (2015) Two new species of madicolous water beetle from South Africa (Coleoptera: Hydraenidae). African Invertebrates 56(1): 181–190. https://doi.org/10.5733/afin.056.0114

Bott R (1960) Crustacea (Decapoda): Potamonidae. In: Hanström B, Brinck P, Rudebeck G (Eds) South African animal life: results of the Lund University expedition in 1950–1951, vol. 7. Almqvist & Wiksells, Uppsala, 13–18.

Calman WT (1918) A new river crab from the Transvaal. Annals & Magazine of Natural History 9(3): 234–236. https://doi.org/10.1080/00222931808562306

Clark VR, Barker NP, Mucina L (2011a) The Great Escarpment of southern Africa: A new frontier for biodiversity exploration. Biodiversity and Conservation 20(12): 2543–2561. https://doi.org/10.1007/s10531-011-0103-3

Clark VR, Barker N, Mucina L (2011b) Taking the scenic route–the southern Great Escarpment (South Africa) as part of the Cape to Cairo floristic highway. Plant Ecology & Diversity 4(4): 313–328. https://doi.org/10.1080/17550874.2011.619584

Cumberlidge N, Daniels SR (2022) A new multilocus phylogeny reveals overlooked diversity in African freshwater crabs (Brachyura: Potamoidea): A major revision with new higher taxa and genera. Zoological Journal of the Linnean Society 194(4): 1268–1311. https://doi.org/10.1093/zoolinnean/zlab082

Cunningham CW, Blackstone NW, Buss LW (1992) Evolution of king crabs from hermit crab ancestors. Nature 355(6360): 539–542. https://doi.org/10.1038/355539a0

Daniels SR (2017) Sympatric colour morphs or distinct taxa? Examining species boundaries among two South African freshwater crabs (Decapoda: Potamonautidae: *Potamonautes* MacLeay, 1838), with the description of a new species. Journal of Crustacean Biology 37(6): 723–731. https://doi.org/10.1093/jcbiol/rux087

Daniels SR, Bayliss J (2012) Neglected refugia of biodiversity: mountainous regions in Mozambique and Malawi yield two novel freshwater crab species (Potamonautidae: *Potamonautes*). Zoological Journal of the Linnean Society 164(3): 498–509. https://doi.org/10.1111/j.1096-3642.2011.00773.x

Daniels SR, Stewart BA, Gibbons M (1998) *Potamonautes granularis* sp. nov (Brachyura, Potamonautidae), a new cryptic species of river crab from the Olifants River system, South Africa. Crustaceana 71(8): 885–903. https://doi.org/10.1163/156854098X00905

Daniels SR, Stewart BA, Burmeister L (2001) Geographic patterns of genetic and morphological divergence amongst populations of a river crab (Decapoda, Potamonautidae) with the description of a new species from mountain streams in the Western Cape, South Africa. Zoologica Scripta 30(3): 181–197. https://doi.org/10.1046/j.1463-6409.2001.00061.x

Daniels SR, Stewart BA, Gouws G, Cunningham M, Matthee CA (2002) Phylogenetic relationships of the southern African freshwater crab fauna (Decapoda: Potamonautidae: *Potamonautes*) derived from multiple data sets reveal biogeographic patterning. Molecular Phylogenetics and Evolution 25(3): 511–523. https://doi.org/10.1016/S1055-7903(02)00281-6

Daniels SR, Phiri EE, Bayliss J (2014) Renewed sampling of inland aquatic habitats in southern Africa yields two novel freshwater crab species (Decapoda: Potamonautidae: *Potamonautes*). Zoological Journal of the Linnean Society 171(2): 356–369. https://doi.org/10.1111/zoj.12139

Daniels SR, Busschau T, Cumberlidge N (2019) Two new species of freshwater crabs of the genus *Potamonautes* MacLeay, 1838 (Decapoda: Brachyura: Potamonautidae) from the forests of KwaZulu-Natal, South Africa. Journal of Crustacean Biology 39(4): 426–435. https://doi.org/10.1093/jcbiol/ruz024

Daniels SR, Barnes A, Marais H, Gouws G (2021) Surveys of Afrotemperate forests yields two new freshwater crabs (Decapoda: Potamonautidae: *Potamonautes* MacLeay, 1838) from South Africa. European Journal of Taxonomy 782: 82–107. https://doi.org/10.5852/ejt.2021.782.1591

Daniels SR, Busschau T, Gullacksen G, Marais H, Gouws G, Barnes A (2022) Cryptic and widespread: a recipe for taxonomic misidentification in a freshwater crab species (Decapoda: Potamonautidae: *Potamonautes sidneyi*) as evident from species delimitation

methods. Zoological Journal of the Linnaean Society, zlac068. [Online early] https://doi.org/10.1093/zoolinnean/zlac068

Darriba D, Taboada GL, Doallo R, Posada D (2012) jModelTest 2: More models, new heuristics and parallel computing. Nature Methods 9(8): 772. https://doi.org/10.1038/nmeth.2109

de Brito Capello F (1864) Descripção de tres especies novas de crustaceos da Africa occidental e observações ácerca do *Penoeus bocagei* Johnson. Especie nova dos mares de Portugal. Typographia da Academia, Lisboa, 11 pp.

Galley C, Bytebier B Bellstedt, Linder PH (2007) The Cape element in the Afrotemperate flora: from Cape to Cairo? Proceedings of the Royal Society B, Biological Sciences 274: 535–543. https://doi.org/10.1098/rspb.2006.0046

Geldenhuys CJ, MacDevette DR (1989) Conservation status of coastal and montane evergreen forest. In: Huntley BJ (Ed.) Biotic diversity in southern Africa: concepts and conservation. Oxford University Press, Cape Town, 224–238.

Gouws G, Stewart BA, Coke M (2000) Evidence for a new species of river crab (Decapoda, Brachyura, Potamonautidae) from the Drakensberg, South Africa. Journal of Crustacean Biology 20(4): 743–758. https://doi.org/10.1163/20021975-99990096

Gouws G, Stewart BA, Reavell PE (2001) A new species of freshwater crab (Decapoda, Potamonautidae) from the swamp forests of KwaZulu-Natal, South Africa: Biochemical and morphological evidence. Crustaceana 74(2): 137–160. https://doi.org/10.1163/156854001750096256

Gouws G, Peer N, Perissinotto R (2015) MtDNA lineage diversity of a potamonautid freshwater crab in KwaZulu-Natal, South Africa. Koedoe 57(1): #1324. [12 pages] https://doi.org/10.4102/koedoe.v57i1.1324

Gouws G, Daniels SR, MacDonald AH, Chakona A, Barker NP (2018) Development and characterization of a microsatellite library for the freshwater crab *Potamonautes danielsi* Peer, Gouws, Lazo-Wasem, Perissinotto & Miranda, 2017 (Brachyura: Potamonautidae) and its transferability across three congeneric species. Journal of Crustacean Biology 38: 765–771. https://doi.org/10.1093/jcbiol/ruy081

Griffiths C, Day J, Picker M (2015) Freshwater Life: A Field Guide to the Plants and Animals of Southern Africa. Struik Nature, Cape Town, South Africa, 368 pp.

Janks MR (2014) Montane wetlands of the South African Great Escarpment: plant communities and environmental drivers. (MSc thesis) Rhodes University, South Africa.

Katoh K, Toh H (2008) Recent developments in the MAFFT multiple sequence alignment program. Briefings in Bioinformatics 9(4): 286–298. https://doi.org/10.1093/bib/bbn013

Katoh K, Kuma K, Toh H, Miyata T (2005) MAFFT version 5: Improvement in accuracy of multiple sequence alignment. Nucleic Acids Research 33(2): 511–518. https://doi.org/10.1093/nar/gki198

Kok AD, Parker DM, Barker NP (2012) Life on high: The diversity of small mammals at high altitude in South Africa. Biodiversity and Conservation 21(11): 2823–2843. https://doi.org/10.1007/s10531-012-0340-0

Krauss F (1843) Südafrikanischen Crustaceen. Eine Zusammenstellung aller bekannten Malacostraca, Bemerkungen über deren Liebenswiese und geographische Verbreitung, nebst beschreibung und Abbildung mehrer neuen arten. E. Schweizerbart'sche Verlagsbuchhandlung, Stuttgart, 81 pp. https://doi.org/10.5962/bhl.title.4825

Larkin MA, Blackshields G, Brown NP, Chenna R, McGettigan PA, McWilliam H, Valentin F, Wallace IM, Wilm A, Lopez R, Thompson JD, Gibson TJ, Higgins DG (2007) Clustal W and Clustal X version 2.0. Bioinformatics 23(21): 2947–2948. https://doi.org/10.1093/bioinformatics/btm404

Milne Edwards H (1834–1840) Histoire naturelle des Crustacés, comprenant l'anatomie, la physiologie et la classification des ces animaux. 2nd edn. Librairie encyclopédique de Roret, Paris, 546 pp. https://doi.org/10.5962/bhl.title.16170

Mucina L, Rutherford MC (2006) The Vegetation of South Africa, Lesotho and Swaziland. Strelitzia 19. Pretoria, South Africa: South African National Biodiversity Institute: Pretoria, South Africa, 807 pp.

Myburgh AM, Daniels SR (2022) Between the Cape Fold Mountains and the deep blue sea: Comparative phylogeography of selected codistributed ectotherms reveals asynchronous cladogenesis. Evolutionary Applications 15(12): 1967–1987. https://doi.org/10.1111/eva.13493

Peer N, Perissinotto R, Gouws G, Miranda NAF (2015) Description of a new species of Potamonautes MacLeay, 1838, from the iSimangaliso Wetland Park, South Africa. ZooKeys 503: 23–43. https://doi.org/10.3897/zookeys.503.9532

Peer N, Gouws G, Lazo-Wasem E, Perissinotto R, Miranda NAF (2017) Redescription of *Potamonautes sidneyi* (Rathbun, 1904) (Decapoda, Potamonautidae) and description of a new congeneric species from KwaZulu-Natal, South Africa. ZooKeys 657: 1–28. https://doi.org/10.3897/zookeys.657.11623

Phiri EE, Daniels SR (2013) Hidden in the highlands: the description and phylogenetic position of a novel endemic freshwater crab species (Potamonautidae: *Potamonautes*) from Zimbabwe. Invertebrate Systematics 27(5): 530–539. https://doi.org/10.1071/IS13012

Phiri EE, Daniels SR (2014) Disentangling the divergence and cladogenesis in the freshwater crab species (Potamonautidae: *Potamonautes perlatus* sensu lato) in the Cape Fold Mountains, South Africa, with the description of two novel cryptic lineages. Zoological Journal of the Linnean Society 170(2): 310–332. https://doi.org/10.1111/zoj.12103

Phiri EE, Daniels SR (2016) Multilocus coalescent species delimitation reveals widespread cryptic differentiation among Drakensberg mountain-living freshwater crabs (Decapoda: *Potamonautes*). Invertebrate Systematics 30(1): 60–74. https://doi.org/10.1071/IS15035

Rathbun MJ (1904) Les Crabes d'Eau Douce (Potamonidae) 2. Nouvelles Archives du Muséum d'Histoire Naturelle (Paris) 7: 159–322.

Sambrook J, Russell DW (2001) Molecular Cloning: A Laboratory Manual. Volume 1. 3rd edn. Cold Spring Harbor Laboratory Press, Cold Spring Harbor, New York, 1546 pp.

Stewart BA (1997) Biochemical and morphological evidence for a new species of river crab *Potamonautes parvispina* sp. nov. (Brachyura, Potamonautidae). Crustaceana 70(6): 737–753. https://doi.org/10.1163/156854097X00168

Stewart BA, Cook PA (1998) Identification of a new species of river crab (Decapoda: Brachyura: Potamonautidae) from South Africa using morphological and genetic data. Journal of Crustacean Biology 18(3): 556–571. https://doi.org/10.2307/1549420

Stewart BA, Coke M, Cook PA (1995) *Potamonautes dentatus*, new species, a fresh-water crab (Brachyura: Potamoidea: Potamonautidae) from KwaZulu-Natal, South Africa. Journal of Crustacean Biology 15(3): 558–568. https://doi.org/10.2307/1548776

Swofford DL (2003) *PAUP*.* Phylogenetic Analysis Using Parsimony (*and Other Methods). Version 4. Sinauer Associates, Sunderland, Massachusetts, 140 pp.

Taylor CL, Barker NP, Barber-James HM, Villet MH, Pereira-da-Conceicoa LL (2020) Habitat requirements affect genetic variation in three species of mayfly (Ephemeroptera, Baetidae) from South Africa. ZooKeys 936: 1–24. https://doi.org/10.3897/zookeys.936.38587

Wood LE, Daniels SR (2016) Genetic and morphological evidence for a new mountain-living freshwater crab species (Decapoda: Potamonautidae: *Potamonautes*) from the Western Cape province of South Africa. Invertebrate Systematics 30(3): 219–230. https://doi.org/10.1071/IS15051

Supplementary material 1

Supplementary infromation

Authors: Gavin Gouws

Data type: phylogenetic

Explanation note: **table S1:** Representatives of valid southern African *Potamonautes* species included in the phylogenetic analysis used to contextualise divergences and confirm the affinities of specimens included in the current study. Four species of *Maritomonautes* were included as outgroup taxa. GenBank accession numbers for the 16S rRNA and cytochrome c oxidase subunit I (COI) included and the data sources are provided; **table S2:** Uncorrected sequence divergences, expressed as percentages, as calculated from a 549 nucleotide alignment of 16S rRNA mtDNA sequences (below diagonal) and a 660 nucleotide alignment of the protein-coding mtDNA cytochrome c oxidase subunit I (COI) fragment (above diagonal), between representative of *Potamonautes* included in the present study. Newly-sampled specimens are identified as *Potamonautes danielsi* and *P. amathole* sp. nov.

Link: https://doi.org/10.3897/zookeys.1160.100844.suppl1

ZooKeys 1160: 109–124 (2023)
doi: 10.3897/zookeys.1160.103110
https://zookeys.pensoft.net

RESEARCH ARTICLE

A peer-reviewed open-access journal
ZooKeys
Launched to accelerate biodiversity research

Adult morphology and redescription of *Lestidiops indopacificus* (Ege, 1953), with comments on the features of related species (Teleostei, Aulopiformes, Paralepididae)

Hsuan-Ching Ho[1,2,3,4], Tzu-Yung Lin[4]

1 *National Museum of Marine Biology and Aquarium, Pingtung, Taiwan* **2** *Institute of Marine Biology, National Donghwa University, Pingtung, Taiwan* **3** *Australian Museum, Sydney, Australia* **4** *Department and Graduate Institute of Aquaculture, National Kaohsiung University of Science and Technology, Kaohsiung, Taiwan*

Corresponding author: Tzu-Yung Lin (plextorx0428@nkust.edu.tw)

Academic editor: Nina Bogutskaya | Received 7 March 2023 | Accepted 14 April 2023 | Published 4 May 2023

https://zoobank.org/ED630F5B-916D-43AD-835B-11D2337EF8DA

Citation: Ho H-C, Lin T-Y (2023) Adult morphology and redescription of *Lestidiops indopacificus* (Ege, 1953), with comments on the features of related species (Teleostei, Aulopiformes, Paralepididae). ZooKeys 1160: 109–124. https://doi.org/10.3897/zookeys.1160.103110

Abstract

Two specimens representing the first known adults of *Lestidiops indopacificus* (Ege, 1953) are reported and described from Taiwan, and the validity and generic assignment of this species are confirmed. The origin of the pelvic fin directly below the dorsal-fin base shows that *L. indopacificus* belongs to the *L. mirabilis* species complex. It can be separated from its congeners by the position of the nostrils above the posterior end of the maxilla, the light body color with unevenly distributed melanophores in adults, and a distinct combination of meristic values and other morphological characteristics. New geographic records are reported for the two other current members of this species complex, *L. mirabilis* (Ege, 1933) and *L. extremus* (Ege, 1953). The diagnostic features that separate these three very similar species are discussed.

Keywords

Biodiversity, biogeography, ichthyofauna, ichthyology, taxonomy

Introduction

The barracudina genus *Lestidiops* was established by Hubbs (1916) but was assigned by Harry (1953a) to one of three subgenera in *Lestidium* before being elevated again by Rofen (1966) to a full genus. *Lestidiops* belongs to the naked paralepidids (subfamily Lestidiinae), which have a scaleless body except for the lateral-line, a single row of short teeth on the gill rakers, and more than 77 vertebrae. *Lestidiops* can be separated from the other genera of Lestidiinae by the following combination of features: head, snout, and body short to moderately slender; nostrils situated slightly to well before a vertical drawn through posterior end of maxilla; light organs and luminescent duct absent; anus close to tip of adpressed pelvic fin; anal-fin rays 25−32; lateral-line usually incomplete (i.e. not reaching caudal-fin base, except in some species); well-developed ventral adipose fin present between anus and anal fin; and unevenly distributed melanophores to uniform black in adults (Harry 1953a; Rofen 1966; this study). There are about 25 nominal species of *Lestidiops*, but no conclusion has been reached as to how many are valid (Ho pers. data).

Recently, two adult specimens of barracudina collected from off southern Taiwan were observed to have the pelvic-fin origin below the dorsal-fin base and no light organs or luminescent duct. They were initially identified as *Lestidiops mirabilis* (Ege, 1933) by the authors; however, both specimens had a much lighter body color compared to the uniformly dark brown to black body of specimens of *L. mirabilis*. More detailed examination has revealed that these two specimens represented the first adults specimens ever recorded of another, little-known species, *Lestidiops indopacificus* (Ege, 1953).

Lestidiops indopacificus, originally *Lestidium indopacificum*, was described based on juveniles collected from the Indian Ocean (Ege 1953: fig. 30), with many larval specimens taken from widely scattered sites across the Indo-West Pacific. At 31.0 mm SL, the holotype has been the largest specimen available until now. Although many specimens in collections have been putatively identified as this species, it has not yet been possible to confirm these. Most literature records have been based on the original description, and others were likely misidentifications (Ho pers. data).

Lestidiops mirabilis, originally *Paralepis mirabilis*, was described by Ege (1933) solely on its holotype (whereabouts unknown), which had been collected from the Sulawesi Sea in the western Pacific. Ege (1953) provided more details of this species based on many juveniles (<47 mm SL) from the tropical Indo-Pacific and western Atlantic oceans. Adults of this species are rather rare, and only a few specimens are known from scattered localities (e.g., Harry 1953b; Uyeno et al. 1983; Gloerfelt-Tarp and Kailola 1984; Ho and Huang 2022). Some additional adult specimens from various localities were examined in the present study.

Recently, Ho and Huang (2022) provided the first description of an adult *Lestidiops extremus* (Ege, 1953) from the Philippines and compared it with *L. mirabilis*. Another specimen from Myanmar, representing the first record of *L. extremus* in the eastern Indian Ocean, is reported in the present work.

This paper provides the first detailed description of adult-stage *L. indopacificus* and a comparison with its most closely related congeneric species. Morphological and biogeographical data pertaining to newly found specimens of *L. mirabilis* and *L. extremus* are also presented.

Material and method

Counts and measurements were made following Ho and Golani (2019) and Ho et al. (2019a), with the addition of pre-nostril length measured from the tip of the snout to the center of the nostrils. The examined specimens are deposited in the Australian Museum, Sydney, Australia (**AMS**), Kochi University, Kochi, Japan (**BSKU**), the National Museum of Marine Biology and Aquarium, Pingtung, Taiwan (**NMMB-P**), the Department of Zoology, National Museum of Nature and Science, Tsukuba, Japan (**NSMT**), the South African Institute for Aquatic Biodiversity, Grahamstown, South Africa (**SAIAB**), and the Zoological Museum, Natural History Museum of Denmark, Copenhagen, Denmark (**ZMUC**).

Morphometric data were not taken from specimens in poor condition, including those that had been bent or damaged. Abbreviations: **DFO**, dorsal-fin origin; **AFO**, anal-fin origin; **VFO**, pelvic-fin origin. **D−A**, horizontal distance between the origins of the dorsal and anal fins (= preanal length minus predorsal length) and **V−A**, horizontal distance between the origins of the pelvic and anal fins (= preanal length minus prepelvic length). **PVLL**, **PDLL**, and **PALL** are numbers of lateral-line scales before VFO, DFO, and AFO, respectively, **TLL** is the total number of lateral-line scales, including large and small scales. **PVV**, **PDV**, and **PAV** are numbers of vertebrae before VFO, DFO, and AFO, respectively, and **PHV**, **CV**, and **TV** are numbers of prehaemal, caudal, and total vertebrae, respectively.

Data used for comparison are taken from Ege (1953), Harry (1953b), and Ho and Huang (2022).

Results

Family Paralepididae

Identity as *Lestidiops indopacificus*

The holotype of *Lestidium indopacificum* (ZMUC P2329237) is in rather poor condition, with its dorsal fin missing entirely. Ventral adipose fins are present on the abdominal ridge and well developed between the anus and the AFO. The eyes are large, the snout is short, and the eye diameter is about half the snout length. There are 32 prepelvic vertebrae, 49 preanal vertebrae, and 80 total vertebrae counted directly from the translucent

specimen. There is neither a light organ around the eye nor a luminescent duct inside the abdominal cavity. The anus is located close to the tips of the adpressed pelvic fins.

The original data for the holotype (31.0 mm SL) provided by Ege (1953) recorded the predorsal length as 53.9% SL and the prepelvic length as 54.8% SL, which implies that the VFO is slightly behind the DFO and under the dorsal-fin base. No drawing of the holotype was provided, but it is notable that the drawing of the largest specimen (21.1 mm SL) provided in Ege (1953: fig. 26) shows its VFO situated on about the same vertical line as its DFO, which is slightly different from the relative positions of the fin origins implied by Ege (1953) for the holotype.

Rofen (1966) later assigned the species to *Lestidiops*, a conclusion accepted here. The total of 80 vertebrae excludes it from Paralepidinae. The position of the VFO slightly behind the DFO excludes it from *Stemonosudis* and *Dolichosudis*. The presence of ventral adipose fins and the position of the anus close to the tips of the adpressed pelvic fins exclude it from *Macroparalepis*, and the lack of light organs or a luminescent duct excludes it from *Lestidium* and *Lestrolepis*. The position of the nostrils above or before the posterior end of the maxilla and the presence of a small pelvic fin exclude it from *Uncisudis*.

If the inferred position of the VFO in the holotype is accepted as standard, *L. indopacificus* shares this feature only with *L. mirabilis* and, by this alone, these two species can be separated from all other nominal congeners. According to Ege (1953), *L. indopacificus* has 79−83 total vertebrae, 34−36 prehaemal vertebrae, and 29−32 anal-fin rays, data that match our two adult specimens well and which are clearly different from those of the two other current members of the *L. mirabilis* complex. In sum, all the available information allows the present specimens to be recognized as adults of *L. indopacificus*.

The *Lestidiops mirabilis* complex

The three species reported below share a distinctive characteristic, namely, the VFO lies clearly behind the DFO, either below the dorsal-fin base or slightly behind that point. Rofen (1966) included *L. mirabilis* and *L. extremus* in the *extremus* complex (= *L. mirabilis* complex herein). However, many members of the scaled genera in the Paralepidinae have in common the VFO behind the DFO and the VFO usually under or slightly behind the dorsal-fin base (Post 1987; Ho and Duhamel 2019). Members of *Lestidium atlanticum* complex, i.e. *L. atlanticum* Borodin, 1928, *L. orientale* Ho, Tsai & Li, 2019, and *L. longilucifer* Ho, Graham & Russell, 2020, usually have the VFO at about same vertical as the DFO, or with the VFO sometimes slightly before or behind the latter (Ho et al. 2020).

Based on our examination, the three current members of the *L. mirabilis* complex can be separated from other species of Paralepidinae by having 80−87 vertebrae in totalal, a single row of small teeth on the gill rakers (vs multiple rows of teeth, slender in many species), and a naked body except for the lateral-line scales (vs a body fully covered with scales). They can be separated from members of the *L. atlanticum* complex by the lack of a luminescent duct inside the abdominal cavity (vs a long duct extending to the gular region).

All other members of *Lestidiops*, regardless of their taxonomic validity, have the VFO situated slightly or well before the DFO.

***Lestidiops indopacificus* (Ege, 1953)**
Figs 1, 2; Tables 1, 2
English name: Gray lightless barracudina

Lestidium indopacificum Ege, 1953: 120, fig. 26 (type locality: off India, Indian Ocean, 1°45'N, 73°03'E, ca 100 m depth).
Lestidiops indopacificus (Ege, 1953): Post 1972: 148 (type catalog).
Lestidiops indopacificum (Ege, 1953): Rofen 1966: 301 (presumably in *Lestidiops*, maybe related to *L. mirabilis*).
Lestidiops indopacificus (Ege, 1953): Paxton et al. 1989: 246 (Australia, probably misidentification); Nakabo 2000: 368 (Ryukyus, juveniles only); Fukui and Ozawa 2004: 293 (list); Mundy 2005: 203 (larvae); Gomon 2008: 267 (Australia, misidentification of other *Lestidiops*).

Material examined. ***Holotype*:** ZMUC P2329237, in poor condition, 31.0 mm SL in original description. Adult specimens: NMMB-P34421 (2, 173–195 mm SL), off Dong-gang, Pingtung, southwestern Taiwan, ca 300 m depth, 30 Jul. 2020.

Diagnosis. Species of *Lestidiops* in the *L. mirabilis* species complex with the VFO under dorsal-fin base and anus farther posteriorly; dorsal portion of body and lateral line covered with melanophores, but large unpigmented areas present on lower portions of head and abdomen; lateral-line scales: PDLL 32–33, PVLL33–34, PALL 47–48, TLL 66–70; vertebrae: PDV 32–33, PVV 33–34, PAV 47–48, PHV 34–35, CV 44–45, TV 80; total number of gill rakers 42–44 (based on adult specimens). Juveniles without dark blotches or bands.

Description. Morphometric and meristic data as provided in Tables 1 and 2. Dorsal-fin rays 10; pectoral-fin rays 13–14; pelvic-fin rays 10; anal-fin rays 30. Lateral-line scales: PDLL 32–33, PVLL 33–34; PALL 47–48; 66–70 in total, with 58–61 large scales and (in rear portion) 6–9 small scales. Vertebrae: PDV 32–33, PVV 33–34, PAV 47–48, PHV 34–35, CV 44–45, 80 in total. Gill rakers: 42–44, with 8–11 on upper limb (epibranchial) and 33–34 on lower limb, including 21 on ceratobranchial + 12–13 on hypobranchial.

Body moderately long, strongly compressed, depth at pectoral fin 12.7–13.2 times in SL. Caudal peduncle short, its length 1.5–1.6 times eye diameter. Ventral adipose fin very weakly developed along abdominal ridge between pectoral and pelvic fins, better developed on margin between pelvic and anal fins. Anus situated above tip of appressed pelvic fin (smaller specimens with anus slightly before fin tip), distance from VFO to anus about 3.5–4.0 times in V–A.

Head moderately slender, long-triangular, its length 4.0–4.1 in SL; snout slender and pointed anteriorly, its length 1.7–1.8 in HL. Mouth terminal, moderately large, its gape extending to about 1.5 times eye diameter in front of eye. Lower jaw slightly upturned at tip, with small distal tab of fleshy tissue. Eye small, its diameter 6.0–6.2 in HL. No light organ around eye. First suborbital bone slender, fifth and sixth bones expanded posteriorly, and seventh small. Interorbital space narrow, its width 11.1–11.2 in HL; some straight ridges present on top of head and snout. Two nostrils located

Figure 1. Adults of *Lestidiops indopacificus* (Ege, 1953), NMMB-P34421 **A, C** 195 mm SL **B, D** 173 mm SL **A, B** fresh, photo by C.-N. Teng **C, D** preserved.

directly above posterior end of maxilla, latter extending to point about 2/3 eye diameter in front of eye. Numerous sensory canals on snout, check, operculum, and jaws; numerous sensory pores on dorsal surface of snout and lower surface of lower jaw.

Gill filaments present on all four gill arches. Fourth arch mostly connected to gill chamber wall by membranes. Pseudobranchs present, their anterior halves included in a deep pocket.

DFO slightly in front of VFO, predorsal length 1.7 in SL. Pectoral-fin base behind posterior margin of gill cover, upper end of fin base slightly below horizontal drawn through lower margin of eye; no small pocket behind fin base. VFO directly under dorsal-fin base, pre-pelvic fin length 1.6 in SL. No axial scale behind pelvic-fin base (probably lost during trawling). Anal fin originating in posterior fourth of body, pre-anal length 1.3 in SL. Dorsal adipose fin over rear portion of anal-fin base, its base length about equal to eye diameter.

Two or three small fangs at tip of upper jaw, followed by single row of numerous small, retrorse teeth, these gradually becoming smaller on posterior part of jaw. Vomerine teeth absent. One or two fangs (either depressible or fixed) at front end of each lower jaw, followed by two rows of fangs arranged in about 6 pairs (more teeth arranged irregularly on right jaw of larger specimen); those of inner row long with knife-like tip and depressible; those in outer row much shorter, curved, and fixed, slightly embedded in tissue. Two rows of fangs on each palatine with anteriormost teeth arranged in 4 widely spaced pairs, those in outer row long and depressible, those in outer row small

Figure 2. Close-up photos of *Lestidiops indopacificus* (NMMB-P34421, 173 mm SL), left side with anterior to left, showing pigmentation and positional details of various structures **A** head, with arrow pointing to the nostrils **B** anterior trunk, arrow point to abdominal ridge **C** posterior trunk, with bars pointing to DFO (upper), VFO (lower left), and AFO (lower right) **D** tail, with arrow pointing to end of lateral line.

Table 1. Morphometric data, as in % SL and % HL, of three species in the *L. mirabilis* complex. * including four specimens from Harry (1953b).

	L. indopacificus		*L. extremus*	*L. mirabilis*	
	NMMB-P34421		**AMS I.36462-006**	***n* = 8***	
SL	195	173	190	131.5–276	SD
In % SL					
Head length (HL)	24.7	24.3	21.4	24.3 (22.7–25.6)	0.9
Body depth	7.9	7.6	6.8	7.5 (7.1–8.0)	0.4
Predorsal length	60.1	59.8	57.9	61.7 (59.9–63.4)	1.1
Prepelvic length	60.8	60.7	63.2	61.9 (59.8–63.6)	1.4
Preanal length	75.8	75.7	76.1	78.3 (75.9–80.1)	1.2
V–A	15.0	15.0	12.9	16.4 (15.2–18.5)	1.1
D–A	15.8	16.0	18.2	16.6 (14.5–17.7)	1.1
Eye diameter	4.0	4.0	3.6	3.4 (3.1–4.0)	0.3
Interorbital width	2.2	2.2	2.6	2.8 (2.5–3.0)	0.2
Snout length	14.0	14.1	10.7	13.0 (12.3–14.4)	0.7
Head depth	6.6	6.4	6.2	6.3 (5.6–7.0)	0.6
Head width	3.4	3.5	–	3.8 (3.6–4.1)	0.2
Upper jaw	12.1	12.1	10.4	12.4 (11.8–13.1)	0.4
Lower jaw	16.2	16.9	13.6	16.2 (15.1–17.3)	1.0
Pectoral-fin length	–	–	9.5	10.3 (8.3–11.8)	1.1
Anal-fin base	17.5	17.7	17.9	15.5 (14.7–16.3)	0.6
Dorsal-fin base	3.5	3.3	3.9	3.7 (3.4–4.1)	0.3
Pre-nostril length	11.6	11.6	8.1	10.4 (10.2–10.6)	0.3
Caudal peduncle depth	2.3	2.4	–	2.6 (2.4–2.8)	0.2
Caudal peduncle length	6.1	6.6	5.6	4.3 (3.5–5.2)	1.2
In % HL					
Pectoral-fin length	–	–	44.2	42.2 (34.3–47.1)	4.6
Eye diameter	16.2	16.6	17.0	14.0 (13.0–15.6)	0.9
Interorbital width	8.9	9.0	12.3	11.2 (9.9–12.7)	1.0
Snout length	56.6	58.0	50.1	53.1 (49.0–56.2)	2.4
Head depth	26.8	26.1	28.7	26.4 (25.1–27.6)	1.2
Pre-nostril length	47.1	47.5	37.8	41.5	–
Upper jaw	49.0	49.6	48.4	50.7 (49.4–52.2)	1.1
Lower jaw	65.4	69.4	63.6	66.3 (63.2–67.9)	2.7

and fixed; single row of small, widely spaced, fixed teeth on posterior part of palatine. One row of small, straight teeth on each side of tongue.

Shield-shaped gill rakers present on epibranchial, ceratobranchial, and hypobranchial parts of each gill arch, each raker with 3–5 (rarely fewer) small teeth on broad base, these teeth barely extending upward beyond margin of gill arch. Teeth on pharyngeal arch short, arranged in oval patch with about 4 rows in middle. Single row of small teeth on fifth ceratobranchial.

Body scaleless, except for single row of lateral-line scales extending from above pectoral girdle to point above approximately two-thirds length of anal-fin base. Lateral-line scales slightly longer than wide, gradually becoming smaller and narrower posteriorly; 2 large pores on each upper and lower corner of most scales and 1 pore at front

Table 2. Meristic data of three species of the *Lestidiops mirabilis* species complex. Counts of both sides provided when different. * including four specimens from Harry (1953b). GR = gill rakers.

	L. indopacificus		*L. extremus*		*L. mirabilis*
	NMMB-P34421		**AMS I.36462-006**	**SAIAB 203471**	***n* = 9***
Dorsal-fin rays	10	10	10	10	9–10
Anal-fin rays	30	30	31	30	28–30
Pectoral-fin rays	14	13	12	13	12–14
Pelvic-fin rays	10	10	10	10	9–10
PVLL	33	33/34	38	37	35–40
PDLL	32	32/33	34	32	36–39
PALL	47	48	51	50	51–56
TLL (large)	58/60	59/61	63	63/62	63–67
TLL (small)	9/6	7/9	8	5/7	8–22
TLL	67/66	66/70	71	68/69	73–85
PHV	34	35	41	41	36–42
CV	44	45	39	40	43–45
PVV	33	34	38	38	36–39
PDV	32	33	33	32	35–38
PAV	47	48	50	50	50–55
TV	80	80	80	81	81–87
GR, epibranchial	8	11	9	9	10–15
GR, ceratobranchial	21	21	15	16	20–26
GR, hypobranchial	13	12	10	9	12–25
Total GR	42	44	34	34	44–61

and 1 pore on each upper and lower corners of those scales on about posterior third of lateral line.

Luminescent duct absent.

Coloration. When fresh, body pale to light gray, somewhat translucent, unevenly covered with melanophores (Fig. 1A, B), and with abdomen bright white. Dorsal fourth of body densely covered with tiny melanophores; slightly larger melanophores beneath extending to lateral line and further downward, gradually becoming scattered; lower third of abdomen pale with large unpigmented areas. Dense melanophores on dorsal surface of head, anterior snout and jaws, and gular region; rest of head pale, with scattered melanophores except in large unpigmented areas on cheek and operculum. Inner surface of operculum pale with large black patch; mouth cavity pale. Abdominal ridge covered with dense melanophores (fewer and scattered in small specimens). Pectoral, dorsal and pelvic fins pale, with scattered melanophores; anal fin covered with dense melanophores except for the paler basal region; caudal fin covered with dense melanophores. When preserved, body light yellow in general, with pigmentation pattern similar to fresh condition (Figs 1C, D, 2A–D). Peritoneal membranes and stomach black; intestine pale.

Distribution. Juveniles widespread in the Indo-West Pacific from Taiwan to Australia and South Africa to French Polynesia (Ege 1953). Adults known only from two specimens collected from off southwestern Taiwan by bottom trawl at an estimated depth of around 300 m based on other fishes collected in the bycatch.

***Lestidiops mirabilis* (Ege, 1933)**
Fig. 3A; Tables 1, 2
English name: Strange pike smelt

Paralepis mirabilis Ege, 1933: 228 (type locality: Sulawesi Sea, western Pacific, 4°03'N, 123°26'E; holotype lost).
Lestidium mirabile (Ege, 1933): Harry 1953a: 240 (assigned to *Lestidium*). Harry 1953b: 197 (record from Hawaii, adults).
Lestidiops mirabilis (Ege, 1933): Rofen 1966: 331, 337 (assigned to *Lestidiops*). Post 1972: 142 (list; type lost). Uyeno et al. 1983: 193 (French Guiana and Suriname, adults). Gloerfelt-Tarp and Kailola 1984 (off Java, Indonesia, adult). Nakabo 2000: 368 (Kyushu, Japan, based on larvae). Ho and Huang 2022: 579 (Australia, adult).

Material examined. ***Non-types*:** AMS I. 29537-004 (1, 210), FRV Kapala, 33°46'S, 151°49'E, east of Sydney, New South Wales, Australia, prawn trawl, 424–439 m, depth 16 Dec. 1980 • BSKU 27461 (1, 238), 27°43'N, 126°26'E, Okinawa Trough, 1,100 m depth, 9 Mar. 1978. NSMT-P 40253 (1, 261), off Suriname, no other data (possibly reported by Uyeno et al. 1983) • SAIAB 82055 (1, 276), 23°57'36"S, 35°51'36"E, off Mozambique, Western Indian Ocean, 814–831 m depth, 13 Oct. 2007. SAIAB 203473 (1, ca 180), 10°20'02.4"N, 96°24'14.4"E, Myanmar, Andaman Sea, 28 May 2015.

Other material (not examined but with reliable identification). BMNH 1984.1.1.50 (1, 145), 8°45'S, 114°17'E, south of Java, Indonesia, eastern Indian Ocean (listed by Gloerfelt-Tarp and Kailola 1984) • USNM 163317 (1, 163), CAS-SU18635 (1, 131.5), ANSP 72175 (1, 170), and POFI 628 (1, 170), all from Hawaii (listed by Harry 1953b; Rofen 1966).

Diagnosis. Species of *Lestidiops* with PVO below dorsal-fin base, anus slightly behind the base; anal-fin rays 28–30; lateral-line scales: PVLL 35–40, PDLL 36–39, PALL 51–56, TLL 63–67+8–22 = 73–85; vertebrae: PHV 36–42, PDV 35–38, PVV 36–39, PAV 50–55, CV 43–45, TV 81–87; total gill rakers 44–61. Adults with body uniformly dark brown to black, densely and evenly covered with melanophores; juveniles pale with broad, dark bands.

Distribution. According to Ege (1953), circumglobal, including the western Atlantic, Indian, and central Pacific oceans based on larvae and juveniles, but more or less restricted to tropical regions. Adult specimens recorded from Indonesia (Gloerfelt-Tarp and Kailola 1984), Hawaii (Harry 1953b), Australia (Ho and Huang 2022), and Suriname and French Guiana (Uyeno et al. 1983); newly reported from Okinawa Trough, Myanmar, and Mozambique in present study. Bathymertic range 424–1,100 m for adults.

Remarks. The information on this species in Tables 1, 2 combines literature data with measurements and counts from examination of voucher specimens in earlier reports (e.g., Harry 1953b; Ho and Huang 2022) and additional specimens. Although *L. mirabilis* is a widespread species, adults appear to be rare, with only about 10 specimens known in collections. The specimen from Mozambique has the most lateral-line scales (85, including 63 large + 22 small), whereas others have 73–80 (64–67 + 8–16).

Figure 3. Photographs of two *Lestidiops* from Myanmar **A** *L. extremus* (Ege, 1953), SAIAB 203471, ca 157 mm SL, with bars indicating DFO (upper), VFO (lower left), and AFO (lower right) **B** *L. mirabilis* (Ege, 1933), SAIAB 203473, ca 180 mm SL, with bars indicating DFO (upper), VFO (lower right), and AFO (lower left) **C** head of specimen as in **B**, with arrow pointing to nostrils.

The number of large scales is fairly constant among specimens, but because most individuals were collected by bottom trawl and either suffered some degree of skin damage or had their body partly broken, it is possible that small scales at the posterior end of the lateral line are missing in some.

Harry (1953b) counted 11–13 pectoral-fin rays in four adults, whereas 13–14 such fin rays were counted in the present material. The first pectoral-fin element of paralepidids has two rays that are closely attached to each other, as can be seen in stained specimens (Ho et al. 2019a); Harry (1953b) probably counted them as a single ray, and, if so, his count should have been 12–14 rays.

The number of gill rakers also shows a large variation. The specimen from Suriname has 44 gill rakers in total (12 on the upper limb + 32 on the lower), whereas other individuals have 53–61 gill rakers (10–14 + 39–51). Rofen (1966) noticed that the vertebral counts are different among specimens from the western Atlantic Ocean (81–83) and New Caledonia (86), which he concluded was due to lack of data, not to the existence of different geographic populations. Our only western Atlantic specimen also has 81 vertebrae, whereas three Pacific specimens have 86 or 87 vertebrae. Examination of more specimens may prove that there are consistent differences among populations.

The only specimen reported from New Zealand (Roberts et al. 2015) shows multiple rows of fine teeth forming tooth plates (in key) and is likely a misidentification of an *Arctozenus* species.

***Lestidiops extremus* (Ege, 1953)**

Fig. 3B; Tables 1, 2

English name: Extreme lightless barracudina

Lestidium extremum Ege, 1953: 136, fig. 29 (type locality: Molucca Passage, 0°18'S, 132°52'E [West Papua, Indonesia], ca 100 m depth). Rofen 1966: 301 (listed). Post 1972: 147 (type catalog; in *Lestidiops*, but possibly referable to *Uncisudis*).

Lestidiops extremus (Ege, 1953): Fukui and Ozawa 2004: 293 (list). Ho and Huang 2022: 580 (redescription, adult).

Material examined. ***Holotype*:** ZMUC P.2136999 (21.8 mm TL), 0°18'S, 132°52'E, West Papua, Indonesia, ca 100 m.

***Non-types*:** AMS I.36462-006 (1, 190 mm SL), about 80 km northwest off Camarines Norte Province, southeastern Luzon, Philippines, 14°50.46'N, 123°17.30'E–14°47.35'N, 123°22.33'E, otter trawl, 760–770 m, 27 Sep. 1995 • SAIAB 203471 (1, ca. 157), 12°42'59.4"N, 96°36'30"E, Myanmar, Andaman Sea, 25 May 2015.

Diagnosis. Species of *Lestidiops* with VFO clearly behind DFO and slightly behind posterior end of dorsal-fin base; anus well behind DFO; posterior end of maxilla extending nearly to vertical drawn through anterior margin of eye; lateral-line scales: PVLL 37–38, PDLL 32–34, PALL 50–51, TLL 68–71, including 62–63 large + 5–8 small scales; vertebrae: PHV 41, CV 39–40, PVV 38, PDV 32–33, PAL 50, TV 80–81; gill rakers 9+25 = 34; anal-fin rays 30–31. Adults uniformly black; juveniles with dark blotches and broad bands.

Distribution. Type series from off West Papua, Indonesia, ca 100 m depth; adults collected from off southeastern Luzon Island, Philippines, at 760–770 m depth.

Remarks. This species was originally described from a type series consisting of three larvae from Indonesia, and the only previously known adult was reported from the Philippines by Ho and Huang (2022). This is a very rare species, with only these four specimens and one additional adult from Myanmar known. This Myanmar specimen represents the first record in the eastern Indian Ocean and suggests that *L. extremus* may have a broader distribution range in the Indo-west Pacific region than has been suspected.

Discussion

Ege (1953) included four species in his *Lestidium indopacificum-mirabilis* group, including *L. indopacificum*, *L. atlanticum*, *L. mirabilis*, and *L. extremum*. He (Ege 1953: 139) distinguished these four nominal species by the proportions of the predorsal, prepelvic, and preanal (measured from tip of snout to anus) lengths, and by the length to the origin of the anal fin (= preanal length herein). He also showed, however, that three of them have similar counts of prehaemal vertebrae, total vertebrae, and anal-fin rays (Ege 1953: 140, no data available for *L. extremum*). The present examination of adults of all three species shows that these length proportions change with growth and become quite similar, even overlapping, as the more slender body shape of adults is attained. Apart from *Lestidium atlanticum*, which remains in that genus, the other three species were later reassigned to *Lestidiops* and are currently in the *L. mirabilis* species complex (Rofen 1966; Post 1972; this study). The differences between the adults of these three species can now be presented and are based both on the present observations and data from the literature.

The snout is quite slender in *L. indopacificus*, moderate in *L. mirabilis*, and rather stout in *L. extremus*. The VFO is slightly but clearly behind the dorsal-fin base in *L. extremus*, whereas it is under the dorsal-fin base in *L. indopacificus* and *L. mirabilis* (Ho and Huang 2022; this study). In *L. extremus*, the posterior end of the maxilla extends nearly to a vertical drawn through the anterior margin of eye, whereas in the two other species, the maxilla only reaches a point well before the eye.

There are 10 dorsal-fin rays in all three species, except that Harry (1953a) counted nine in a specimen of *L. mirabilis*. There are 28 or 29 (29–31 in Ege 1953) anal-fin rays in *L. mirabilis*, 30 in *L. indopacificus*, and 30 or 31 in *L. extremum*. Examination of more adult specimens may reveal overlapping or coincident ranges of counts for these features.

Total gill raker counts for *L. mirabilis* are 44 (Atlantic specimen) or 53–61 (Indo-Pacific specimens) versus 34 total gill rakers in two adults of *L. extremus* and 42–44 in two adults of *L. indopacificus*. The gill rakers are quite closely spaced in *L. mirabilis*, widely spaced in *L. extremus*, and intermediate in *L. indopacificus*. On each gill raker there are usually three or four closely spaced teeth, which are quite long in *L. extremus*, only moderately so in *L. mirabilis*, and short in *L. indopacificus*.

Comparison of the proportional measurements of all three species in the *L. mirabilis* species complex (Table 1) shows that the head is smaller in *L. extremus* compared to the other two species. In addition, the predorsal length is small, and the prepelvic

length larger, in *L. extremus*. While the distance between VFO and AFO (V–A) is clearly smaller in this species than in the other two, the distance between DFO and AFO (D–A) is large. The snout and both jaws are also shorter in *L. extremus* than in the other two species, and the pre-nostril length is smallest in *L. extremus* and longest in *L. indopacificus*, as reflected by the different positions of the nostrils in these species.

As for meristic values (Table 2), *L. indopacificus* has some clearly low vertebral counts (PHV 34–35, PVV 33–34, and PAV 47–48) compared to the other two species, and the latter two counts are consistent with the relatively low lateral-line scale counts (PVLL 33–34, PALL 47–48), which also readily separate *L. indopacificus* from the other two species. *Lestidiops extremus* has the lowest caudal vertebra count (CV 39–40), which clearly separates it from the other two species, and *L. mirabilis* has more PDV (35–38) and PDLL (36–39) than the other two species. Finally, *L. mirabilis* has a higher total count of lateral line scales (TLL 73–85) versus *L. indopacificus* (66–70) and *L. extremus* (68–71).

It is notable that both adult specimens of *L. indopacificus* have their nostrils directly above the posterior end of the maxilla, which is different from the two other species (with nostrils situated well before the end of the maxilla), as well as from most other species of *Lestidiops*, although information on this is lacking for some species (Harry 1953a). The more posterior nostril position of *L. indopacificus* is reminiscent of *Stemonosudis*, which was defined by Harry (1953a) as having the laterally positioned nostrils distinctly behind the posterior ends of the maxillae but later revised by Rofen (1966) to "nostrils varying in position from before to slightly behind a vertical from posterior tip of maxilla." Ho et al. (2019b) found that members of the *S. rothschildi* species complex also have their nostrils situated above or clearly before the posterior ends of the maxillae. More investigation is needed to fully delineate the taxonomic boundary between *Lestidiops* and *Stemonosudis*.

Acknowledgements

This study was supported by the National Museum of Marine Biology and Aquarium, Taiwan, the National Kaohsiung University of Science and Technology, Taiwan, and the Australian Museum, Sydney. Thanks go to P. Psomadakis (FAO) for collecting specimens and curatorial teams at AMS, NSMT, BSKU, SAIAB, and ZMUC. English and stylistic review of an earlier draft of the manuscript were provided by Dr Mark J. Grygier, NMMBA. We also thank A. Steward for critically reviewing the manuscript.

References

Borodin NA (1928) Scientific results of the yacht "Ara" Expedition during the years 1926 to 1928, while in command of William K. Vanderbilt. Fishes. Bulletin of the Vanderbilt Oceanographic Museum 1(1): 1–37. [pls 1–5]

Ege V (1933) On some new fishes of the families Sudidae and Stomiatidae. Preliminary note. Videnskabelige Meddelelser fra Dansk Naturhistorisk Forening. Kjøbenhavn 94: 223–236.

Ege V (1953) Paralepididae I. (*Paralepis* and *Lestidium*). Dana-Report 40: 1–184.

Fukui A, Ozawa T (2004) *Uncisudis posteropelvis*, a new species of barracudina (Aulopiformes: Paralepididae) from the western North Pacific Ocean. Ichthyological Research 51(4): 289–294. https://doi.org/10.1007/s10228-004-0229-3

Gloerfelt-Tarp T, Kailola PJ (1984) Trawled Fishes of Southern Indonesia and Northwestern Australia. Australian Development Assistance Bureau, Sydney, 406 pp.

Gomon MF, Bray DJ, Kuiter RH [Eds] (2008) Fishes of Australia's Southern Coast. New Holland Publishers, Sydney, 928 pp.

Harry RR (1953a) Studies on the bathypelagic fishes of the family Paralepididae. 1. Survey of the genera. Pacific Science 7(2): 219–249.

Harry RR (1953b) Studies on the bathypelagic fishes of the family Paralepididae (order Iniomi). 2. A revision of the North Pacific species. Proceedings. Academy of Natural Sciences of Philadelphia 105: 169–230.

Ho HC, Duhamel G (2019) A new species of the fish genus *Arctozenus* from the Kerguelen Islands, with comments on the lost teeth in adults (Aulopiformes: Paralepididae). Zootaxa 4651(3): 497–512. https://doi.org/10.11646/zootaxa.4651.3.5

Ho HC, Golani D (2019) A new species of *Lestrolepis* from the Red Sea, with redescription of *Lestrolepis pofi* (Harry, 1953) (Aulopiformes: Paralepididae). Zootaxa 4619(3): 571–579. https://doi.org/10.11646/zootaxa.4619.3.10

Ho HC, Huang CH (2022) First adult record of the barracudina *Lestidiops extremus* (Ege, 1953), based on a specimen from the Philippines (Teleostei: Paralepididae). Zootaxa 5195(6): 579–584. https://doi.org/10.11646/zootaxa.5195.6.6

Ho HC, Tsia SY, Li HH (2019a) The barracudina genera *Lestidium* and *Lestrolepis* of Taiwan, with descriptions of two new species (Aulopiformes: Paralepididae). Zootaxa 4702(1): 114–139. https://doi.org/10.11646/zootaxa.4702.1.16

Ho HC, Russell B, Graham K, Psomadakis PN (2019b) Review of the *Stemonosudis rothschildi* species complex, with descriptions of two new species from the Indo-west Pacific Ocean (Aulopiformes: Paralepididae). Zootaxa 4702(1): 216–229. https://doi.org/10.11646/zootaxa.4702.1.19

Ho HC, Graham K, Russell B (2020) Three new species of the barracudina genus *Lestidium* (Aulopiformes: Paralepididae) from the Indo-West Pacific. Zootaxa 4767(1): 71–88. https://doi.org/10.11646/zootaxa.4767.1.3

Hubbs CL (1916) Notes on the marine fishes of California. University of California Publications in Zoology 16(13): 153–169.

Mundy BC (2005) Checklist of the fishes of the Hawaiian Archipelago. Bishop Museum Bulletins in Zoology 6: 1–703.

Nakabo T [Ed.] (2000) Fishes of Japan with Pictorial Keys to the Species (2nd Edn.) (Vol. 1). Tokai University Press, Tokyo, 866 pp. [In Japanese]

Paxton JR, Hoese DF, Allen GR, Hanley JE [Eds] (1989) Zoological Catalogue of Australia (Vol. 7). Pisces. Petromyzontidae to Carangidae (Vol. 7). Australian Government Publishing Service, Canberra, 665 pp.

Post A (1972) Catalogue of type-specimens and designation of lectotypes of the fish-family Paralepididae (Osteichthyes, Myctophoidei). Archiv für Fischereiwissenschaft 23(2): 136–165.

Post A (1987) Results of the research cruises of FRV "Walther Herwig" to South America. LXVII. Revision of the subfamily Paralepidinae (Pisces, Aulopiformes, Alepisauroidei, Paralepididae). I. Taxonomy, morphology, and geographical distribution. Archiv für Fischereiwissenschaft 38(1/2): 75–131.

Roberts CD, Stewart AL, Struthers CD [Eds] (2015) The Fishes of New Zealand (Vol. 3). Systematic Accounts. Te Papa Press, Wellington, 577–1152.

Rofen RR (1966) Family Paralepididae. In: Mead GW, Bigelow HB, Olsen YH, Breder CM, Schroeder WC, Cohen DM, Schultz LP, Merriman D, Tee-Van J (Eds) Memoirs, Sears Foundation of Marine Research. No. I. Fishes of the Western North Atlantic. Part 5. Yale University, New Haven, 205–461.

Uyeno T, Matsuura K, Fujii E [Eds] (1983) Fishes Trawled off Suriname and French Guiana. Japan Marine Fishery Resource Research Center, 519 pp. [In Japanese and English]

ZooKeys 1160: 125–144 (2023)
doi: 10.3897/zookeys.1160.95694
https://zookeys.pensoft.net

RESEARCH ARTICLE

A peer-reviewed open-access journal
ZooKeys
Launched to accelerate biodiversity research

A new Neotropical ant species of genus *Linepithema* Mayr (Hymenoptera, Formicidae, Dolichoderinae) with partial revision of the *L. fuscum* group based on males

Stefano Cantone[1,2], Andrea Di Giulio[1,2]

1 *Department of Science, University 'Roma Tre', Viale G. Marconi, 446, 00146 Rome, Italy* **2** *NBFC, National Biodiversity Future Center, Palermo 90133, Italy*

Corresponding author: Andrea Di Giulio (andrea.digiulio@uniroma3.it)

Academic editor: Jeffrey Sosa-Calvo | Received 27 September 2022 | Accepted 30 March 2023 | Published 9 May 2023

https://zoobank.org/783F4624-B87C-4872-B396-AE8F517FABC8

Citation: Cantone S, Di Giulio A (2023) A new Neotropical ant species of genus *Linepithema* Mayr (Hymenoptera, Formicidae, Dolichoderinae) with partial revision of the *L. fuscum* group based on males. ZooKeys 1160: 125–144. https://doi.org/10.3897/zookeys.1160.95694

Abstract

The genus *Linepithema* was erected by Mayr (1866) for his male-based species *L. fuscum*. In this study a new species is described also based on male morphology, *L. paulistana* **sp. nov.**, collected in the city of São Paulo, Brazil, which is attributed to the *fuscum* group (Formicidae: Dolichoderinae). *Linepithema paulistana* **sp. nov.** is the only species of *fuscum* group present in the eastern part of South America. It is easily distinguishable from the other species of the group because of the presence of a triangular volsellar tooth, which is distally situated between the digitus and the basivolsellar process. By using SEM and optical microscopy, the external genitalia of *L. paulistana* **sp. nov.** were analyzed and illustrated and some characters and previous interpretations have been re-evaluated in the *Linepithema fuscum* group. The male external genitalia are also comparatively analyzed in three species representative of the three *Linepithema* species groups, those of *fuscum*, *humile*, and *neotropicum*. The present work confirms that the morphological characters of male ants, especially those of male external genitalia, are effective for the identification of genera or species. Given the discrete morphological differences between the external genitalia of the *fuscum* group and the other species of this genus, a re-evaluation of the generic status of *Linepithema* is suggested.

Keywords

External genitalia, *Linepithema paulistana*, male ants, taxonomic status, winged ants

Introduction

The Neotropical ant genus *Linepithema* Mayr, 1866 (Formicidae: Dolichoderinae) includes 20 species that are widely distributed in Central and South America and the Caribbean (Wild 2007; Bolton 2022). Workers of this genus are monomorphic, and the males and queens are winged. The best known and most studied species is the invasive Argentine ant *L. humile* Mayr, 1868, which shows a cosmopolitan distribution due to its ability to adapt to different climatic conditions and to the plasticity of its reproductive strategies (Ward 1987; Aron et al. 1994, 2001; Aron 2001; Roura-Pascual et al. 2004; Menke and Holway 2006). The genus was erected based on males collected in Lima, Peru, which was described as *Linepithema fuscum* Mayr, 1866. Shattuck (1992a) subdivided the dolichoderine genus *Iridomyrmex* Mayr, 1862, transferring the Neotropical species to *Linepithema*, including *L. humile*, based on the examination of workers associated with males. In his generic review of Dolichoderinae, Shattuck (1992b) provided a diagnosis of *Linepithema* for the worker, queen, male, and the larval stage, and divided the genus into two male-based species groups, those of *fuscum* and *humile*.

Linepithema was later revised by Wild (2007), who followed Shattuck's species-group classification and suggested that the *fuscum* group may be monophyletic, and the *humile* group may be paraphyletic, as it lacks distinct synapomorphies. Subsequently, Wild (2009), confirmed the monophyly of the *fuscum* group via molecular phylogenetics, and subdivided the *humile* group into three species groups: *humile* group, *iniquum* group, and *neotropicum* group. Unfortunately, *L. fuscum* could not be included in this phylogenetic analysis. According to Wild (2007, 2009), the *fuscum* group includes seven species, two of which, *L. cryptobioticum* Wild, 2007 and *L. flavescens* Wheeler & Mann, 1914, have unknown males. The highly distinctive characters of the males of the *Linepithema fuscum* group, compared to the other species groups, have been highlighted by both Shattuck (1992b) and Wild (2007), and mainly refer to: i) the submarginal cells of the forewings; ii) the ventral petiolar process; iii) the pygostyle; and iv) the paramere and volsella, which are parts of the external genitalia. Notably, the female castes of *L. fuscum* remain unknown, with the intersex association based solely on geography (Wild 2007), and no COI DNA barcode analysis was performed (Wild 2009).

In the present study we describe a new species of *Linepithema*, collected in the city of São Paulo (Brazil), based on males. Due to its genitalic form, we attribute the species to the *fuscum* group. The morphology of the new species is described by using optical and scanning electron (SEM) microscopy; these are the first SEM illustrations of a *fuscum* group male and include figures of the external genitalia. The male genitalia are compared to three species, representing three of the four species groups (*fuscum*, *humile*, and *neotropicum*). The morphological interpretation and terminology used for external genitalia in previous *Linepithema* descriptions is revised. Finally, an updated key to males of the species *Linepithema* in the *fuscum* group is presented, and a new species distribution map of the *Linepithema fuscum*-group is supplied.

Materials and methods

Material examined

Males of *Linepithema paulistana* sp. nov., *L. humile*, and *L. neotropicum* Wild, 2007 were captured in São Paulo city (Brazil), 23°35'16"S, 46°38'55"W, altitude 800 m a.s.l. via two light traps ("Luiz de Queiroz" model), equipped with 15-watt UV black-blue lamps. The traps were left in the same position, attached to the same tree at 3 m and 7 m from the ground, kept active continuously from 01 August 2012 to 01 September 2014 and checked weekly (Cantone 2018b), with the specimens preserved in 70% ethanol. We identified the specimens using the works of Mayr (1866), Emery (1912), Shattuck (1992b), and Wild (2004, 2007). We had the following material at our disposal: *Linepithema paulistana* sp. nov. (*fuscum* group), 12 male specimens collected from March to August 2013, and in January, February, and June 2014; *L. humile* (*humile* group), ten male specimens collected in April 2012, September to December 2013, and March 2014; and *L. neotropicum* (*neotropicum* group), 20 male specimens collected in the months of October to December 2012, January to April 2013 and July to December 2013. The holotype (MZUR3-HF0001) and seven paratypes (unique ID codes MZUR3-HF0002 to MZUR3-HF0008) of *L. paulistana* sp. nov., and specimens of *L. humile* and *L. neotropicum* are deposited in the Museum of Zoology of 'Roma Tre' University (Rome, Italy; **MZUR3**); two paratype males (MZUR3-HF0009 and MZUR3-HF0010) will be deposited in the Museum of Zoology of São Paulo University (**MZUSP**).

Morphological analysis

The identifications and dissections were performed with Leica MZ12 (Leica Microsystems, Wetzlar, Germany) and Olympus SZX16 (Olympus, Tokyo, Japan) stereomicroscopes equipped respectively with Olympus Highlight 2100 and Olympus KL1500 LCD fiber optic lights. Dissected specimens were mounted on slides in Canada balsam and examined with an Olympus BX51 (Olympus, Tokyo, Japan) microscope. Optical micrographs of slide mounted specimens were taken with an Olympus BX51 microscope equipped with an om-d e-m5 digital camera (Olympus, Tokyo, Japan) with either a 10 × or 20 × objective. Remaining pictures of holotype were acquired with a Zeiss Axio Zoom V16 (Carl Zeiss AG; Oberkochen, Germany) and an Axiocam 503 (Carl Zeiss Microimaging Gmbh, Jena, Germany) equipped with Led dual spot-lights Photonic Optische (Vienna, Austria). Scanning electron microscopy was performed at L.I.M.E. lab (University of Roma Tre, Rome, Italy). Samples were dehydrated in a graded ethanol series (70%, 85%, 95%, 30 min each followed by 100% for 2 h), critical point dried (Balzer Union CPD 030 unit), mounted on aluminum stubs with a conductive adhesive carbon disk, sputtered with a thin layer (30 nm) of gold in a Emithech K550 sputter coater (Emithech, Kent, UK), and analyzed with a Zeiss Gemini 300 field emission SEM microscope at a voltage of 5 kV (Carl Zeiss AG, Jena, Germany).

The terminology used in this study represents a combination between classical studies on Hymenoptera and more specific studies on Formicidae and it based on

Snodgrass (1941) for the external genitalia; Mason (1986) for the wing venation; Schulmeister (2001, 2003) for the external genitalia; Yoshimura and Fisher (2007, 2009, 2011) for the male general morphology and wing venation; Perfilieva (2010) for the wing venation; Boudinot (2013, 2015, 2018) for the external genitalia and mesosoma; Barden et al. (2017) for the external genitalia; Cantone (2017, 2018a) and Cantone and Von Zuben (2019) for the wing venation; Delsine et al. (2019) for the general morphology of Formicidae; Beutel et al. (2020) for the legs; Richter et al. (2019, 2020, 2021) for the head. When conflicting terminology was found, we prioritized the most recent reference studies applied to the family Formicidae.

Measurements

In order to make comparisons with the other species of the genus *Linepithema*, measurements of *L. paulistana* sp. nov. follow the system of Wild (2007). We provided all measurements for the holotype and the morphometric variation (minimum and maximum) based on ten specimens (holotype and nine paratypes). In Table 1 we compared these measurements with those of all species of the *fuscum* group with known males.

Table 1. The most relevant morphological characters that differentiate the males of the *Linepithema fuscum* group from the males of the other *Linepithema* species. This table is based on the comparative tables by Shattuck (1992b) and Wild (2007). The new or re-evaluated diagnostic characters of the *fuscum* group resulting from this study are indicated in bold.

Morphological characters	Male *Linepithema fuscum* group	Male *Linepithema*, other species
ventral petiolar process	**slightly developed (Figs 1D, 3D)**	**well developed (Fig. 5A, B)**
forewings	two submarginal cells (Fig. 1E)	one submarginal cell
proctiger	**well developed (Fig. 4A–C)**	**slightly developed (Fig. 5C–D)**
pygostyles	very long (Fig. 4A)	short (Fig. 5C)
basimere	strongly thinned dorsally and shortened distally (Fig. 4C, F)	developed dorsally and distally (Fig. 5C, D)
telomere	narrow and very long ribbon-like, digitiform distally (Fig. 4A–C)	short and lobe form (Fig. 5C, D)
basivolsellar process	**reduced (Fig. 4C, D)**	**developed (Fig. 5E, F)**
digitus	dorsal and very long (Fig. 4B)	medial and short (Fig. 5C, D)
cuspis	**lateral and very reduced (Fig. 4D)**	**lateral and developed (Fig. 5C, D)**
valviceps lamina	**dentate ventral edge straight (Fig. 1J)**	**dentate ventral edge strongly convex and rounded (Fig. 5G, H)**

Abbreviations for morphological characters

HL Head length, in full face view. The midline distance from the level of the maximum posterior projection of the margin of the head (not including the ocelli) to the level of the most anterior projection of the anterior clypeal margin.

HW Head width, in full face view, the maximum width of the head posterior to the compound eyes.

MOD Median ocellus diameter.
SL Antennal scape length, measured from the apex of the first antennal segment to the base, excluding the radicle.
FL Profemur length, in posterior view, measured along the longitudinal axis from the apex to the junction with the trochanter.
LHF Metafemur length.
LHT Metatibial length, in dorsal view, measured along the longitudinal axis from the apex to the level of the lateral condyles, excluding the medial proximal condyle.
LHTa Metabasitarsus length.
EL Eye length, in full face view, the length of the compound eye along the longitudinal axis.
EW Eye width, with eye held in focal plane facing the viewer, the maximum transverse width of the compound eye.
MML Maximum mesosomal length, the distance from the maximum anterior projection of the mesosoma to the maximum posterior projection of the propodeum.
WL Forewing length, the maximum distance between the insertion of the sclerotized wing veins to the distal margin of the wing.
WHL Hindwing length, the maximum distance between the insertion of the sclerotized wing veins to the distal margin of the wing
ES Eye size index. 100 × EL × EW
CI Cephalic index. 100 × HW/HL
SI Scape index. 100 × SL/HL
OI Ocular index. 100 × EL/HL
WI Wing index. 10 × WL/MML
FI Femoral index. 100 × FL/MML

Results

Class Insecta Linnaeus, 1758
Order Hymenoptera Linnaeus, 1758
Family Formicidae Latreille, 1809
Subfamily Dolichoderinae, Forel, 1878
Genus *Linepithema* Mayr, 1866

***Linepithema paulistana* sp. nov.**
https://zoobank.org/48DC08BF-0E4B-4946-9142-F26224830832
Figs 1–6

Type material. ***Holotype*** male: Brazil, São Paulo city, 07–13 July 2013, light trap. Museum of Zoology of the Roma Tre University (Rome, Italy), MZUR3-HF0001.

***Paratypes*:** Same data as holotype, 10 specimens deposited in the Museum of Zoology of the Roma Tre University (Rome, Italy), MZUR3-HF0002 to MZUR3-HF0008.

Holotype male description. ***Measurements*** **(in mm):** HL: 0.70; HW: 0.65; MOD: 0.15; SL: 0.19; FL: 1.10; LHT: 1.11; LHF: 1.36; LHTa: 1.1; EL: 0.35; EW: 0.25; MML: 1.56; WL: 4.05; WHL: 3.28.

Indices**:** ES: 8.75; CI: 92.9; SI: 27.1; OI: 50.0; WI: 26.0; FI: 70.5.

Male diagnosis**:** notauli absent; forewing with two submarginal cells, marginal cell closed; petiole without ventral process; proctiger well developed; telomere narrow and elongated, digitiform distally; digitus dorsally long, spine-like distally; basivolsellar process reduced ventrally; volsellar tooth present distally between digitus and basivolsellar process; cuspis laterally very reduced.

Habitus (Fig. 1A): slender ant, with metasoma elongated, longer than mesosoma. Dense pubescence present throughout the body, with sparse elongate, erected setae on head and mesosoma. Color of head and body medium brown; antennae and legs yellowish.

Head (Figs 1B, C, 2A–G): longer that broad in full face view; with pubescence; eyes relatively large, occupying much of the anterolateral side of the head, separated from the insertion of the mandibles by a distance less than 1/3 than the length of the antennal scape. Two very long erect setae posterior to the median ocellus. Antennae filiform with 13 articles, regularly tapering to the apex; scape short, ~ 1/2 the length of the second funicular article; first article of the funiculus very short and cylindric, barrel shaped, ~ 1/3 the length of the second; second funicular article longest; articles of funiculus 9–12 short; antennal condylar bulb with series of spiniform Böhm sensilla, scape and first article of funiculus with recumbent sensilla; articles of funiculus 2–12 with erected sensilla. Anterior clypeal margin convex medially, with erect setae; medial part of the clypeus with two long erect setae. Labrum small, bilobed, separated by a deep notch, each lobe laterally reduced and pointed and medially produced into a round plate dorsally with multiple setae. Epipharynx unsclerotized, exceeding the length of labrum and distinctly visible in dorsal view. Mandibles large, with masticatory margin long and broad; apical tooth long and pointed; preapical tooth short and subtriangular, followed by a series of teeth and denticles; basal margin short and strongly diverging; basal part of the mandible covered by dense pubescence on dorsal and lateral surface; masticatory margin without pubescence, with very long setae (6 or 7 dorsally and 9–11 ventrally). Maxillae with subrectangular stripes, pubescent dorsolaterally and not setose ventrally. Maxillary palps with six articles, together with a total length that exceeds half the length of head; article I very short, II subequal in length and diameter to III; IV subequal in length and minor in diameter to III; V and VI thin and short. Dorsal surface of galea not pubescent, with short, scattered setae basally, long setae laterally and distally; ental margin of galea with maxillary comb medially projected. Lacinia comb composed of teeth alternating with stout setae. Labium with prementum subrectangular and elongate, wider and with two very long setae ventrally; postmentum with spinulate microsculpture; glossa with comb-like, backward directed fringes; labial palps of four articles: article I subequal in length to II; III and IV shorter and thinner than II. Hypostoma with anteromedial stipital notch.

Mesosoma (Figs 1A, D–F, 3A–D, F, G): shorter in length than metasoma. Pronotum short, with recumbent pubescence, laterally projecting over the

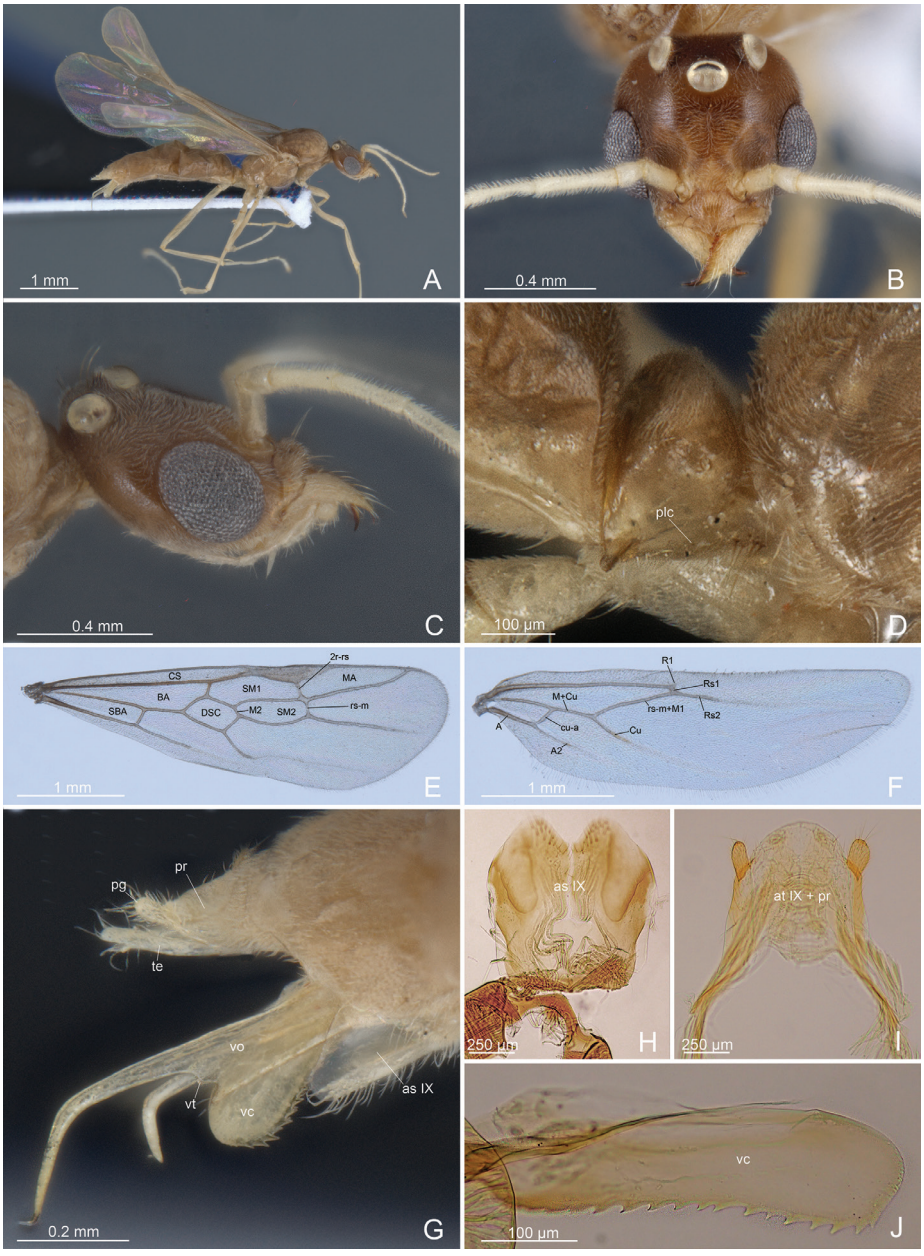

Figure 1. *L. paulistana* sp. nov.: **A** habitus **B** head in dorsal view **C** head in lateral view **D** petiole in lateral view **E** forewing **F** hindwing **G** external genitalia in lateral view **H** abdominal sternite IX **I** tergite IX+proctiger **J** valviceps lamina. Abbreviations: A: anal vein; atIX: abdominal tergite IX; asIX: abdominal sternite IX; BA: basal cell; CS: costal cell; Cu: cubital vein; cu-a: cubito-anal crossvein; DSC: discoidal cell; MA: marginal cell; M+Cu: medio-cubital vein; plc: petiole ventral postero-lateral carina; pg: pygostyle; pr: proctiger; Rs1: radial sector 1 vein; Rs2: radial sector 2 vein; rs-m+M1: radial sector-media crossvein; rs-m: radial sector-media cross-vein; 2r-rs: 2 radius-radial sector crossvein; R1: Radius 1; Rs1: Radial sector 1; Rs2: Radial sector 2; SBA: subbasal cell; SM1: submarginal 1 cell; SM2: submarginal cell 2; te: telomere; vc: valviceps; vo: volsella; vt: volsellar tooth.

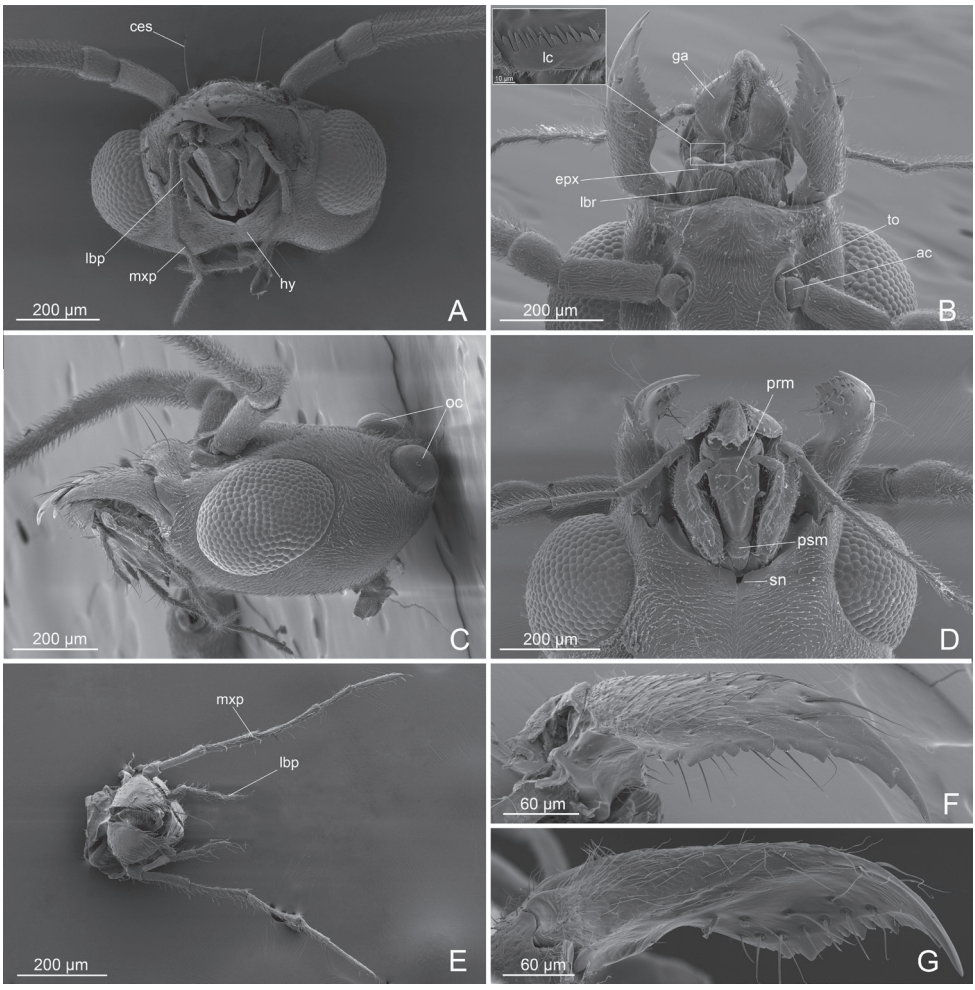

Figure 2. *L. paulistana* sp. nov.: **A** head oral view **B** head dorsal view **C** head lateral view **D** head ventral view **E** maxillar palp and labial palp **F**, **G** mandible. Abbreviations: ac: antennal condyle; ces: clypeal long erect setae; epx: epipharynx; ga: galea; hy: hypostoma; lbp: labial palp; lbr: labrum; lc: lacinia comb; mxp: maxilar palp; oc: ocelli; psm: postmentum; prm: prementum; sn: stipital notch; to: torulus.

anepisternum. Mesoscutum strongly convex in lateral view, not overhanging the pronotum, totally covered by recumbent pubescence; notauli absent; parapsidal lines evident. Mesoscutellum swelling, separated from mesoscutum by a deep scutoscutellar sulcus, smooth dorsally and with recumbent pubescence laterally. Metascutellum convex, lower than mesoscutellum and not overlapping with the propodeum, with recumbent pubescence and long setae dorsomedially. Metapleural gland orifice very large and posterolateral. Forewings (WL: 4,05; WI: 25,95) with two submarginal cells, discoidal cell, marginal cell closed and large, dark pterostigma, two radius-radial sector cross-vein almost in line with radial sector-media, two media vein present; tegula with row of small hairs. Hindwings (WHL: 3,27)

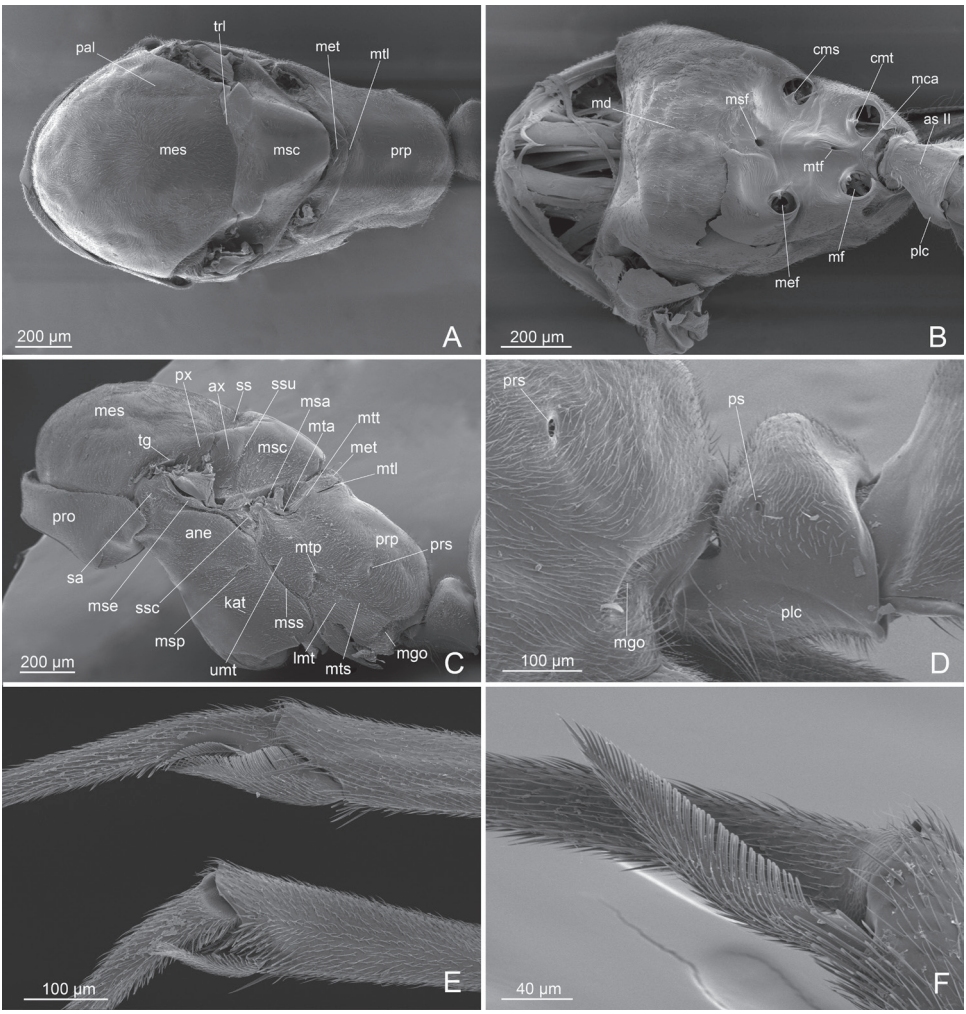

Figure 3. *L. paulistana* sp. nov.: **A** mesosoma dorsal view **B** mesosoma ventral view **C** mesosoma dorsal view **D** tegula **E** petiole **F** protibial spur and mesotibial spur **G** metatibial spur. Abbreviations: ane: anepisternum; asII: abdominal sternum II; ax: axilla; cms: medial coxal articular process of the mesopectus; cmt: medial coxal articular process of the metapectus; lmt: lower metapleuron; kat: katespisternum; mca: medial coxal articular process of the metapectus; md: mesodiscrimen; mef: mesocoxal foramen; mf: metacoxal foramen; mes: mesoscutum; msc: mesoscutellum; met: metascutellum; mgo: metapleural gland orifice; msa: mesoscutellar arm; mse: mesepimeron; msf: mesoprefurcal pit; mtf: metaprefurcal pit; msp: mesopleural pit; mss: mesopleural suture; mta: metascutellar arm; mtl: metascutellar line; mtp: metatentorial pit; mts: metapleuropropodeal suture; mtt: metascutellar trough; pal: parapsidal line; plc: petiole ventral posterolateral carina; pro: pronotum; prp: propodeum; prs: propodeal spiracle; ps: petiole spiracle; px: preaxilla; sa: subalar area; ss: scutoscutellar sulcus; ssc: spiracular sclerite; ssu: scutoscutellar suture; trl: transscutal line; tg: tegula; umt: upper metapleuron.

without two medial vein; one radius vein nebulous and one radial sector present but short; 8–11 hamuli. Legs (FI: 70,5); profemur (FL: 1,10); metafemur (LHF: 1,36); metatibia (LHT: 1,11) with single apical very long spur pectinate on the in-

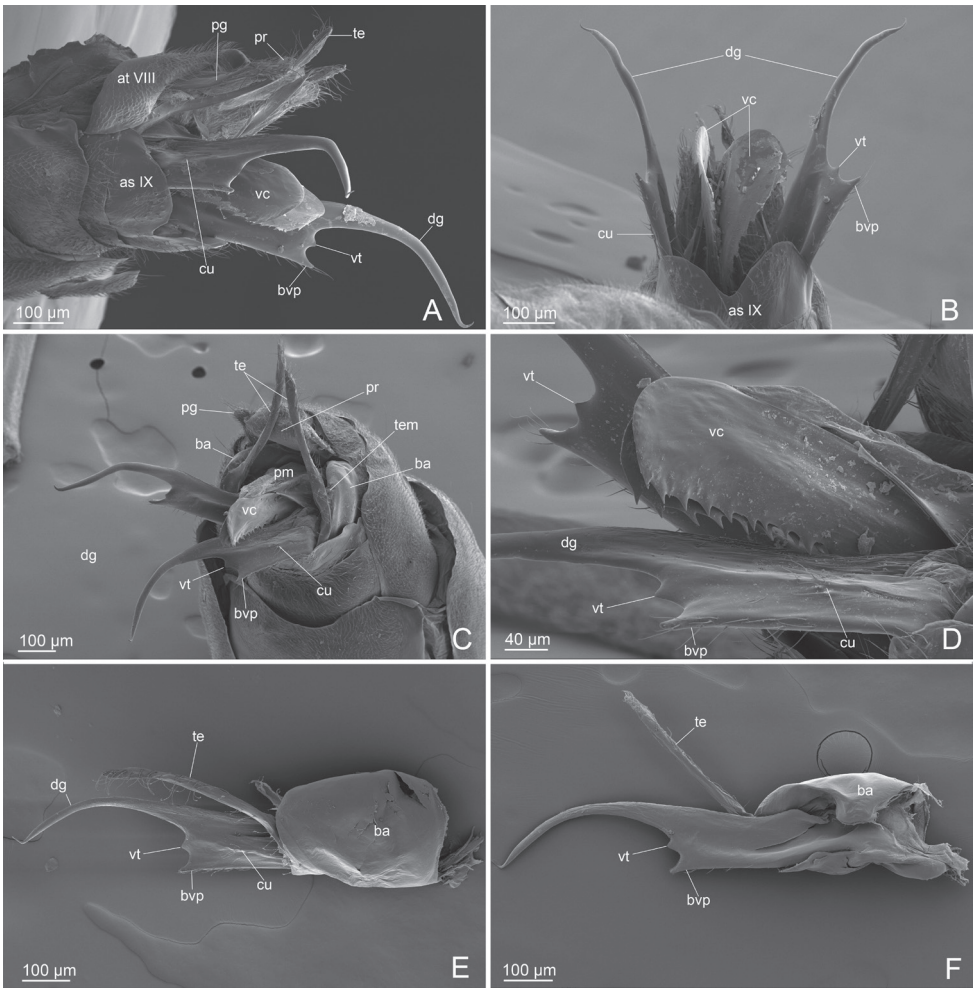

Figure 4. *L. paulistana* sp. nov.: **A** external genitalia lateral view **B** external genitalia ventral view **C** external genitalia ventro-lateral view **D** volsella and valviceps lateral view **E** basimere and volsella in lateral view **F** basimere and volsella in medial view. Abbreviations: asIX: abdominal sternite IX; atVIII: abdominal tergite VIII; pr: proctiger; ba: basimere; bvp: basivolsellar process; cu: cuspis; dg: digitus; pg: pygostyle; pm: penisvalve membrane; te: telomere; tem: telomere membrane; vc: valviceps; vo: volsella; vt: volsellar tooth.

ner margin and with small cuticular fringes on the external margin; metabasitarsus long (LHTa: 1,09); mesotibia with short apical spur pectinate; pretarsal claw simple with arolium and planta developed. Propodeum in lateral view slightly convex dorsally and straight posteriorly; propodeal spiracle orifice lateral and rounded. Sternal region as in Fig. 3B.

Metasoma (Figs 1A, D, 3D): Petiole erect, taller than wide in lateral view and rounded dorsally, anterior profile convex and posterior concave; setae and pubescence present in the anterior face, posterior face without setae or pubescence; petiolar tergosternal suture with small posterior lobe; ventral profile of petiole only slightly convex, without subpetiolar process, with long setae anteriorly and erect setae posteriorly; petiole articulated ventrally with abdominal segment III. Gaster elongate, with dense pubescence on tergites and sternites, hairs of pubescence longer on last sternites where long setae are also present laterally; pygostyles very long and apical erected setae; proctiger well developed, extending posteriorly beyond the IX abdominal tergite in the form of a large lamina, straight distally and light colored.

External genitalia (Figs 1G–J, 4A–F): IX abdominal sternite bilobed distally, due to a deep medial notch. Paramere composed of a short basimere, dish-like, strongly thinned dorsally, and shortened distally, and telomere narrow and very long ribbon-like, digitiform distally, that extends postero-dorsally overcoming the proctiger. Volsella composed of i) parossiculus (basivolsella+cuspis) with small and pointed ventral basivolsellar process and with apical and ventral setae along the edge; lateral cuspis very reduced to a ridge, bearing long setae on apical part; ii) very long falcate dorsal digitus, downturned, distally spine-like; iii) triangular volsellar tooth posteromedially placed, between basivolsellar process and digitus, without setae. Penis valve very long with valviceps lamina ventrally straight and multidentate with 13 or 14 teeth, apically rounded.

Remarks. Queen and worker unknown. Currently only known from São Paulo city, Brazil. Mating flight January to August.

Derivatio nominis. The name *paulistana* refers to the Brazilian appellation of the citizens of São Paulo city, where several males of the new species were captured.

Description of the male external genitalia of *Linepithema humile* (*humile* group) and *L. neotropicum* (*neotropicum* group)

External genitalia (Fig. 5A–F). The two species *L. humile* and *L. neotropicum* show a similar structure of the following features: IX abdominal sternite distally concave medially; paramere composed of a short dish-like basimere, which extends dorsally, and a distally lobate telomere; volsella composed of: i) parossiculus (basivolsella+cuspis) with posteroventral basivolsellar process developed, lobate, with long setae along its margin and lateral cuspis developed, with apical setae; ii) median falcate digitus, downturned, distally spine-like and slightly longer than the telomere; penisvalve with valviceps lamina ventrally strongly convex, rounded and multidentate with 16 or 17 teeth in *L. humile* and 13 teeth in *L. neotropicum*. The two species are clearly distinguished by the shape of the valviceps lamina and for structure of the volsella, that in *L. neotropicum* is characterized by having a lateral cuspis lobate apically and parallel to the median digitus; instead in *L. humile* the lateral cuspis is slightly pointed apically and more ventral than the digitus.

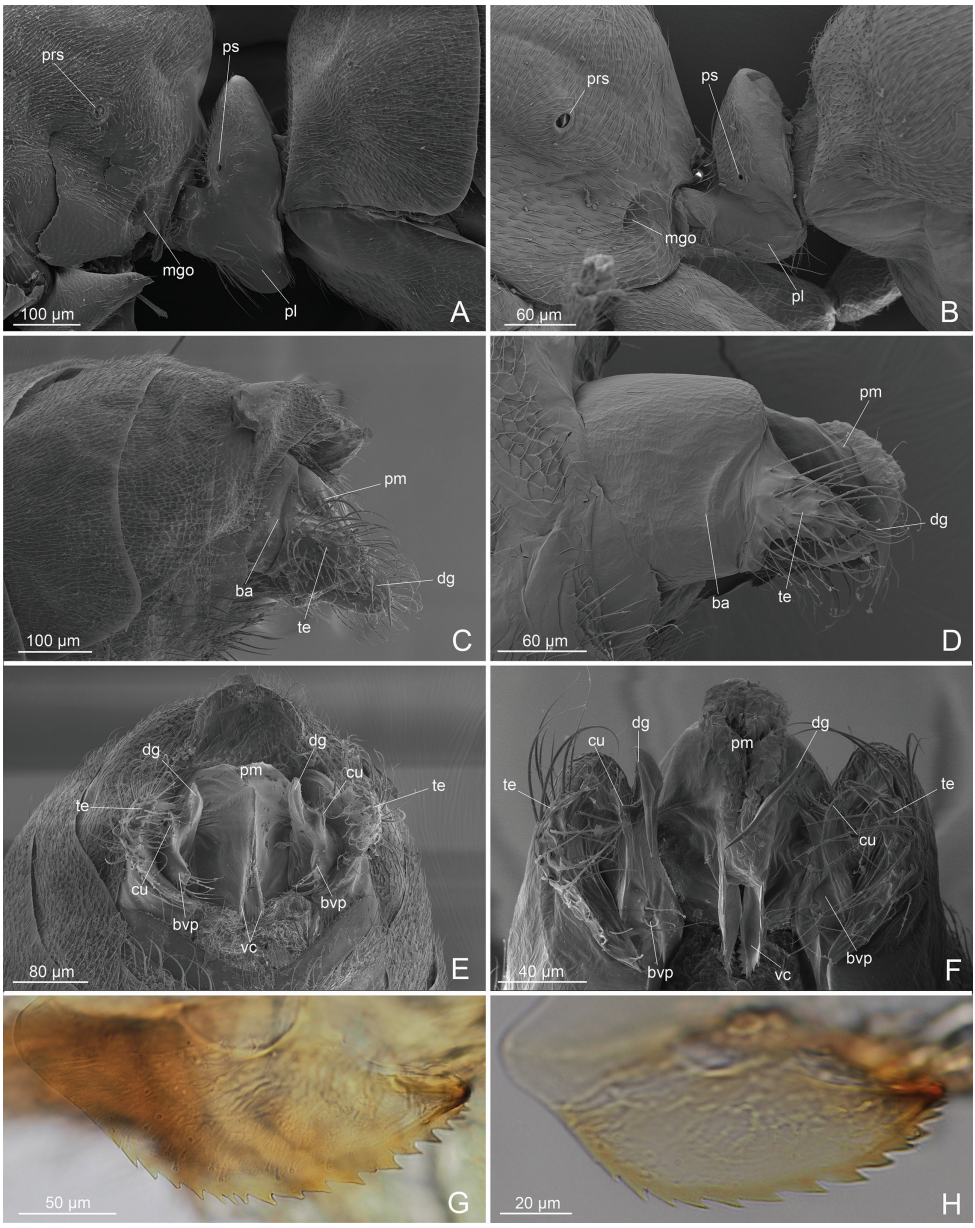

Figure 5. *L. humile*: **A** petiole in lateral view **C** external genitalia in lateral view **E** external genitalia in posterior view **G** valviceps lamina. *L. neotropicum* **B** petiole in lateral view **D** external genitalia in lateral view **F** external genitalia in posterior view **H** valviceps lamina. Abbreviations: ba: basimere; bvp: basivolsellar process; cu: cuspis; dg: digitus; mgo: metapleural gland orifice; ps: petiole spiracle; prs: propodeal spiracle; pl: ventral petiolar process; pm: penisvalve membrane; te: telomere; vc: valviceps lamina.

In Table 1 we report an updated and comparative list of the most relevant diagnostic characters that differentiate the males of the *Linepithema fuscum* group from the males of the other species of the same genus.

Morphometrics

See Table 2.

Table 2. Most relevant morphometric male characters of *L. paulistana* sp. nov. and species of the *Linepithema fuscum*-group. The measurements of *L. angulatum*, *L. fuscum*, *L. keiteli*, *L. piliferum*, and *L. tsachila* are taken from Wild (2007). Abbreviations are listed in Materials and methods and follow the system of Wild (2007). *n* = number of specimens measured.

	***L. paulistana* sp. nov. (*n* = 10)**	***L. angulatum* (*n* = 4)**	***L. fuscum* (*n* = 5)**	***L. keiteli* (*n* = 4)**	***L. piliferum* (*n* = 5)**	***L. tsachila* (*n* = 4)**
HL	0.67–0.71	0.73–0.77	0.68–0.74	0.61–0.70	0.66–0.71	0.71–0.74
HW	0.64–0.67	0.67–0.71	0.63–0.70	0.56–0.65	0.63–0.78	0.69–0.71
SL	0.19–0.20	0.20–0.21	0.19–0.21	0.21–0.22	0.23–0.24	0.21–0.24
FL	1.07–1.11	1.13–1.25	1.01–1.07	0.88–1.06	0.91–1.03	1.10–1.15
LHT	1.06–1.12	1.09–1.25	1.01–1.07	0.85–1.10	0.90–1.02	1.09–1.13
EL	0.33–0.37	0.32–0.35	0.32–0.37	0.24–0.28	0.34–0.37	0.39–0.43
MML	1.46–1.58	0.76–0.95	1.48–1.67	1.31–1.61	1.44–1.57	1.53–1.62
WL	4.03–4.14	4.1–4.75	4.16–4.49	3.66–4.68	4.4–4.9	4.35–4.51
CI	88–93	92–95	92–97	85–98	90–97	93–97
SI	26–29	27–30	27–30	31–34	32–35	30–32
OI	47–52	43–47	48–52	37–42	51–53	55–58
WI	25–27	26–28	26–28	28–29	29–31	27–28
FI	66–69	70–73	63–68	66–68	61–66	70–71

Geographic distribution

The species of the *fuscum* group are geographically distributed as follows: *L. angulatum* Emery, 1894, in Costa Rica south, west South America to the Brazilian Pantanal; *L. fuscum* Mayr, 1866, in Peru and Ecuador; *L. keiteli* Forel, 1906, in Hispaniola;

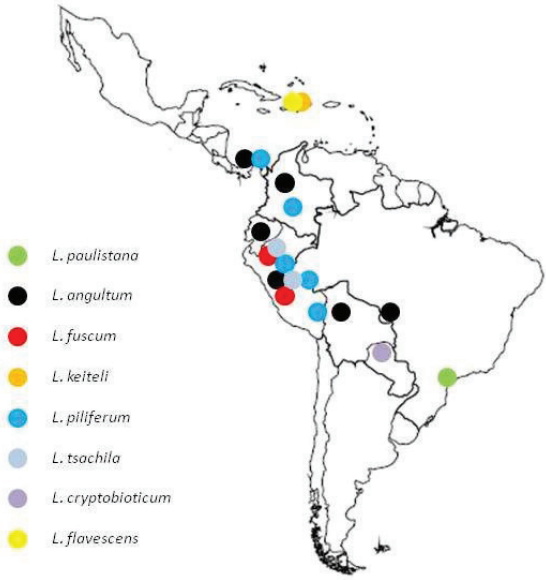

Figure 6. Distribution map of the *Linepithema fuscum* group of species in Central and South America.

L. piliferum Mayr, 1870, in mountains of northwestern South America to Costa Rica; *L. tsachila* Wild, 2007, in Colombia and Ecuador; *L. cryptobioticum* Wild, 2007, Paraguai; *L. flavescens* Wheeler & Mann, 1914, Hispaniola (Wild 2007; Escarga and Guerrero 2016); and *L. paulistana* sp. nov. São Paulo, Brazil (Fig. 6).

Key

A dichotomous key to identify the males of known species of the *fuscum* group is presented. The form of the volsella in the species of *Linepithema fuscum* group is the main morphological feature used by Wild (2007) to differentiate the species. The digitus was divided by Wild (2007) into proximal arm and distal arm (Fig. 7D). We follow this criterion, which gives the possibility to compare this new species with the other described species of the *fuscum* group (Fig. 7). In *L. paulistana* sp. nov. the distal arm is similar in length to the proximal arm.

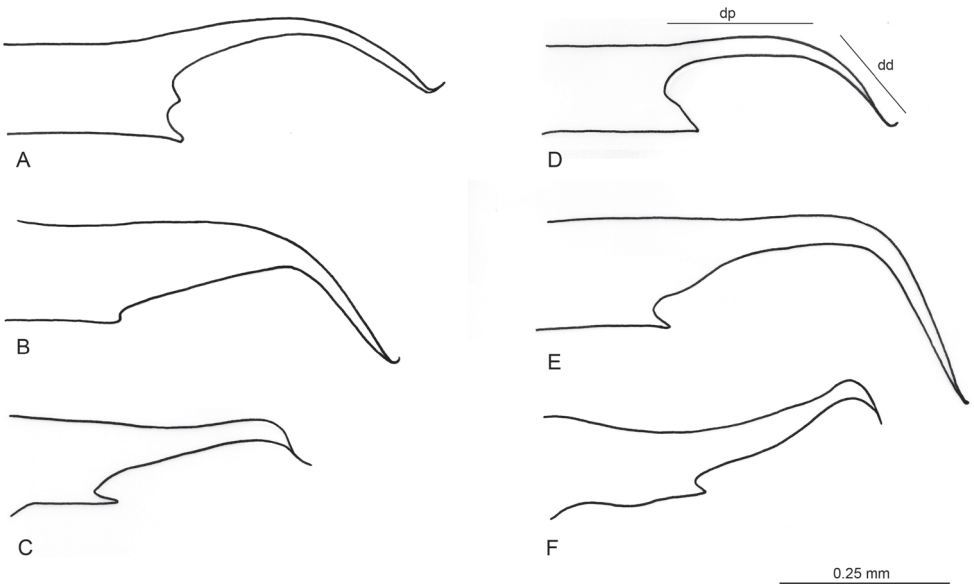

Figure 7. Shape of volsella in males of the *Linepithema* Fuscum-group **A** *L. paulistana* sp. nov. **B** *L. angulatum* **C** *L. piliferum* **D** *L. fuscum* **E** *L. keiteli* **F** *L. tsachila*. Abbreviations: dp = proximal arm of digitus; dd = distal arm of digitus. **B–F** re-drawn from Wild (2007).

1 Forewings with one submarginal cell; petiole with ventral process well developed (Fig. 5A, B); pygostyle short (Fig. 5C); proctiger slightly developed (Fig. 5E, F); telomere short and lobiform (Fig. 5C, D); lateral cuspis developed (Fig. 5E, F); ventral basivolsellar process developed (Fig. 5E, F)..... ..... ***Linepithema* species not in the *fuscum* group**

– Forewings with two submarginal cells (Fig. 1E); petiole with ventral process slightly developed consisting of a slight convexity (Figs 1D, 3D); pygostyle very

long (Fig. 4A); proctiger well developed (Fig. 1G, I); telomere very long and narrow (Fig. 4C); lateral cuspis very reduced (Fig. 4E); ventral basivolsellar process reduced (Fig. 4D)..... ***Linepithema fuscum* group 2**

2 Digitus very long, downturned, falcate (Fig. 7A, B, D, E)..... **3**

– Digitus moderately long, not downturned, not falcate (Fig. 7C, F)..... **6**

3 Basivolsellar process not pointed apically (Fig. 7B)..... ***L. angulatum***

– Basivolsellar process pointed apically (Fig. 7A, D, E) **4**

4 Digitus downturned with almost a 90° angle (Fig. 7E); ocular index OI = 37–42; Hispaniola island ..... ***L. keiteli***

– Digitus downturned with 45° angle (Fig. 7A, D); ocular index OI = 47–52 ..... **5**

5 Volsellar tooth present distally between basivolsellar process and digitus (Fig. 7A); São Paulo, Brazil ..... ***L. paulistana* sp. nov.**

– Volsellar tooth absent (Fig. 7D); Peru and Ecuador..... ***L. fuscum***

6 Digitus strongly concave dorsally (Fig. 7F)..... ***L. tsachila***

– Digitus straight to slightly concave (Fig. 7C) ..... ***L. piliferum***

Discussion

The genus *Linepithema* was designated by Mayr (1866) for males that he described as *L. fuscum*, for which workers and queens remain unknown. Regardless, males of the *fuscum* group are easily distinguished from other *Linepithema* species due to the synapomorphic features indicated by Shattuck (1992b) and Wild (2007). We report these features in Table 1 together with new or updated characters, while in Table 2 we report the male morphometrics for all species of the *L. fuscum* group with the addition of our proposed new species. Currently, males of the *L. fuscum* group are known for five out of seven species and are recognizable by the peculiar morphology of the volsella (digitus and basivolsellar process, Fig. 6), which was used as the main species-specific feature by Wild (2007) in his dichotomous key to males. *Linepithema paulistana* sp. nov. shows all diagnostic features of *fuscum* group and is distinguished from the other species by the presence of a triangular tooth situated on the volsella distally, between digitus and basivolsellar process (Figs 1G, 4A–F). For this reason, in the present description of *L. paulistana* sp. nov. we emphasized the morphology of the external genitalia (in particular of the volsella).

The first description of the external genitalia in *L. fuscum* was made by Mayr (1866), later revised by Emery (1912), who supplied a new description of all the three paired valves, figured by a schematic drawing. Subsequently, the external genitalia of the genus *Linepithema fuscum* group have been described by Shattuck (1992b) and Wild (2007). According to careful studies of several authors, the volsella is composed of two separate sclerites: the lateroventral parossiculus and the medial digitus (Snodgrass 1941); both sclerites are united longitudinally by a narrow, sclerotized suture (Schulmeister 2001); the parossiculus is a unique sclerite (Schulmeister 2001), consisting in a basal basivolsella, a ventral basivolsellar process and a lateral cuspis (Snodgrass 1941). The distal apex of the cuspis and the ventral and apical basivolsellar process are usually recognizable by the presence of setae (Boudinot 2013). By using SEM and optical microscopy

we analyzed the external genitalia of *L. paulistana* sp. nov. and re-evaluated some characters and previous interpretations in the *Linepithema fuscum* group.

In *L. paulistana* sp. nov. we found that: i) the cuspis is very reduced but clearly recognizable as a ridge by the presence of long setae on apical part (Fig. 4C–E), probably due to a lateromedial flattening of the volsella, and not absent as claimed by Shattuck (1992b) and Wild (2007) in the diagnosis of the *fuscum* group. In our opinion, the presence of the cuspis in males of other species of the *fuscum* group should be reconsidered. ii) The "ventrodistal process" of the volsella described by Wild (2007) is the basivolsellar process, which is reduced and with apical and ventral setae (Fig. 4A–F). The *L. fuscum* group is, to our knowledge, an exception in the subfamily Dolichoderinae: the paramere shows a telomere very elongated, narrow, ribbon-like and digitiform apically, extending anterodorsally up the proctiger (Fig. 4A–C). Otherwise, the external genitalia of the subfamily Dolichoderinae, based on the diagnosis by Boudinot (2015), is characterized by a paramere, with basimere dorsally and distally developed, and a telomere strongly reduced and lobed, representing a synapomorphy of the subfamily (Yoshimura and Fisher 2011; Boudinot 2015). As for the paramere (basimere+telomere), in the males of the *fuscum* group, including *L. paulistana* sp. nov., the term telomere should be preferred to gonostylus, utilized in the previous descriptions (Shattuck 1992b), consistently with the same lobate structures of other dolichoderine males, as suggested by Boudinot (2013).

In order to show the morphological diversity of the male external genitalia within the *Linepithema* species-groups, we also analyzed and illustrated by SEM the species *L. humile* (representative of *humile* group) and *L. neotropicum* (representative of the *neotropicum* group), and we compared these species with *L. paulistana* sp. nov. (representative of the *fuscum* group). We highlighted, in particular, that: i) in *L. humile* and *L. neotropicum* the basivolsellar process is well developed, located ventrally, with lateral cuspis and medial digitus (Fig. 5C–F). In males of the *fuscum* group, due to elongation and flattening lateromedially of the volsella, the cuspis is reduced laterally to the digitus and the basivolsellar process is reduced ventrally (Fig. 4A–F). ii) The morphology of the dentate valviceps lamina in *L. humile* and *L. neotropicum* has a rounded profile dentate ventral edge strongly convex and rounded, while in *L. paulistana* sp. nov. has a dentate ventral edge straight (Figs 1J, 4D, 5G, H). iii) The proctiger in *L. paulistana* sp. nov. is well developed (Figs 1G, I, 4A, C), probably representing a morphological character of the *fuscum* group, given that in *L. tsachila* and *L. fuscum* is present (AntWeb 2022). The proctiger is very reduced in the males of the other *Linepithema* species-groups (Fig. 5C, D). Relevant morphological characters that distinguish the species of the *Linepithema fuscum* group from the other species of the same genus are reported in Table 1.

Concerning the morphometric characters reported in Table 2, *L. paulistana* sp. nov. shows several similarities with *L. fuscum*, but differs in having smaller head (CI), much smaller wings (WL), and longer profemora (FL). However, the possibility that *L. paulistana* sp. nov. could represent an allopatric population of *L. fuscum*, with some morphological differences, seems highly unlikely due to: i) different morphology and dimensions of the volsella, an acknowledged species-specific character; ii) the great geographic distance between the species, *L. fuscum* from the Pacific side and *L. paulistana*

sp. nov. from of the Atlantic side, separated by the Andes Mountains; iii) the different climatic and ecological conditions where the two species live.

As the *fuscum* group is male-based, the assignment of the species to this group should be verified by using male characters. However, based on worker morphology (Wild 2007), two species of *Linepithema* with unknown males, *L. flavescens* and *L. cryptobioticum*, were assigned to the *fuscum* group (Wild 2007). For *L. cryptobioticum* this assignment was supported by a molecular study (Wild 2009). Since the workers of the new species here described are still unknown, we cannot exclude *a priori* the possibility that males of *L. paulistana* sp. nov. could be part of the aforementioned species. However, this is unlikely based on the following arguments: 1) The species *L. cryptobioticum*, *L. flavescens* and *L. paulistana* sp. nov. have allopatric distribution: *L. flavescens* is very far from the other species and shows very localized distribution in the Northern hemisphere, being only present in the Hispaniola Island; *L. cryptobioticum* is only present in Paraguay; *L. paulistana* sp. nov. is only present in São Paulo city. 2) The species *L. cryptobioticum* was included in the molecular phylogeny of Wild (2009) and was found to be a daughter species of *L. angulatum*. For this reason, we hypothesize that male of *L. cryptobioticum* is morphologically very similar to that of *L. angulatum*. Comparing the males of *L. angulatum* and *L. paulistana* sp. nov. we find the following distinctive differences that widely reduce the possibility of a close relationship between the two species: the volsella is very different in shape (Fig. 7A, B) and the morphometric dimensions are very different (see for example HL, HW, FL, MML, OI in Table 2). However, we cannot exclude that *L. paulistana* sp. nov. is a derived offshoot within the "*angulatum*" cluster. For these reasons, in order to have more clarity about the relationships in this intricate species group, we will have to wait until the discovery of males of *L. cryptobioticum*, as well as *L. angulatum* males from other representative localities within the wide range of distribution, spanning from Meso-America to the Pantanal.

Finally, it is remarkable that *L. paulistana* sp. nov. is the only species of the *fuscum* group present in the eastern part of South America, extending the former distribution of this species group (Fig. 6), widely distributed i western South America. This finding represents an important range expansion of the genus, which opens the possibility to find additional species of *L. fuscum* group also in other parts of eastern South America.

Conclusions

The present work confirms that the information on morphological characters of male, especially of male external genitalia, is effective for the identification of ant genera and species, as in most insects (Bolton 2003; Yoshimura and Fisher 2007; Yoshimura and Fisher 2011; Boudinot 2013, 2015; Cantone 2017). We are strongly convinced that a greater knowledge of the male caste would greatly help the identification of most ant species, genera, or species groups, like *Linepithema*, where workers are very difficult to identify at the species level. Unfortunately, in the family Formicidae the knowledge on the male caste is very limited and the taxonomy is traditionally mainly based on workers. *Linepithema* is one of the very rare genera described on male caste and allows

to describe a new species, like *L. paulistana* sp. nov., based on male specimens. In our opinion the great morphological differences between the external genitalia of species of the *fuscum* group and all the other species formerly assigned to the genus *Iridomyrmex*, like *L. humile*, and now included in three different *Linepithema* species groups, suggest that a re-evaluation of the taxonomic status of this genus is urgently needed.

Acknowledgements

We thank Alexander L. Wild, author of the great revision of the genus *Linepithema*, Jeffrey Sosa-Calvo, and an anonymous referee who carefully revised the manuscript and greatly improved this paper with their helpful suggestions.

References

AntWeb (2022) Version 8.75.3. California Academy of Science. [Online at:] https://www.antweb.org [Accessed 27/09/2022]

Aron S (2001) Reproductive strategy: An essenzial component in the success of incipient colonies of the invasive Argentine ant. Insectes Sociaux 48(1): 25–27. https://doi.org/10.1007/PL00001740

Aron S, Passera L, Keller L (1994) Queen-worker conflict over sex ratio: A comparison of primary and secondary sex ratios in the Argentine ant, *Iridomyrmex humilis*. Journal of Evolutionary Biology 7(4): 403–418. https://doi.org/10.1046/j.1420-9101.1994.7040403.x

Aron S, Keller L, Passera L (2001) Role of resource availability on sex, caste and reproductive allocation ration in the Argentine ant *Linepithema humile*. Journal of Animal Ecology 70(5): 831–839. https://doi.org/10.1046/j.0021-8790.2001.00545.x

Barden P, Boudinot B, Lucki A (2017) Where Fossil Dare and Male Matter: combined morphological and molecular analysis untangles the evolutionary history of the spider ant genus *Leptomyrmex* Mayr (Hymenoptera: Dolichoderinae). Invertebrate Systematics 31(6): 765–780. https://doi.org/10.1071/IS16067

Beutel RG, Richter A, Keller RA, Hita Garcia F, Matsumura Y, Economo EP, Gorb SN (2020) Distal leg structures of the Aculeata (Hymenoptera): A comparative evolutionary study of *Sceliphron* (Sphecidae) and *Formica* (Formicidae). Journal of Morphology 281(7): 737–753. https://doi.org/10.1002/jmor.21133

Bolton B (2003) Synopsis and Classification of Formicidae. Memoirs of the American Entomological Institute, vol. 71. The American Entomological Institute, Gainsville, FL, 370 pp. [ISBN: I-887988-15-7]

Bolton B (2022) An online catalog of the ants of the world. [Available from:] http://antcat.org [Accessed 27/09/2022]

Boudinot BE (2013) The male genitalia of ants: Musculature, homology, and functional morphology (Hymenoptera, Aculeata, Formicidae). Journal of Hymenoptera Research 30: 29–49. https://doi.org/10.3897/jhr.30.3535

Boudinot BE (2015) Contribution to the knowledge of Formicidae (Hymenoptera, Aculeata): A new diagnosis of the family, the first global male-based key to subfamilies, and a treatment of early branching lineages. European Journal of Taxonomy 120(120): 1–62. https://doi.org/10.5852/ejt.2015.120

Boudinot BE (2018) A general theory of genital homologies for the Hexapoda (Pancrustacea) derived from skeletomuscolar correspondences, with emphasis on the Endopterygota. Arthropod Structure & Development 47(6): 563–613. https://doi.org/10.1016/j.asd.2018.11.001

Cantone S (2017) Winged Ants, The Male. Dichotomous key to genera of winged ♂♂ ants in the World; Behavioral Ecology of Mating flight. In: Cantone S (Ed.) Catania, Italy. [ISBN-A 10.979.12200/23948] https://antcat.org/references/143115

Cantone S (2018a) Winged Ants, The Queen. Dichotomous key to genera of winged queen ants in the world. The wings of ants: morphological and systematic relationships. Cantone S (Ed.) Catania, Italy. [ISBN-A 10.979.12200/37075] https://antwiki.org/wiki/images/8/87/Cantone%2C_S._2018._Winged_ants._The_Queen.pdf

Cantone S (2018b) Winged Ants in the city of São Paulo, Brazil: Analysis of the mating flights. International Journal of Entomological Research 3(6): 47–54. https://www.entomologyjournals.com/archives/2018/vol3/issue6/3-6-18

Cantone S, Von Zuben JC (2019) The Hindwings of Ants: A Phylogenetic analysis. Psyche: A Journal of Entomology 2019: [Article ID] 7929717. https://doi.org/10.1155/2019/7929717

Delsine T, Serna FJ, Leponce M, Boudinot BE (2019) Glossario de morfologia. Capitulo 13. In: Fernandez F, Guerrero RJ, Delsine T, Hormigas de Colombia. Universidad Nacional de Colombia, Bogotà, 387–457. [1198 pp] [ISBN 978-958-783-765-0; ISBN 978-958-783-766-7]

Emery C (1912) Hymenoptera Fam. Formicidae Subfam. Dolichoderinae. Genera Insectorum, Fascicule. Hymenoptera 137: 1–50.

Escarga M, Guerrero RJ (2016) The ant genus *Linepithema* (Formicidae: Dolichoderinae) in Colombia. Zootaxa 4208(5): 446–458. https://doi.org/10.11646/zootaxa.4208.5.3

Mason WRM (1986) Standard drawing conventions and definitions for venational and other features of wings of Hymenoptera. Proceedings of the Entomological Society of Washington 88(1): 1–7.

Mayr GL (1866) Myrmecologische Beitrage. Sitzungsberichte der Kaiserlichen Akademie der Wissenschaften in Wien. Mathematisch-Naturwissenscaftliche Classe. Abteilung I 53: 484–517.

Menke SB, Holway DA (2006) Abiotic factor control invasion by Argentine ants at the community scale. Journal of Animal Ecology 75(2): 368–376. https://doi.org/10.1111/j.1365-2656.2006.01056.x

Perfilieva KS (2010) Trend in Evolution of Ant Wing Venation (Hymenoptera, Formicidae). Entomological Review 90(7): 857–870. https://doi.org/10.1134/S0013873810070043

Richter A, Keller RA, Rosumek FB, Economo EP, Hita Garcia F, Beutel RG (2019) The cephalic anatomy of workers of the ant species *Wasmannia affinis* (Formicidae, Hymenoptera, Insecta) and its evolutionary implications. Arthropod Structure & Development 49: 26–49. https://doi.org/10.1016/j.asd.2019.02.002

Richter A, Hita Garcia F, Keller RA, Billen J, Economo EP, Beutel RG (2020) Comparative analysis of worker head anatomy of *Formica* and *Brachyponera* (Hymenoptera: Formicidae). Arthropod Structure & Phylogeny 78(1): 133–170. https://doi.org/10.26049/ASP78-1-2020-06

Richter A, Hita Garcia F, Keller RA, Billen J, Katzke J, Boudinot BE, Economo EP, Beutel RG (2021) The head anatomy of *Protanilla lini* (Hymenoptera: Formicidae: Leptanillinae), with a hypothesis of their mandibular movement. Myrmecological News 31: 85–114. https://doi.org/10.25849/myrmecol.news_031:085

Roura-Pascual N, Suarez AV, Gomez C, Pons P, Touyama Y, Wild AL, Peterson T (2004) Geographical potential of Argentine ants (*Linepithema humile* Mayr) in the face of global climate change. Proceedings of the Royal Society B, Biological Sciences 271(1557): 2527–2535. https://doi.org/10.1098/rspb.2004.2898

Schulmeister S (2001) Functional morphology of the male genitalia and copulation in lower Hymenoptera, with special emphasis on the Tenthredinoidea s. str. (Insecta, Hymenoptera, 'Symphyta'). Acta Zoologica (Stockholm, Sweden) 82(4): 331–349. https://doi.org/10.1046/j.1463-6395.2001.00094.x

Schulmeister S (2003) Genitalia and terminal abdominal segments of male basal Hymenoptera (Insecta): Morphology and evolution. Organisms, Diversity & Evolution 3(4): 253–279. https://doi.org/10.1078/1439-6092-00078

Shattuck SO (1992a) Review of the Dolichoderinae ant genus *Iridomyrmex* Mayr with description of three new genera (Hymenoptera: Formicidae). Journal of the Australian Entomological Society 31(1): 13–18. https://doi.org/10.1111/j.1440-6055.1992.tb00453.x

Shattuck SO (1992b) Generic revision of the ant subfamily Dolichoderinae (Hymenoptera: Formicidae. Sociobiology 21(1): 1–181.

Snodgrass RE (1941) The male genitalia of Hymenoptera. Smithsonian Miscellaneous Collections 99: 1–86.

Ward PS (1987) Distribution of the Introduced Argentine Ant (*Iridomyrmex humilis*) in Natural Habitats of the Lower Sacramento Valley and Its Effects on the Indigenous Ant Fauna. Hilgardia 55(2): 1–16. https://doi.org/10.3733/hilg.v55n02p016

Wild AL (2004) Taxonomy and Distribution of the Argentine Ant, *Linepithema humile* (Hymenoptera: Formicidae). Annals of the Entomological Society of America 97(6): 1204–1215. https://doi.org/10.1603/0013-8746(2004)097[1204:TADOTA]2.0.CO;2

Wild AL (2007) Taxonomic Revision of the Ant Genus *Linepithema* (Hymenoptera: Formicidae). University of California publications, Entomology 126: 1–151. [ISBN: 9780520098589] http://repositories.cdlib.org/ucpress/

Wild AL (2009) Evolution of the Neotropical ant genus *Linepithema*. Systematic Entomology 34(1): 49–62. https://doi.org/10.1111/j.1365-3113.2008.00435.x

Yoshimura M, Fisher B (2007) A revision of male of the Malagasy region (Hymenoptera: Formicidae): Key to subfamilies and treatment of the genera of Ponerinae. Zootaxa 1654(1): 21–40. https://doi.org/10.11646/zootaxa.1654.1.2

Yoshimura M, Fisher B (2009) A revision of male ants of the Malagasy region (Hymenoptera: Formicidae): key to genera of the subfamily Proceratiinae. Zootaxa 2216(1): 1–21. https://doi.org/10.11646/zootaxa.2216.1.1

Yoshimura M, Fisher B (2011) A revision of male ants of the Malagasy region (Hymenoptera: Formicidae): Key to genera of the subfamily Dolichoderinae. Zootaxa 2794(1): 1–34. https://doi.org/10.11646/zootaxa.2794.1.1

ZooKeys 1160: 145–167 (2023)
doi: 10.3897/zookeys.1160.100818
https://zookeys.pensoft.net

RESEARCH ARTICLE

A peer-reviewed open-access journal
ZooKeys
Launched to accelerate biodiversity research

The complete mitochondrial genome of *Aeschrocoris tuberculatus* and *A. ceylonicus* (Hemiptera, Pentatomidae) and its phylogenetic implications

Wang Jia[1], Jiufeng Wei[1], Minmin Niu[1], Hufang Zhang[2], Qing Zhao[1]

1 *College of Plant Protection, Shanxi Agricultural University, Taigu 030801, Shanxi, China* **2** *Department of Biology, Xinzhou Teachers University, Xinzhou 034000, Shanxi, China*

Corresponding author: Qing Zhao (zhaoqing86623@163.com)

Academic editor: Wenjun Bu | Received 20 January 2023 | Accepted 13 April 2023 | Published 9 May 2023

https://zoobank.org/CAF0F319-41E5-4B7F-8C4E-7DF79D2BBBB6

Citation: Jia W, Wei J, Niu M, Zhang H, Zhao Q (2023) The complete mitochondrial genome of *Aeschrocoris tuberculatus* and *A. ceylonicus* (Hemiptera, Pentatomidae) and its phylogenetic implications. ZooKeys 1160: 145–167. https://doi.org/10.3897/zookeys.1160.100818

Abstract

Aeschrocoris tuberculatus and *A. ceylonicus* (Hemiptera, Pentatomidae, Pentatominae) are mainly distributed in southern China, India, Myanmar, and Sri Lanka. Both species are also common agricultural pests. However, only the morphology of the genus *Aeschrocoris* has previously been studied, and molecular data have been lacking. In this study, the whole mitochondrial genomes of *A. tuberculatus* and *A. ceylonicus* are and annotated. The lengths of the complete mitochondrial genomes of the two species are 16,134 bp and 16,142 bp, respectively, and both contain 37 typical genes, including 13 protein-coding genes (PCGs), two ribosomal RNA genes (rRNAs), 22 transfer RNA genes (tRNAs), and a control region. The mitochondrial genome structure, gene order, nucleotide composition, and codon usage of *A. tuberculatus* and *A. ceylonicus* are consistent with those of typical Pentatomidae. Most PCGs of both species use ATN as the start codon, except *atp8*, *nad1*, and *cox1*, which use TTG as the start codon. *cox1*, *cox2*, and *atp6* use a single T, and *nad1* use TAG as the stop codon; the remaining PCGs have TAA as the stop codon. The A+T contents of the two species are 73.86% and 74.08%, respectively. All tRNAs have a typical cloverleaf structure, with the exception of *trnS1*, which lacks a dihydrouridine arm. The phylogenetic tree is reconstructed using the maximum-likelihood method based on the newly obtained mitochondrial genome sequences and 87 existing mitochondrial genomes of Pentatomoidea from the NCBI database and two species of Lygaeoidea as outgroups. The phylogenetic trees strongly support the following relationships: (Urostylididae + ((Acanthosomatidae + ((Cydnidae + (Dinidoridae + Tessaratomidae)) + (Scutelleridae + Plataspidae))) + Pentatomidae). This study enriches the mitochondrial genome database of Pentatomoidea and provides a reference for further phylogenetic studies.

Keywords
Mitogenome, Pentatomoidea, phylogenetic analysis

Introduction

The insect mitochondrial genome is a circular double-stranded DNA molecule with a length of about 16–18 kb, which code 37 genes: 13 protein-coding genes (PCGs), two ribosomal RNA (rRNA) genes, and 22 transfer RNA (tRNA) genes (Boore 1999). In addition, the mitochondrial genome usually includes a noncoding region of variable length that plays a regulatory role in transcription and replication, known as the mitochondrial control region (Cameron 2014). In recent years, with the development of sequencing technology and the amplification through universal primers for mitochondrial genes (Simon et al. 1994, 2006), the number of insect mitochondrial genomes has rapidly increased, and the characteristics and evolutionary patterns of insect mitochondrial genomes are becoming more and more clear; their applications in phylogenetic studies are gradually increasing. The mitochondrial genome contains important molecular evolutionary information such as base composition and codon usage (Yuan et al. 2022). It has been widely used in research on molecular evolution, phylogeny, genealogy, and population genetic structure because of its stable gene composition, relatively conserved order, matrilineal inheritance, and minimal recombination (Ballard and Whitlock 2004; Simon and Hadrys 2013; Cameron 2014).

Pentatomoidea (Hemiptera, Heteroptera, Pentatomomorpha) consists of more than 8,000 species in 18 families, of which Pentatomidae is the largest family containing 940 genera and about 5,000 species (Rider et al. 2018). Pentatomidae is a species-rich group, so it is difficult to propose defining characteristics that can be applied to all groups. All stinkbugs of Pentatomidae are terrestrial insects, most of which are phytophagous; only Asopinae are predatory species, and some are used as biological control agents (De Clercq et al. 2003).

The tribe Aeschrocorini was first proposed by Distant (1902) and included two genera, *Aeschrocoris* Bergroth, 1887 and *Scylax* Distant, 1887. It remained little known until Cachan (1952) added a new genus to the tribe. The Aeschrocorini is still relatively small, currently with only eight genera (Rider et al. 2018). Hassan et al. (2016) provided a brief record of Indian species of *Aeschrocoris*. Despite the complex taxonomic relationships within the Aeschrocorini, numerous scholars have consistently assigned the genus *Aeschrocoris* to Aeschrocorini (Rider et al. 2018). *Aeschrocoris* was reported to have five species in China and eight in the world. *Aeschrocoris tuberculatus* (Stål, 1865) and *A. ceylonicus* Distant, 1899 are mainly distributed in southern China, India, Myanmar, and Sri Lanka, and both are also common agricultural pests (Fan 2011). However, most studies of the genus *Aeschrocoris* have focused on morphological descriptions and lack molecular data.

In this study, we analyze the mitochondrial genomes of *A. tuberculatus* and *A. ceylonicus* in detail, including genome structure, nucleotide composition, and codon

usage. Meanwhile, we also construct the genome structure of RNA. In addition, we analyze the phylogenetic relationship of eight families of Pentatomoidea and explore the phylogenetic location of these two species. The results of this study will provide a reference for phylogenetic analyses and identification of the Pentatomoidea.

Materials and methods

Sample collection

Adult specimens of *Aeschrocoris tuberculatus* and *A. ceylonicus* were collected from Baihua Ling (Baoshan City, Yunnan Province, China; 25°16'43"N, 98°48'12"E) on 13 August 2015 and from Guanlan Ting (Taohua Island, Zhoushan City, Zhejiang Province, China; 29°50'31"N, 122°14'13"E) on 4 August 2016. All samples were immediately placed in anhydrous ethanol and stored in a refrigerator at –25 °C until DNA was extracted. The species were identified by Qing Zhao.

DNA extraction and sequencing

Whole-genome DNA was extracted from the thoracic muscle of the samples using the Genomic DNA Extraction Kit (BGI, Wuhan, Hubei, China). Concentrations of samples were detected using Qubit Fluorometer and microplate reader (Mardis and McCombie 2017). The integrity of the samples was tested by agarose gel electrophoresis. High-throughput pair-ended sequencing (PE150) was performed on DNBSEQ platform for the complete mitochondrial genomes of the two species (Chen et al. 2018). All the above operations were carried out in the high-throughput laboratory at Wuhan BGI Technology Services Co., Ltd. (Wuhan, Hubei, China).

Genome annotation and sequence analysis

When the assembly was complete, the complete mitogenomes were manually annotated using Geneious v. 11.0 software (Kearse et al. 2012). Two reference sequences (*Eurydema gebleri* and *Brachymna tenuis*) for annotation were obtained from the Basic Local Alignment Search tool (BLAST) in the NCBI database. The boundaries of the PCGs were determined using Open Reading Frame Finder on the NCBI website (http://www.ncbi.nlm.nih.gov/gorf/gorf.html). MEGA v. 11.0 (Tamura et al. 2021) was used to translate the proteins to verify the start codons, stop codons, and amino acid sequences and to ensure the accuracy of the sequences. We annotated tRNA sequences using tRNAscan-SE 2.0 (http://lowelab.ucsc.edu/tRNAscan-SE/; Lowe and Eddy 1997) or used automatic annotation done by MITOS (http://mitos.bioinf.uni-leipzig.de/index.py/; Bernt et al. 2013) with the invertebrate mitochondrial code. The boundaries of the rRNA genes were completed based on the positions of adjacent genes and published rRNA gene sequences (Boore 2006). The control region was identified through the boundary of the neighboring genes.

The base composition, codon usage (RSCU), and amino acid composition of the mitogenome were analyzed using MEGA v. 11.0. The skew of the nucleotide composition was calculated as follows: AT-skew = (A – T) / (A + T) and GC-skew = (G – C) / (G + C) (Perna and Kocher 1995; Hassanin et al. 2005; Bernt et al. 2013). DnaSP6 software (Rozas et al. 2017) was used to count the non-synonymous substitutions (Ka) and synonymous substitutions (Ks) of 13 PCGs of Pentatomoidea and to calculate the Ka/Ks values. The ratio Ka/Ks indicated the rate of evolution, the higher the ratio, and the faster the rate of evolution.

Phylogenetic analyses

In this study, we used the two newly sequenced species, 87 species from other eight families of Pentatomoidea, and two species (*Geocoris pallidipennis* and *Kleidocerys resedae* as the outgroup) from Lygaeoidea to analyze the phylogenetic position of *A. tuberculatus* and *A. ceylonicus* and the phylogenetic relationships within Pentatomoidea (Table 1). DNA alignment was inferred from the amino-acid alignment of the 13 PCGs using MUSCLE with default settings in MEGA v. 11 (Edgar 2004).

Table 1. List of species used to construct the phylogenetic tree.

Classification	Family	Species	Accession number	Reference
Outgroup				
Lygaeoidea	Lygaeidae	*Geocoris pallidipennis*	EU427336	Hua et al. 2008
		Kleidocerys resedae	KJ584365	Li et al. 2016
Ingroup				
Pentatomoidea	Acanthosomatidae	*Acanthosoma labiduroides*	JQ743670	Li et al. 2017
		Anaxandra taurina	NC042801	Liu et al. 2019
		Sastragala edessoides	JQ743676	Li et al. 2017
		Sastragala esakii	MW847247	Xu et al. 2021
	Cydnidae	*Adrisa magna*	NC042429	Liu et al. 2019
		Aethus nigritus	MW847231	Xu et al. 2021
		Macroscytus gibbulus	EU427338	Hua et al. 2008
		Macroscytus subaeneus	MW847241	Xu et al. 2021
		Scoparipes salvazai	NC042800	Liu et al. 2019
	Dinidoridae	*Coridius brunneus*	MW899158	Unpublished
		Cyclopelta parva	NC037739	Jiang 2017
		Megymenum gracilicorne	NC042810	Liu et al. 2019
	Pentatomidae	***Aeschrocoris ceylonicus***	OP526368	This study
		Aeschrocoris tuberculatus	OP526367	This study
		Arma custos	NC051562	Wu et al. 2020
		Anaxilaus musgravei	NC061538	Unpublished
		Brachymna tenuis	NC042802	Liu et al. 2019
		Carbula sinica	NC037741	Jiang 2017
		Catacanthus incarnatus	NC042804	Liu et al. 2019
		Caystrus obscurus	NC042805	Liu et al. 2019
		Cazira horvathi	NC042817	Liu et al. 2019
		Dalpada cinctipes	NC058967	Xu et al. 2021
		Dalsira scabrata	NC037374	Jiang 2017
		Deroploa parva	NC063299	Unpublished
		Dinorhynchus dybowskyi	NC037724	Zhao et al. 2018
		Dolycoris baccarum	NC020373	Zhang et al. 2013
		Eocanthecona furcellata	MZ440302	Unpublished
		Eocanthecona thomsoni	NC042816	Liu et al. 2019
		Eurydema dominulus	NC044762	Zhao et al. 2019b

Classification	Family	Species	Accession number	Reference
Pentatomoidea	Pentatomidae	*Eurydema gebleri*	NC027489	Yuan et al. 2015
		Eurydema liturifera	NC044763	Zhao et al. 2019b
		Eurydema maracandica	NC037042	Zhao et al. 2017b
		Eurydema oleracea	NC044764	Zhao et al. 2019b
		Eurydema qinlingensis	NC044765	Unpublished
		Eurydema ventralis	MG584837	Unpublished
		Erthesina fullo	NC042202	Ji et al. 2019
		Eysarcoris aeneus	MK841489	Zhao et al. 2019a
		Eysarcoris annamita	MW852483	Li et al. 2021
		Eysarcoris gibbosus	MW846868	Li et al. 2021
		Eysarcoris guttigerus	NC047222	Chen et al. 2020
		Eysarcoris montivagus	MW846867	Li et al. 2021
		Eysarcoris rosaceus	MT165687	Li et al. 2021
		Glaucias dorsalis	NC058968	Xu et al. 2021
		Gonopsis affinis	NC036745	Chen et al. 2017
		Graphosoma rubrolineatum	NC033875	Wang et al. 2017
		Halyomorpha halys	NC013272	Lee et al. 2009
		Hippotiscus dorsalis	NC058969	Xu et al. 2021
		Hoplistodera incisa	NC042799	Liu et al. 2019
		Menida violacea	NC042818	Liu et al. 2019
		Nezara viridula	NC011755	Hua et al. 2008
		Neojurtina typica	NC058971	Xu et al. 2021
		Palomena viridissima	NC050166	Unpublished
		Pentatoma metallifera	NC058972	Xu et al. 2021
		Pentatoma rufipes	MT861131	Zhao et al. 2021
		Pentatoma semiannulata	NC053653	Unpublished
		Picromerus griseus	NC036418	Zhao et al. 2017a
		Picromerus lewisi	NC058610	Mu et al. 2022
		Placosternum urus	NC042812	Liu et al. 2019
		Plautia crossota	NC057080	Wang et al. 2019
		Plautia fimbriata	NC042813	Liu et al. 2019
		Plautia lushanica	NC058973	Xu et al. 2021
		Priassus spiniger	OK546352	Unpublished
		Scotinophara lurida	NC042815	Liu et al. 2019
		Tholosanus proximus	NC063300	Unpublished
		Zicrona caerulea	NC058303	Zhao et al. 2020
	Plataspidae	*Brachyplatys subaeneus*	MW847232	Xu et al. 2021
		Calacta lugubris	MW847233	Xu et al. 2021
		Coptosoma bifaria	EU427334	Hua et al. 2008
		Coptosoma variegatum	OP123035	Zhu et al. 2022
		Megacopta bituminata	OP123020	Zhu et al. 2022
		Megacopta caliginosa	OP123022	Zhu et al. 2022
		Megacopta centronubila	OP123024	Zhu et al. 2022
		Megacopta cribraria	JF288758	Unpublished
		Megacopta cribriella	OP123025	Zhu et al. 2022
		Megacopta distanti	OP123028	Zhu et al. 2022
		Megacopta horvathi	OP123029	Zhu et al. 2022
		Megacopta lobata	OP123031	Zhu et al. 2022
	Scutelleridae	*Cantao ocellatus*	MF497713	Liu et al. 2019
		Chrysocoris stollii	NC051942	Unpublished
		Eurygaster testudinaria	NC042808	Liu et al. 2019
		Poecilocoris druraei	MW847246	Xu et al. 2021
	Tessaratomidae	*Dalcantha dilatata*	JQ910981	Li et al. 2017
		Eusthenes cupreus	NC022449	Song et al. 2013
		Mattiphus splendidus	NC053743	Xu et al. 2020
		Pycanum ochraceum	MW899159	Wang et al. 2021
		Tessaratoma papillosa	NC037742	Jiang 2017
	Urostylididae	*Urostylis flavoannulata*	NC037747	Jiang 2017
		Urolabida histrionica	MW847249	Xu et al. 2021
		Urochela quadrinotata	NC020144	Li et al. 2012

To determine whether the sequences contained phylogenetic information, we tested nucleotide substitution saturation and plotted transition and transversion rates against the TN93 distances for two datasets: all codon positions of the 13 PCGs (PCG123) and first and second codon positions of PCGs (PCG12) using DAMBE to further validate the feasibility of constructing a phylogenetic tree (Xia and Xie 2001; Xia and Lemey 2009). Heterogeneity in sequence divergence in the two datasets was analyzed by using AliGROOVE with the default sliding window size (Kück et al. 2014). PartitionFinder was used to provide the best fit model (Kalyaanamoorthy et al. 2017). IQtree v. 1.6.12 was used to construct the ML tree (Nguyen et al. 2015), and node confidence was assessed with 500,000 replications for bootstrap (Hoang et al. 2018). The phylogenetic trees were constructed using two datasets, PCG123 and PCG12. Finally, the generated phylogenetic trees were visualized using the online editing tool Chipolt (https://www.chiplot.online).

Results

Genomic features

The complete mitogenomes of *Aeschrocoris tuberculatus* (16,134 bp, GenBank accession no. OP56367) and *A. ceylonicus* (14,142 bp, GenBank accession no. OP56368) were obtained (Fig. 1). The mitogenomes of the two species contain a control region and 37 genes (13 PCGs, 22 tRNA genes, and two rRNA genes). The composition of genes is similar to those described in other pentatomid insects (Lee et al. 2009; Zhao et al. 2017a, 2017b; Chen et al. 2019). In addition, the mitochondrial genomes of both species have similar overlapping regions and gene spacer regions. In *A. tuberculatus*, the intergenic overlap region is 34 bp in length and contains seven overlapping regions of 1–8 bp in length. The longest overlapping regions are located between *trnW*/*trnC* and *nad6*/*cytb*. The intergenic spacer is 127 bp in length and contains 17 spacers ranging from 1 to 25 bp in size. The longest spacer (25 bp) is located between *trnS2* and *nad1*. In *A. ceylonicus*, seven intergenic overlapping regions were examined with varying lengths of 1–8 bp, and the longest overlapping region is at the same position (between *trnW* and *trnC*, *nad6*, and *cytb*) as in *A. tuberculatus*. The intergenic spacers are the same in *A. ceylonicus* as in *A. tuberculatus*, and the longest spacer (33 bp) region is also situated between *trnS2* and *nad1* (Table 2).

Nucleotide composition and codon usage

The nucleotide composition of two species shows the predominance of A+T in the complete mitochondrial genome (Table 3). The order of base composition of the entire sequence in *A. tuberculatus* and *A. ceylonicus* is A (42.32%) > T (31.55%) > C (15.20%) > G (10.94%) and A (42.36%) > T (31.72%) > C (14.94%) > G (10.98%), respectively. This bias was observed in the complete mitochondrial genome. The A+T

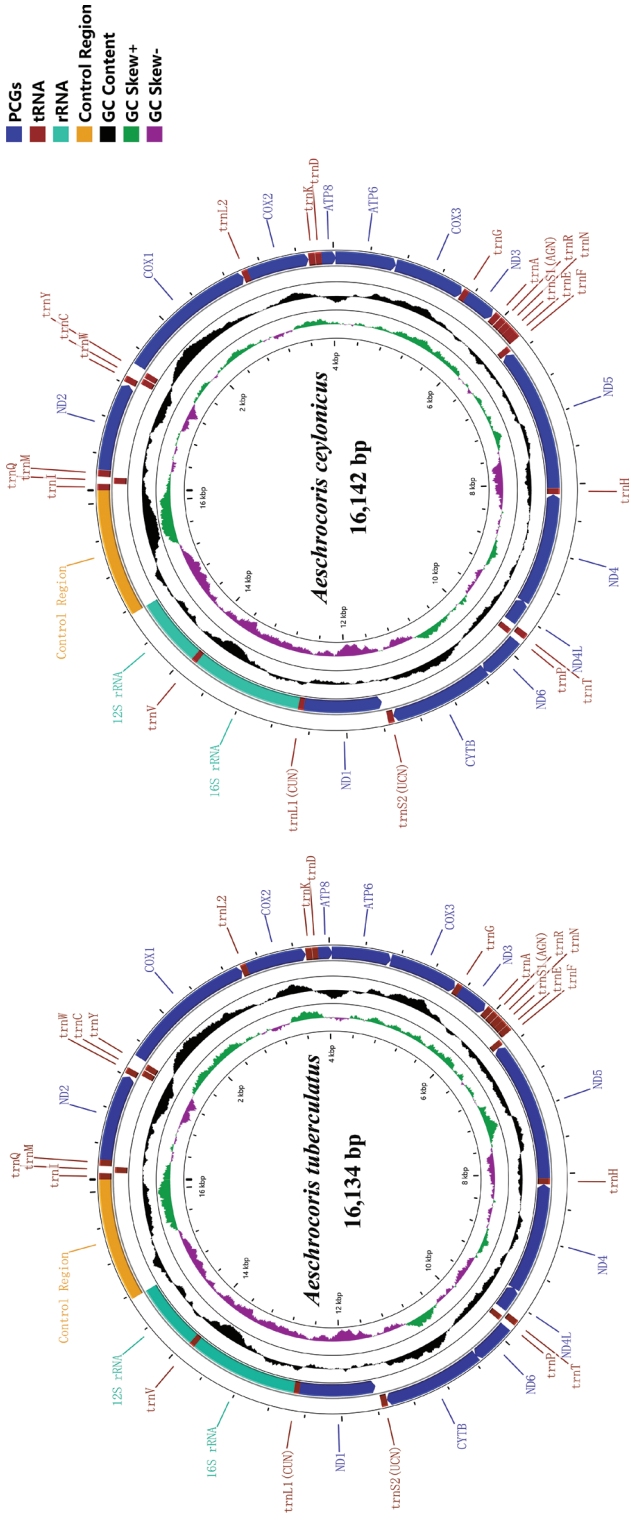

Figure 1. Mitochondrial genome structure of *Aeschrocoris tuberculatus* and *A. ceylonicus*. Arrows indicate the orientation of gene transcription. PCGs are shown as blue arrows; tRNAs are named using single-letter amino acid abbreviations.

content of the two species is 73.09% and 72.79% in PCGs, 76.11% and 76.63% in tRNAs, 75.97% and 76.60% in rRNAs and 73.99% and 77.35% in the control region, respectively. The complete genomes of both also show a clear AC skew (GC skew = –0.16, AT skew = 0.15, GC skew = –0.15, and AT skew = 0.14), suggesting a greater abundance of A than T and a higher abundance of C than G.

The composition of nucleotides is also reflected in the use of codons. The RSCUs of the two species show some differences and are compared to each other in Fig. 2. The most frequently used codons are UUA (Leu2), and most of the codons with high frequency ended in A/T. These results indicate that in the codon composition of *Aeschrocoris* mitogenomes, AT was superior to GC.

Table 2. Organization of the mitochondrial genomes of *Aeschrocoris tuberculatus* and *A. ceylonicus*.

			A. tuberculatus					*A. ceylonicus*				
Gene	**Strand**	**Anticodon**	**Position**	**Size (bp)**	**Initiation codon**	**Stop codon**	**Intergenic nucleotide**	**Position**	**Size (bp)**	**Initiation codon**	**Stop codon**	**Intergenic nucleotide**
trnI	J	GAT	1–71	71			0	1–71	71			0
trnQ	N	TTG	80–148	69			8	79–147	69			7
trnM	J	CAT	154–224	71			5	152–222	71			4
nad2	J		225–1208	984	ATA	TAA	0	226–1206	981	ATA	TAA	3
trnW	J	TCA	1226–1292	67			17	1223–1290	68			16
trnC	N	GCA	1285–1352	68			–8	1283–1350	68			–8
trnY	N	GTA	1366–1434	69			13	1364–1429	66			13
cox1	J		1450–2986	1537	TTG	T	15	1445–2981	1537	TTG	T	15
trnL2	J	TAA	2987–3053	67			0	2982–3048	67			0
cox2	J		3054–3732	679	ATA	T	0	3049–3727	679	ATA	T	0
trnK	J	CTT	3733–3804	72			0	3728–3799	72			0
trnD	J	GTC	3808–3873	66			3	3803–3869	67			3
atp8	J		3874–4035	162	TTG	TAA	0	3870–4031	162	TTG	TAA	0
atp6	J		4029–4701	673	ATG	T	–7	4025–4697	673	ATG	T	–7
cox3	J		4702–5490	789	ATG	TAA	0	4698–5486	789	ATG	TAA	0
trnG	J	TCC	5490–5555	66			–1	5486–5550	65			–1
nad3	J		5556–5909	354	ATT	TAA	0	5551–5904	354	ATT	TAA	0
trnA	J	TGC	5914–5982	69			4	5909–5977	69			4
trnR	J	TCG	5991–6058	68			8	5988–6056	69			10
trnN	J	GTT	6064–6131	68			5	6061–6128	68			4
trnS1	J	GCT	6133–6202	70			1	6130–6199	70			1
trnE	J	TTC	6207–6275	69			4	6200–6269	70			0
trnF	N	GAA	6274–6341	68			–2	6268–6335	68			–2
nad5	N		6346–8052	1707	ATG	TAA	4	6340–8046	1707	ATG	TAA	4
trnH	N	GTG	8055–8123	69			2	8049–8117	69			2
nad4	N		8127–9455	1329	ATG	TAA	3	8121–9449	1329	ATG	TAA	3
nad4l	N		9449–9736	288	ATT	TAA	–7	9443–9730	288	ATT	TAA	–7
trnT	J	TGT	9739–9807	69			2	9733–9801	69			2
trnP	N	TGG	9808–9871	64			0	9802–9865	64			0
nad6	J		9880–10353	474	ATA	TAA	8	9868–10347	480	TTG	TAA	2
cytb	J		10346–11482	1137	ATG	TAA	–8	10340–11476	1137	ATG	TAA	–8
trnS2	J	TGA	11482–11550	69			–1	11476–11534	68			–1
nad1	N		11576–12499	924	TTG	TAG	25	11568–12491	924	TTG	TAG	33
trnL1	N	TAG	12500–12565	66			0	12492–12557	66			0
rrnL	N		12566–13874	1309			0	12558–13859	1302			0
trnV	N	TAC	13875–13942	68			0	13860–13927	68			0
rrnS	N		13943–14751	809			0	13928–14740	813			0
OH	J		14752–16134	1383			0	14741–16142	1402			0

Table 3. Nucleotide composition of the mitogenomes of *Aeschrocoris tuberculatus* and *A. ceylonicus*.

A. tuberculatus								
Feature	**Length (bp)**	**A%**	**C%**	**G%**	**T%**	**A+T%**	**AT-skew**	**GC-skew**
Whole genome	16134	42.32	15.20	10.94	31.55	73.86	0.15	–0.16
PCGs	11036	32.63	13.54	13.37	40.46	73.09	–0.11	0.01
tRNA	1503	38.39	10.18	13.71	37.72	76.11	0.01	0.15
rRNA	2118	32.39	8.40	15.63	43.58	75.97	–0.15	0.30
Control region	1383	38.41	14.49	11.52	35.58	77.99	0.04	–0.11
A. ceylonicus								
Feature	**Length (bp)**	**A%**	**C%**	**G%**	**T%**	**A+T%**	**AT-skew**	**GC-skew**
Whole genome	16142	42.36	14.94	10.98	31.72	74.08	0.14	–0.15
PCGs	11040	32.40	13.65	13.56	40.39	72.79	–0.11	0.00
tRNA	1502	38.08	9.85	13.52	38.55	76.63	–0.01	0.16
rRNA	2115	32.77	8.32	15.08	43.83	76.60	–0.14	0.29
Control region	1402	39.40	12.58	10.06	37.96	77.35	0.02	–0.11

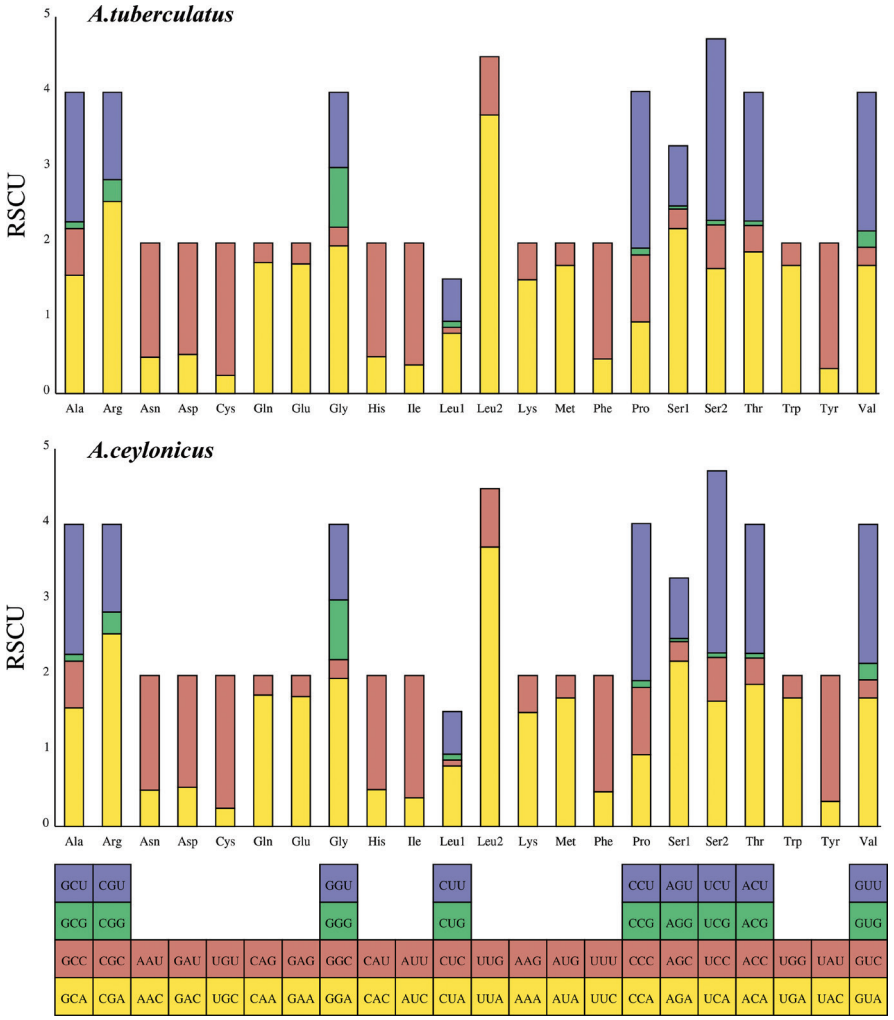

Figure 2. Relative synonymous codon usage (RSCU) within *Aeschrocoris tuberculatus* and *A. ceylonicus*. Codon families are shown on the *x*-axis and the frequency of RSCU on the *y*-axis.

Protein-coding genes

The length of PCGs in *A. tuberculatus* and *A. ceylonicus* is 11,036 bp and 11,040 bp, respectively. For the 13 PCGs, nine (*cox1*, *cox2*, *cox3*, *atp6*, *atp8*, *nad2*, *nad3*, *nad6*, and *cytb*) are encoded on the major strand (J-strand), whereas the other four are encoded on the minor strand (N-strand). The typical ATN (five with ATG, three with ATA, and two with ATT) are used as the start codon in most PCGs of these species, except for the *atp8*, *nad1*, and *cox1* genes, which use TTG as the start codon. *cox1*, *cox2*, and *atp6* sequences terminate with a single T, the terminal codon of *nad1* sequences is TAG, and the stop codon for the remaining genes was TAA.

In addition, we calculated non-synonymous substitutions (Ka), synonymous substitutions (Ks), and Ka/Ks ratios for the 13 PCGs of the Pentatomoidea (Fig. 3), and the evolutionary rates of the 13 PCGs are compared. The results clearly show that *atp8* evolved at the fastest rate (Ka/Ks = 0.75), *cox1* evolved at the slowest rate (Ka/Ks = 0.06), and the other genes evolved in the order of *nad6* > *nad2* > *nad4* > *nad5* > *nad4l* > *atp6* > *nad3* > *nad1* > *cox2* > *cox3* > *cytb*. Furthermore, all 13 PCGs have Ks values greater than Ka values and Ka/Ks ratios less than 1, indicating that these genes are affected by purifying selection.

Transfer and ribosomal RNAs

The total lengths of the tRNAs of *A. tuberculatus* and *A. ceylonicus* are 1,503 bp and 1,502 bp, respectively. And the length of tRNA genes are from 64 bp to 72 bp. Fourteen genes (*trnA*, *trnE*, *trnD*, *trnG*, *trnK*, *trnI*, *trnL2*, *trnM*, *trnN*, *trnR*, *trnS1*, *trnS2*,

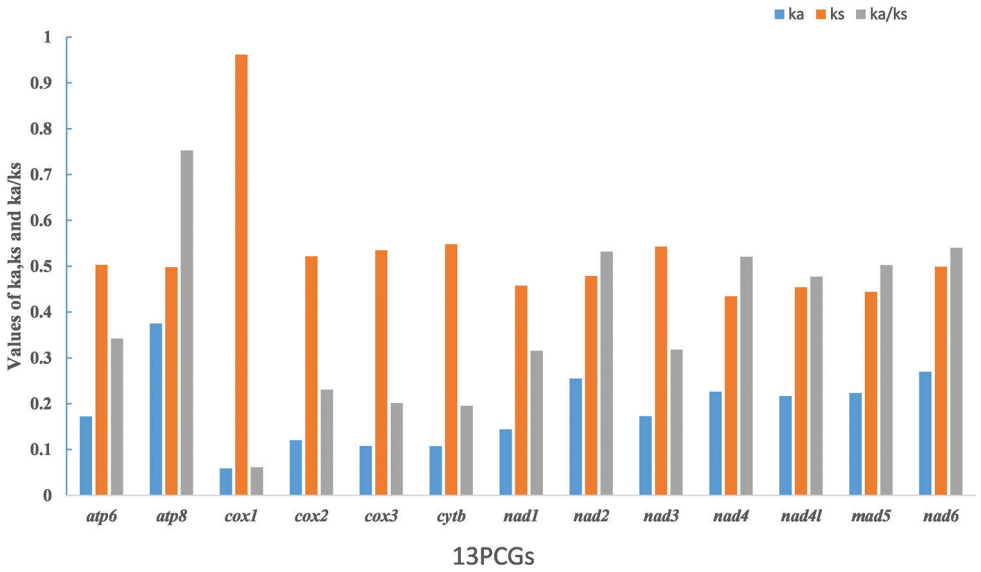

Figure 3. Evolutionary rates of 13 PCGs in Pentatomoidea. Rate of non-synonymous substitutions (Ka), rate of synonymous substitutions (Ks), and ratio of rate of non-synonymous substitutions to rate of synonymous substitutions (Ka/Ks) are calculated for each PCG.

trnT, and *trnW*) are located on the J-strand, and other eight genes on the N-strand. Only *trnS1* lacks a dihydrouridine (DHU) arm; the other tRNA genes all have the classic cloverleaf secondary structure. In addition to the typical base pairs (A-U and G-C), some wobble G-U pairs appear in these secondary structures, which can form stable chemical bonds between G and U (Fig. 4).

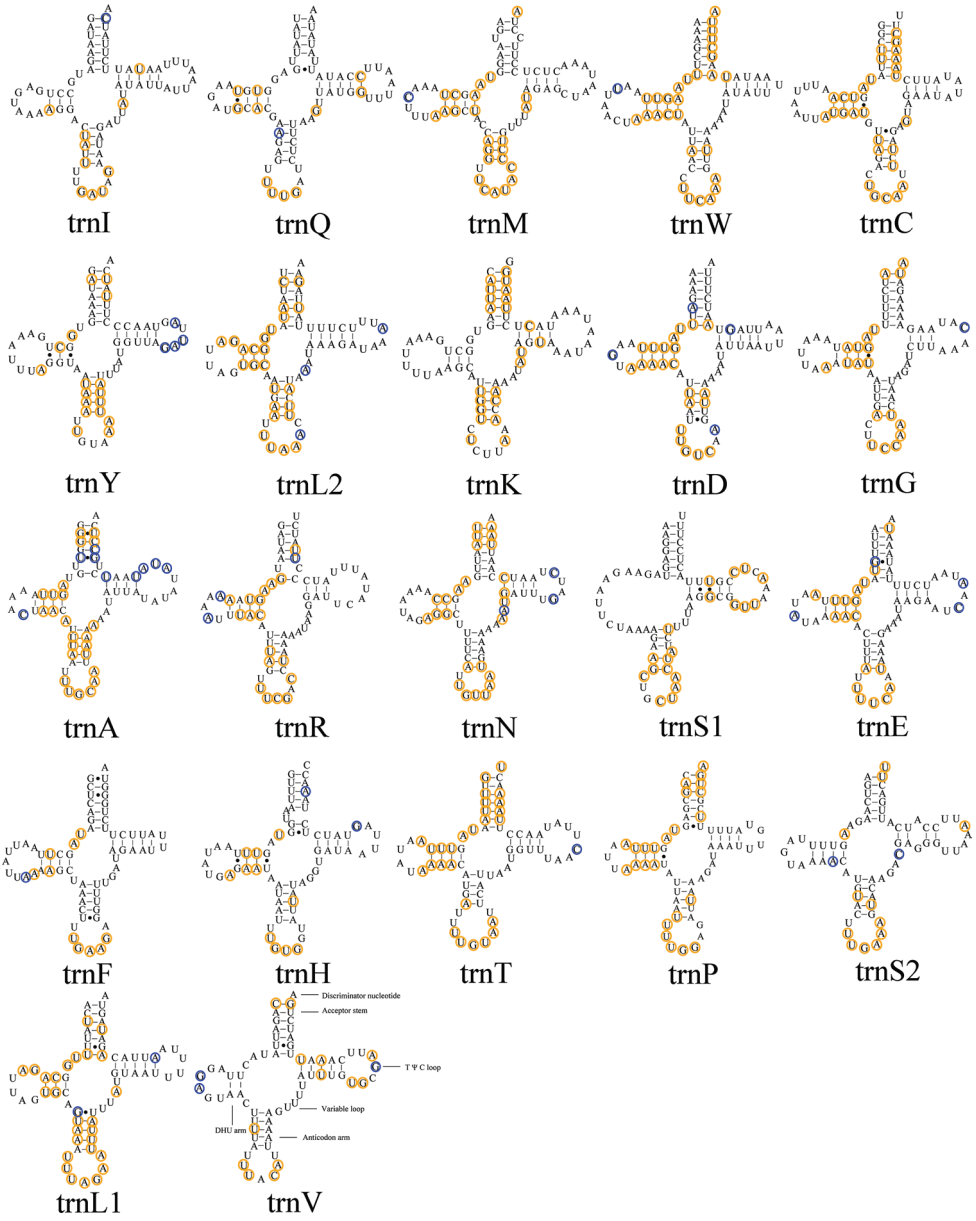

Figure 4. Predicted secondary structure of tRNA genes in *Aeschrocoris tuberculatus*. Conserved sites in Pentatomoidea are marked orange. Nonconserved sites in *A. tuberculatus* and *A. ceylonicus* are marked blue.

The *rrnL* and *rrnS* genes have the same situation in the two species. The *rrnL* gene is located between *trnL1* (CUN) and *trnV*, and the *rrnS* gene is located between *trnV* and the control region; they are encoded on the N-strand. The lengths of the two genes in *A. tuberculatus* are 1,309 bp (*rrnL*) and 809 bp (*rrnS*); the complete secondary structures are shown in Figs 5, 6. In *A. ceylonicus*, the two genes are 1,302 bp (*rrnL*) and 813 bp (*rrnS*) in length. The order of the base content of the rRNA genes is T (43.58%) > A (32.39%) > G (15.63%) > C (8.40%) and T (43.83%) > A (32.77%) > G (15.08%) > C (8.32%), respectively. The AT-skews are negative, and the GC-skews are positive.

The control region

The control is the main regulatory region for replication and transcription of the mitochondrial genome (Taanman 1999; Stewart and Beckenbach 2006; Cameron 2014). The variation in length of the control region is mainly caused by the lengths and numbers of repeating units. In conclusion, the sequence and structure of the mitochondrial control region is highly variable in Hemiptera (Moreno et al. 2010). The control region of *A. tuberculatus*, located between *rrnS* and *trnI* genes, is 1,383 bp in length, and the A + T content is 73.99%. The length of the control region of *A. ceylonicus*, at 1,402 bp, is similar to *A. tuberculatus*, and the A + T content is 77.35%. Moreover, both species have a variety of different tandem repeat units (Fig. 7).

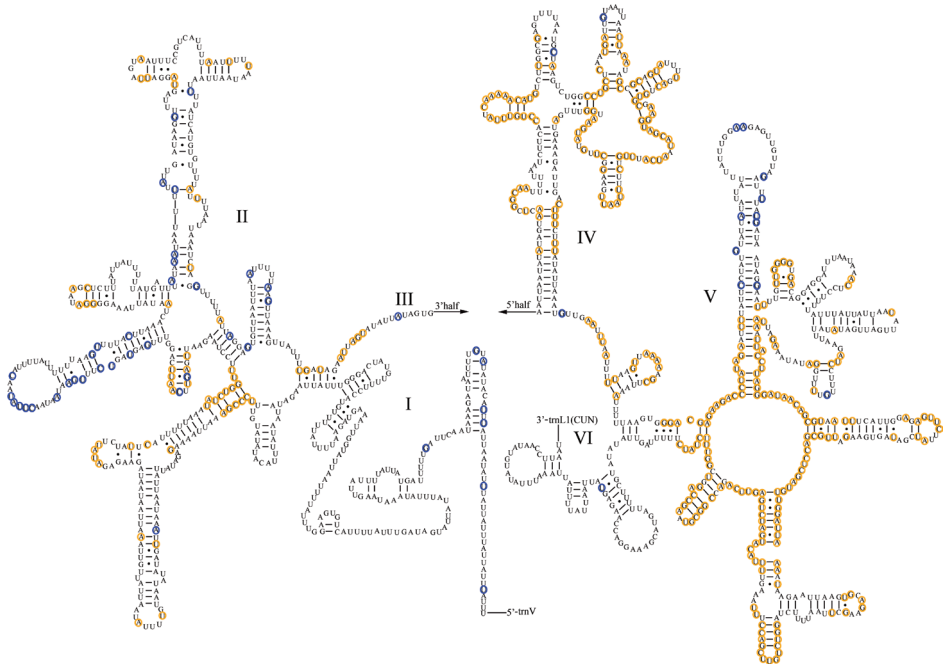

Figure 5. Predicted secondary structure of the *rrnL* in *Aeschrocoris tuberculatus*. Conserved sites in Pentatomoidea are marked orange. Nonconserved sites in *A. tuberculatus* and *A. ceylonicus* are marked blue.

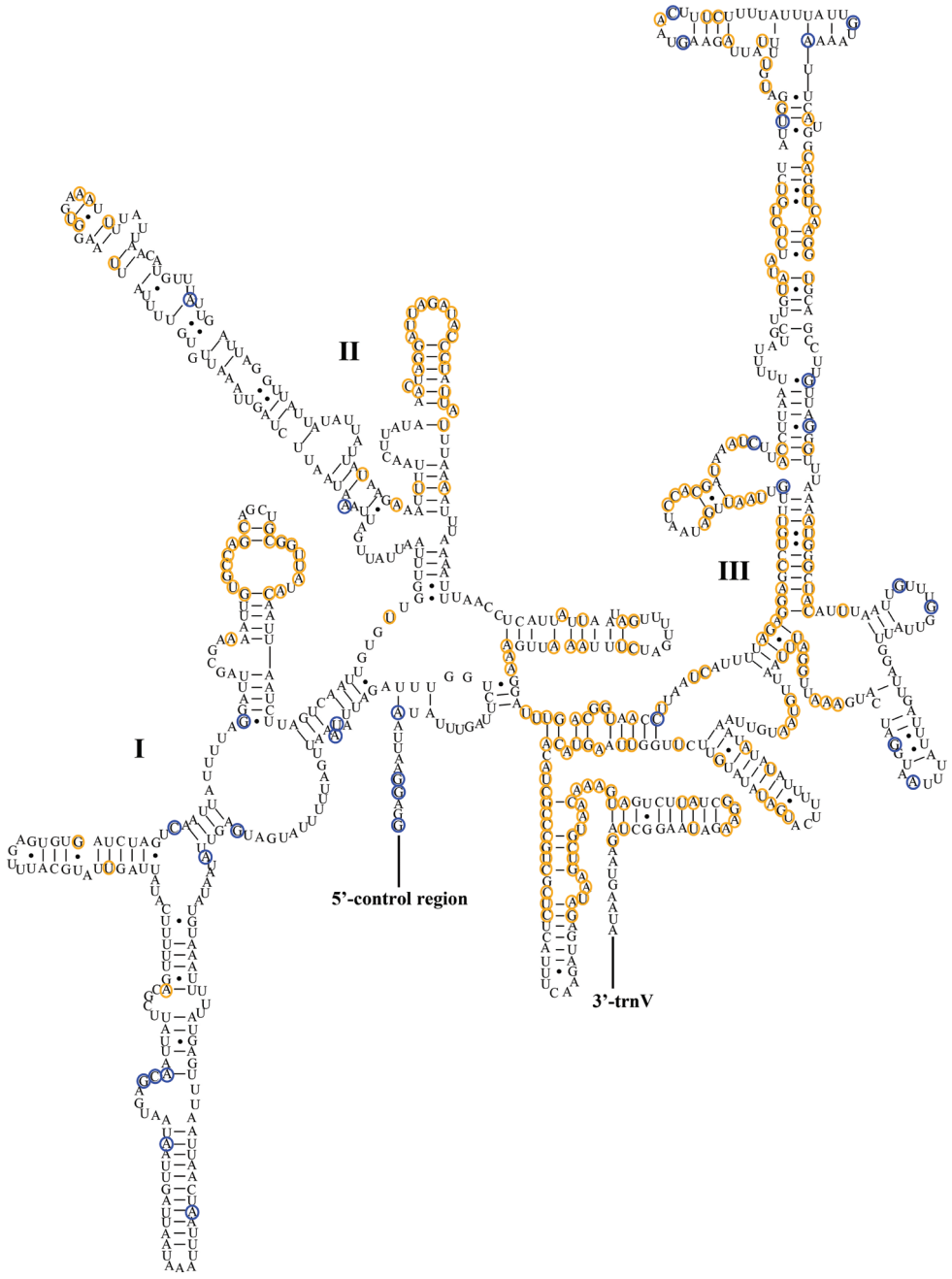

Figure 6. Predicted secondary structure of the *rrnS* in *Aeschrocoris tuberculatus*. Conserved sites in Pentatomoidea are marked orange. Nonconserved sites in *A. tuberculatus* and *A. ceylonicus* are marked blue.

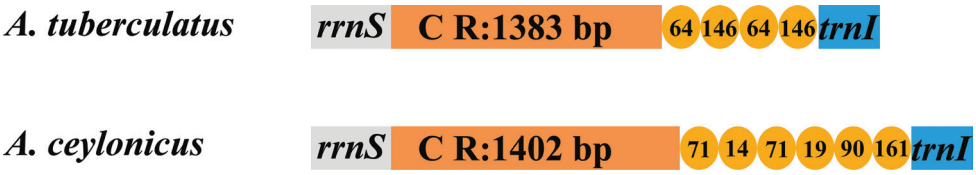

Figure 7. Organization of the control region in the mitochondrial genomes of *Aeschrocoris tuberculatus* and *A. ceylonicus*. The tandem repeats are shown by yellow ovals with repeat length inside. CR indicates the length of the sequence of the control region.

Tests of substitution saturation and heterogeneity

Before constructing the phylogenetic tree, we evaluated the substitution saturation of the PCG123 and PCG12 datasets. The results show that the Xia saturation index (Iss) is below the critical values for a symmetric (Iss.cSym) and asymmetric (Iss.cAsym) topology (Fig. 8). Meanwhile, the conversion rate and modified genetic distance both increase linearly, indicating that the nucleotide sequences of two datasets are not saturated.

Our analysis of the heterogeneity of the base composition in the two datasets show that the heterogeneity of PCG123 is higher than in PCG12, thus indicating a higher heterogeneity of the third site of the codon. The degree of heterogeneity between the two datasets is certainly consistent with the construction of a phylogenetic tree, which can be used for phylogenetic analysis (Fig. 9).

Phylogenetic analyses

We constructed phylogenetic trees of Pentatomoidea based on the two datasets using the ML method (Figs 10, 11). The results show that the topological structure of the tree is reliable. The relationship is as follows: (Urostylididae + ((Acanthosomatidae + ((Cydnidae + (Dinidoridae + Tessaratomidae)) + (Scutelleridae + Plataspidae))) + Pentatomidae)). All analyses also show that *A. tuberculatus* and *A. ceylonicus* are the earliest diverging lineage within Pentatomidae and cluster as a sister group. The monophyly of Pentatominae and Podopinae is rejected, as both are scattered within the Pentatomidae clade. However, we recovered the monophyly of Asopinae and Phyllocephalinae with strong support values and high internal node support values. The two subfamilies are nested in one of the Pentatominae clades, so the subfamilies of Pentatomidae need further research.

Discussion and conclusions

In this study, we sequenced and annotated the complete mitogenomes of *Aeschrocoris tuberculatus* and *A. ceylonicus* using NGS technology and Geneious v. 11.0. Our analysis comparing of the mitochondrial genomes of the two species show that the gene arrangement is highly conserved, which is consistent with other published mitochondrial genomes of Hemiptera (Hua et al. 2008; Lee et al. 2009; Song et al. 2013).

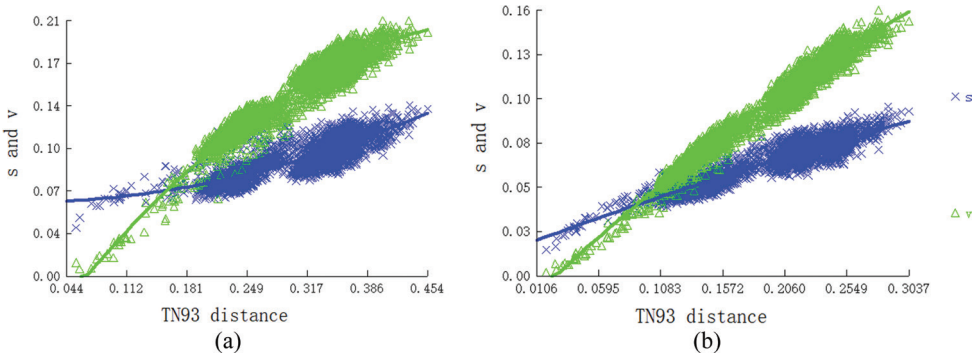

Figure 8. The substitution saturation analysis of two datasets **a** PCG123 **b** PCG12.

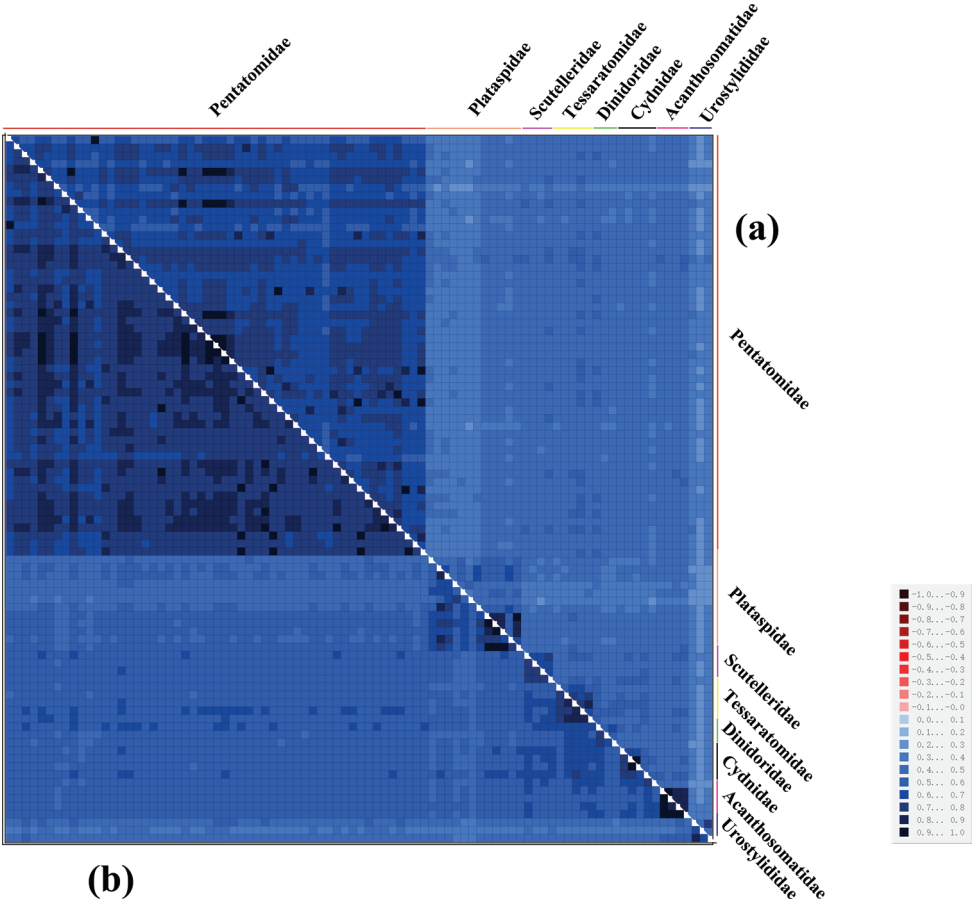

Figure 9. AliGROOVE analysis of 89 Pentatomoidea species **a** based on PCG123 **b** based on PCG12. The mean similarity score between sequences is represented by colored squares, based on AliGROOVE scores ranging from –1, which indicates a great difference in rates from the remainder of the data set (= heterogeneity, red color) to +1, which indicates rates that matched all other comparisons (blue color, as in this case).

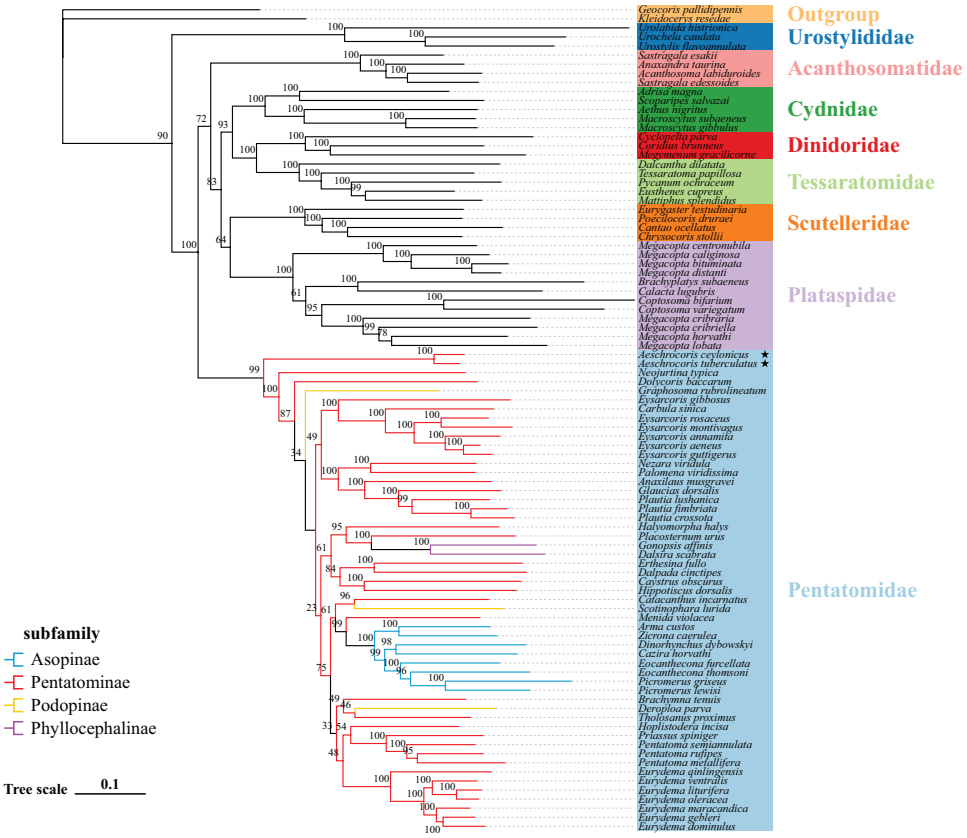

Figure 10. Phylogenetic tree using ML analyses based on PCG123. Numbers at the node are bootstrap values.

The lengths of the mitochondrial genomes of *A. tuberculatus* and *A. ceylonicus* are 16,134 bp and 16,142 bp, respectively. There were four overlapping regions in the mitochondrial genome of these two species. The positions of their overlapping regions re identical. One of the longest overlaps, located between *trnW* and *trnC*, is 8 bp in length, and the overlapping bases are AAGCTTTA, which is common in pentatomid species (Yuan et al. 2015; Zhao et al. 2019a). The other two pairs of genes, namely *atp8*/*atp6* and *nad4*/*nad4l*, overlap by 7 bp, and both overlapping bases are ATGATAA. Specifically, an overlap of 8 bp between *nad6* and *cytb* was also observed, and the overlapping bases are ATGAATAA. This is different from that found in previous studies on Pentatomidae. Between *trnS2* and *nad1*, the longest spacer region appeared in both, which is consistent with the findings of other studies (Hua et al. 2008; Zhao et al. 2019a). The difference of mitogenome size between *A. tuberculatus* and *A. ceylonicus* is due to the length difference of the noncoding region.

In most Pentatomidae mitochondrial genomes, only *cox1* has TTG as its start codon, and the remaining 12 PCGs use ATN as their start codon (Hua et al. 2008; Li et al. 2012). However, there is a difference between *A. tuberculatus* and *A. ceylonicus* in that

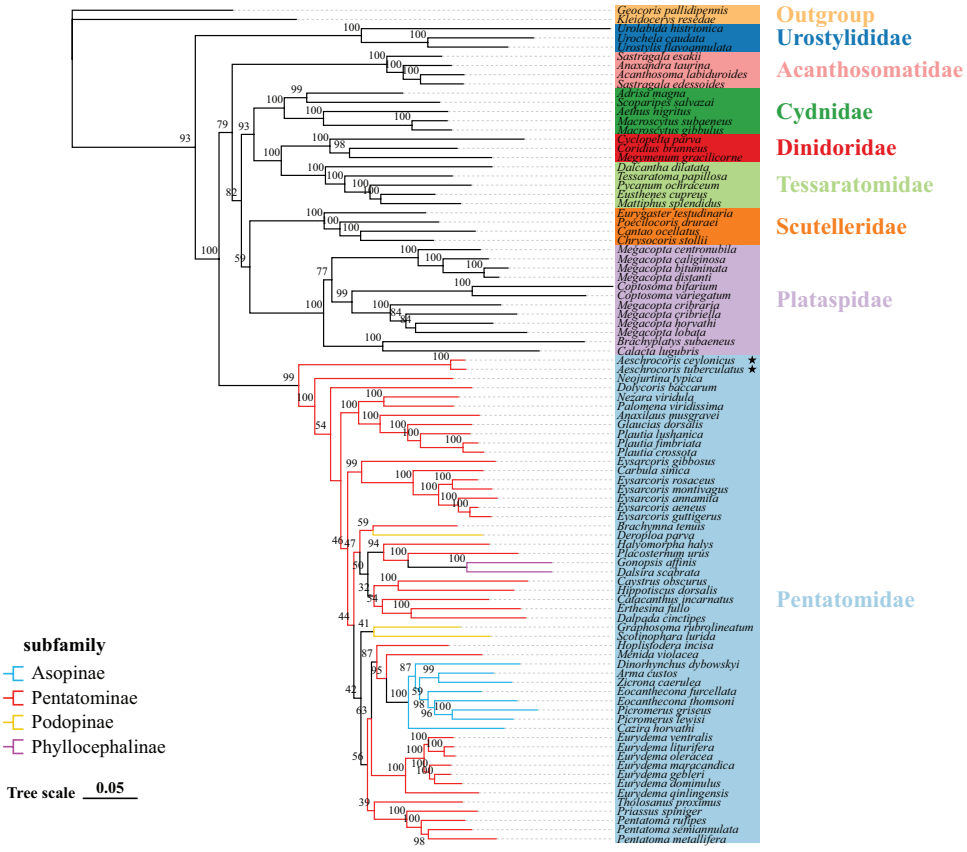

Figure 11. Phylogenetic tree using ML analyses based on PCG12. Numbers at the node are bootstrap values.

nine PCGs have the same start codons ATN, and four PCGs (*nad1*, *cox1*, *atp8*, and *nad6*) use TTG as the start codon. Most PCGs use the TAA as the stop codon; nevertheless, in some insects, *nad1*, *cox2*, and some other genes use the single T or TAG as the stop codon (Liu et al. 2012; Song et al. 2013). In this study, our results show most PCGs stop with TAA, and three PCGs (*cox1*, *cox2*, and *atp6*) stop with a single T. However, one PCG (*nad1*) stops with TAG. In PCGs, *cox1* is commonly used for barcode analysis and genus or species identification due to its slow rate of evolution (Hebert et al. 2004).

The composition of the four bases in *A. tuberculatus* and *A. ceylonicus* is A>T>C>G. There is a clear AT preference in nucleotide composition. Most tRNAs have the typical cloverleaf secondary structure as observed in Hemiptera. However, the lack of a DHU arm in the *trnS1* is common in hemipteran mitogenomes (Wolstenholme 1992; Shi et al. 2012). *rrnL* and *rrnS* in *A. tuberculatus* and *A. ceylonicus* lie between *trnL1* (CUN) and *trnV*, and between *trnV* and the control region, respectively. In Pentatomoidea, *rrnS* contains 19.37% conserved sites and included three domains. The *rrnL* contains 26.81% conserved sites and six domains (domain III is absent), and the IV and V domains are relatively conservative.

Through the topological structure of the trees, the clade including Urostylididae is found to be the earliest clade lineage. It forms a sister group to the other families. The relationship of (Cydnidae + (Dinidoridae + Tessaratomidae)) was recovered in our phylogenetic results with high support; these results are consistent with previous studies (Grazia et al. 2008; Yuan et al. 2015; Wu et al. 2018; Zhao et al. 2018; Xu et al. 2021). Xu et al. (2021) used PCGRNA and PCG12RNA data sets to recover the sister-group relationship of (Plataspidae + Scutelleridae) and (Dinidoridae + Tessaratomidae), and we also obtained this result. Of course, there are still other conclusions to be made based on the phylogenetic studies of Pentatomoidea. Previously, two sister groups (Plataspidae + Pentatomidae) and (Cydnidae + Scutelleridae) were recovered (Zhao et al. 2018; Liu et al. 2019). Possible reasons include, for example, the number of samples, the selection of outliers, the selection of data sets, and the influence of branches. In addition, the saturation and heterogeneity of the third site of PCG has little effect on the topological structure of the trees. In the study of Hemiptera insects, retention of the third site of PCG does not reduce the reliability of the phylogenetic results (Fenn et al. 2008). Although in many studies, the results obtained from different data sets and inference methods show that there are some contradictions among the relationships among families, our results based on more species have higher reliability. This study also confirms that adding more mitochondrial genome sequences is the key to solve the phylogenetic relationships of Pentatomoidea at various different taxonomic levels.

We studied the genus *Aeschrocoris* at a molecular level for the first time and preliminarily identified its taxonomic position and evolution in phylogenetic relationships. This study not only discusses the relationships among families, but it also adds new molecular data for Pentatomidae. These results demonstrate that mitochondrial genomes can effectively reveal the phylogenetic relationships among differing taxonomic hierarchies. We should sequence more mitochondrial genes to provide greater evidence for exploring the phylogenetic relationships among taxa.

Acknowledgements

This research was funded by the National Science Foundation Project of China (no. 31872272 and 32100370); the Research Project Supported by Shanxi Scholarship Council of China (no. 2020-064 and 2020-065), Natural Science Research General Project of Shanxi Province (No.202103021224331 and 202103021224132).

References

Ballard JWO, Whitlock MC (2004) The incomplete natural history of mitochondria. Molecular Ecology 13(4): 729–744. https://doi.org/10.1046/j.1365-294X.2003.02063.x

Bernt M, Donath A, Jühling F, Externbrink F, Florentz C, Fritzsch G, Pütz J, Middendorf M, Stadler PF (2013) MITOS: Improved de novo metazoan mitochondrial genome annotation. Molecular Phylogenetics and Evolution 69(2): 313–319. https://doi.org/10.1016/j.ympev.2012.08.023

Boore JL (1999) Animal mitochondrial genomes. Nucleic Acids Research 27(8): 1767–1780. https://doi.org/10.1093/nar/27.8.1767

Boore JL (2006) The use of genome-level characters for phylogenetic reconstruction. Trends in Ecology & Evolution 21(8): 439–446. https://doi.org/10.1016/j.tree.2006.05.009

Cachan P (1952) Les Pentatomidae de Madagascar (Hemipteres Heteropteres). Mémoires de l'Institut Scientifique de Madagascar (E) 1: 231–462.

Cameron SL (2014) Insect mitochondrial genomics: Implications for evolution and phylogeny. Annual Review of Entomology 59(1): 95–117. https://doi.org/10.1146/annurev-ento-011613-162007

Chen C, Wei J, Ji W, Zhao Q (2017) The first complete mitochondrial genome from the subfamily Phyllocephalinae (Heteroptera: Pentatomidae) and its phylogenetic analysis. Mitochondrial DNA. Part B, Resources 2(2): 938–939. https://doi.org/10.1080/23802359.2017.1413313

Chen Y, Chen Y, Shi C, Huang Z, Zhang Y, Li S, Li Y, Ye J, Yu C, Li Z, Zhang X, Wang J, Yang H, Fang L, Chen Q (2018) SOAPnuke: A MapReduce acceleration-supported software for integrated quality control and preprocessing of high-throughput sequencing data. GigaScience 7(1): gix120. https://doi.org/10.1093/gigascience/gix120

Chen D-B, Zhang R-S, Bian H-X, Li Q, Xia R-X, Li Y-P, Liu Y-Q, Lu C (2019) Comparative mitochondrial genomes provide new insights into the true wild progenitor and origin of domestic silkworm *Bombyx mori*. International Journal of Biological Macromolecules 131: 176–183. https://doi.org/10.1016/j.ijbiomac.2019.03.002

Chen Q, Niu X, Fang Z, Weng Q (2020) The complete mitochondrial genome of Eysarcoris guttigerus (Hemiptera: Pentatomidae). Mitochondrial DNA. Part B, Resources 5(1): 687–688. https://doi.org/10.1080/23802359.2020.1714498

De Clercq P, Peeters I, Vergauwe G, Thas O (2003) Interaction between *Podisus maculiventris* and *Harmonia axyridis* two predators used in augmentative biological control in greenhouse crops. BioControl 48(1): 39–55. https://doi.org/10.1023/A:1021219714684

Distant WL (1902) The Fauna of British India, Including Ceylon and Burma. In: Blanford WT (Ed.) Vol. 1. Heteroptera. Taylor & Francis, London, [xxxviii +] 438 pp.

Edgar RC (2004) MUSCLE: A multiple sequence alignment method with reduced time and space complexity. BMC Bioinformatics 5(1): 113. https://doi.org/10.1186/1471-2105-5-113

Fan ZH (2011) The Study on Systematics of Pentatominae from China (Hemiptera: Heteroptera: Pentatomidae). PhD, Nankai University, Tianjin.

Fenn JD, Song H, Cameron SL, Whiting MF (2008) A preliminary mitochondrial genome phylogeny of Orthoptera (Insecta) and approaches to maximizing phylogenetic signal found within mitochondrial genome data. Molecular Phylogenetics and Evolution 49(1): 59–68. https://doi.org/10.1016/j.ympev.2008.07.004

Grazia J, Schuh RT, Wheeler WC (2008) Phylogenetic relationships of family groups in Pentatomoidea based on morphology and DNA sequences (Insecta: Heteroptera). Cladistics 24(6): 932–976. https://doi.org/10.1111/j.1096-0031.2008.00224.x

Hassan M, Mukherjee P, Biswas B (2016) A new species of *Aeschrocoris* Bergroth (Hemiptera: Heteroptera: Pentatomidae: Pentatominae) from India. Munis Entomology & Zoology 11: 246–249.

Hassanin A, Leger N, Deutsch J (2005) Evidence for multiple reversals of asymmetric mutational constraints during the evolution of the mitochondrial genome of Metazoa, and consequences for phylogenetic inferences. Systematic Biology 54(2): 277–298. https://doi.org/10.1080/10635150590947843

Hebert PDN, Stoeckle MY, Zemlak TS, Francis CM (2004) Identification of birds through DNA barcodes. PLoS Biology 2(10): e312. https://doi.org/10.1371/journal.pbio.0020312

Hoang DT, Chernomor O, Von Haeseler A, Minh BQ, Vinh LS (2018) UFBoot2: Improving the ultrafast bootstrap approximation. Molecular Biology and Evolution 35(2): 518–522. https://doi.org/10.1093/molbev/msx281

Hua J, Li M, Dong P, Cui Y, Xie Q, Bu W (2008) Comparative and phylogenomic studies on the mitochondrial genomes of Pentatomomorpha (Insecta: Hemiptera: Heteroptera). BMC Genomics 9(1): 610. https://doi.org/10.1186/1471-2164-9-610

Ji H, Xu X, Jin X, Yin H, Luo J, Liu G, Zhao Q, Chen Z, Bu W, Gao S (2019) Using high-resolution annotation of insect mitochondrial DNA to decipher tandem repeats in the control region. RNA Biology 16(6): 830–837. https://doi.org/10.1080/15476286.2019.1591035

Jiang P (2017) Studies on the comparative mitochondrial genomics and phylogeny of Heteroptera (insecta: Hemiptera). PhD, China Agricultural University, Beijing.

Kalyaanamoorthy S, Minh BQ, Wong TK, Von Haeseler A, Jermiin LS (2017) ModelFinder: Fast model selection for accurate phylogenetic estimates. Nature Methods 14(6): 587–589. https://doi.org/10.1038/nmeth.4285

Kearse M, Moir R, Wilson A, Stones-Havas S, Cheung M, Sturrock S, Buxton S, Cooper A, Markowitz S, Duran C, Thierer T, Ashton B, Meintjes P, Drummond A (2012) Geneious Basic: An integrated and extendable desktop software platform for the organization and analysis of sequence data. Bioinformatics 28(12): 1647–1649. https://doi.org/10.1093/bioinformatics/bts199

Kück P, Meid SA, Groß C, Wägele JW, Misof B (2014) AliGROOVE–Visualization of heterogeneous sequence divergence within multiple sequence alignments and detection of inflated branch support. BMC Bioinformatics 15(1): 294. https://doi.org/10.1186/1471-2105-15-294

Lee W, Kang J, Jung C, Hoelmer K, Lee SH, Lee S (2009) Complete mitochondrial genome of brown marmorated stink bug *Halyomorpha halys* (Hemiptera: Pentatomidae), and phylogenetic relationships of hemipteran suborders. Molecules and Cells 28(3): 155–165. https://doi.org/10.1007/s10059-009-0125-9

Li H, Jiang P, Song F, Ye Z, Yuan X, Chang J, Cai W (2012) Sequence and organization of the mitochondrial genome of an urostylidid bug, *Urochela quadrinotata* Reuter (Hemiptera: Urostylididae). Entomotaxonomia 34: 613–623.

Li T, Yi W, Zhang H, Xie Q, Bu W (2016) Complete mitochondrial genome of the birch catkin bug *Kleidocerys resedae resedae*, as the first representative from the family Lygaeidae (Hemiptera: Heteroptera: Lygaeoidea). Mitochondrial DNA. Part A, DNA Mapping, Sequencing, and Analysis 27: 618–619. https://doi.org/10.3109/19401736.2014.908372

Li H, Leavengood Jr JM, Chapman EG, Burkhardt D, Song F, Jiang P, Liu J, Zhou X, Cai W (2017) Mitochondrial phylogenomics of Hemiptera reveals adaptive innovations driving the diversification of true bugs. Proceedings of the Royal Society B, Biological Sciences 284(1862): 20171223. https://doi.org/10.1098/rspb.2017.1223

Li R, Li M, Yan J, Bai M, Zhang H (2021) Five mitochondrial genomes of the genus *Eysarcoris* Hahn, 1834 with phylogenetic implications for the Pentatominae (Hemiptera: Pentatomidae). Insects 12(7): 597. https://doi.org/10.3390/insects12070597

Liu L, Li H, Song F, Song W, Dai X, Chang J, Cai W (2012) The mitochondrial genome of *Coridius chinensis* (Hemiptera: Dinidoridae). Zootaxa 3537(1): 29–40. https://doi.org/10.11646/zootaxa.3537.1.2

Liu Y, Li H, Song F, Zhao Y, Wilson JJ, Cai W (2019) Higher-level phylogeny and evolutionary history of Pentatomomorpha (Hemiptera: Heteroptera) inferred from mitochondrial genome sequences. Systematic Entomology 44(4): 810–819. https://doi.org/10.1111/syen.12357

Lowe TM, Eddy SR (1997) tRNAscan-SE: A program for improved detection of transfer RNA genes in genomic sequence. Nucleic Acids Research 25(5): 955–964. https://doi.org/10.1093/nar/25.5.955

Mardis E, McCombie WR (2017) Library quantification: fluorometric quantitation of double-stranded or single-stranded DNA samples using the qubit system. Cold Spring Harbor Protocols 2017: pdb.prot094730. https://doi.org/10.1101/pdb.prot094730

Moreno M, Marinotti O, Krzywinski J, Tadei WP, James AA, Achee NL, Conn JE (2010) Complete mtDNA genomes of *Anopheles darlingi* and an approach to anopheline divergence time. Malaria Journal 9(1): 127. https://doi.org/10.1186/1475-2875-9-127

Mu Y-L, Zhang C-H, Zhang Y-J, Yang L, Chen X-S (2022) Characterizing the complete mitochondrial genome of *Arma custos* and *Picromerus lewisi* (Hemiptera: Pentatomidae: Asopinae) and conducting phylogenetic analysis. Journal of Insect Science 22(1): 6. https://doi.org/10.1093/jisesa/ieab105

Nguyen L-T, Schmidt HA, Von Haeseler A, Minh BQ (2015) IQ-TREE: A fast and effective stochastic algorithm for estimating maximum-likelihood phylogenies. Molecular Biology and Evolution 32(1): 268–274. https://doi.org/10.1093/molbev/msu300

Perna NT, Kocher TD (1995) Patterns of nucleotide composition at fourfold degenerate sites of animal mitochondrial genomes. Journal of Molecular Evolution 41(3): 353–358. https://doi.org/10.1007/BF01215182

Rider DA, Schwertner CF, Vilímová J, Rédei D, Kment P, Thomas DB (2018) Higher systematics of the Pentatomoidea. In: McPherson JE (Ed.) Invasive Stink Bugs and Related Species (Pentatomoidea): Biology, Higher Systematics, Semiochemistry, and Management. CRC Press, Boca Raton, 25–204. https://doi.org/10.1201/9781315371221-2

Rozas J, Ferrer-Mata A, Sánchez-DelBarrio JC, Guirao-Rico S, Librado P, Ramos-Onsins SE, Sánchez-Gracia A (2017) DnaSP 6: DNA sequence polymorphism analysis of large data sets. Molecular Biology and Evolution 34(12): 3299–3302. https://doi.org/10.1093/molbev/msx248

Shi A, Li H, Bai X, Dai X, Chang J, Guilbert E, Cai W (2012) The complete mitochondrial genome of the flat bug *Aradacanthia heissi* (Hemiptera: Aradidae). Zootaxa 3238(1): 23–38. https://doi.org/10.11646/zootaxa.3238.1.2

Simon S, Hadrys H (2013) A comparative analysis of complete mitochondrial genomes among Hexapoda. Molecular Phylogenetics and Evolution 69(2): 393–403. https://doi.org/10.1016/j.ympev.2013.03.033

Simon C, Frati F, Beckenbach A, Crespi B, Liu H, Flook P (1994) Evolution, weighting, and phylogenetic utility of mitochondrial gene sequences and a compilation of conserved poly-

merase chain reaction primers. Annals of the Entomological Society of America 87(6): 651–701. https://doi.org/10.1093/aesa/87.6.651

Simon C, Buckley TR, Frati F, Stewart JB, Beckenbach AT (2006) Incorporating molecular evolution into phylogenetic analysis, and a new compilation of conserved polymerase chain reaction primers for animal mitochondrial DNA. Annual Review of Ecology, Evolution, and Systematics 37(1): 545–579. https://doi.org/10.1146/annurev.ecolsys.37.091305.110018

Song W, Li H, Song F, Liu L, Wang P, Xun H, Dai X, Chang J, Cai W (2013) The complete mitochondrial genome of a tessaratomid bug, *Eusthenes cupreus* (Hemiptera: Heteroptera: Pentatomomorpha: Tessaratomidae). Zootaxa 3620(2): 260–272. https://doi.org/10.11646/zootaxa.3620.2.4

Stewart J, Beckenbach A (2006) The complete mitochondrial genome sequence of a giant stonefly, *Pteronarcys princeps*, asymmetric directional mutation bias, and conserved plecopteran A+ T-region elements. Genome 49(7): 815–824. https://doi.org/10.1139/g06-037

Taanman J-W (1999) The mitochondrial genome: Structure, transcription, translation and replication. Biochimica et Biophysica Acta (BBA) –. Bioenergetics 1410(2): 103–123. https://doi.org/10.1016/S0005-2728(98)00161-3

Tamura K, Stecher G, Kumar S (2021) MEGA11: Molecular Evolutionary Genetics Analysis version 11. Molecular Biology and Evolution 38(7): 3022–3027. https://doi.org/10.1093/molbev/msab120

Wang J, Zhang L, Yang X-Z, Zhou M-Q, Yuan M-L (2017) The first mitochondrial genome for the subfamily Podopinae (Hemiptera: Pentatomidae) and its phylogenetic implications. Mitochondrial DNA. Part B, Resources 2(1): 219–220. https://doi.org/10.1080/23802359.2017.1310605

Wang Y, Duan Y, Yang X (2019) The complete mitochondrial genome of *Plautia crossota* (Hemiptera: Pentatomidae). Mitochondrial DNA. Part B, Resources 4(2): 2281–2282. https://doi.org/10.1080/23802359.2019.1627924

Wang Y-C, Li G-L, Liu X-Y, He Q-J, Yi C-H, Yang C, Zhu E-J (2021) The complete mitochondrial genome of *Pycanum ochraceum* Distant, 1893 (Hemiptera: Tessaratomidae). Mitochondrial DNA, Part B, Resources 6(12): 3383–3385. https://doi.org/10.1080/23802359.2021.1997659

Wolstenholme DR (1992) Animal mitochondrial DNA: Structure and evolution. International Review of Cytology 141: 173–216. https://doi.org/10.1016/S0074-7696(08)62066-5

Wu YZ, Rédei D, Eger Jr J, Wang YH, Wu HY, Carapezza A, Kment P, Cai B, Sun XY, Guo PL, Luo J-Y, Xie Q (2018) Phylogeny and the colourful history of jewel bugs (Insecta: Hemiptera: Scutelleridae). Cladistics 34(5): 502–516. https://doi.org/10.1111/cla.12224

Wu Y, Yang H, Zhou W, Song F, Cai W, Li H (2020) Characterization of the complete mitochondrial genome of *Arma custos* (Hemiptera: Pentatomidae). Mitochondrial DNA. Part B, Resources 5(3): 2624–2626. https://doi.org/10.1080/23802359.2020.1780985

Xia X, Lemey P (2009) Assessing substitution saturation with DAMBE. In: Lemey P, Salemi M, Vandamme AM (Eds) The Phylogenetic Handbook: a Practical Approach to DNA and Protein Phylogeny. 2nd edn. Cambridge University Press, Cambridge, 615–630. https://doi.org/10.1017/CBO9780511819049.022

Xia X, Xie Z (2001) DAMBE: Software package for data analysis in molecular biology and evolution. The Journal of Heredity 92(4): 371–373. https://doi.org/10.1093/jhered/92.4.371

Xu S, Wu Y, Cai W, Song F (2020) The complete mitochondrial genome of the lychee stinkbug *Mattiphus splendidus* (Hemiptera: Tessaratomidae). Mitochondrial DNA, Part B, Resources 5(1): 321–322. https://doi.org/10.1080/23802359.2019.1703609

Xu S, Wu Y, Liu Y, Zhao P, Chen Z, Song F, Li H, Cai W (2021) Comparative mitogenomics and phylogenetic analyses of Pentatomoidea (Hemiptera: Heteroptera). Genes 12(9): 1306. https://doi.org/10.3390/genes12091306

Yuan M-L, Zhang Q-L, Guo Z-L, Wang J, Shen Y-Y (2015) Comparative mitogenomic analysis of the superfamily Pentatomoidea (Insecta: Hemiptera: Heteroptera) and phylogenetic implications. BMC Genomics 16(1): 460. https://doi.org/10.1186/s12864-015-1679-x

Yuan L, Liu H, Ge X, Yang G, Xie G, Yang Y (2022) A mitochondrial genome phylogeny of cleridae (Coleoptera, cleroidea). Insects 13(2): 118. https://doi.org/10.3390/insects13020118

Zhang Q-L, Yuan M-L, Shen Y-Y (2013) The complete mitochondrial genome of *Dolycoris baccarum* (Insecta: Hemiptera: Pentatomidae). Mitochondrial DNA 24(5): 469–471. https://doi.org/10.3109/19401736.2013.766182

Zhao Q, Wei J, Zhao W, Cai B, Du X, Zhang H (2017a) The first mitochondrial genome for the subfamily Asopinae (Heteroptera: Pentatomidae) and its phylogenetic implications. Mitochondrial DNA, Part B, Resources 2(2): 804–805. https://doi.org/10.1080/23802359.2017.1398599

Zhao W, Zhao Q, Li M, Wei J, Zhang X, Zhang H (2017b) Characterization of the complete mitochondrial genome and phylogenetic implications for *Eurydema maracandica* (Hemiptera: Pentatomidae). Mitochondrial DNA, Part B, Resources 2(2): 550–551. https://doi.org/10.1080/23802359.2017.1365649

Zhao Q, Wang J, Wang M-Q, Cai B, Zhang H-F, Wei J-F (2018) Complete mitochondrial genome of *Dinorhynchus dybowskyi* (Hemiptera: Pentatomidae: Asopinae) and phylogenetic analysis of Pentatomomorpha species. Journal of Insect Science 18(2): 44. https://doi.org/10.1093/jisesa/iey031

Zhao Q, Chen C, Liu J, Wei J (2019a) Characterization of the complete mitochondrial genome of *Eysarcoris aeneus* (Heteroptera: Pentatomidae), with its phylogenetic analysis. Mitochondrial DNA, Part B, Resources 4(2): 2096–2097. https://doi.org/10.1080/23802359.2019.1622465

Zhao W, Zhao Q, Li M, Wei J, Zhang X, Zhang H (2019b) Comparative mitogenomic analysis of the *Eurydema* genus in the context of representative Pentatomidae (Hemiptera: Heteroptera) taxa. Journal of Insect Science 19(6): 20. https://doi.org/10.1093/jisesa/iez122

Zhao Q, Cassis G, Zhao L, He Y, Zhang H, Wei J (2020) The complete mitochondrial genome of *Zicrona caerulea* (Linnaeus) (Hemiptera: Pentatomidae: Asopinae) and its phylogenetic implications. Zootaxa 4747(3): 547–561. https://doi.org/10.11646/zootaxa.4747.3.8

Zhao L, Wei J, Zhao W, Chen C, Gao X, Zhao Q (2021) The complete mitochondrial genome of *Pentatoma rufipes* (Hemiptera, Pentatomidae) and its phylogenetic implications. ZooKeys 1042: 51–72. https://doi.org/10.3897/zookeys.1042.62302

Zhu X, Zheng C, Dong X, Zhang H, Ye Z, Xue H, Bu W (2022) Species boundary and phylogeographical pattern provide new insights into the management efforts of *Megacopta cribraria* (Hemiptera: Plataspidae), a bean bug invading North America. Pest Management Science 78(11): 4871–4881. https://doi.org/10.1002/ps.7108

ZooKeys 1160: 169–190 (2023)
doi: 10.3897/zookeys.1160.101594
https://zookeys.pensoft.net

RESEARCH ARTICLE

A peer-reviewed open-access journal
ZooKeys
Launched to accelerate biodiversity research

On four new species of the orb-weaver spider genus *Araneus* Clerck, 1757 (Araneae, Araneidae) from southern China

Yibei Wu[1], Cheng Wang[1], Nanfei Wu[2], Mengfei Zhang[2], Xiaoqi Mi[1]

1 *College of Agriculture and Forestry Engineering and Planning, Guizhou Provincial Key Laboratory of Biodiversity Conservation and Utilization in the Fanjing Mountain Region, Tongren University, Tongren 554300, Guizhou, China* **2** *Central South Inventory and Planning Institute of National Forestry and Grassland Administration, Changsha, Hunan 410014, China*

Corresponding author: Xiaoqi Mi (mixiaoqi1018@163.com)

Academic editor: Sarah Crews | Received 7 February 2023 | Accepted 19 April 2023 | Published 9 May 2023

https://zoobank.org/25047ED1-4915-4DC4-AF72-3FD0BA7CDB5D

Citation: Wu Y, Wang C, Wu N, Zhang M, Mi X (2023) On four new species of the orb-weaver spider genus *Araneus* Clerck, 1757 (Araneae, Araneidae) from southern China. ZooKeys 1160: 169–190. https://doi.org/10.3897/zookeys.1160.101594

Abstract

Four new species of *Araneus* Clerck, 1757 from southern China are described: *A. mayanghe* Mi & Wang, **sp. nov.** (♂♀) from Guizhou, *A. shiwandashan* Mi & Wang, **sp. nov.** (♂♀) from Guangxi, and *A. zhoui* Mi & Wang, **sp. nov.** (♂♀) from Hainan are assigned to the *A. sturmi* group, and *A. fenzhi* Mi & Wang, **sp. nov.** (♂♀) from Hunan, Guizhou and Jiangxi is not assigned to any species group. A new combination is also proposed: *Aoaraneus octumaculalus* (Han & Zhu, 2010) **comb. nov.**

Keywords

Arachnida, biodiversity, diagnosis, morphology, new combination, taxonomy

Introduction

Araneidae is the third most speciose family in the order Araneae, and 3119 species in 188 genera are known worldwide, of which 437 species in 54 genera have been recorded from China (WSC 2023). Data on the family in China is far from complete. For example, ongoing surveys of Araneidae from Xishuangbanna Tropical Botanical Garden in Yunnan Province, southwestern China has produced more than 120 species and about two-fifths are new to science (Mi and Li 2021a, b, 2022).

As the largest genus of the family, *Araneus* Clerck, 1757 includes 555 species worldwide (WSC 2023), and for centuries it has been a dumping ground for araneid species, making it polyphyletic, as shown by the multi-gene phylogenetic analysis of Scharff et al. (2020).

A comprehensive study of Chinese *Araneus* species was conducted by Yin et al. (1997), and a total of 79 *Araneus* species were described and illustrated. Fifteen Chinese *Araneus* species published before 1997 were not included: *A. anjonensis* Schenkel, 1963, *A. basalteus* Schenkel, 1936, *A. fengshanensis* Zhu & Song, 1994, *A. haruspex* (O. Pickard-Cambridge, 1885), *A. loczyanus* (Lendl, 1898), *A. mangarevoides* (Bösenberg & Strand, 1906), *A. metellus* (Strand, 1907), *A. paitaensis* Schenkel, 1953, *A. pecuensis* (Karsch, 1881), *A. pseudoconicus* Schenkel, 1936, *A. roseomaculatus* Ono, 1992, *A. scutellatus* Schenkel, 1963, *A. transversivittiger* (Strand, 1907), *A. triangulus* (Fox, 1938), and *A. zygielloides* Schenkel, 1963. Since then, 35 new species and a new record of the genus *Araneus* have been reported (Zhu et al. 1998, 2005; Hu 2001; Zhang and Zhang 2002; Zhang et al. 2006; Yin et al. 2007, 2009; Han and Zhu 2010; Guo et al. 2011; Zhou et al. 2017; Liu et al. 2019, 2022; Mi and Li 2022). To date, including generic changes of 11 species (*A. acusisetus* Zhu & Song, 1994, *A. baotianmanensis* Hu, Wang & Wang, 1991, *A. henanensis* (Hu, Wang & Wang, 1991), *A. himalayaensis* Tikader, 1975, *A. inustus* (L. Koch, 1871), *A. mitificus* (Simon, 1886), *A. nigromaculatus* Schenkel, 1963, *A. nympha* (Simon, 1889), *A. pentagrammicus* (Karsch, 1879), *A. pineus* Yin, Wang, Xie & Peng, 1990, and *A. pseudocentrodes* Bösenberg & Strand, 1906 were transferred from *Araneus* to other genera), a total of 118 *Araneus* species have been recorded in China.

Yin et al. (1997) placed 69 *Araneus* species into six species groups (Table 1). The following 10 species were not assigned to any of the above groups because original descriptions were too simple and/or illustrations not clear enough: *A. badiofoliatus* Schenkel, 1963, *A. badongensis* Song & Zhu, 1992, *A. decentellus* Strand, 1907, *A. diffinis* Zhu, Tu & Hu, 1988, *A. doenitzellus* Strand, 1906, *A. hetian* Hu & Wu, 1989, *A. nigromaculatus*, *A. pavlovi* Schenkel, 1953, *A. pichoni* Schenkel, 1963, and *A. virgus* (Fox, 1938).

While examining the Araneidae specimens collected in several national nature reserves in southern China, four new species of *Araneus* are identified, and they are described in this paper.

Table 1. Yin et al.'s (1997) grouping of 69 *Araneus* species.

Species group	Included species
A. dehaani group	*A. dehaani* (Doleschall, 1859), *A. albomaculatus* Yin, Wang, Xie & Peng, 1990 and *A. shunhuangensis* Yin, Wang, Xie & Peng, 1990
A. ejusmodi group	*A. cercidius* Yin, Wang, Xie & Peng, 1990, *A. ejusmodi* Bösenberg & Strand, 1906, *A. elongatus* Yin, Wang & Xie, 1989, *A. inustus*, *A. mitificus*, *A. pseudocentrodes*, *A. tengxianensis* Zhu & Zhang, 1994 and *A. viridiventris* Yaginuma, 1969
A. sturmi group	*A. acusisetus*, *A. auriculatus* Song & Zhu, 1992, *A. circellus* Song & Zhu, 1992, *A. colubrinus* Song & Zhu, 1992, *A. dayongensis* Yin, Wang, Xie & Peng, 1990, *A. nympha*, *A. octodentalis* Song & Zhu, 1992, *A. pseudosturmii* Yin, Wang, Xie & Peng, 1990, *A. sturmi* (Hahn, 1831), *A. vermimaculatus* Zhu & Wang, 1994, *A. viperifer* Schenkel, 1963, *A. wulongensis* Song & Zhu, 1992 and *A. yuanminensis* Yin, Wang, Xie & Peng, 1990
A. diadematus group	*A. affinis* Zhu, Tu & Hu, 1988, *A. aksuensis* Yin, Xie & Bao, 1996, *A. ancurus* Zhu, Tu & Hu, 1988, *A. angulatus* Clerck, 1757, *A. baotianmanensis*, *A. beijiangensis* Hu & Wu, 1989, *A. bicavus* Zhu & Wang, 1994, *A. biprominens* Yin, Wang & Xie, 1989, *A. boesenbergi* (Fox, 1938), *A. chunhuaia* Zhu, Tu & Hu, 1988, *A. circumbasilaris* Yin, Wang, Xie & Peng, 1990, *A. diadematoides* Zhu, Tu & Hu, 1988, *A. diadematus* Clerck, 1757, *A. flagelliformis* Zhu & Yin, 1998, *A. flavidus* Yin, Wang, Xie & Peng, 1990, *A. gratiolus* Yin, Wang, Xie & Peng, 1990, *A. guandishanensis* Zhu, Tu & Hu, 1988, *A. himalayaensis*, *A. licenti* Schenkel, 1953, *A. linshuensis* Yin, Wang, Xie & Peng, 1990, *A. marmoreus* Clerck, 1757, *A. marmoroides* Schenkel, 1953, *A. motuoensis* Yin, Wang, Xie & Peng, 1990, *A. nidus* Yin & Gong, 1996, *A. pahalgaonensis* Tikader & Bal, 1981, *A. pentagrammicus*, *A. pinguis* (Karsch, 1879), *A. taigunensis* Zhu, Tu & Hu, 1988, *A. tetraspinulus* (Yin, Wang, Xie & Peng, 1990), *A. tubabdominus* Zhu & Zhang, 1993, *A. tsuno* Yaginuma, 1972, *A. xianfengensis* Song & Zhu, 1992 and *A. zebrinus* Zhu & Wang, 1994
A. vermimaculatus group	*A. menglunensis* (Yin, Wang, Xie & Peng, 1990), *A. miquanensis* Yin, Wang, Xie & Peng, 1990, *A. pineus*, *A. pseudoventricosus*, *A. tartaricus* (Kroneberg, 1875), *A. tenerius* Yin, Wang, Xie & Peng, 1990, *A. tricoloratus* Zhu, Tu & Hu, 1988, *A. variegatus* Yaginuma, 1960, *A. ventricosus* (L. Koch, 1878) and *A. yuzhongensis* Yin, Wang, Xie & Peng, 1990
A. henanensis group	*A. henanensis* and *A. yunnanensis* Yin, Peng & Wang, 1994

Materials and methods

All specimens were collected by beating shrubs or by hand and are preserved in 75% ethanol. Type specimens of the new species are deposited in the Museum of Tongren University, China (**TRU**). The specimens were examined with an Olympus SZX16 stereomicroscope. The epigynes were cleared in lactic acid for examination and imaging. The left male pedipalp was dissected in ethanol for examination, description, and imaging. Photographs of the habitus and copulatory organs were taken with a Kuy Nice digital camera mounted on an Olympus BX43 compound microscope. Compound focus images were generated using Helicon Focus v. 6.7.1. The paths of the left copulatory ducts were drawn using Adobe Illustrator CC 2018.

All measurements are given in millimeters. Leg measurements are given as total length (femur, patella + tibia, metatarsus, tarsus). Abbreviations used in the text and figures are as follows: **ALE** anterior lateral eye; **AME** anterior median eye; **C** conductor; **CD** copulatory duct; **CO** copulatory opening; **E** embolus; **EL** embolic lamella; **ET** embolic tooth; **FD** fertilization duct; **MA** median apophysis; **MOA** median ocular area; **PLE** posterior lateral eye; **PME** posterior median eye; **Sc** scape; **Sp** spermatheca; **ST** subterminal apophysis; **TA** terminal apophysis.

Taxonomy

Family Araneidae Clerck, 1757

Genus *Araneus* Clerck, 1757

Araneus Clerck, 1757: 22.

Type species. *Araneus angulatus* Clerck, 1757.

Comments. Although the four new species are different from the generotype *A. angulatus* in thier smaller body size and having the abdomen lacking a pair of anterolateral humps, the epigynal base not elongated, and a shorter scape which does not extend far beyond the epigastric furrow, we provisionally place them in this genus because they share a very similar habitus and copulatory organs with other *Araneus* species. There is no doubt that their generic position needs confirmation, but it is not discussed here due to limited evidence.

Araneus fenzhi Mi & Wang, sp. nov.

https://zoobank.org/4F58C4BE-5F33-44A6-BD75-3233B75D7E48
Figs 1, 2, 9A–D, 10

Type material. ***Holotype*** ♂ (TRU-Araneidae-136), China: Hunan Province, Shaoyang City, Suining County, Zhaishi Township, Huangsang National Nature Reserve (26°23.51'N, 110°9.56'E, ca 1620 m), 11.VII.2022, X.Q. Mi & C. Wang leg. ***Paratypes*****:** 1♂2♀ (TRU-Araneidae-137–139), same data as for holotype; 2♂4♀ (TRU-Araneidae-140–145), Guizhou Province, Qiandongnan Miao and Dong Autonomous Prefecture, Leishan County, Danjiang Township, Leigongshan National Nature Reserve (26°22.99'N, 108°12.08'E, ca 1990 m), 20.VII.2017, C. Wang et al. leg.; 1♂ (TRU-Araneidae-146), Jiangxi Province, Ji'an City, Anfu County, Taishan Township, Wugongshan (27°27.50'N, 114°10.08'E, ca 1270 m), 23.VI.2022, Z.G. Huang et al. leg.

Etymology. The specific name is derived from the Chinese pinyin "fenzhi", meaning branched, referring to the threadlike branch of the embolus.

Diagnosis. The new species resembles *A. albabdominalis* Zhu, Zhang, Zhang & Chen, 2005 in having pale green coloration in life and a similar shape of the median apophysis and conductor, but it can be distinguished as follows: 1) epigyne scape not twisted into an S-shape vs S-shaped (Zhu et al. 2005: fig. 3B); 2) copulatory openings wedge-shaped in ventral view vs round (Zhu et al. 2005: fig. 3B); 3) embolus of male pedipalp U-shaped in prolateral view vs straight (Zhu et al. 2005: fig. 3D); 4) the branch on the embolus is threadlike vs lamellar (Zhu et al. 2005: fig. 3D); and 5) carapace unicolor vs with a pair of lateral longitudinal patches (Zhu et al. 2005: fig. 3A).

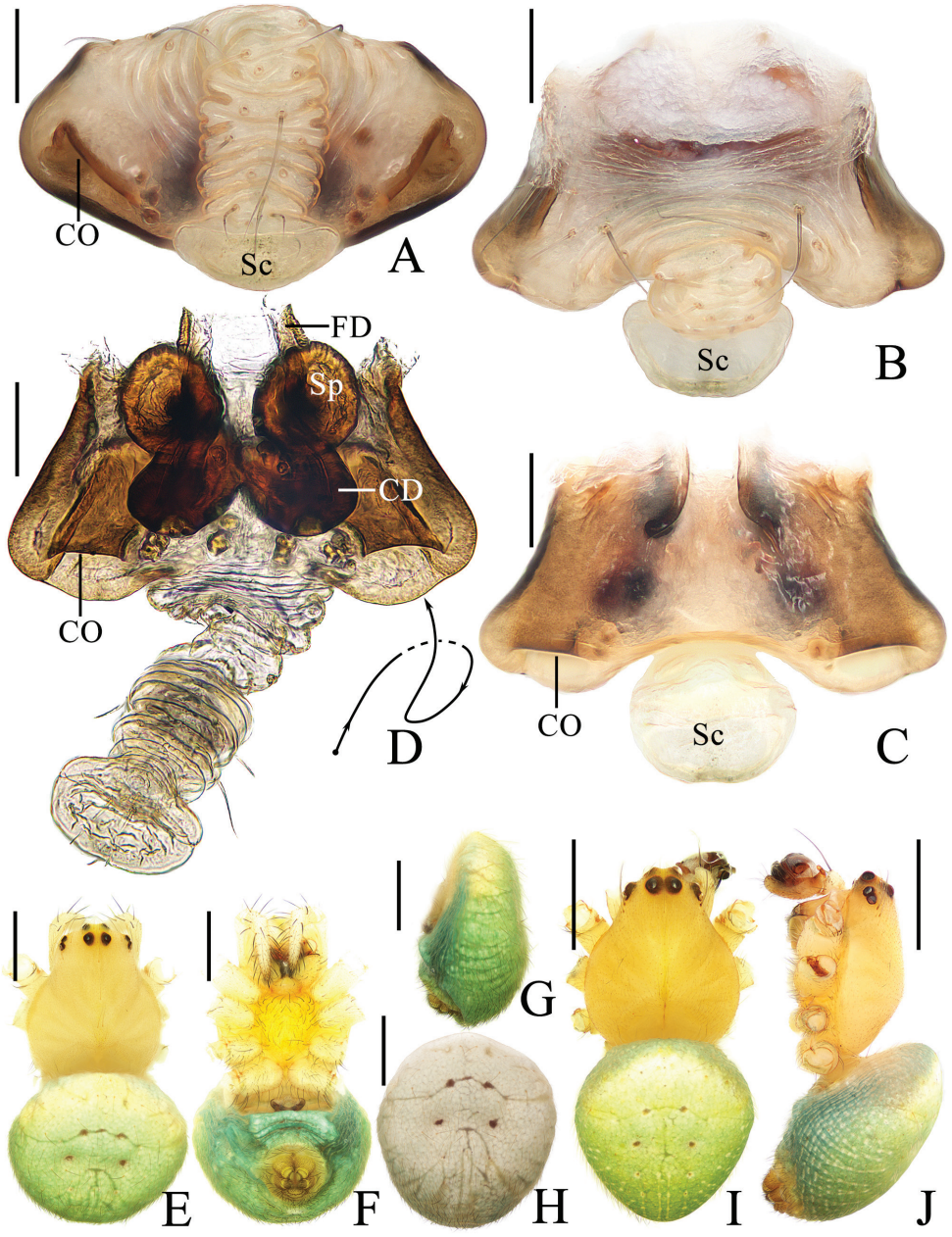

Figure 1. *Araneus fenzhi* sp. nov. **A–H** female paratype TRU-Araneidae-137 **I, J** male holotype **A** epigyne, ventral view **B** ibid., anterior view **C** ibid., posterior view **D** vulva, posterior view **E** habitus, dorsal view **F** ibid., ventral view **G** abdomen, lateral view **H** ibid., dorsal view **I** habitus, dorsal view **J** ibid., lateral view. Scale bars: 0.1 mm (**A–D**); 1 mm (**E–J**).

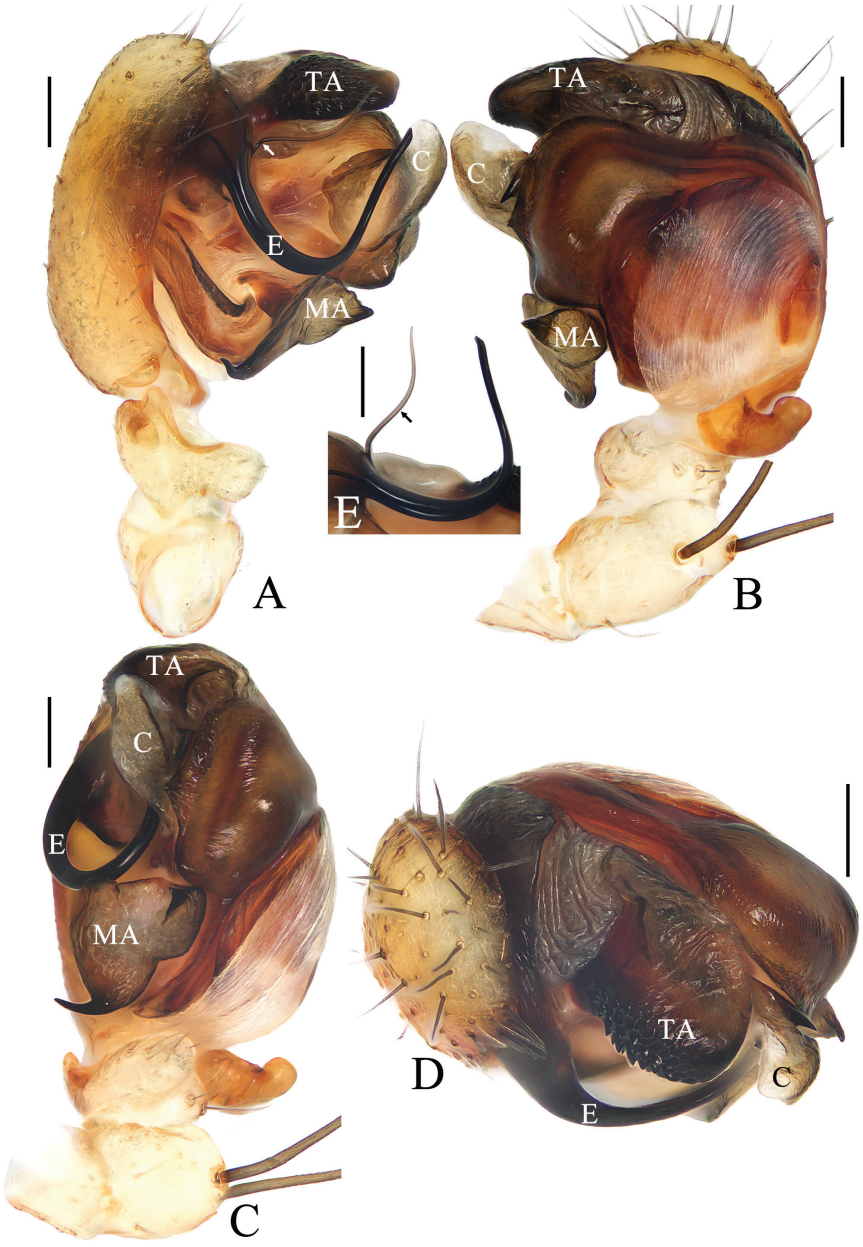

Figure 2. *Araneus fenzhi* sp. nov. **A, E** male paratype TRU-Araneidae-138 **B–D** male holotype **A** pedipalp, prolateral view **B** ibid., retrolateral view **C** ibid., ventral view **D** ibid., apical view **E** embolus. Scale bars: 0.1 mm.

Description. Male (holotype, Figs 1I, J, 2B–D, 9A–D; paratype TRU-Araneidae-138, Fig. 2A, E). Total length 3.35. Carapace 1.75 long, 1.20 wide. Abdomen 2.10 long, 1.65 wide. Clypeus 0.10 high. Eye sizes and interdistances: AME 0.10, ALE 0.06, PME 0.11, PLE 0.06, AME–AME 0.15, AME–ALE 0.15, PME–PME

0.13, PME–PLE 0.20, MOA length 0.33, anterior width 0.35, posterior width 0.33. Leg measurements: I 6.90 (2.05, 2.40, 1.70, 0.75), II 6.45 (1.95, 2.20, 1.60, 0.70), III 3.60 (1.20, 1.10, 0.80, 0.50), IV 5.25 (1.70, 1.70, 1.30, 0.55). Carapace pear-shaped, yellow; base of eyes brown. Cervical groove inconspicuous; fovea longitudinal. Chelicerae yellow; four promarginal and three retromarginal teeth. Endites almost square, yellow with very narrow, dark anterior edge, with tooth-like process laterally. Labium triangular, yellow. Sternum cordiform, yellow with dark setae. Legs yellow to brown, without annuli; femur I with eight macrosetae; tibia I with 10 macrosetae; tibia II with 12 macrosetae; tibia III with nine macrosetae; tibia IV with seven macrosetae. Abdomen oval, ~1.3× longer than wide, yellowish green with pale yellow spots; venter whitish green. Spinnerets yellowish brown.

Pedipalp (Fig. 2) with a basal femoral protrusion; patella with two bristles; median apophysis almost triangular, with a single long, slender, curved spur and a shorter broad spur; embolus twisted into a U-shape, with a threadlike branch at base, without cap (see arrows in Fig. 2A, E); conductor membranous, with a spur at base; terminal apophysis blunt, with dense denticles.

Female (paratype TRU-Araneidae-137, Fig. 1A–H). Total length 4.40. Carapace 2.35 long, 1.85 wide. Abdomen 2.80 long, 2.55 wide. Clypeus 0.10 high. Eye sizes and interdistances: AME 0.11, ALE 0.08, PME 0.13, PLE 0.08, AME–AME 0.18, AME–ALE 0.25, PME–PME 0.15, PME–PLE 0.33, MOA length 0.40, anterior width 0.40, posterior width 0.38. Leg measurements: I 8.30 (2.45, 2.95, 2.05, 0.85), II 7.70 (2.25, 2.70, 1.95, 0.80), III 4.75 (1.55, 1.50, 1.05, 0.65), IV 6.85 (2.25, 2.30, 1.60, 0.70). Habitus similar to that of male, but abdomen ~1.1× wider than long.

Epigyne (Fig. 1A–D) ~1.65× wider than long; scape with nearly parallel sides, spoon shaped distally; copulatory openings wedge shaped in ventral view, near posterior margin; copulatory ducts coiled ~360°, ~2× longer than a spermatheca diameter; spermathecae spherical, ~1/4 spermatheca diameter apart.

Variation. Total length: ♂♂ 2.95–3.40 (*n* = 5); ♀♀ 4.15–5.65 (*n* = 6). Preserved specimens grayish white. The embolic branch is generally broken off.

Distribution. Hunan, Guizhou, Jiangxi.

Comment. The oval abdomen is similar to that of members of the *A. ejusmodi* group, but the long, distally spoon-shaped scape differs greatly than in those species, and thus the group to which the new species belongs is unclear.

Araneus mayanghe **Mi & Wang, sp. nov.**

https://zoobank.org/0151AD54-FB49-424C-980D-21E4D80229DA

Figs 3, 4, 9E–H, 10

Type material. ***Holotype*** ♂ (TRU-Araneidae-147), China: Guizhou Province, Tongren City, Yanhe Tujia Autonomous County, Siqu Township, Dabao Village, Mayanghe National Nature Reserve (28°39.48'N, 108°12.80'E, ca 690 m), 19.IV.2022, X.Q. Mi et al. leg. ***Paratypes*****:** 4♂10♀ (TRU-Araneidae-148–161), same data as for holotype.

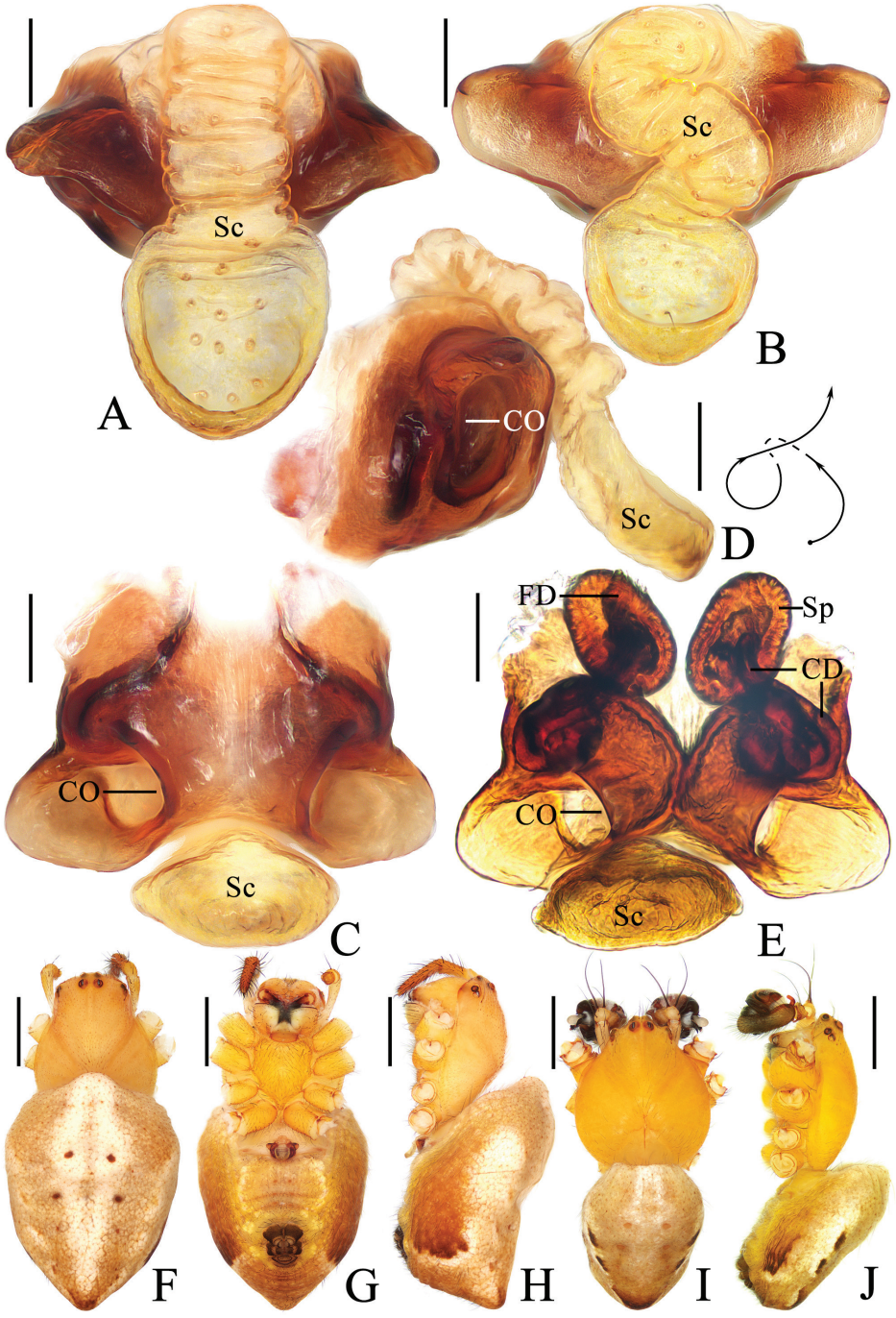

Figure 3. *Araneus mayanghe* sp. nov. **A, C–H** female paratype TRU-Araneidae-149 **B** female paratype TRU-Araneidae-150 **I, J** male holotype **A** epigyne, ventral view **B** ibid., ventral view **C** ibid., posterior view dorsal view **D** ibid., lateral view **E** vulva, posterior view **F** habitus, dorsal view **G** ibid., ventral view **H** ibid., lateral view habitus **I** ibid., dorsal view **J** ibid., lateral view. Scale bars: 0.1 mm (**A–E**); 1 mm (**F–J**).

Etymology. The specific name is a noun in apposition and refers to the type locality.

Diagnosis. The new species resembles *A. ryukyuanus* Tanikawa, 2001, *A. tsurusakii* Tanikawa, 2001, *A. polydentatus* Yin et al., 2007, and *A. yuanminensis* Yin, Wang, Xie & Peng, 1990 in appearance, but differs from *A. ryukyuanus* in having 1) the copulatory openings located on the posterior surface vs the ventral surface (Tanikawa 2001: fig. 20); 2) the embolus long, reaching the base of the conductor vs short and not reaching the conductor (Tanikawa 2001: fig. 21); and 3) the embolus somewhat S-shaped distally vs C-shaped (Tanikawa 2001: fig. 21). It can be distinguished from *A. tsurusakii* in having 1) the epigyne scape almost straight or slightly twisted vs extremely twisted (Tanikawa 2001: fig. 14); 2) the copulatory opening about ~0.8× the median plate width vs ~0.33× the median plate width (Tanikawa 2001: fig. 15); and 3) the embolus somewhat S-shaped distally vs C-shaped (Tanikawa 2001: figs 16–18). It differs from *A. polydentatus* in having 1) the epigyne scape almost straight vs S-shaped (Yin et al. 2007: fig. 1g); 2) the embolus S-shaped distally vs straight (Yin et al. 2007: fig. 1b); and 3) the embolus long, reaching the base of the conductor vs short and not reaching the conductor (Yin et al. 2007: fig. 1b). It differs from *A. yuanminensis* in having 1) the copulatory openings located on the posterior surface vs on the ventral surface (Yin et al. 1990: figs 66–68); 2) the spermathecae oval vs spherical (Yin et al. 1990: fig. 68); and 3) the spinnerets at the posterior 1/3 of abdomen vs at the middle of abdomen (Yin et al. 1990: fig. 65).

Description. Male (holotype, Figs 3I, J, 4A–D, 9E–H; paratype TRU-Araneidae-148, Fig. 4E). Total length 4.00. Carapace 2.05 long, 1.80 wide. Abdomen 2.45 long, 1.65 wide. Clypeus 0.10 high. Eye sizes and interdistances: AME 0.08, ALE 0.08, PME 0.11, PLE 0.08, AME–AME 0.15, AME–ALE 0.23, PME–PME 0.10, PME–PLE 0.28, MOA length 0.30, anterior width 0.33, posterior width 0.33. Leg measurements: I 7.30 (2.30, 2.65, 1.60, 0.75), II 7.05 (2.15, 2.65, 1.55, 0.70), III 3.75 (1.10, 1.35, 0.80, 0.50), IV 5.35 (1.80, 2.00, 1.00, 0.55). Carapace pear-shaped, yellow with dark setae; posterior eyes with brown base. Cervical groove obvious; fovea longitudinal. Chelicerae yellow; four promarginal and three retromarginal teeth. Endites yellow with very narrow, dark anterior edge, with tooth-like process laterally. Labium triangular, yellow. Sternum cordiform, yellow with dark setae. Legs yellow to dark brown, without annuli; femur I with seven macrosetae; tibia I with 11 macrosetae; tibia II with 11 macrosetae; tibia III with 10 macrosetae, tibia IV with 11 macrosetae. Abdomen oval, blunt anteriorly and pointed posteriorly, ~1.5× longer than wide, covered with gray setae; dorsum yellow with a large terminal dark patch and two pairs of lateral dark patches; venter grayish yellow. Spinnerets dark brown.

Pedipalp (Fig. 4) with basal femoral protrusion; patella with two bristles; median apophysis large, bifurcated, dorsal ramus long, curved, pointed at tip; ventral ramus short with serrated tip; embolus stout at base, slender and twisted into an S-shape distally, without cap; conductor subquadrate in retrolateral view, thickened at tip, with spur at base; terminal apophysis weakly sclerotized, digitiform; subterminal apophysis large, heavily sclerotized, concave medially.

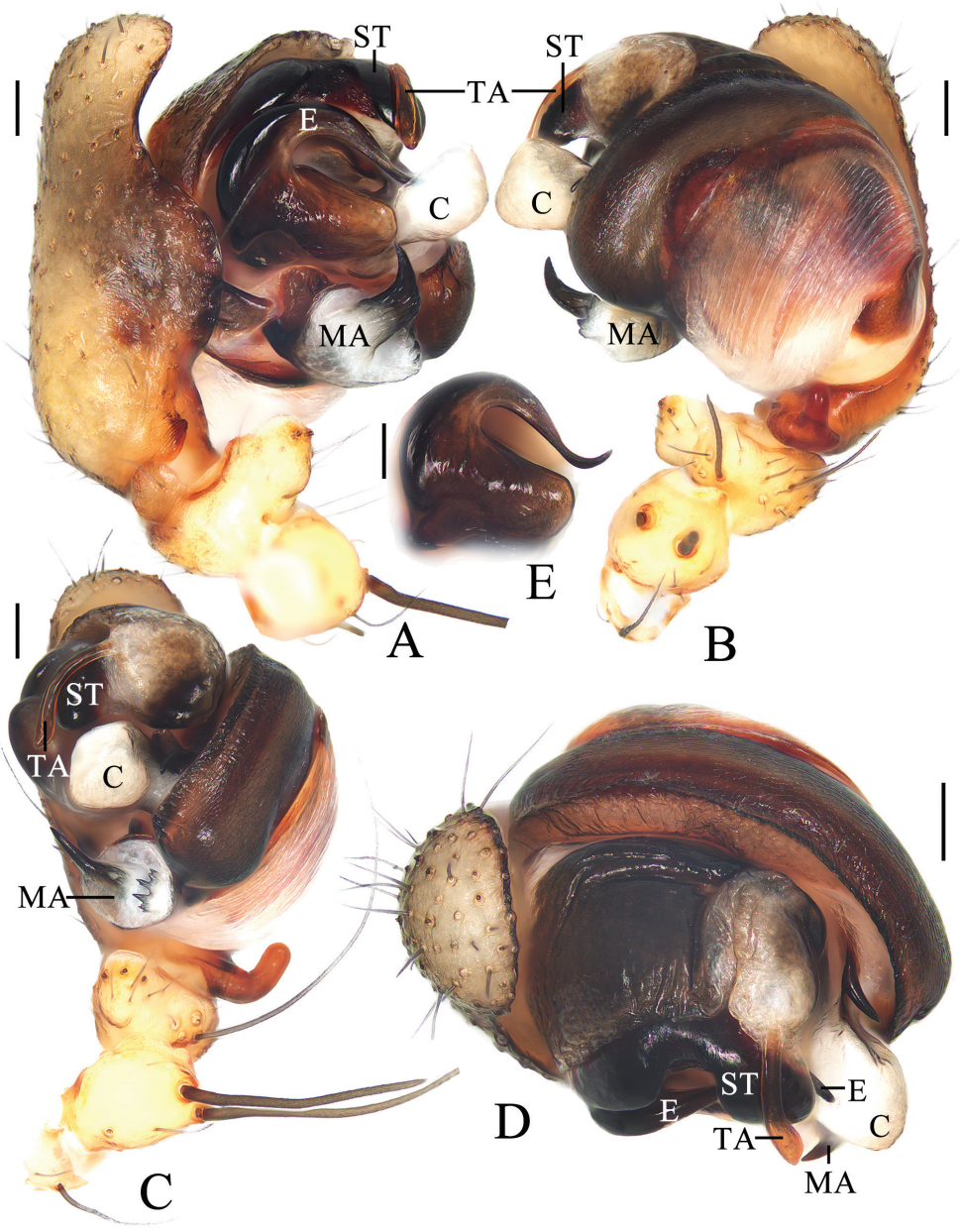

Figure 4. *Araneus mayanghe* sp. nov. **A–D** male holotype **E** male paratype TRU-Araneidae-148 **A** pedipalp, prolateral view **B** ibid., retrolateral view **C** ibid., ventral view **D** ibid., apical view. **E** embolus, prolateral view. Scale bars: 0.1 mm.

Female (paratype TRU-Araneidae-149, Fig. 3A, C–H; paratype TRU-Araneidae-150, Fig. 3B). Total length 4.95. Carapace 2.25 long, 1.60 wide. Abdomen 3.45 long, 2.65 wide. Clypeus 0.08 high. Eye sizes and interdistances: AME 0.09, ALE

0.09, PME 0.13, PLE 0.09, AME–AME 0.15, AME–ALE 0.30, PME–PME 0.15, PME–PLE 0.33, MOA length 0.33, anterior width 0.30, posterior width 0.35. Leg measurements: I 7.70 (2.40, 2.90, 1.65, 0.75), II 6.85 (2.10, 2.60, 1.45, 0.70), III 4.15 (1.35, 1.45, 0.85, 0.50), IV 6.10 (2.00, 2.20, 1.35, 0.55). Habitus similar to that of male but pointed anteriorly and abdominal patches much paler.

Epigyne (Fig. 3A, C–E) scape almost straight, distally spoon-shaped; copulatory openings on posterior surface; copulatory ducts twisted, longer than spermatheca; spermathecae oval, not touching.

Variation. Total length: ♂♂ 3.55–4.00 (*n* = 5); ♀♀ 4.15–5.55 (*n* = 10). Scape of female paratype TRU-Araneidae-149 slightly twisted into an S-shape (Fig. 3B). Abdomen of male paratype TRU-Araneidae-151 dorsally with a large, grayish brown, triangular patch.

Distribution. Known only from the type locality (Guizhou).

Comment. The oval, posteriorly pointed abdomen and the long, distally spoon-shaped scape indicate that the new species belongs to the *A. sturmi* group. Based on the similarities of the somatic morphology and genitalia, the new species is most similar to *A. polydentatus*, *A. ryukyuanus*, *A. tsurusakii*, *A. viperifer*, and *A. yuanminensis*.

Araneus shiwandashan **Mi & Wang, sp. nov.**
https://zoobank.org/DF107666-FB11-4133-BFA7-8FED554A5C99
Figs 5, 6, 9I–L, 10

Type material. ***Holotype*** ♂ (TRU-Araneidae-162), China: Guangxi Zhuang Autonomous Region, Fangchenggang City, Shangsi County, Shiwandashan National Nature Reserve (21°52.97'N, 107°54.88'E, ca 720 m), 6.X.2018, X.Q. Mi et al. leg. ***Paratype***: 1♀ (TRU-Araneidae-163), same data as for holotype.

Etymology. The specific name is a noun in apposition and refers to the type locality.

Diagnosis. The new species resembles *Araneus floriformis* Liu, Li, Mi & Peng, 2022 in somatic morphology and pedipalp structures, but differs in having 1) the median apophysis bifurcated vs uniramous (Liu et al. 2022: fig. 4A–C); 2) the embolic lamella covering the embolus medially in prolateral view vs not covering the embolus medially (Liu et al. 2022: fig. 4A, D); 3) copulatory openings at the posterior surface vs laterally (Liu et al. 2022: fig. 4G, H); and 4) the epigyne scape triangular vs spoon-shaped (Liu et al. 2022: fig. 4G, H).

Description. Male (holotype, Figs 5G, H, 6, 9I–L). Total length 4.70. Carapace 2.50 long, 2.05 wide. Abdomen 2.80 long, 1.75 wide. Clypeus 0.13 high. Eye sizes and interdistances: AME 0.15, ALE 0.13, PME 0.15, PLE 0.13, AME–AME 0.15, AME–ALE 0.28, PME–PME 0.08, PME–PLE 0.33, MOA length 0.38, anterior width 0.38, posterior width 0.35. Leg measurements: I 9.35 (2.80, 3.40, 2.30, 0.85), II 8.60 (2.60, 3.10, 2.10, 0.80), III 4.90 (1.60, 1.65, 1.05, 0.60), IV 6.95 (2.15, 2.40, 1.70, 0.70). Carapace pear-shaped, yellow, with dark setae on sides of cephalic region. Cervical groove inconspicuous; fovea longitudinal. Chelicerae yellow; four promarginal and three retromarginal teeth. Endites yellow with very narrow, dark anterior edge, with

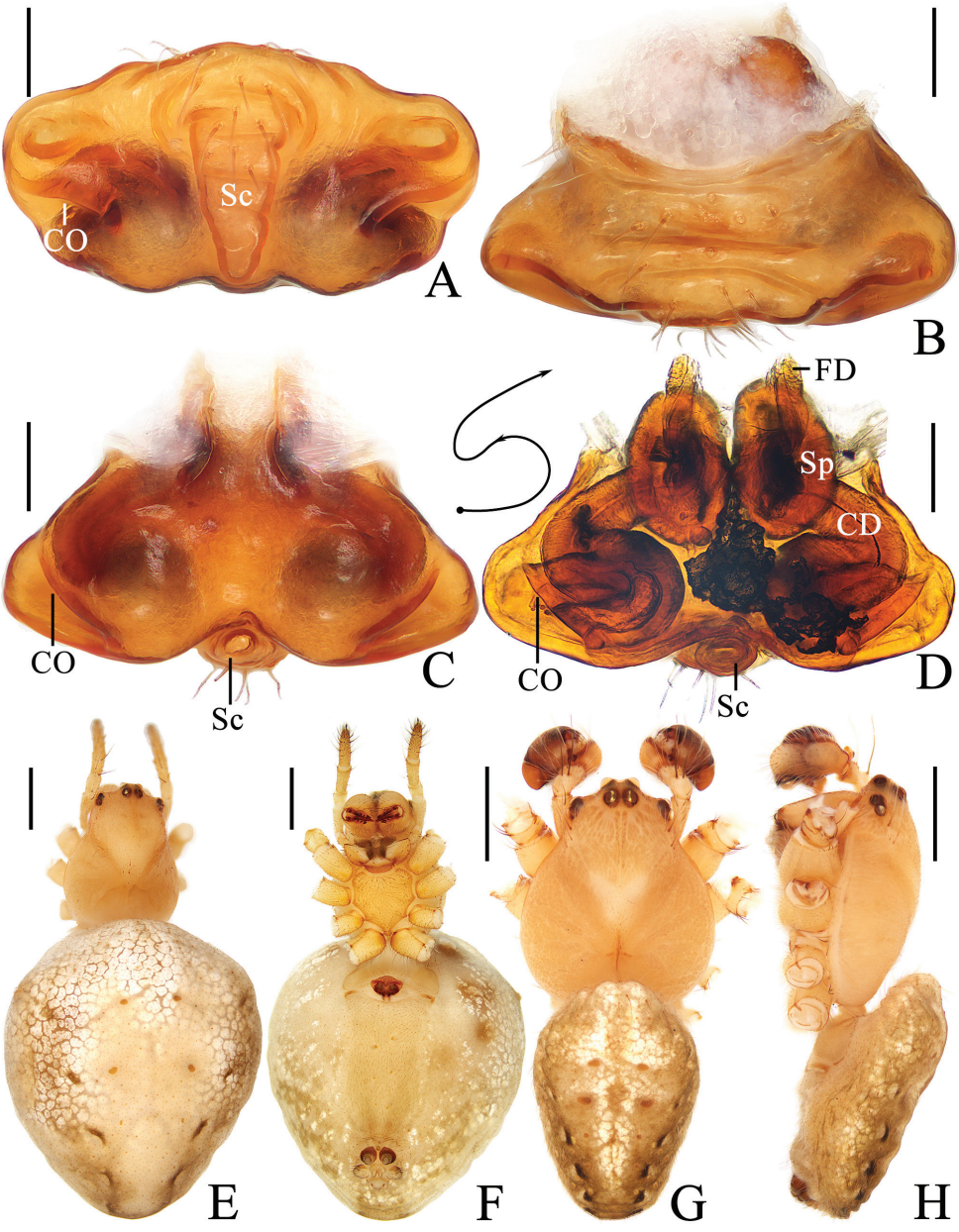

Figure 5. *Araneus shiwandashan* sp. nov. **A–F** female paratype TRU-Araneidae-163 **G, H** male holotype **A** epigyne, ventral view **B** ibid., anterior view **C** ibid., posterior view **D** vulva, posterior view **E** habitus, dorsal view **F** ibid., ventral view **G** ibid., dorsal view **H** ibid., lateral view. Scale bars: 0.1 mm (**A–D**); 1 mm (**E–H**).

tooth-like process laterally. Labium triangular, yellow, paler at tip. Sternum cordiform, yellow with dark setae. Legs yellow with indistinct, yellowish-brown annuli; femur I with seven macrosetae; tibia I with 10 macrosetae; tibia II with 12 macrosetae, tibia III

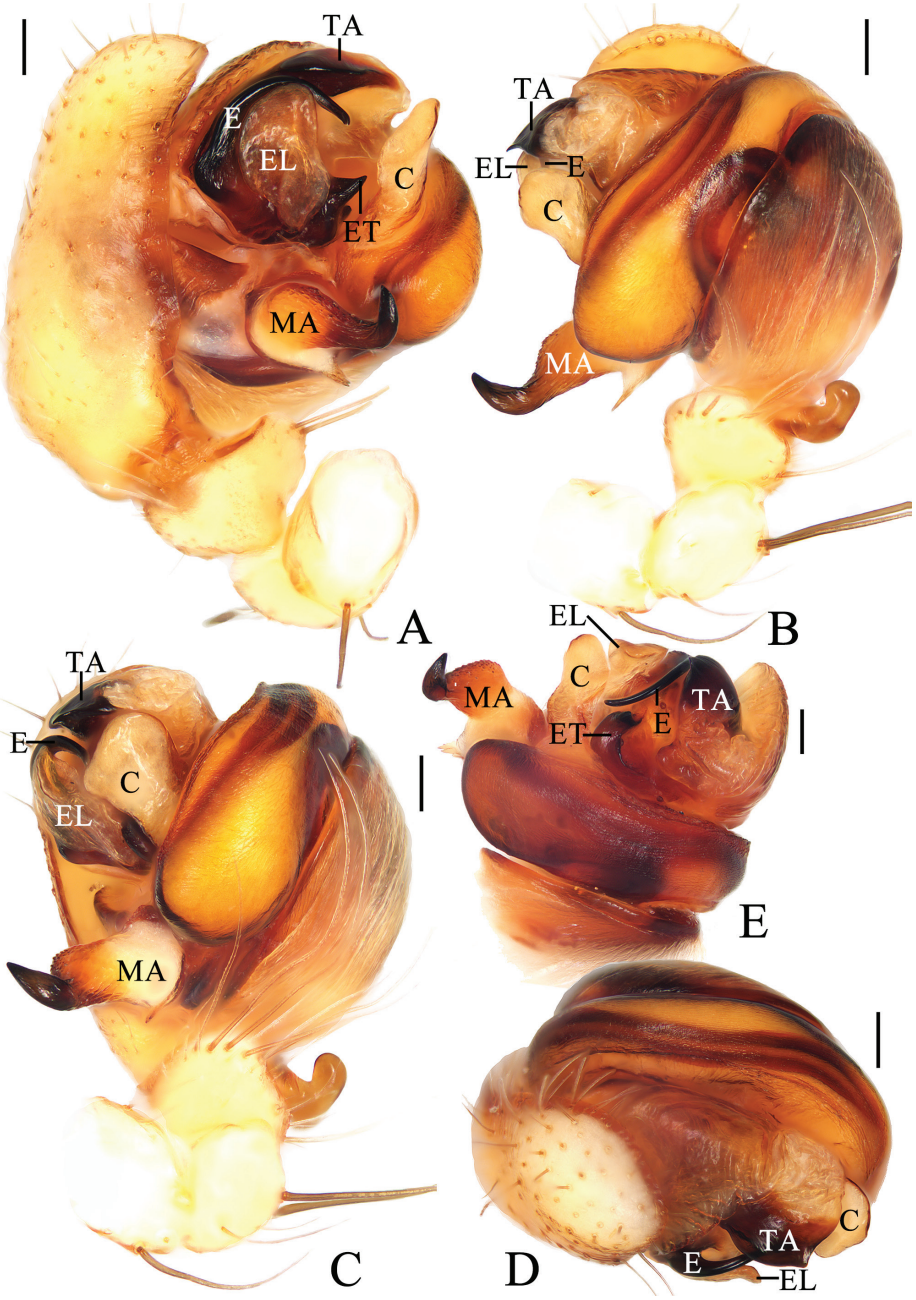

Figure 6. *Araneus shiwandashan* sp. nov. male holotype **A** pedipalp, prolateral view **B** ibid., retrolateral view **C** ibid., ventral view **D** ibid., apical view **E** expanded bulb, retrolateral view. Scale bars: 0.1 mm.

with eight macrosetae; and tibia IV with 11 macrosetae. Abdomen oval, ~1.6× longer than wide, covered with pale setae; dorsum whitish yellow with six pairs of lateral patches; posterior patches darker; venter grayish yellow. Spinnerets brown.

Pedipalp (Fig. 6) with basal femoral protrusion; patella with two bristles; median apophysis prominent, bifurcate, dorsal ramus long, curved, ventral ramus short, straight; embolus strongly sclerotized, with basal tooth, distally semicircular, embolic lamella long, covering part of embolus; conductor membranous, subquadrate in ventral view; terminal apophysis flattened, heavily sclerotized distally.

Female (paratype TRU-Araneidae-163, Fig. 5A–F). Total length 7.25. Carapace 2.45 long, 2.00 wide. Abdomen 5.10 long, 4.55 wide. Clypeus 0.08 high. Eye sizes and interdistances: AME 0.15, ALE 0.13, PME 0.15, PLE 0.13, AME–AME 0.15, AME–ALE 0.33, PME–PME 0.10, PME–PLE 0.40, MOA length 0.35, anterior width 0.38, posterior width 0.33. Leg measurements: I 7.85 (2.30, 2.85, 1.90, 0.80), II 7.10 (2.15, 2.50, 1.70, 0.75), III 4.30 (1.45, 1.40, 0.90, 0.55), IV 6.35 (2.10, 2.10, 1.50, 0.65). Femur I with a distinct macroseta prolaterally, tibia I with three distinct macrosetae prolaterally. Habitus similar to that of male.

Epigyne (Fig. 5A–D) ~1.9× wider than long; scape triangular, ~1.8× longer than wide, directed posteriorly; copulatory openings concave, located at posterolaterally; copulatory ducts twisted into an S-shape, longer than spermatheca; spermathecae elliptical, touching each other.

Distribution. Known only from the type locality (Guangxi).

Comments. The oval abdomen and the male pedipalp with a bifurcated median apophysis and arched terminal apophysis indicate that the new species belongs to the *A. sturmi* group, although the scape is not twisted or widened distally. Based on the somatic morphology and genitalia, the new species is most similar to *A. breviscapus*, *A. floriformis*, and *A. pianmaensis*.

Araneus zhoui **Mi & Wang, sp. nov.**

https://zoobank.org/C2732937-19D2-4F05-BBA9-019024985A53

Figs 7, 8, 9M–P, 10

Type material. ***Holotype*** ♂ (TRU-Araneidae-164), China: Hainan Province, Ledong Li Autonomous County, Jianfeng Township, Jianfengling National Nature Reserve (18°43.11'N, 108°52.32'E, ca 1400 m), 16.IV.2019, C. Wang & Y.F. Yang leg. ***Paratypes*****:** 3♂6♀ (TRU-Araneidae-165–173), same data as for holotype.

Comparative material. *Araneus colubrinus* Song & Zhu, 1992, 5♀, China: Guizhou Province, Yinjiang Tujia Autonomous County, Ziwei Township, Dayuanzhi Village, Huguosi (27°54.54'N, 108°46.57'E, ca 1660 m), 9.V.2020, X.Q. Mi et al. leg.

Etymology. The species is named after Mr Runbang Zhou who helped us with specimen collections; noun in genitive case.

Diagnosis. The new species resembles *A. conexus* Liu, Irfan, Yang & Peng, 2019 and *A. colubrinus* Song & Zhu, 1992 in somatic morphology and genital structures, but it can be distinguished from *A. conexus* in having 1) the female carapace with two short spines anterior to the fovea vs lacking (Liu et al. 2019: fig. 1D); 2) the anterior abdomen slightly elevated in lateral view vs extremely elevated to a pointed tip

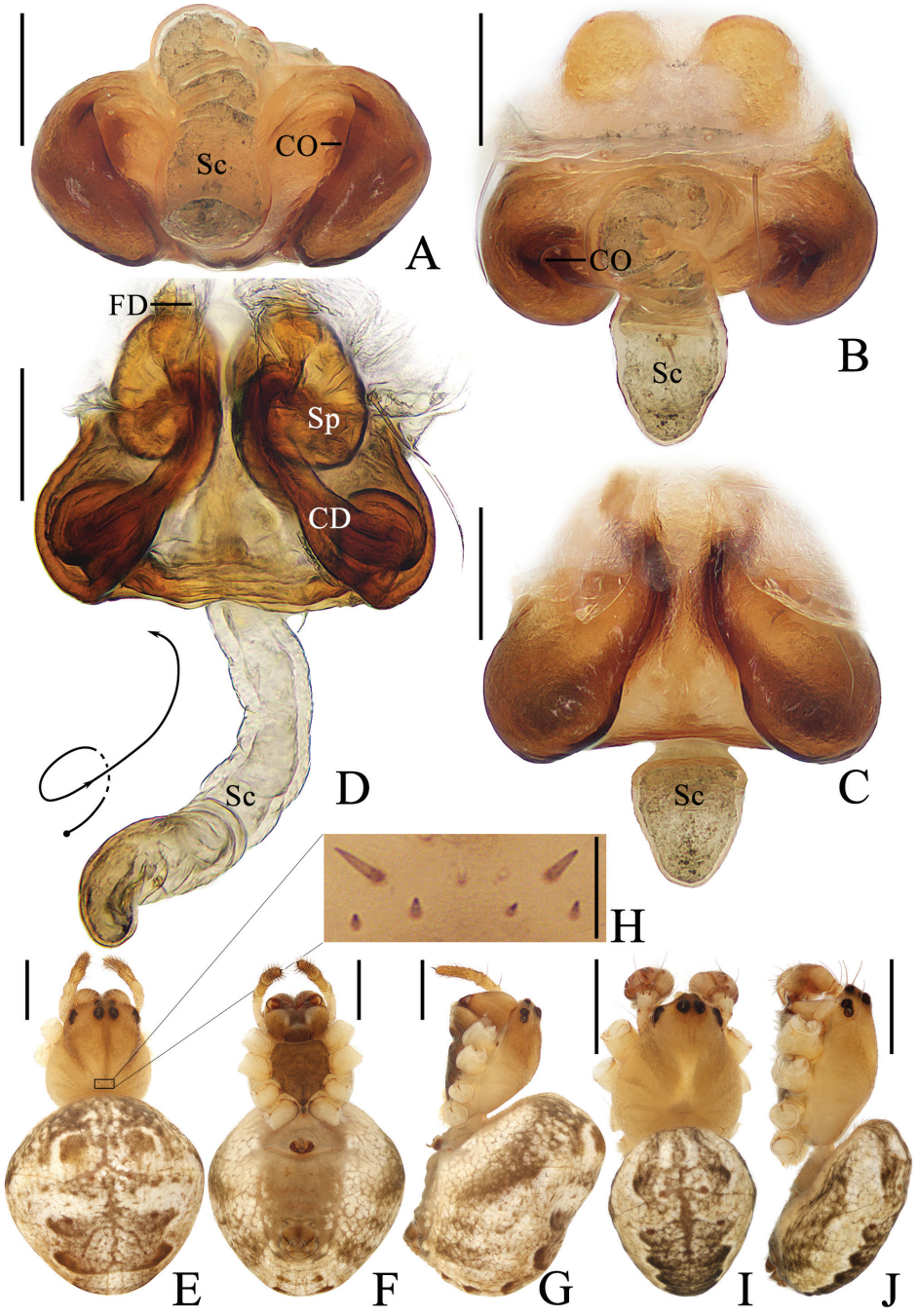

Figure 7. *Araneus zhoui* sp. nov. **A–H** female paratype TRU-Araneidae-165 **I, J** male holotype **A** epigyne, ventral view **B** ibid., anterior view **C** ibid., posterior view **D** vulva, posterior view **E** habitus, dorsal view **F** ibid., ventral view **G** ibid., lateral view **H** part of carapace, dorsal view **I** habitus, dorsal view **J** ibid., lateral view. Scale bars: 0.1 mm (**A–D, H**); 1 mm (**E–G, I, J**).

(Liu et al. 2019: fig. 1E); 3) the terminal apophysis long, touching the conductor in prolateral view vs short and not touching the conductor (Liu et al. 2019: fig. 2A, B, D, E); and 4) the distal end of the subterminal apophysis rounded in prolateral view vs concave (Liu et al. 2019: fig. 2A, D). It differs from *A. colubrinus* in having 1) the epigyne scape almost straight vs S-shaped and twisted (Song and Zhu 1992: fig. 4); and 2) the spermathecae touching each other vs separated by ~1.6× of the spermatheca width.

Description. Male (holotype, Figs 7I, J, 8, 9M–P). Total length 3.20. Carapace 1.60 long, 1.40 wide. Abdomen 1.95 long, 1.55 wide. Clypeus 0.05 high. Eye sizes and interdistances: AME 0.09, ALE 0.08, PME 0.11, PLE 0.08, AME–AME 0.08, AME–ALE 0.18, PME–PME 0.08, PME–PLE 0.23, MOA length 0.28, anterior width 0.25, posterior width 0.30. Leg measurements: I 6.15 (1.85, 2.15, 1.50, 0.65), II 5.45 (1.65, 1.90, 1.30, 0.60), III 3.35 (1.10, 1.10, 0.70, 0.45), IV 4.45 (1.40, 1.50, 1.05, 0.50). Carapace pear-shaped, yellow, paler anterior to fovea; ALEs, PMEs, and PLEs with black base. Cervical groove inconspicuous; fovea depressed. Chelicerae yellow; four promarginal and three retromarginal teeth. Endites yellow with very narrow, dark anterior edge, with tooth-like process laterally. Labium triangular, yellow with paler tip. Sternum cordiform, yellow with grayish brown patches, with brown setae. Legs yellow with yellowish-brown annuli; femur I with eight macrosetae; tibia I with 14 macrosetae, distally with constriction (see arrow in Fig. 9M); tibia II with 12 macrosetae; tibia III with six macrosetae; tibia IV with nine macrosetae. Abdomen oval, ~1.25× longer than wide; dorsum whitish yellow, with large grayish brown patch extending from anterior edge to posterior end, bearing four pairs of constrictions; venter grayish brown with pair of longitudinal yellow patches laterally. Spinnerets grayish brown.

Pedipalp (Fig. 8) with basal femoral protrusion; patella with two bristles; median apophysis with prolateral spur and four or five small retrolateral teeth; embolus tapered, curved counterclockwise at tip; conductor membranous, widest at base; terminal apophysis approximately equal in length to bulb diameter, distally touching conductor, subterminal apophysis with blunt tip in prolateral view.

Female (paratype TRU-Araneidae-165, Figs 7A–H). Total length 3.80. Carapace 1.60 long, 1.40 wide. Abdomen 2.85 long, 2.55 wide. Clypeus 0.03 high. Eye sizes and interdistances: AME 0.10, ALE 0.09, PME 0.13, PLE 0.09, AME–AME 0.15, AME–ALE 0.25, PME–PME 0.13, PME–PLE 0.30, MOA length 0.28, anterior width 0.28, posterior width 0.30. Leg measurements: I 5.10 (1.55, 1.90, 1.10, 0.55), II 4.45 (1.35, 1.65, 0.95, 0.50), III 2.90 (1.00, 0.95, 0.55, 0.40), IV 4.00 (1.25, 1.40, 0.90, 0.45). Habitus similar to that of male but anterior abdominal elevation more obvious, carapace with two short spines and four teeth anterior to fovea.

Epigyne (Fig. 7A–D): ~1.7× wider than long; scape with nearly parallel sides, distally directed ventrally; copulatory openings slit-like, ventral; copulatory ducts coiled ~360°, widest at origin, longer than spermatheca; spermathecae elliptical, touching each other.

Variation. Total length: ♂♂ 2.85–3.20 (n = 4); ♀♀ 2.95–4.20 (n = 6). Some female carapaces only have two short spines anterior to fovea rather than four short spines.

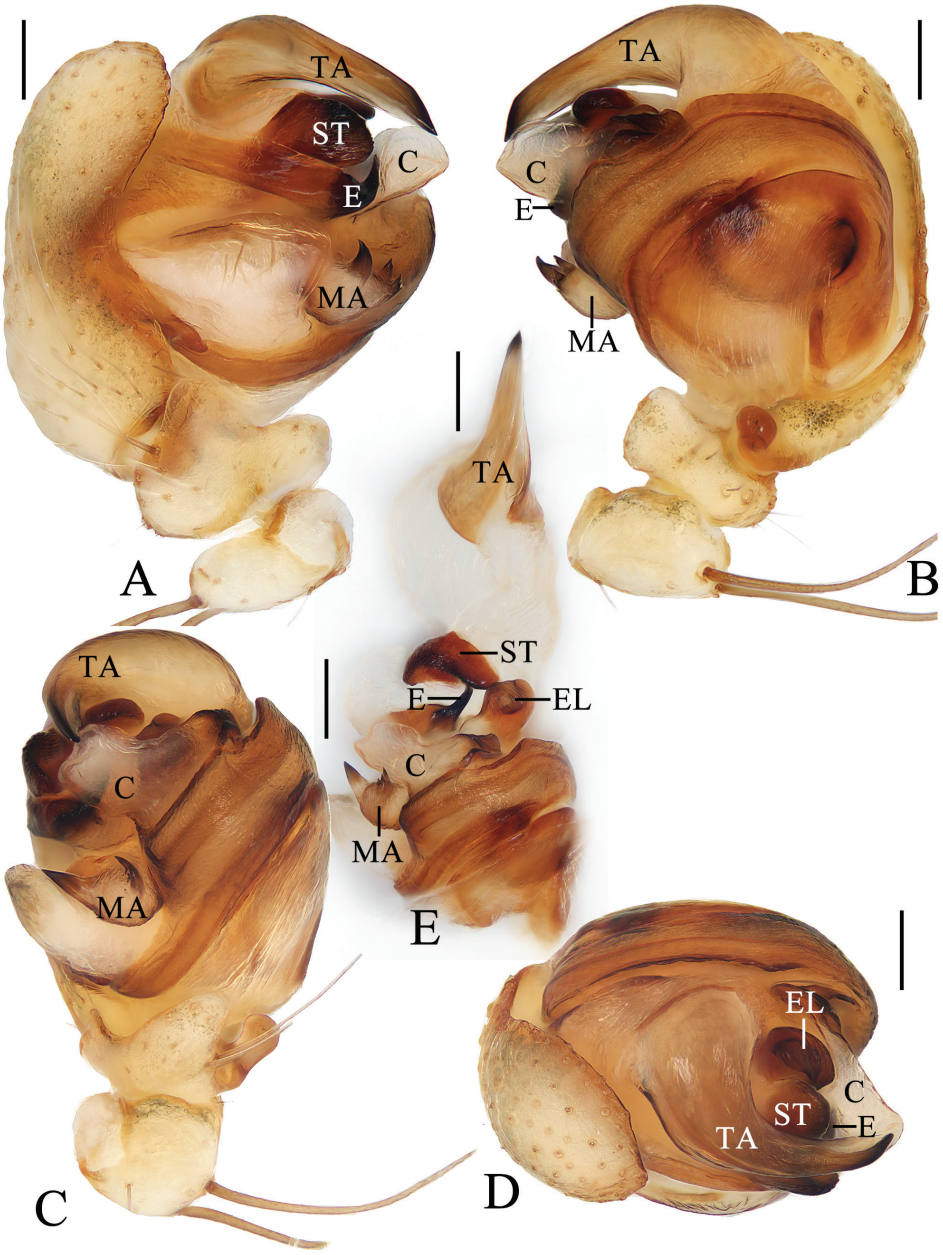

Figure 8. *Araneus zhoui* sp. nov. male holotype **A** pedipalp, prolateral view **B** ibid., retrolateral view **C** ibid., ventral view **D** ibid., apical view **E** expanded bulb, ventral view. Scale bars: 0.1 mm.

Distribution. Known only from the type locality (Hainan).

Comments. The oval abdomen and the long, twisted, distally spoon-shaped scape indicate that the new species belongs to the *A. sturmi* group. The somatic morphology and genitalia indicate that the new species is most similar to *A. colubrinus* and *A. conexus*.

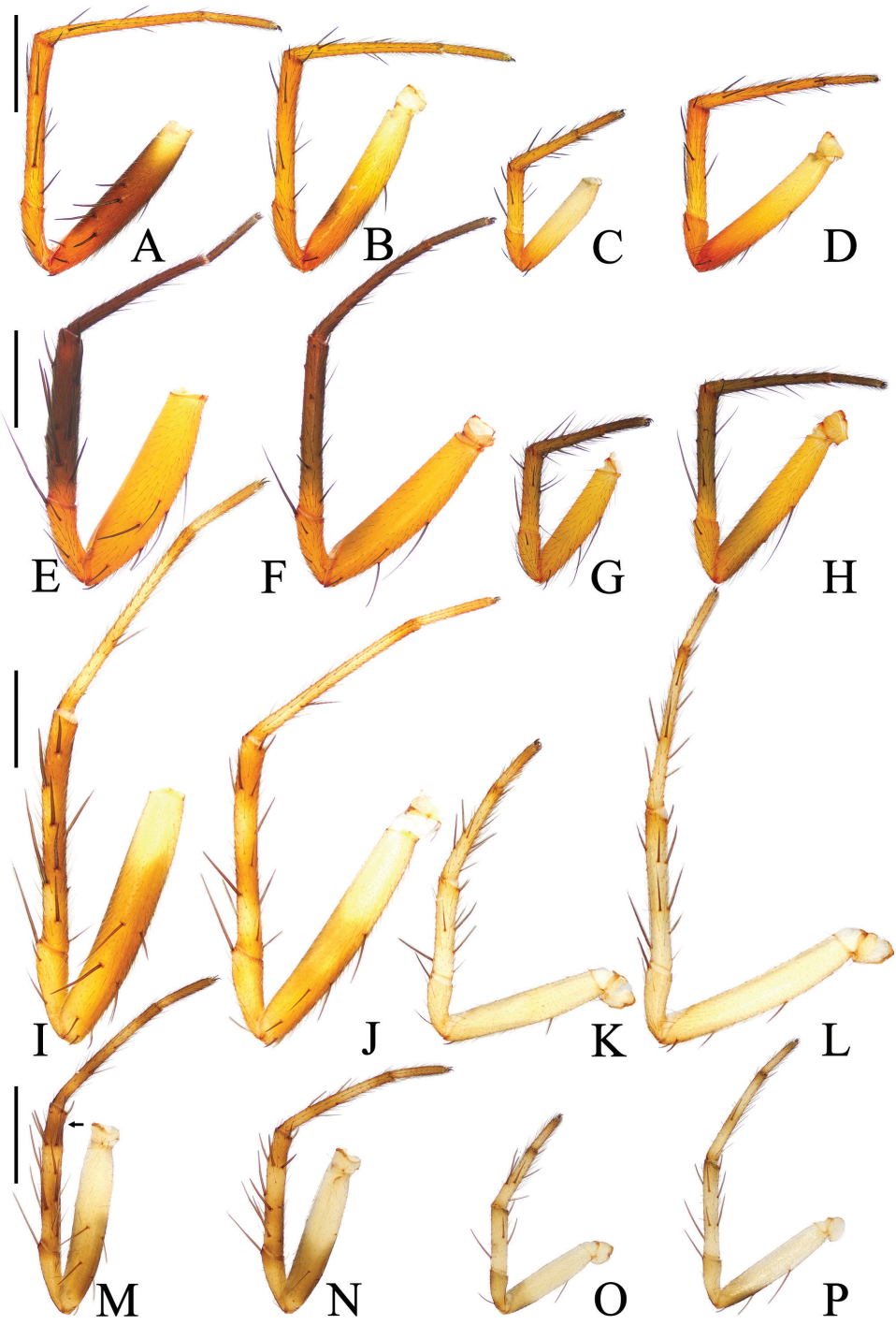

Figure 9. Legs of *Araneus* spp., male holotypes, prolateral view **A–D** *A. fenzhi* sp. nov. **E–H** *A. mayanghe* sp. nov. **I–L** *A. shiwandashan* sp. nov. **M–P** *A. zhoui* sp. nov. **A, E, I, M** legs I; **B, F, J, N** legs II; **C, G, K, O** legs III; **D, H, L, P** legs IV. Scale bars: 1 mm.

Genus *Aoaraneus* Tanikawa, Yamasaki & Petcharad, 2021

Aoaraneus Tanikawa, Yamasaki & Petcharad, 2021: 89.

Type species. *Aoaraneus pentagrammicus* (Karsch, 1879).

***Aoaraneus octumaculalus* (Han & Zhu, 2010), comb. nov.**
Fig. 10

Araneus octumaculalus Han & Zhu, 2010: 58, figs 1–6. (Type material not examined.)

Material examined. 1♀ (TRU-Araneidae-174), China: Hainan Province, Ledong Li Autonomous County, Jianfeng Township, Jianfengling National Nature Reserve, around Tianchi pond (18°44.45'N, 108°51.49'E, ca 860 m), 11.IV.2019, C. Wang & Y.F. Yang leg.; 1♀ (TRU-Araneidae-175), same locality and collectors (18°45.24'N, 108°51.57'E, ca 850 m), 14.IV.2019; 1♀ (TRU-Araneidae-176), Jianfengling National Nature Reserve, around the peak of Jianfengling (18°43.11'N, 108°52.32'E, ca 1400 m), 16.IV.2019, same collectors; 1♂ (TRU-Araneidae-177), Hainan Province, Wuzhishan City, Shuiman Township, around Yatai Rainforest Hotel (18°54.37'N, 109°40.70'E, ca 750 m), 11.VIII.2020, X.Q. Mi et al. leg.

Description. See Han and Zhu (2010).

Comments. The type locality of *A. octumaculalus* is in Changjiang County, Hainan Province. The type specimens were not examined because this species was well described and illustrated (Han and Zhu 2010), and both male and female specimens of this species from nearby localities in Hainan were examined. The new combination is based on the following characters of *Aoaraneus*: long, wrinkled and flexible scape with bent tip; long terminal and subterminal apophyses, median apophysis with apical and basal projections; male endite with lateral tooth, male coxa I with ventral hook, and male femur II with groove.

Discussion

The *Araneus dehaani* group of Yin et al. (1997) included three species. The extreme sexual dimorphism of the species "*A. dehaani*" (now *Parawixia dehaani*) was discussed by Scharff et al. (2020), and molecular phylogenetic analysis has indicated that this species belonged to a new genus in the Backobourkiines. Because *A. albomaculatus* also shows extreme sexual dimorphism (female ~6.2× longer than male) and the morphology is similar to "*A. dehaani*", it is likely in the same genus. However, a third species, *A. shunhuangenesis*, does not show extreme sexual dimorphism, and the long triangular epigyne, rather flattened pedipalp bulb, single macroseta on the male pedipalp patella, and the enlarged male tibia II (Yin et. al 2007) indicate that it may belong to another genus.

Figure 10. Distribution map of the species.

Yin et al. (1997) based the *A. ejusmodi* group on the following characters: the oval or elongate-oval abdomen and the epigyne with a short scape. The characters of the male padipalp were not thoroughly considered, making the *A. ejusmodi* group somewhat arbitrary. Further taxonomic and systematic work must be conducted to clarify the aforementioned issues.

Acknowledgements

This manuscript benefitted greatly from comments by subject editor Sarah Crews and two reviewers, Volker W. Framenau and Anna Šestáková. We are grateful to Jiahui Gan, Tianjun Liu, Feng'e Li, Tingrong Peng, Xian Li, Guijie Tian, Yuanfa Yang, Hong Liu, Siyi Yan, Ke Wen, Zongguang Huang, Yun Liang, Rongrong Liao, and Yingli

Wen for collecting the specimens. This research was supported by the Science and Technology Project Foundation of Guizhou Province ([2020]1Z014), the National Natural Science Foundation of China (NSFC-31660609, 32200369), and the Key Laboratory Project of Guizhou Province ([2020]2003), and it was partly supported by the program of investigation of biodiversity resources in Hunan Province and the Open Project of Ministry of Education Key Laboratory for Ecology of Tropical Islands, Hainan Normal University, China.

References

Clerck C (1757) Aranei Svecici. Svenska spindlar, uti sina hufvud-slågter indelte samt under några och sextio särskildte arter beskrefne och med illuminerade figurer uplyste. Laurentius Salvius, Stockholmiae, 154 pp. https://doi.org/10.5962/bhl.title.119890

Guo S, Zhang F, Zhu M (2011) Two new species of the genera *Araneus* and *Gibbaranea* from Liupan Mountain, China (Araneae, Araneidae). Acta Zootaxonomica Sinica 36: 213–217.

Han G, Zhu M (2010)[2009] A new species of the genus *Araneus* (Araneae: Araneidae) from China. Acta Arachnologica 58(2): 67–68. https://doi.org/10.2476/asjaa.58.67

Hu J (2001) Spiders in Qinghai-Tibet Plateau of China. Henan Science and Technology Publishing House, Zhengzhou, 658 pp.

Liu P, Irfan M, Yang S, Peng X (2019) Two new species of *Araneus* Clerck, 1757 (Araneae, Araneidae) and first description of *A. wulongensis* male from China. ZooKeys 886: 61–77. https://doi.org/10.3897/zookeys.886.31163

Liu P, Li S, Mi X, Peng X (2022) Three new spider species of *Araneus* Clerck, 1757 (Araneae, Araneidae) from the Gaoligong Mountains of Yunnan, China. Zootaxa 5200(6): 576–586. https://doi.org/10.11646/zootaxa.5200.6.5

Mi X, Li S (2021a) On nine species of the spider genus *Eriovixia* (Araneae, Araneidae) from Xishuangbanna, China. ZooKeys 1034: 199–236. https://doi.org/10.3897/zookeys.1034.60411

Mi X, Li S (2021b) Nine new species of the spider family Araneidae (Arachnida, Araneae) from Xishuangbanna, Yunnan, China. ZooKeys 1072: 49–81. https://doi.org/10.3897/zookeys.1072.73345

Mi X, Li S (2022) On eleven new species of the orb-weaver spider genus *Araneus* Clerck, 1757 (Araneae, Araneidae) from Xishuangbanna, Yunnan, China. ZooKeys 1137: 75–108. https://doi.org/10.3897/zookeys.1137.96306

Scharff N, Coddington J, Blackledge T, Agnarsson I, Framenau V, Szűts T, Hayashi C, Dimitrov D (2020) Phylogeny of the orb-weaving spider family Araneidae (Araneae: Araneoidea). Cladistics 36(1): 1–21. https://doi.org/10.1111/cla.12382

Song D, Zhu M (1992) On new species of the family Araneidae (Araneae) from Wuling Mountains area, southwestern China. Journal of Hubei University, Natural Science Edition 14: 167–173.

Tanikawa A (2001) Twelve new species and one newly recorded species of the spider genus *Araneus* (Araneae: Araneidae) from Japan. Acta Arachnologica 50(1): 63–86. https://doi.org/10.2476/asjaa.50.63

Tanikawa A, Yamasaki T, Petcharad B (2021) Two new genera of Araneidae (Arachnida: Araneae). Acta Arachnologica 70(2): 87–101. https://doi.org/10.2476/asjaa.70.87

WSC (2023) World Spider Catalog, version 23.5. Natural History Museum Bern. https://doi.org/10.24436/2

Yin C, Wang J, Xie L, Peng X (1990) New and newly recorded species of the spiders of family Araneidae from China (Arachnida, Araneae). In: Spiders in China: One Hundred New and Newly Recorded Species of the Families Araneidae and Agelenidae. Hunan Normal University Press, Changsha, 171 pp.

Yin C, Wang J, Zhu M, Xie L, Peng X, Bao Y (1997) Fauna Sinica: Arachnida: Araneae: Araneidae. Science Press, Beijing, 460 pp.

Yin C, Griswold C, Xu X (2007) One new species and two new males of the family Araneidae from China (Arachnida: Araneae). Acta Arachnologica Sinica 16: 1–6.

Yin C, Griswold C, Yan H, Liu P (2009) Four new species of the spider genus *Araneus* from Gaoligong Mountains, Yunnan Province, China (Araneae, Araneidae). Acta Arachnologica Sinica 18: 1–10.

Zhang F, Zhang C (2002) Notes on one new species and one newly recorded species of the family Araneidae (Arachnida: Araneae) from Taihang Mountains, China. Acta Arachnologica Sinica 11: 22–24.

Zhang C, Song D, Kim J (2006) A new species of the spider genus *Araneus* from Tibet, China (Araneae: Araneidae). Korean Arachnology 22: 1–5.

Zhou H, Zhu J, Zhang Z (2017) Two new and four newly recorded species of orbweaver spiders from China (Araneae: Araneidae). Acta Arachnologica Sinica 26(1): 6–12.

Zhu M, Zhang W, Gao L (1998) A new species of *Araneus* (Araneae: Araneidae) from China. Acta Arachnologica Sinica 7: 30–32.

Zhu M, Zhang J, Zhang Z, Chen H (2005) Arachnida: Araneae. In: Yang M, Jin D (Eds) Insects from Dashahe Nature Reserve of Guizhou. Guizhou People's Publishing House, Guiyang, 490–555.

ZooKeys 1160: 191–205 (2023)
doi: 10.3897/zookeys.1160.103596
https://zookeys.pensoft.net

RESEARCH ARTICLE

A peer-reviewed open-access journal
ZooKeys
Launched to accelerate biodiversity research

A revision of the genus *Trichohoplorana* Breuning, 1961 (Arthropoda, Insecta, Coleoptera, Cerambycidae, Lamiinae, Acanthocinini)

Gui-Qiang Huang[1], Dong-Shuo Liu[2], Rong-Chuan Xiong[1]

1 *School of Biological Science and Technology, Liupanshui Normal University, Liupanshui 553004, Guizhou, China* **2** *Unaffiliated, 401, Unit 1, Building 11, Xiying Qianjie, Tongzhou District, 101149, Beijing, China*

Corresponding author: Rong-Chuan Xiong (691477843@qq.com)

Academic editor: Francesco Vitali | Received 16 March 2023 | Accepted 23 April 2023 | Published 10 May 2023

https://zoobank.org/DD3B08DE-AF5E-4AF5-9E9F-E623C147308D

Citation: Huang G-Q, Liu D-S, Xiong R-C (2023) A revision of the genus *Trichohoplorana* Breuning, 1961 (Arthropoda, Insecta, Coleoptera, Cerambycidae, Lamiinae, Acanthocinini). ZooKeys 1160: 191–205. https://doi.org/10.3897/zookeys.1160.103596

Abstract

A taxonomic revision of the genus *Trichohoplorana* Breuning, 1961 is presented. A junior synonym of *Trichohoplorana*, *Ipochiromima* Sama & Sudre, 2009, **syn. nov.**, is proposed. A junior synonym of *T. dureli* Breuning, 1961, *I. sikkimensis* (Breuning, 1982), **syn. nov.**, is proposed. *Trichohoplorana* is newly recorded from Vietnam. A new species, *T. nigeralba* **sp. nov.** is described from Vietnam. *Trichohoplorana luteomaculata* Gouverneur, 2016 is newly recorded from China and Vietnam. Hind wings and male terminalia of *T. luteomaculata* are described for the first time. *Trichohoplorana* is redescribed, and a key to *Trichohoplorana* species is presented.

Keywords

Hind wings, male terminalia, new faunistic records, new species, synonyms

Introduction

The genus *Trichohoplorana* was established by Breuning (1961) for *Trichohoplorana dureli* Breuning, 1961. It presently consists of six species from Asia (Tavakilian and Chevillotte 2022). Mitono (1943) described *Acanthocinus shirakii* from China (Taiwan), then Gressitt (1951) transferred *A. shirakii* Mitono, 1943 to *Neacanista* Gressitt, 1940, and finally, Gouverneur (2016) transferred *N. shirakii* to *Trichohoplorana* and

described *T. luteomaculata* from Laos (Houa Phan). Holzschuh (1989, 1990, 2015) described *T. juglandis*, *T. mutica*, and *T. tenuipes*, respectively, from South Asia.

In this work, new synonyms, new faunistic records, and a new species are provided. Wings and male terminalia are described for the first time. Consequently, *Trichohoplorana* now consists of seven species from Asia. A redescription and a key to all species of *Trichohoplorana* are presented.

Material and methods

Specimens examined are deposited in following institutions and private collections:

CDSL Collection Dong-Shuo Liu, Beijing, China
CHS Collection Carolus Holzschuh, Villach, Austria
CWW Collection Andreas Weigel, Wernburg, Germany
CXG Collection Xavier Gouverneur, Rennes, France
LPSNU School of Biological Science and Technology, Liupanshui Normal University, Liupanshui, Guizhou, China
MNHN Muséum national d'Histoire naturelle, Paris, France
SYSU The Museum of Biology, Sun Yat-sen University, Guangzhou, China

The methods of taking photographs for Figs 2C–G, 4B–F, 6A–E followed Huang et al. (2020), and methods of photographing Fig. 3A–J mainly followed Huang and Li (2019) but were taken with a E3ISPM21000KPA camera and ImageView software. The terminology of hind wings vein follows Švácha and Lawrence (2014). The terminology of male terminalia follows Ślipiński and Escalona (2013).

Taxonomy

Trichohoplorana Breuning, 1961

Trichohoplorana Breuning, 1961: 548; Breuning 1963: 534; Breuning 1978: 49; Löbl and Smetana 2010: 213. Type species: *Trichohoplorana dureli* Breuning, 1961, by original designation.
Trichhoplorana Breuning 1977: 115 (misspelling).
Ipochiromima Sama and Sudre 2009: 384 (replacement name for *Mimipochira* Breuning, 1982: 25); Löbl and Smetana 2010: 209. Type species: *Mimipochira sikkimensis* Breuning, 1982, by original designation. Syn. nov.

Redescription. Head distinctly narrower than prothorax, frons with a narrow, median furrow extending from base of clypeus up to apical margin of pronotum; eyes coarsely faceted, lower lobes of eyes distinctly far away from each other and longer than genae;

antennae slender, distinctly longer than body, scape strongly expanded before apex, pedicle distinctly longer than broad. Pronotum transverse, with a tubercle on each side, punctured, with a pair of subuliform tubercles at sides of middle; prosternal process broad, with a longitudinal depression in middle, procoxal cavities closed posteriorly. Scutellum linguiform. Elytra covered with black or brown spots and a series of black or brown spots along suture; disc elongate, distinctly broader than pronotum at base, gradually narrow from near apical third, punctured, with a pair of tubercles at base and near scutellum, with a pair of bumps behind the tubercles; humeral angles rounded and slightly processed forward. Mesocoxal cavities closed externally to mesepimera. Femora strongly clavate.

Diagnosis. *Trichohoplorana* is very similar to *Neacanista* Gressitt, 1940 in having the pronotum with a tubercle at each side, with a pair of tubercles at the sides of the middle, the elytra with a pair of tubercles at the base and near the scutellum, with a pair of bumps behind the tubercles, and a strongly clavate femora. However, *Trichohoplorana* differs from *Neacanista* in having the antennal scape strongly expanded before the apex (gradually thickened before the apex in *Neacanista*) and the pedicle distinctly longer than broad (broader than long in *Neacanista*).

Distribution. Bhutan, China, India, Laos, Nepal, Vietnam (**new country record**).

Remarks. Breuning (1982) established *Mimipochira* for *M. sikkimensis* Breuning, 1982, but this genus was a junior homonym of *Mimipochira* Breuning, 1956. Hence, Sama and Sudre (2009) introduced the new name *Ipochiromima*. After comparing photographs of the holotypes of *T. dureli* Breuning, 1961 (Fig. 1A) and *M. sikkimensis* (Fig. 1B, C), we consider these two species as belonging to the same genus, based on above redescribed characters. Thus, we treat *Ipochiromima* as a junior synonym of *Trichohoplorana*.

Trichohoplorana dureli Breuning, 1961

Fig. 1A–D

Trichohoplorana dureli Breuning, 1961: 548 (type locality: "Pedong, Sikkim, India"); Breuning 1963: 534 (catalogue); Breuning 1978: 49 (redescription), pl. IV, fig. 15 (holotype); Löbl and Smetana 2010: 213 (catalogue).

Ostedes dureli: Breuning and Heyrovský 1961: 143.

Mimipochira sikkimensis Breuning, 1982: 26 (type locality: "Sikkim, India"). Syn. nov.

Ipochiromima sikkimensis: Sama and Sudre 2009: 384 (catalogue); Löbl and Smetana 2010: 209 (catalogue).

Type material examined. *Trichohoplorana dureli* Breuning, 1961: ***holotype***, ♂ (MNHN), Pedong, Sikkim, India, 1914, L. Durel leg., [examined from a photograph (Fig. 1A)]; *Mimipochira sikkimensis* Breuning, 1982: ***holotype***, ♂ (MNHN), Sikkim, India [examined from three photographs (Fig. 1B–D)].

Distribution. Bhutan, India (Sikkim).

Remarks. The differences between *T. dureli* and *I. sikkimensis* (Fig. 1A–C) mainly reflect in the shape of the elytral brown spots: the large spots near elytral middle, at

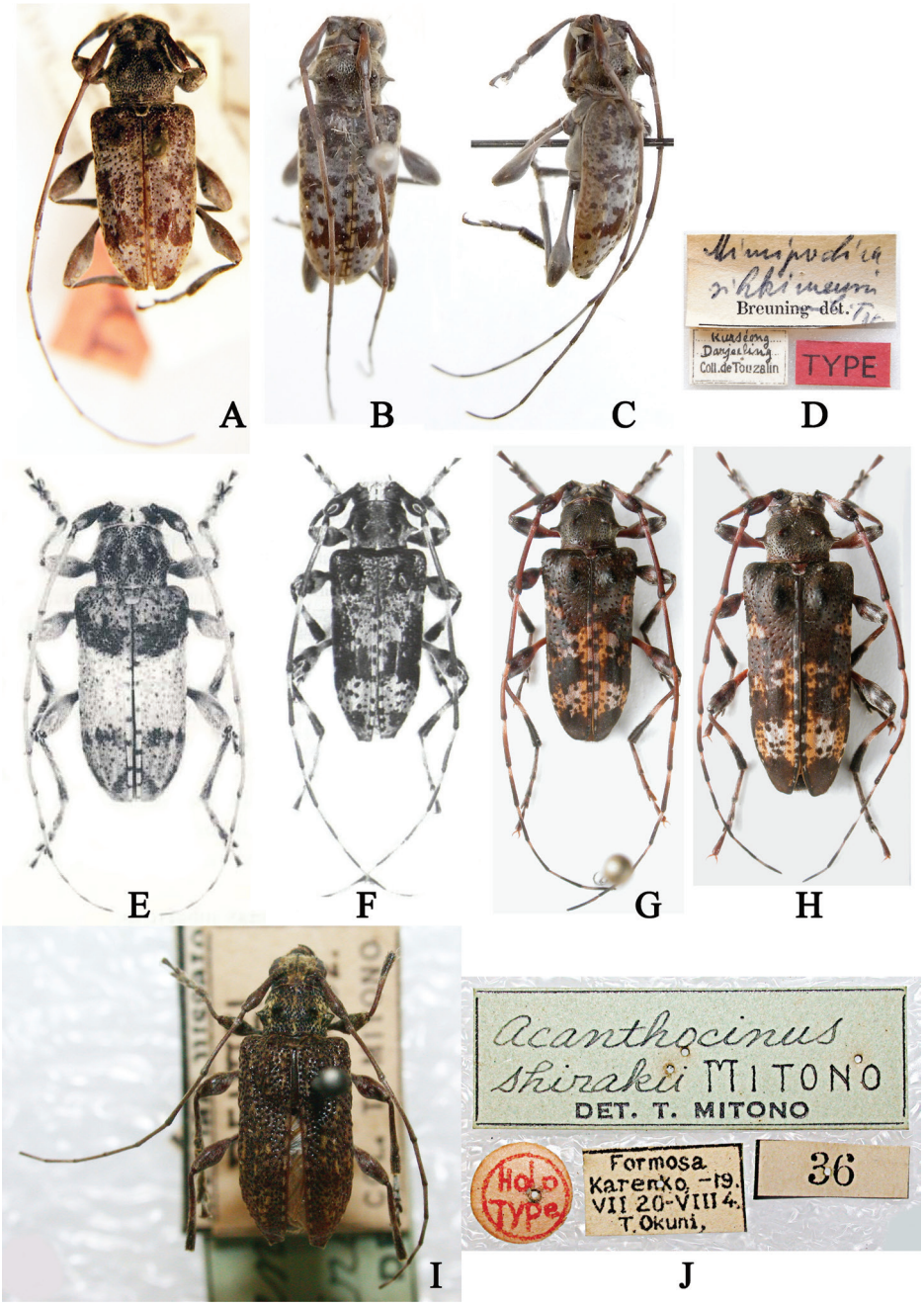

Figure 1. Types of *Trichohoplorana* spp. **A** *Trichohoplorana dureli*, holotype, male habitus, dorsal view (photo by Andreas Weigel) **B–D** *Mimipochira sikkimensis* **B** holotype, male habitus, dorsal view **C** holotype, male habitus, lateral view **D** labels (photos by Xavier Gouverneur) **E** *Trichohoplorana juglandis*, holotype, male habitus, dorsal view (photo reproduced from Holzschuh 1989) **F** *Trichohoplorana mutica*, holotype, male habitus, dorsal view (photo reproduced from Holzschuh 1990) **G, H** *Trichohoplorana tenuipes* **G** holotype, male habitus, dorsal view **H** paratype, female habitus, dorsal view (photos provided by Holzschuh) **I, J** *Acanthocinus shirakii*: **I** holotype, male habitus, dorsal view **J** labels (photos reproduced from Huang et al. 2015).

apical third, and at apex. They are actually intraspecific differences; thus, we treat *I. sikkimensis* as a junior synonym of *T. dureli*.

Trichohoplorana juglandis Holzschuh, 1989

Fig. 1E

Trichohoplorana juglandis Holzschuh, 1989: 401 (type locality: "Menchunang, East Dochu-La, Thimphu district, West Bhutan"), fig. 8 (holotype, male); Löbl and Smetana 2010: 213 (catalogue); Weigel 2012: 408 (catalogue), pl. XXVII, fig. b; Lazarev 2019: 154 (catalogue).

Distribution. Bhutan (Thimphu), India (Arunachal Pradesh).

Trichohoplorana mutica Holzschuh, 1990

Fig. 1F

Trichohoplorana mutica Holzschuh, 1990: 193 (type locality: "Footpath from Sherpagaon to Ghora Tabela, Langtang Khola, Nawakot, C-Nepal"), fig. 11 (holotype, male); Weigel 2006: 506 (catalogue); Löbl and Smetana 2010: 213 (catalogue).

Distribution. Nepal (Nawakot).

Trichohoplorana tenuipes Holzschuh, 2015

Fig. 1G, H

Trichohoplorana tenuipes Holzschuh, 2015: 473 (type locality: "Bhalukhop, district of Taplejung, East Nepal"), figs 3 (holotype, male) and 4 (paratype, female).

Type material examined. ***Holotype***, ♂ (CHS), Bhalukhop, district of Taplejung, East Nepal, alt. 3000m, 11–21.V.2013, Emil Kučera leg., [examined from a photograph (Fig. 1G)]; ***paratype***, 1 ♀ (CHS), data same as holotype, [examined from a photograph (Fig. 1H)].

Distribution. Nepal (Taplejung).

Trichohoplorana shirakii (Mitono, 1943)

Fig. 1I, J

Acanthocinus shirakii Mitono, 1943: 584 (type locality: "Reimei, Hassenzan, Taiwan").
Neacanista shirakii: Gressitt 1951: 518 (catalogue); Breuning 1978: 40 (redescription); Hua 1982: 99 (catalogue); Nakamura, Makihara and Saito 1992: 95 (catalogue);

Hua 2002: 218 (catalogue); Chou 2004: 326, fig (male); Hua et al. 2009: 95, pl. XCV, fig. 1091 (male and female); Löbl and Smetana 2010: 210 (catalogue); Huang et al. 2015: 560 (catalogue), figs 32 (holotype, male), 33 (holotype, labels), and 34 (4 in map).

Trichohoplorana shirakii: Gouverneur 2016: 72, figs 2a (holotype, male) and 2b (holotype, labels).

Distribution. China (Taiwan).

Trichohoplorana luteomaculata Gouverneur, 2016

Figs 2–5

Trichohoplorana luteomaculata Gouverneur, 2016: 69 (type locality: "Ban Saleui, Massif du Mont Phou Pan, Houa Phan Province, Northeast Laos"), figs 1a, b (holotype, male) and 1c (paratype, female).

Type material examined. ***Holotype***, ♂ (CXG), Ban Saleui, Massif du Mont Phou Pan, Houa Phan Province, Northeast Laos, alt. 1300–1900m, 1.V.2012, local collector leg., [examined from two photographs (Fig. 2A, B)]; ***paratype***, 1 ♀ (CXG), data same as holotype, but 2.V.2014 [examined from a photograph (Fig. 4A)].

Additional material examined. China: 1 ♀ (SYSU), Suoli village, Tongdao County, Huaihua City, Hunan Province, V.1981, Li-Jun Zhang leg.; 1♂1♀ (CDSL, figs 2C–G, 3, 4B–F), Jianfengling National Natural Reserve, Hainan Province, 7.VI.2021, 18°42'34.75"N, 108°52'34.50"E, alt. 954 m, Dong-Shuo Liu leg., collected by light trap (Fig. 5); **Vietnam:** 1 ♀ (LPSNU), Yen Bai Province, August 2020, local collector leg.; 1 ♀ (CWW), Gem. Ta Pin, Kreis Sapa, Lao Cai Province, 22°22.196'N, 103°48.701'E, alt. 2318 m, 26.VI–01.VII.2017, N.H. Binh leg., [examined from a photograph provided by Andreas Weigel].

Supplementary description. Male (Figs 2C–G, 3). Hind wings (Fig. 2G) with AA_{3+4} vein bifurcate near apical third; AA_4 vein and AA_3 vein closed to each other apically and not extending to margin; AA_3 vein connected with Cu vein near apical third; CuA_2 vein connected with MP_{3+4} vein near basal third of MP_{3+4} vein and not extending to margin; MP_{3+4} vein bifurcate near middle; MP_4 vein, MP_3 vein and MS vein not extending to margin; a short and vague uncertain vein (?, either a crossvein or base of MP_{3+4} vein) located between Cu vein and MP_{1+2} vein.

Male terminalia. Tergite VIII (Fig. 3A) sparsely covered with short brown setae apically and at sides of apical third, nearly truncated at apex. Sternite VIII (Fig. 3B) anchor-shaped, sparsely covered with short brown setae at apical sides, apical margin slightly depressed; spiculum relictum distinctly longer than sternite VIII. Stem of spiculum gastrale more than 2.0 times as long as branches and curved towards dorsum at base (Fig. 3C). Parameres of tegmen sparsely covered with short brown setae on apical third and several long setae near apical fifth; each paramere gradually constricted from base to apex, but

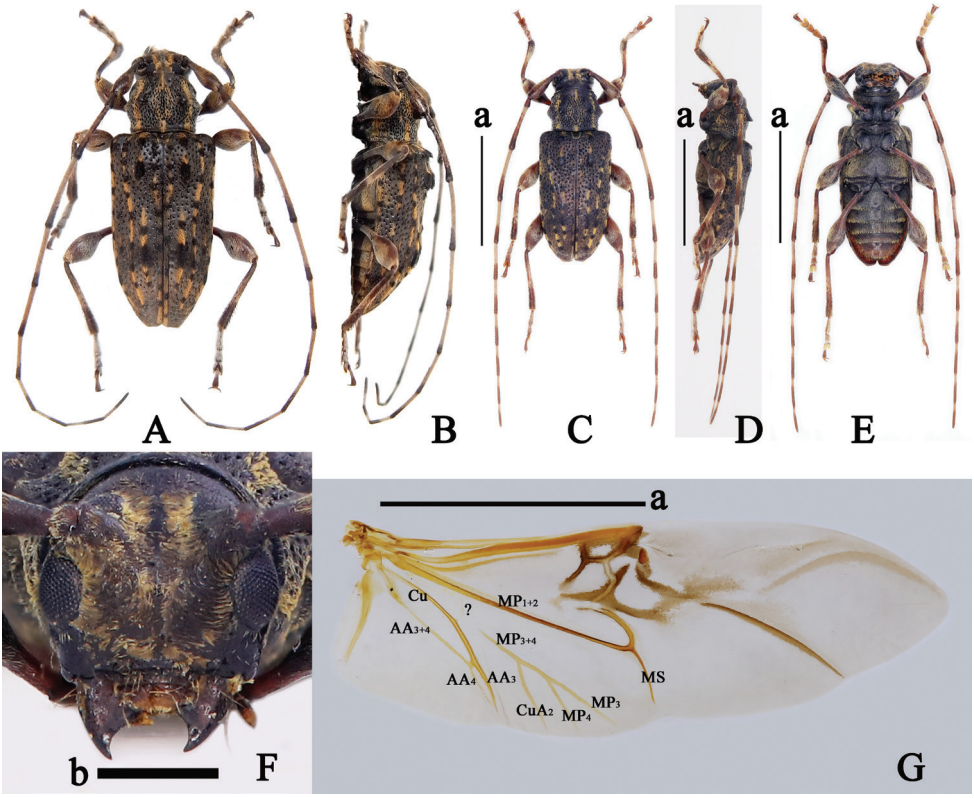

Figure 2. *Trichohoplorana luteomaculata*, males **A, B** holotype habitus **A** dorsal view **B** lateral view (photos by Xavier Gouverneur) **C–G** material from Hainan, China **C** habitus, dorsal view **D** habitus, lateral view **E** habitus, ventral view **F** head, frontal view **G** right hind wing, dorsal view. Abbreviations: A: anal, Cu: cubital, MP: medial posterior, MS: medial spur, ?: a vein of uncertain homology (either a crossvein or base of MP_{3+4} vein). Scale bars: 5 mm (**a**); 1 mm (**b**).

external margin slightly expanded near apex; apex of both parameres rounded and closed together; phallobase nearly 3.0 times as long as parameres and processed outward near middle; anterior tegminal strut curved outward (Fig. 3D–F). Penis curved towards venter, ventral plate distinctly longer and broader than dorsal plate and slightly sharp at apex; dorsal plate widely rounded at apex; apex of dorsal struts obliquely truncated (Fig. 3G–J).

Female (Fig. 4B–F). Hind wings (Fig. 4F) with AA_{3+4} vein bifurcate near apical third; AA_4 vein and AA_3 vein fused apically and not extending to margin; AA_3 vein connected with Cu vein near apical third; CuA_2 vein connected with MP_{3+4} vein near basal fifth of MP_{3+4} vein and not extending to margin; MP_{3+4} vein bifurcate near middle, MP_4 vein, MP_3 vein and MS vein not extending to margin; a short uncertain vein (?, either a crossvein or base of MP_{3+4} vein) located between Cu vein and MP_{1+2} vein.

Distribution. China (Hainan, Hunan), Laos (Houa Phan), Vietnam (Lao Cai, Yen Bai).

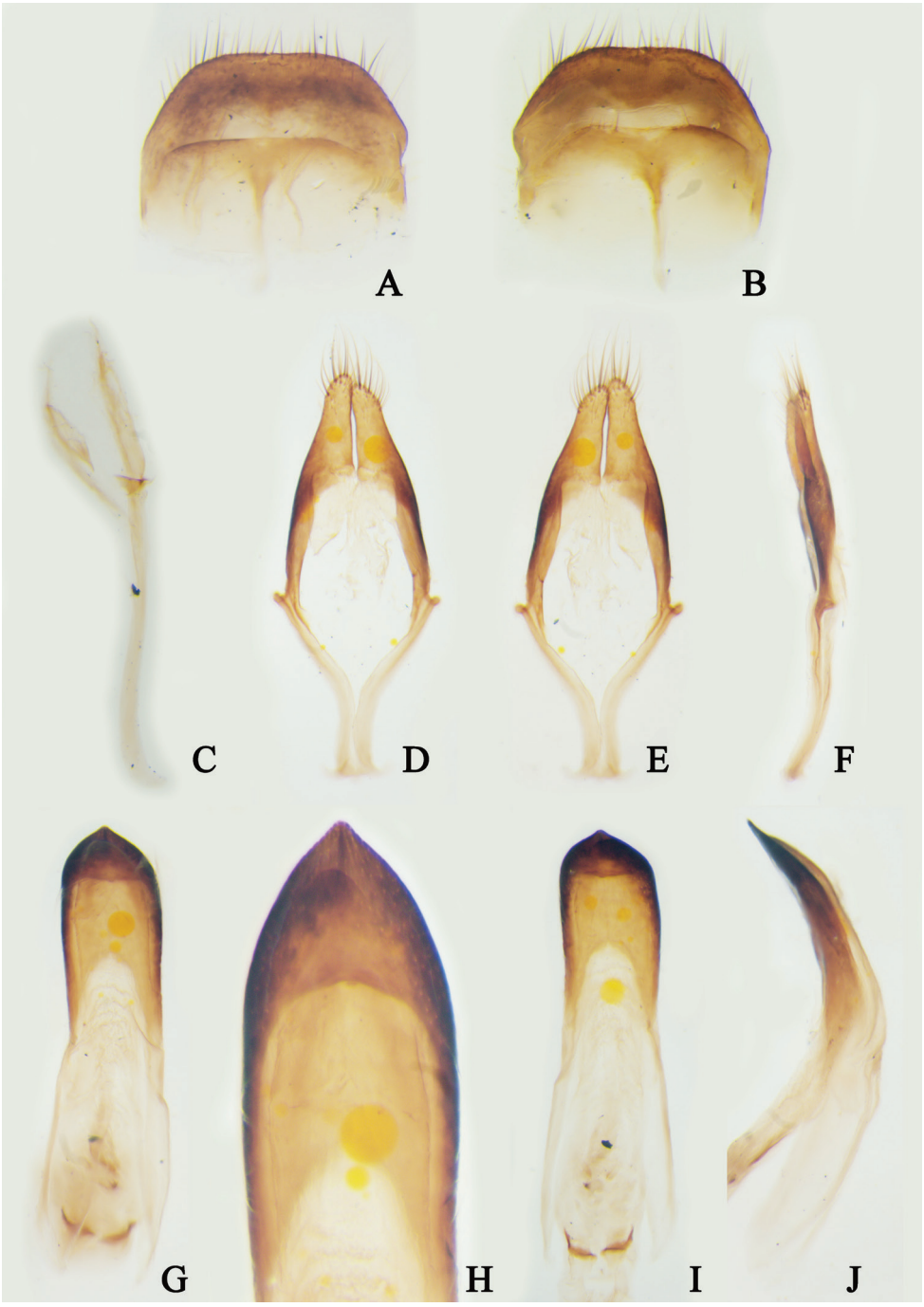

Figure 3. Male terminalia of *Trichohoplorana luteomaculata* from Hainan, China **A** tergite VIII, dorsal view **B** sternite VIII, verntral view **C** spiculum gastrale, dorsal view **D–F** tegmen **D** dorsal view **E** ventral view **F** lateral view **G–J** penis **G** dorsal view **H** dorsal view **I** ventral view **J** lateral view. Not to scale.

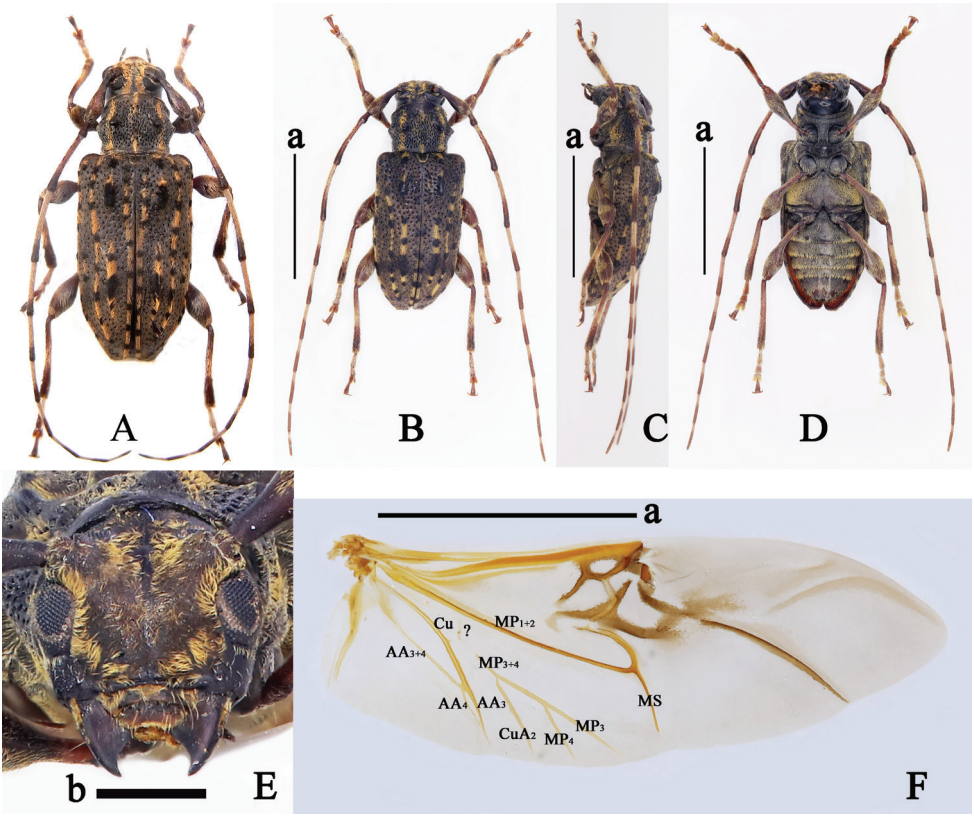

Figure 4. *Trichohoplorana luteomaculata*, females **A** paratype habitus, dorsal view (photo by Xavier Gouverneur) **B–F** material from Hainan, China **B** habitus, dorsal view **C** habitus, lateral view **D** habitus, ventral view **E** head, frontal view **F** right hind wing, dorsal view. Abbreviations: A: anal, Cu: cubital, MP: medial posterior, MS: medial spur, ?: a vein of uncertain homology (either a crossvein or base of MP_{3+4} vein). Scale bars: 5 mm (**a**), 1 mm (**b**).

Figure 5. Scene showing collecting *Trichohoplorana luteomaculata* by light trap from Hainan, China (photos by Dong-Shuo Liu).

***Trichohoplorana nigeralba* sp. nov.**
https://zoobank.org/68605399-2CE3-485B-96B7-2530C1A471B8
Fig. 6

Type material examined. ***Holotype***, ♀ (LPSNU), Yen Bai Province, Vietnam, V.2019, local collector leg.

Description. Female, holotype. Body length: 14.0 mm, humeral width: 5.2 mm. Body black, antennal scape (except for outside of apex), pedicel, antennomeres III (except for apex), IV (except for apex), V (basal half), VI (basal half), elytra (apical half), protibiae (basal half), mesofemora (basal half), mesotibiae (basal half), metafemora (most of parts) and metatibiae (basal half) reddish brown; claws yellowish brown (Fig. 6A–C).

Frons (Fig. 6D) densely covered with short yellow and white hairs. Vertex densely covered with short white hairs on middle and short yellow hairs on center (Fig. 6A). Antennae sparsely covered with sub-erect, short, white setae; scape sparsely covered with short, brown setae; pedicel sparsely covered with short, brown setae, with several short, white setae at internal side of apex; antennomere III sparsely covered with short, white setae basally, other parts densely with short, brown setae; antennomeres IV–XI densely covered with short white setae on the basal half and densely with short, brown setae on the apical half; antennomeres III–VII fringed with several long, black setae ventrally; antennomeres VIII–X fringed with one or two long, black setae ventrally; antennae 1.5 times as long as body, length (mm) of each antennomere: scape = 2.7, pedicel= 0.8, III = 3.0, IV= 3.0, V = 2.2, VI = 2.0, VII = 1.7, VIII = 1.6, IX = 1.6, X = 1.5, X I = 1.3; antennomeres III and IV curved inward (Fig. 6A–C). Pronotum (Fig. 6A) covered with three yellow haired bands: two located at sides and starting from near anterior margin to posterior margin, one located in middle and starting from anterior margin to posterior margin; disc with a pair of subtriangular, yellow haired spots located at sides of middle; near anterior of pronotum distinctly expanded outward, pronotum densely punctured (except for apex and base), base of the subuliform tubercles on pronotum expanded forward. Prosternum (sides) and propleuron (venter) sparsely covered with short, yellow hairs (Fig. 6B, C). Scutellum (Fig. 6A) sparsely covered with short black hairs, densely covered with yellow hairs at apex, depressed in middle of apical margin. Elytra (Fig. 6A, B) sparsely covered with short black hairs on the basal half, a short yellow haired band at lateral margins of base, several yellow haired spots arranging into an longitudinal line starting from near posterior humeral angle to basal third, a yellow haired spot located behind the bumps, and several yellow spots along suture from basal fourth to middle; the tubercles at elytral base and near scutellum, and the bumps behind the tubercles densely covered with short, black setae; apical half of each elytron densely covered with short white hairs and four longitudinal yellow haired bands (first band located at lateral margin, second and third bands located in middle and fused at apical half, forth band located near suture); disc 1.9 times as long as wide at base, rounded apically, moderately covered with dense coarse punctures at basal half. Mesosternum, mesepisternum, and mesepimeron sparsely covered with short, yellow hairs; metasternum, metepisternum, and metepimeron densely covered with short,

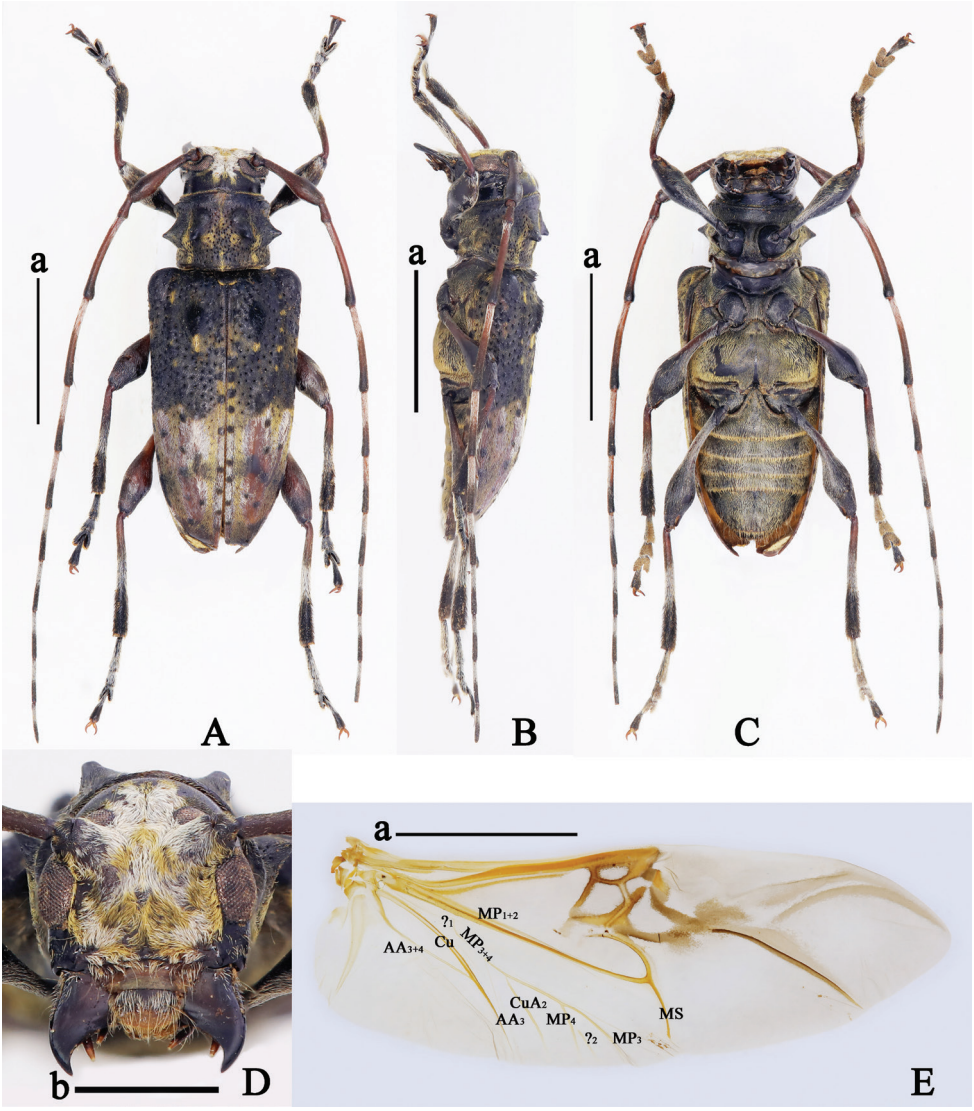

Figure 6. *Trichohoplorana nigeralba*, holotype, female **A** habitus, dorsal view **B** habitus, lateral view **C** habitus, ventral view **D** head, frontal view **E** right hind wing, dorsal view. Abbreviations: A: anal, Cu: cubital, MP: medial posterior, MS: medial spur, $?_1$: a vein of uncertain homology (either a crossvein or base of MP_{3+4} vein), $?_2$: an uncertain vein. Scale bars: 5 mm (**a**), 2 mm (**b**).

yellow hairs (Fig. 6C). Femora sparsely covered with short white setae and several suberect, long, white setae at external side; tibiae covered with extremely sparse, suberect, long, white setae, sparsely with short, thin, black setae on the basal third, densely with short, white setae in middle, and densely with short, thick, black setae on the apical third; tarsomere I–III (except for venter) densely covered with short white and sparsely suberect, long, white setae dorsally, tarsomere V (except for venter) sparsely covered

with short, white setae at basal half and short, black setae on the apical half, with more sparse long black setae at apex (Fig. 6A–C). Abdominal ventrites I–V densely covered with short, yellow hairs, the hairs more dense at apices of ventrites I–IV; apex and sides of ventrite V sparsely covered with long, yellow pubescences (Fig. 6C).

Hind wings (Fig. 6E) with AA_{3+4} vein not bifurcate, AA_4 vein missed, AA_3 vein connected with Cu vein near apical 1/3 and not extending to margin; CuA_2 vein connected with MP_{3+4} vein near basal 1/3 of MP_{3+4} vein and not extending to margin; MP_{3+4} vein bifurcate near apical 1/3, some parts of base of MP_{3+4} vein missed, a short and vague uncertain vein ($?_1$, either a crossvein or base of MP_{3+4} vein) connected with base of MP_{3+4} vein; MP_4 vein, MP_3 vein and MS vein not extending to margin; a short uncertain vein ($?_2$) located between MP_4 vein and MP_3 vein, not extending to margin. Abdominal ventrite V raised at apical sides and truncated apically (Fig. 6C).

Male. Unknown.

Etymology. The specific epithet of this new species is derived from the Latin words "*niger*" and "*albus*" referring to most of parts of elytral basal half sparsely covered with short, black hairs and most of parts of elytral apical half densely with short, white hairs.

Distribution. Vietnam (Yen Bai).

Diagnosis. This new species can be distinctly distinguished from other species of *Trichohoplorana* by its peculiar elytral pattern (Fig. 6A).

Remarks. When the senior author received the holotype of this new species, the right antennomere XI was missing and the elytral apex was broken. Then, the head, left antennomere XI, and prothorax were separated from the body due to his carelessness, and he correspondingly glued to the body the separated portions with white emulsoid. Consequently, some hairs on the antennae, elytra, metaventrite, and legs were worn so that some characters are unclear.

Key to species of *Trichohoplorana*

1 Elytra with a broad transverse white haired band on the middle..... ***T. juglandis***
– Elytra without a broad transverse white haired band on the middle **2**
2 Elytra not covered with short white or grayish-white hairs **3**
– Elytra covered with short white or grayish-white hairs..... **4**
3 Tips of the lateral tubercles of the prothorax obtuse, elytral apex slightly obliquely truncated, with the marginal angle obtuse and not distinctly processed, elytral punctuations fine ..... ***T. luteomaculata***
– Tips of the lateral tubercles of the prothorax pointed, elytral apex distinctly obliquely truncated, with the marginal angle pointed and distinctly stretched, elytral punctuations coarse ..... ***T. shirakii***
4 Most of parts of elytra densely covered with grayish-white hairs..... ***T. dureli***
– Most of parts of elytra not densely covered with grayish-white hairs..... **5**
5 Elytra with a yellow haired spot located behind bumps, most of parts of elytral apical half densely covered with short white hairs..... ***T. nigeralba***
– Elytra without a yellow haired spot located behind bumps, most of parts of elytral apical half not densely covered with short, white hairs **6**

6 Lateral tubercles of prothorax thick, elytra with a transverse band behind bumps, marginal angles distinctly processed ..... ***T. mutica***
– Lateral tubercles of prothorax thin, elytra with a transverse band on the middle, rounded apically ..... ***T. tenuipes***

Acknowledgements

We sincerely appreciate Mr Xavier Gouverneur (CXG) for providing photographs of the holotype of *Trichohoplorana luteomaculata* and *Mimipochira sikkimensis*, Dr Andreas Weigel (CWW) for providing a photograph of the holotype of *Trichohoplorana dureli*, Dr Carolus Holzschuh (CHS) for providing photographs of the type of *Trichohoplorana tenuipes*. We are very grateful to Andreas Weigel for providing material of *T. luteomaculata* and literature, to Dr Ping Wang (Yangtze University, Jingzhou, Hubei, China) for providing literature, and to Prof Hong Pang (SYSU), Dr Bing-Lan Zhang (SYSU), and Mr Wei-Cai Xie (SYSU) for providing kind help during the senior author's visits to SYSU. We express our special appreciation to Mr Ming-Zhi Zhao (South China Agricultural University, Guangzhou, Guangdong, China) for obtaining materials of *T. luteomaculata* and *T. nigeralba*. We also thank the reviewers Dr Eduard Vives (Natural Science Museum of Barcelona, Spain), Mr Xavier Gouverneur (Rennes, France), and Dr Francesco Vitali (Academic Editor for Cerambycidae) for improving our manuscript.

This research was supported by Guizhou Provincial Science and Technology Foundation (黔科合基础-ZK[2022]一般527), the Fund Project of the Education Department of Guizhou Province (黔教技[2022]091号, 黔教技[2022]054号, 黔教技[2022]338号), the Science and Technology Innovation Team Project of Liupanshui Normal University (LPSSYKJTD201602).

References

Breuning S (1961) Nouveaux Cerambycidae des collections du Muséum de Paris. Bulletin du Muséum National d'Histoire Naturelle de Paris (2ème série) 32(6) [1960]: 536–548.

Breuning S (1963) Catalogue des Lamiaires du Monde (Col. Céramb.). Verlag des Museums G. Frey, Tutzing bei München (7): 463–555.

Breuning S (1977) Révision de la tribu des Acanthocinini de la région Asiato-Australienne (Coleoptera: Cerambycidae), première partie. Mitteilungen aus dem Zoologischen Museum in Berlin 53(1): 111–155. https://doi.org/10.1002/mmnz.19770530103

Breuning S (1978) Révision de la tribu des Acanthocinini de la région Asiato-Australienne (Coleoptera: Cerambycidae), troisième partie. Mitteilungen aus dem Zoologischen Museum in Berlin 54(1): 3–78. https://doi.org/10.1002/mmnz.19780540102

Breuning S (1982) Diagnoses préliminaires de nouveaux Lamiinae du Muséum national d'Histoire naturelle de Paris [Coleoptera, Cerambycidae]. Annales de la Société Entomologique de France, Paris (N. S.) 18(1): 9–29. https://doi.org/10.3406/bsef.1960.20510

Breuning S, Heyrovský L (1961) Die Himalaja-Cerambyciden im Museum A. Koenig in Bonn. Bonner Zoologische Beitrage 1/2(12): 142–144.

Chou W-I (2004) The Atlas of Taiwanese Cerambycidae (2nd edn.). Owl Publishing House, Taipei, 408 pp.

Gouverneur X (2016) Description d'une nouvelle espèce du genre *Trichohoplorana* Breuning, 1961 du Laos (Coleoptera, Cerambycidae, Lamiinae, Acanthocinini). Les Cahiers Magellanes (NS) 23: 72–76.

Gressitt JL (1951) Longicorn beetles of China. Longicornia 2: 1–667.

Holzschuh C (1989) Beschreibung von 8 neuen Bockkäfern aus Bhutan (Coleoptera, Cerambycidae). Entomologica Basiliensa 13: 391–402.

Holzschuh C (1990) Beschreibung von neuen Bockkäfern aus dem Himalaya (Insecta: Coleoptera, Cerambycidae). Berichte des Naturwissenschaftlich-Medizinischen Vereins in Innsbruck 77: 185–197.

Holzschuh C (2015) Zwei neue Bockkäfer aus Nepal (Insecta: Coleoptera: Cerambycidae). In: Hartmann M, Weipert J (Eds) Biodiversität und Naturausstattung im Himalaya V. Verein der Freunde und Förderer des Naturkundemuseums Erfurt e. V: 471–474.

Hua L-Z (1982) A Check List of the Longicorn Beetles of China (Coleoptera: Cerambycidae). Zhongshan University, Guangzhou, 158 pp.

Hua L-Z (2002) List of Chinese Insects. Vol. II. Zhongshan (Sun Yat-sen) University Press, Guangzhou, 612 pp.

Hua L-Z, Nara H Saemulson [misspelling of Samuelson] GA, Lingafelter SW (2009) Iconography of Chinese Longicorn Beetles (1406 Species) in Color. Sun Yat-sen University Press, Guangzhou, xii, 474 pp.

Huang G-Q, Li S (2019) Review of the genus *Falsotrachystola* Breuning, 1950 (Coleoptera: Cerambycidae: Lamiinae: Morimopsini). Zootaxa 4555(1): 45–55. https://doi.org/10.11646/zootaxa.4555.1.3

Huang G, Liu B, Gouverneur X (2015) Note on the genus *Neacanista* Gressitt, 1940 (Coleoptera: Cerambycidae: Lamiinae: Acanthocinini). Zootaxa 3981(4): 553–564. https://doi.org/10.11646/zootaxa.3981.4.6

Huang G-Q, Yan K, Li S (2020) Description of *Pseudoechthistatus rugosus* n. sp. from Yunnan, China (Coleoptera: Cerambycidae: Lamiinae: Lamiini). Zootaxa 4747(3): 593–600. https://doi.org/10.11646/zootaxa.4747.3.12

Lazarev MA (2019) Catalogue of Bhutan longhorn beetles (Coleoptera, Cerambycidae). Humanity space-International Almanac 8(2): 141–198.

Löbl I, Smetana A (2010) Catalogue of Palaearctic Coleoptera. Vol. 6. Chrysomeloidea. Apollo Books, Stenstrup, 924 pp. https://doi.org/10.1163/9789004260917

Mitono T (1943) Descriptions of some new species and varieties of longicorn-beetles from Taiwan. Transactions of the Natural History Society of Formosa 33: 578–588.

Nakamura S, Makihara H, Saito A (1992) Check-list of longicorn-beetles of Taiwan. Hiba Society of Natural History, Shobara, Hiroshima, 126 pp.

Sama G, Sudre J (2009) New nomenclatural acts in Cerambycidae. II. (Coleoptera). Bulletin de la Société Entomologique de France, Paris 114(3): 383–388. https://doi.org/10.3406/bsef.2009.2751

Ślipiński A, Escalona HE (2013) Australian Longhorn Beetles (Coleoptera: Cerambycidae). Vol. 1. Introduction and Subfamily Lamiinae. ABRS, Canberra & CSIRO Publishing, Melbourne, 504 pp. https://doi.org/10.1071/9781486300044

Švácha P, Lawrence JF (2014) 2.4 Cerambycidae Latreille, 1802. In: Leschen RAB, Beutel RG (Eds) Handbook of zoology, Coleoptera, Beetles. Vol. 3. Morphology and Systematics (Phytophaga). Walter de Gruyter, Berlin, 77–177. https://doi.org/10.1515/9783110274462.77

Tavakilian G, Chevillotte H (2022) Titan: International Database on Worldwide Cerambycidae or Longhorn Beetles. http://titan.gbif.fr/index.html [accessed 18 March 2022]

Weigel A (2006) Checklist and Bibliography of Longhorn Beetles from Nepal (Insecta: Coleoptera: Cerambycidae). In: Hartmann M, Weipert J (Eds) Biodiversität und Naturausstattung im Himalaya II. Verein der Freunde und Förderer des Naturkundemuseums Erfurt e. V., 495–510.

Weigel A (2012) Beitrag zur Bockkäferfauna von Arunachal Pradesh (Indien) mit Beschreibung einer neuen Art aus der Gattung Acalolepta Pascoe, 1858 (Insecta: Coleoptera: Cerambycidae). In: Hartmann M, Weipert J (Eds), Biodiversität und Naturausstattung im Himalaya IV. Verein der Freunde und Förderer des Naturkundemuseums Erfurt e. V., 405–411.